

N O T I C E

THIS DOCUMENT HAS BEEN REPRODUCED FROM
MICROFICHE. ALTHOUGH IT IS RECOGNIZED THAT
CERTAIN PORTIONS ARE ILLEGIBLE, IT IS BEING RELEASED
IN THE INTEREST OF MAKING AVAILABLE AS MUCH
INFORMATION AS POSSIBLE

JPL PUBLICATION 81-65

(NASA-CR-168643) CONVENTIONAL ENGINE
TECHNOLOGY. VOLUME 1: STATUS OF OTTO CYCLE
ENGINE TECHNOLOGY (Jet Propulsion Lab.)
216 p HC A10/MF A01

N82-19542

CSSL 21A

Unclas

G3/37 09289

Conventional Engine Technology

Volume I: Status of OTTO Cycle Engine Technology

M. W. Dowdy



December 15, 1981

Prepared for
U.S. Department of Energy
Through an Agreement with
National Aeronautics and Space Administration
by
Jet Propulsion Laboratory
California Institute of Technology
Pasadena, California

JPL PUBLICATION 81-65

Conventional Engine Technology

Volume I: Status of OTTO Cycle Engine Technology

M. W. Dowdy

December 15, 1981

Prepared for
U.S. Department of Energy
Through an Agreement with
National Aeronautics and Space Administration
by
Jet Propulsion Laboratory
California Institute of Technology
Pasadena, California

Prepared by the Jet Propulsion Laboratory, California Institute of Technology,
for the U.S. Department of Energy through an agreement with the National
Aeronautics and Space Administration.

This report was prepared as an account of work sponsored by an agency of the
United States Government. Neither the United States Government nor any
agency thereof, nor any of their employees, makes any warranty, express or
implied, or assumes any legal liability or responsibility for the accuracy, com-
pleteness, or usefulness of any information, apparatus, product, or process
disclosed, or represents that its use would not infringe privately owned rights.

Reference herein to any specific commercial product, process, or service by trade
name, trademark, manufacturer, or otherwise, does not necessarily constitute or
imply its endorsement, recommendation, or favoring by the United States
Government or any agency thereof. The views and opinions of authors
expressed herein do not necessarily state or reflect those of the United States
Government or any agency thereof.

PRECEDING PAGE BLANK NOT FILMED

ABSTRACT

Federally-mandated emissions standards have led to major changes in automotive technology during the last decade. Efforts to satisfy the new standards have been directed more toward the use of add-on devices, such as catalytic converters, turbochargers, and improved fuel metering, than toward complete engine redesign. The resulting changes are described in this volume, and the improvements brought about by them in fuel economy and emissions levels are fully documented.

Four specific categories of gasoline-powered internal combustion engines are covered, including subsystem and total engine development. Also included are the results of fuel economy and exhaust emissions tests performed on representative vehicles from each category.

PREFACE

This report was prepared by the Jet Propulsion Laboratory for the U.S. Department of Energy, Office of Transportation Programs, for the Vehicle Systems Program managed by Albert Chesnes. This work was done at JPL in the Energy and Control Division by the Propulsion System Section as part of Vehicle Systems Tasks managed by Eugene Baughman. Dr. M.W. Dowdy, the author of this volume, is no longer an employee of JPL. He is presently with Mechanical Technology, Incorporated, in Latham, New York.

The work was performed by the Jet Propulsion Laboratory and was sponsored by the U.S. Department of Energy under Interagency Agreements DE-A101-76CS51011 and DE-A101-80CS50194 through NASA Task RD 152, Amendment 165.

The purpose of this vehicle systems task was to perform a technical assessment of conventional automotive engine status and report the results. The status of the technology reported is that which was available through April 1981. This volume is part of the final report consisting of three volumes.

Volume I presents the status of Otto cycle engine technologies; Volume II presents the status of Diesel engine technology and Volume III compares these conventional engine types and discusses their future potential.

CONTENTS

1.	INTRODUCTION	1-1
1.1	TRANSPORTATION NEEDS	1-1
1.2	LEGISLATIVE CONSTRAINTS	1-1
1.3	MARKET EFFECTS	1-7
1.4	INDUSTRY TRENDS	1-7
2.	UNIFORM CHARGE ENGINES WITH THREE-WAY CATALYST EMISSION CONTROL SYSTEMS	2-1
2.1	INTRODUCTION	2-1
2.2	COMPONENT CHARACTERISTICS AND LIMITATIONS	2-3
2.2.1	Three-Way Catalysts	2-3
2.2.2	Oxygen Sensors	2-15
2.2.3	Fuel/Air Mixture Preparation	2-27
2.2.4	Control Systems	2-45
2.3	VEHICLE SYSTEMS	2-46
2.3.1	General Description	2-46
2.3.2	Systems with Fuel Injection	2-48
2.3.3	Systems with Carburetors	2-55
2.3.4	Systems with Throttle-Body Injection	2-61
2.4	VEHICLE FUEL ECONOMY AND EMISSIONS RESULTS	2-72
3.	LEAN BURN (FAST BURN) ENGINE CONCEPTS	3-1
3.1	INTRODUCTION	3-1
3.2	TECHNOLOGY DEVELOPMENTS AND VEHICLE SYSTEMS	3-6
3.3	VEHICLE FUEL ECONOMY AND EMISSIONS RESULTS	3-34

4.	STRATIFIED-CHARGE ENGINE CONCEPTS	4-1
4.1	INTRODUCTION	4-1
4.2	TECHNOLOGY DEVELOPMENTS AND VEHICLE SYSTEMS	4-5
4.3	VEHICLE FUEL ECONOMY AND EMISSIONS RESULTS	4-25
5.	ROTARY ENGINE CONCEPTS	5-1
5.1	INTRODUCTION	5-1
5.2	TECHNOLOGY DEVELOPMENTS AND VEHICLE SYSTEMS	5-2
5.3	VEHICLE FUEL ECONOMY AND EMISSIONS RESULTS	5-20
6.	REFERENCES	6-1
7.	BIBLIOGRAPHY	7-1

SECTION I

INTRODUCTION

1.1 TRANSPORTATION NEEDS

In order to continue to improve or even maintain present standards of living, it is necessary in an industrial society like the United States to maintain personal mobility. In the long term, this need can be met either by continuing to use personal automobiles or by developing effective public mass transportation. However, in many cases, personal automobiles are the only viable short-term option. This is especially true in some American cities (e.g., Los Angeles) whose development has been predicated on the availability of personal automobiles. Other impediments to the development of effective mass transportation systems are the tremendous capital investment required to build the system, and in many cases, a reluctance of people to give up their automobiles and utilize public transportation. Only developments in automotive technology will be discussed in this report.

During the last decade, many changes have occurred in the environment in which automobiles must operate. The need to improve air quality to protect the public health has led to the passage of Federal emissions standards for controlling exhaust emissions from automobiles. Also, Federal safety regulations have had a significant impact on automotive design. Early attempts by automotive manufacturers to meet these emissions standards with conventional engines led to significant fuel economy penalties. Several times during the last decade petroleum shortages have highlighted the dependence of the United States on imported oil and have helped focus the need for energy conservation, especially in the use of petroleum for transportation. To encourage production of more fuel-efficient automobiles, Federal fuel economy standards have been imposed on new automobiles. These fuel economy standards have led automotive manufacturers to produce smaller, lighter-weight vehicles powered by more fuel-efficient conventional engines. Also, fuel prices and fuel availability have drastically changed the attitudes of consumers, leading to the present strong trend toward smaller vehicles.

1.2 LEGISLATIVE CONSTRAINTS

The general trends in exhaust emissions and fuel economy regulations have led to changes in automotive technology in recent years (shown in Figure 1-1) and considerable reductions in gaseous exhaust emissions have been mandated during the last decade. Further changes in automotive technology are anticipated as fuel economy and exhaust emissions standards become more stringent in future years.

Specific gaseous exhaust emissions standards are given in Table 1-1 for production automobiles since the 1973 model year. For the 1980 model year, the 49-state standards for hydrocarbon (HC) and carbon monoxide (CO) emissions have been reduced to 0.41 g/mi and 7.0 g/mi respectively, with the nitrogen oxide (NO_x) requirement staying at 2.0 g/mi. The California standards for

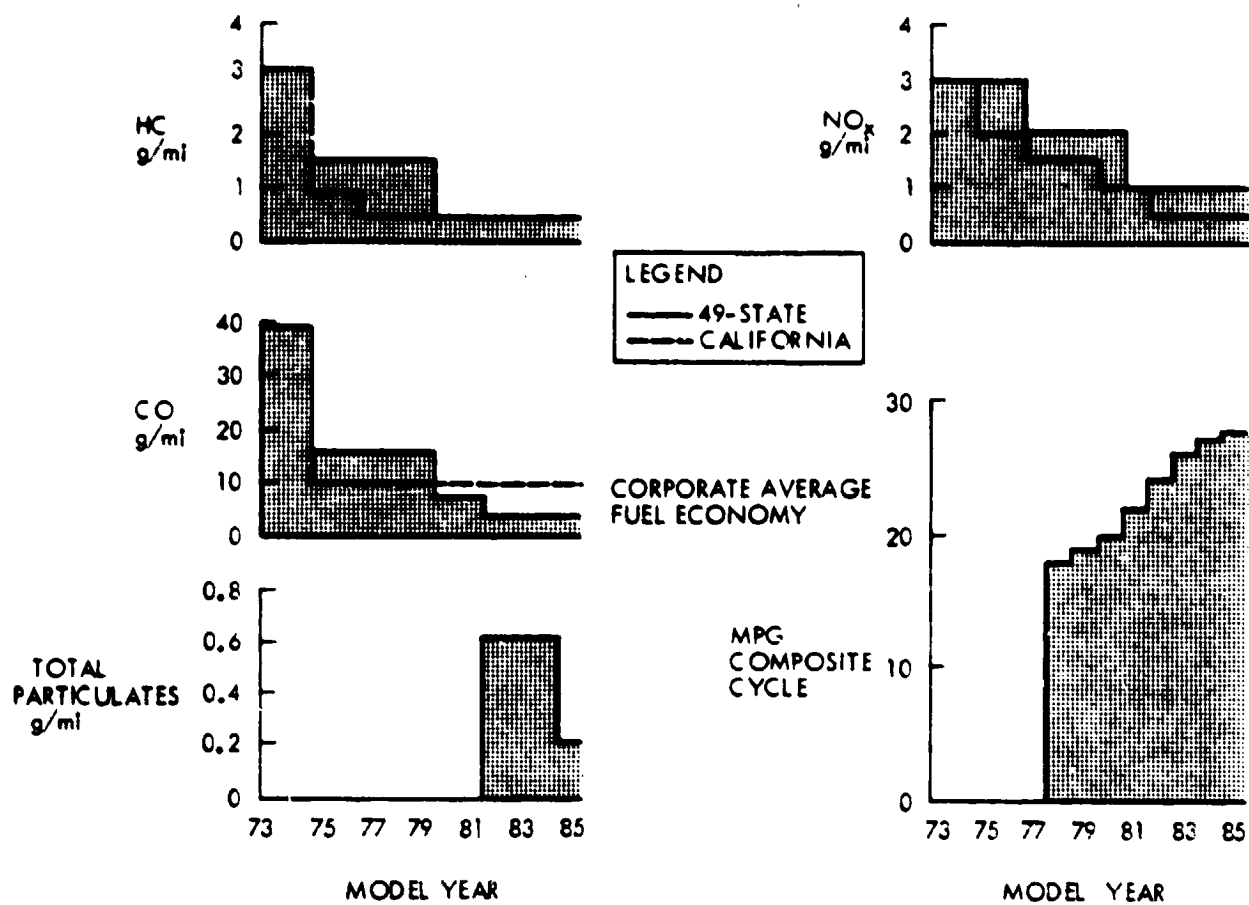


Figure 1-1. Exhaust Emissions and Fuel Economy Regulations

Table 1-1. Exhaust Emissions Standards For Light-Duty Vehicles

Year	Emission Standards, g/mi					
	California			Other 49 States and Federal		
	HC	CO	NO _x	HC	CO	NO _x
1973 ⁽¹⁾	3.2	39.0	3.0	3.2	39.0	3.0
1974 ⁽¹⁾	3.2	39.0	3.0	3.2	29.0	3.0
1975 ⁽²⁾	0.9	9.0	2.0	1.5	15.0	3.0
1976	0.9	9.0	2.0	1.5	15.0	3.0
1977	0.4	9.0	1.5	1.5	15.0	2.0
1978	0.4	9.0	1.5	1.5	15.0	2.0
1979	0.4	9.0	1.5	1.5	15.0	2.0
1980 ⁽⁸⁾	0.39 ⁽⁴⁾	9.0	1.0 ⁽⁵⁾	0.41	7.0	2.0
1981 ⁽⁷⁾	0.39	3.4 ^(7.0)	1.0 ^(0.7)	0.41	3.4 ⁽⁶⁾	1.0 ⁽³⁾
1982 ⁽⁷⁾	0.39	7.0 ^(7.0)	0.4 ^(0.7)	0.41	3.4	1.0
1983	0.39	7.0	0.4	0.41	3.4	1.0
1984	0.39	7.0	0.4	0.41	3.4	1.0
1985	0.39	7.0	0.4	0.41	3.4	1.0

- (1) 1972 CVS-C test procedures used for 1973-74.
- (2) 1975 CVS-CH test procedure used for 1975 and beyond.
- (3) EPA has granted waivers for some diesel models permitting NO_x emissions up to 1.5 g/mi.
- (4) Standard based on non-methane hydrocarbon emissions.
- (5) CARB has granted waiver for some diesel models while requiring 100,000 mile warranty on emission control systems.
- (6) EPA has granted waivers for some models permitting CO emissions up to 7.0 g/mi.
- (7) CARB has given manufacturers two options for certification of NO_x and CO levels in 81-82 model years.
- (8) CARB introduced "anti-tampering" regulation requiring that idle mixture adjustment be made inaccessible to owner. Also, reduced allowable maintenance on certification durability vehicle.

HC and NO_x have been reduced to 0.39 g/mi and 1.0 g/mi respectively, with the CO requirement remaining at 9.0 g/mi. The 49-state HC standard is based on a measurement of total hydrocarbon emissions, whereas the California HC standard is based on the nonmethane hydrocarbon emissions. Because typically about 50 percent of the hydrocarbon emissions are methane, the 49-state standard is actually more stringent than the California standard. Many diesel models have had difficulty in certifying to the California NO_x standard (1.0 g/mi). As a result, the California Air Resources Board (CARB) granted waivers for some diesel models by permitting certification to the 2.0 g/mi NO_x level but requiring a 100,000 mile warranty on the emission control systems. CARB also introduced an "anti-tampering" regulation requiring that the idle mixture adjustment on 1980 models be made inaccessible to the owner. In addition, the allowable maintenance on certification durability vehicles was reduced for 1980, as shown in Table 1-2.

For the 1981 model year, the 49-state standards for CO and NO_x are being reduced to 3.4 g/mi and 1.0 g/mi respectively, with the HC requirement staying at 0.41 g/mi. Already, EPA has granted waivers for some diesel models, permitting certification to NO_x levels up to 1.5 g/mi (level depends on vehicle). Also, some gasoline models have been granted waivers permitting certification to CO levels of 7.0 g/mi. In California, vehicle manufacturers may choose between two NO_x options for certification of 1981-82 models. They can either (1) remain at the 1.0 g/mi NO_x level and meet the 3.4 g/mi Federal CO standard in 1981, then meet the 7.0 g/mi CO and 0.4 g/mi NO_x standards in 1982 or (2) meet 0.7 g/mi NO_x and 7.0 g/mi CO in 1981 and 1982, and postpone the 0.4 g/mi NO_x standard until 1983.

During the last two years, exhaust particulate standards have been proposed for light duty diesel vehicles, as some preliminary data indicate that diesel particulates are mutagenic and may be carcinogenic. The proposed standards regulate total mass of particulate matter emitted from the vehicle and require meeting 0.6 g/mi in the 1982 model year and 0.2 g/mi in the 1985 model year. Originally, these standards were to be implemented in the 1981 model year (0.6 g/mi) and the 1983 model year (0.2 g/mi); however, current diesel engine technology would not permit that schedule. Although there is as yet no legislation, an increasing interest is also being shown in pollutants such as sulfur dioxide, sulfates, polynuclear aromatics, cyanides, etc.

In addition to the emissions regulations, fuel economy improvement is required in future model years according to the schedule shown in Table 1-3. The requirement for the 1980 model year is 20 mpg over the composite cycle for the corporate average fuel economy (CAFE) for each automobile manufacturer. This mileage increases by 2 mpg for 1981 models and continues to increase each year, reaching 27.5 mpg for 1985 models. Earlier, automobile manufacturers felt this fuel economy time-table could not be met, but recent market trends toward smaller vehicles and diesel-powered vehicles has made this requirement seem feasible. In fact, GM President, Elliott M. Estes, recently predicted that by 1985 the company's CAFE will reach a minimum of 31 mpg. The National Highway Traffic Safety Administration (NHTSA) is currently studying automotive technology trends to form a sound basis for possibly setting higher fuel economy standards for model years beyond 1985.

Table 1-2. Summary of Allowable Maintenance on Certification Durability Vehicle

(Reference 1)

Item	EPA Interval (miles)	California Interval (miles)
Drive Belts	12,500	30,000
Valve Lash	12,500	15,000
Spark Plugs	12,500	30,000
Fuel and Air Filter	12,500	30,000
O ₂ Sensor	(a)	30,000
Choke Service	12,500	30,000
Break-in Maintenance	<5,000	<5,000
Idle Mixture and Speed	12,500	not allowed
Inlet Air and Exhaust Valves	12,500	not allowed
Bolt Torque	12,500	not allowed
PCV System	12,500	not allowed
EGR System	(b)	not allowed
Catalyst	(c)	not allowed
Ignition System	12,500	not allowed

(a) Not listed, but manufacturers can request additional scheduled maintenance of emissions related parts.

(b) Up to 3 times in 50,000 miles with audible signal.

(c) Once in 50,000 miles.

Table 1-3. Fuel Economy Standards for Light-Duty Vehicles

Year	CORPORATE AVERAGE FUEL ECONOMY mpg (1)
1978	18
1979	19
1980	20
1981	22
1982	24
1983	26
1984	27
1985	27.5
(1) Composite - 55% urban cycle, 45% highway cycle	

1.3 MARKET EFFECTS

One of the most difficult jobs for automobile manufacturers is to accurately predict what kind of products the buying public will want in the future. This is especially critical for the automotive industry where tooling investment is high and product lines cannot change rapidly. During the Arab oil embargo in 1973, the American public did show a switch to buying smaller automobiles; however, the switch was temporary and large automobiles soon regained strength in the marketplace. Recently, as the result of a new fuel shortage and drastically higher fuel prices, buying trends have again switched to the smaller automobiles. In this case, indications are that the switch is more permanent than before. The reduced demand for large American automobiles has been drastic and shows no sign of recovery. Continued escalation of fuel prices and high inflation rates also oppose any recovery.

1.4 INDUSTRY TRENDS

Throughout much of the last two decades, many of the significant changes in automobiles produced by the American automotive industry have been in response to government regulations in the areas of safety, exhaust emissions, and fuel economy. Early attempts to meet the exhaust emissions standards resulted in sizeable fuel economy penalties. The development of three-way catalyst emissions control systems has enabled the industry to recover most of this fuel economy penalty. To help meet the fuel economy standards starting with the 1978 model year, vehicle weight reduction programs were used and some models were downsized. The added impetus of another fuel shortage, greatly increased fuel cost, changing consumer buying trends, and heightened competition from foreign imports has accelerated this trend toward smaller, lighter-weight automobiles.

Most automobiles in use today are powered by uniform-charge, spark-ignited, internal combustion engines (UC Otto) based on the Otto cycle and using gasoline as a fuel. As new fuel economy and exhaust emissions demands have been placed on the automobile, the tremendous economic investments in the UC Otto engine have led the automotive industry to attempt meeting these demands with add-on devices, rather than introducing alternative engine systems. As a result of the need to improve vehicle fuel economy, several manufacturers have added diesel engines as standard or optional equipment in their passenger cars. Developments have continued on both the pre-chamber and direct injection versions of the stratified charge Otto (SC Otto) engines, although only one SC Otto engine is currently in production. Rotary engine development work is continuing in both the UC Otto and SC Otto versions; however, only one rotary engine is currently being produced. Turbocharging is being used in production UC Otto and diesel engines to increase their vehicle performance. The Department of Energy (DOE) has significant programs aimed at the development of advanced alternative engine systems (Brayton and Stirling) for future automotive applications.

This report will concentrate on the current state of automotive technology related to the UC Otto and SC Otto engines.

SECTION 2

UNIFORM CHARGE ENGINES WITH THREE-WAY CATALYST EMISSION CONTROL SYSTEMS

2.1 INTRODUCTION

Since the introduction of the automobile, the predominant powerplant for automobiles has been the uniform-charge, spark-ignited, internal combustion engine (UC Otto) based on the Otto cycle. Although many alternative powerplants have been evaluated in the past and continue to be studied today, the UC Otto engine continues to power most automobiles produced. In spite of the new fuel economy and exhaust emissions demands which have been placed on the automobile, the large investments in the UC Otto engine have led automotive manufacturers to attempt meeting these demands with add-on devices. Early emissions control approaches (e.g., retarded spark timing, exhaust gas recirculation, manifold reactors, etc.) led to significant fuel economy penalties as engines were tuned to meet more stringent emissions standards. A significant advance in emissions control was achieved with the introduction of oxidation catalysts to remove unburned hydrocarbons (HC) and carbon monoxide (CO) from the exhaust. A major breakthrough in controlling nitrogen oxide (NO_x) emissions in UC Otto engines without severe fuel economy penalties came with the development of the three-way catalyst emissions control systems.

The first vehicle introduced in the United States with a three-way catalyst emissions control system was the 1977 Volvo (Model B21) which was certified in California. Although the emissions of the Volvo vehicle were low (0.2 g/mi HC, 2.8 g/mi CO, 0.17 g/mi NO_x), the most stringent proposed standards (0.41 g/mi HC, 3.4 g/mi CO, 0.4 g/mi NO_x) were not satisfied, because some individual test points exceeded the CO and NO_x emissions levels (Ref. 2). As emissions levels became more difficult to meet, the success of the Volvo system led other manufacturers to introduce variations of the three-way catalyst emissions control system on their automobiles. In fact, during the 1980 model year, most California automobiles used some form of three-way catalyst system for emissions control. It is expected that most 1981 automobiles produced for the other 49 states will also use three-way catalyst systems to meet the 1.0 g/mi NO_x standard. The remainder of this section of the report will discuss three-way catalyst systems.

Efficient three-way catalyst performance requires precise control of air-fuel ratio. This is evident in Figure 2-1, which shows the variation of HC, CO and NO_x emissions as a function of inlet air-fuel ratio. The solid lines represent the emissions at the converter inlet and the dotted lines represent converter outlet emissions. Effective conversion of all three pollutants is achieved only within a very narrow air-fuel ratio band around stoichiometric. Present carburetors and even fuel injection systems, which can control air-fuel ratio to about 3 percent, fall short of the required air-fuel ratio control when operation is based on system calibration (open-loop control) (Ref. 3). To achieve the required accuracy and speed of response in mixture preparation under continuous transient engine operating conditions, it is necessary to introduce a feedback control loop into the system (closed-

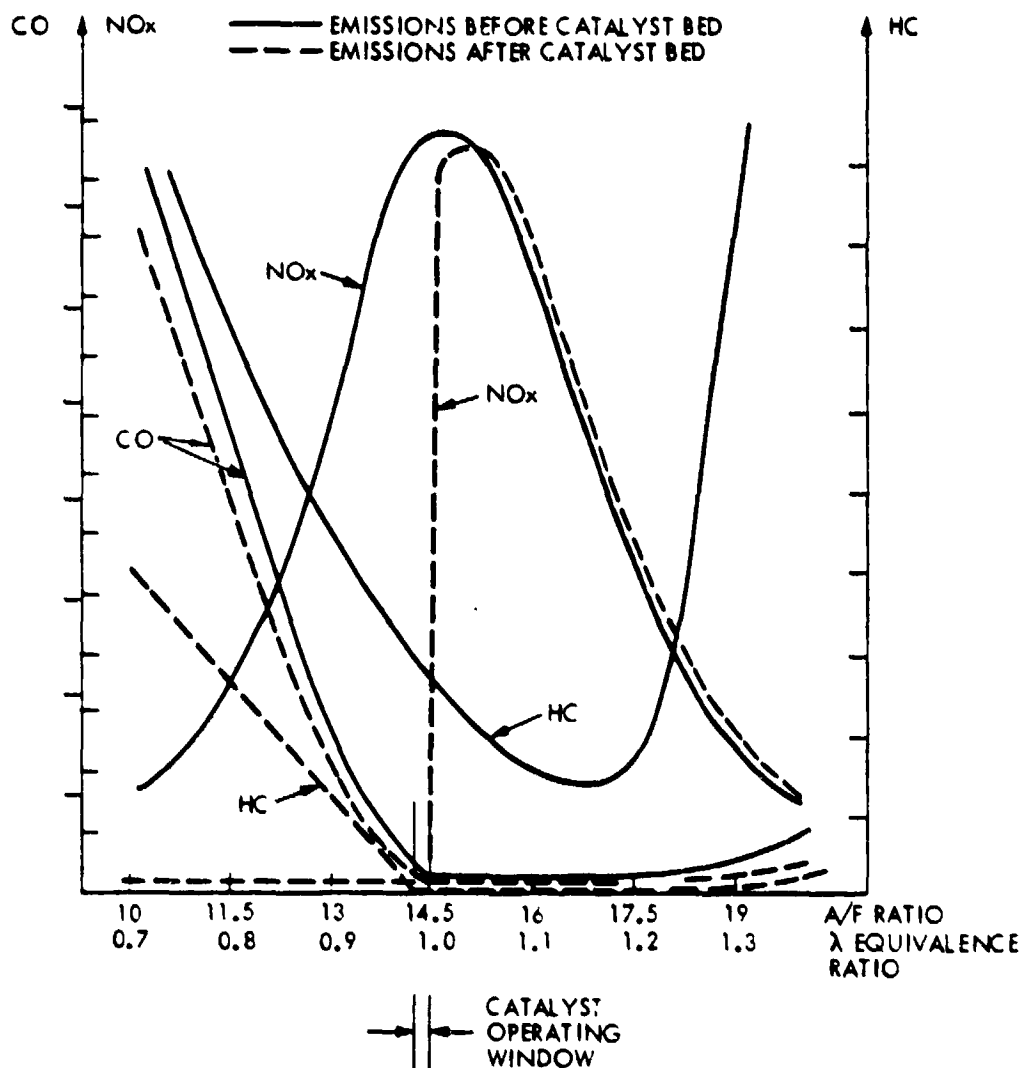


Figure 2-1. Variation of Exhaust Emissions as a Function of Air-Fuel (A/F) Ratio (Ref. 3)

loop control). The typical mechanization for a three-way catalyst, closed-loop system is shown in Figure 2-2. Major elements of the system are the three-way catalyst, oxygen sensor, electronic control unit, and fuel-metering system. The oxygen sensor, located upstream of the three-way catalyst unit, detects the instantaneous partial pressure of oxygen in the exhaust gas which gives an indication of whether the inlet air-fuel ratio is rich or lean of stoichiometric. The sensor output signal, shown in Figure 2-3, is continuous and nonlinear and shows an almost step change in signal as the exhaust gas composition moves either rich or lean of stoichiometric. The signal from the oxygen sensor is used by the electronic control unit (ECU) to control its output signal which drives the fuel metering actuator to accurately maintain the engine air-fuel ratio at stoichiometric conditions.

The ECU contains the electronics necessary to achieve the control algorithm needed for the required air-fuel ratio control. The control algorithm can range from simple proportional or integral control laws to more complex control schemes which compensate for engine speed, temperature, load, altitude, or any other factors that may influence driveability. Depending on the complexity of the control algorithm, the input signals to the ECU may be only the oxygen sensor output signal, or it may include engine speed, temperature, throttle position, and air-flow rate. Fuel metering systems used in three-way catalyst emissions control systems are generally either closed-loop carburetors or fuel injection systems. To date, the closed-loop carburetors are mechanized using either metering rods, carburetor injectors, or variable venturies. Fuel injection is accomplished electronically, i.e., electronic fuel injection (EFI), or with continuous mechanical fuel injection (MFI).

2.2 COMPONENT CHARACTERISTICS AND LIMITATIONS

2.2.1 Three-Way Catalysts

A three-way catalyst (Ref. 4) selectively promotes certain chemical reactions in the exhaust gas from an engine to simultaneously lower unburned hydrocarbons (HC), carbon monoxide (CO), and nitrogen oxides (NO_x) without creating new pollutants. The exhaust gas composition coming from the engine is a mixture of H_2O , H_2 , CO_2 , HC, O_2 , NO_x and SO_2 , in varying amounts, depending on fuel composition and air-fuel ratio relative to a stoichiometric mixture. With this exhaust gas mixture, various reactions can take place on a catalyst. In steady-state operation, the products resulting from the interaction of a gaseous mixture with a catalyst depend on gas composition, catalyst composition, temperature, and residence time of the gas within the catalyst bed. Although many transition metals, both base and noble metals, have been shown to be active in converting various components of exhaust gases under certain conditions, relatively few are active and/or durable enough to meet the demanding rate requirement over the range of gas compositions present in exhaust gases. This is a result of competing reactions which take place within the range of temperatures and space velocities present

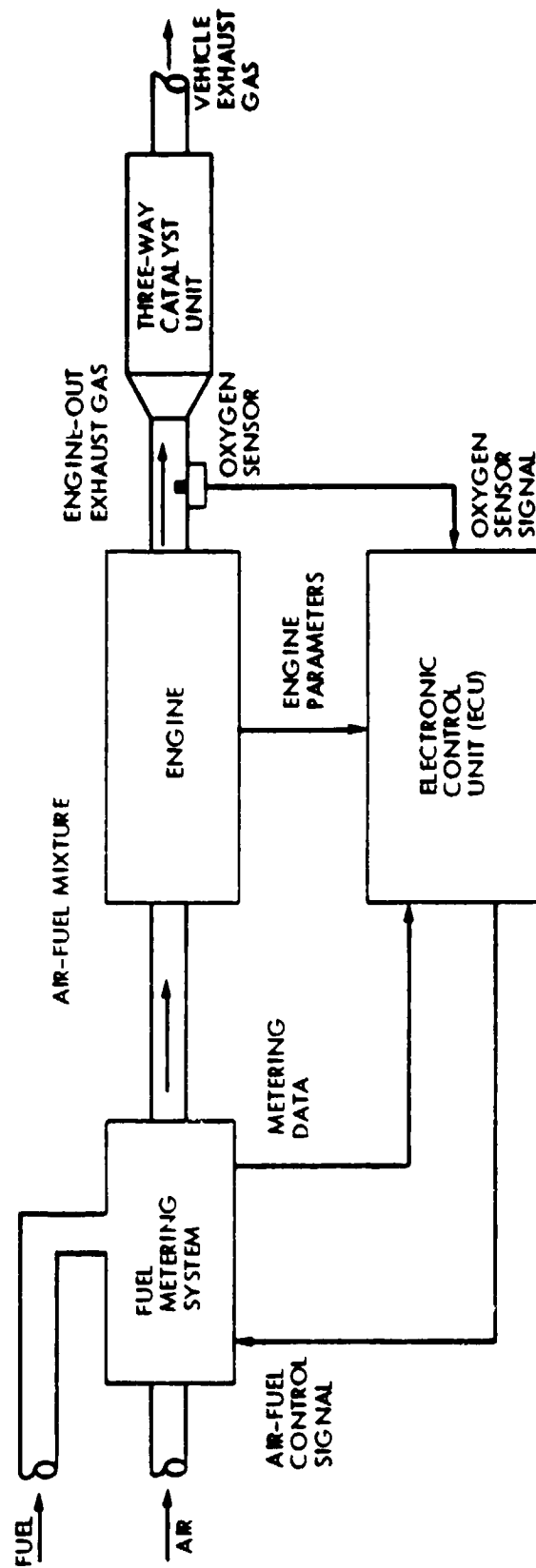


Figure 2-2. Typical Three-Way Catalyst Emissions Control System

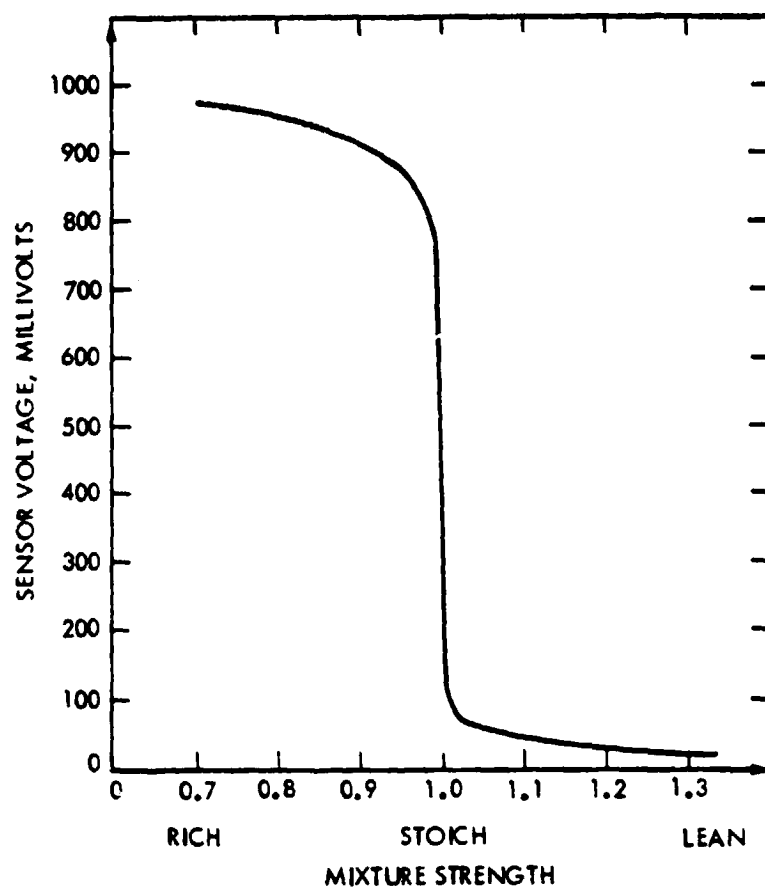
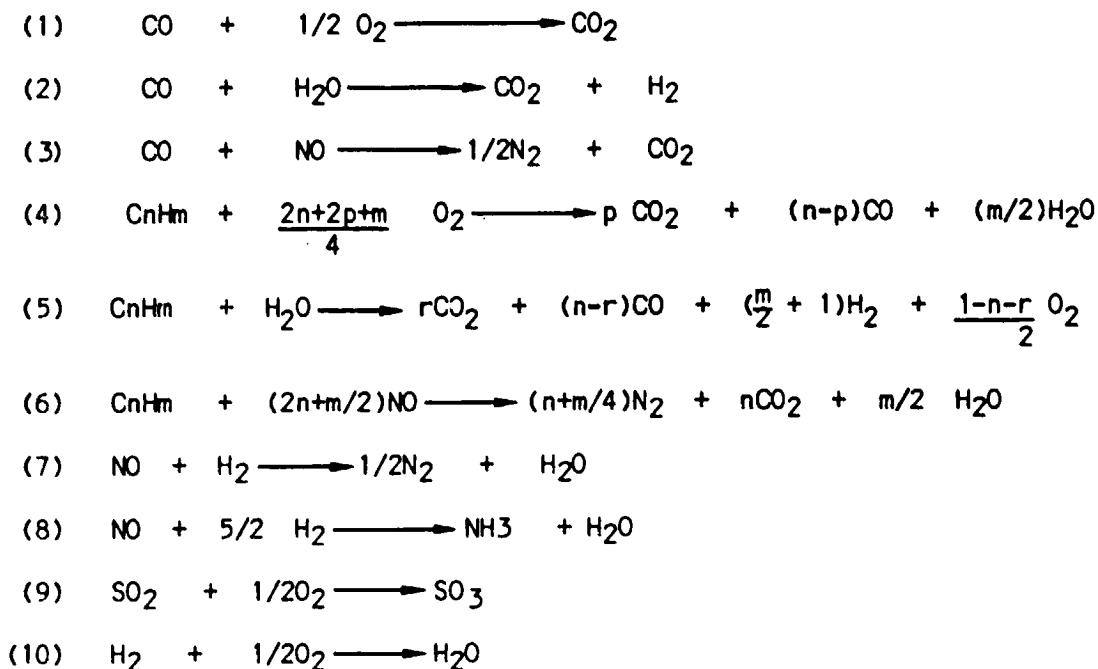


Figure 2-3. ZrO₂ Sensor Output as a Function Inlet Mixture (Ref. 3)

in engine exhausts. Competing reactions which can take place at various rates within three-way catalyst beds are as follows:



The air-fuel ratio ranges in which some of these reactions are important are shown in Figure 2-4.

Various catalysts enhance the rates of different reactions under steady conditions. However, even with some control on engine operation (i.e., closed-loop feedback) the exhaust gas composition variation alters the rates appreciably, (particularly the reduction of NO_2) as the oxygen content increases with lean operation. Ideally, a three-way catalyst would selectively promote reactions 1, 2, 4, and 5 when the engine is operating rich, and specifically enhance 3, 6, 7, 8, 9, 10 during lean engine operation, while keeping reactions 8 and 9 consistently low. At relatively low temperatures (300-1500°F) certain transition metals are more capable of enhancing some of the desired reactions under the varying gas composition of exhaust gases.

In addition to the role of the transition metal as catalyst, the thermal environment in which the metal is held is also important. Advances are still being made in maintaining and aiding the catalytic activity of the transition metals under hydrothermal conditions. Preparation of a material which will retain maximum pore size and density and hinder sintering and crystallite growth of the catalyst (which reduce catalyst activity) under the specific conditions encountered in the automotive application has constituted a major effort. In monoliths, a washcoat material applied over the commonly used cordierite support probably aids the catalytic processes when the system is hot, when some reaction rates become mass-transfer limited and are not controlled by chemical kinetics. In addition to maintaining their

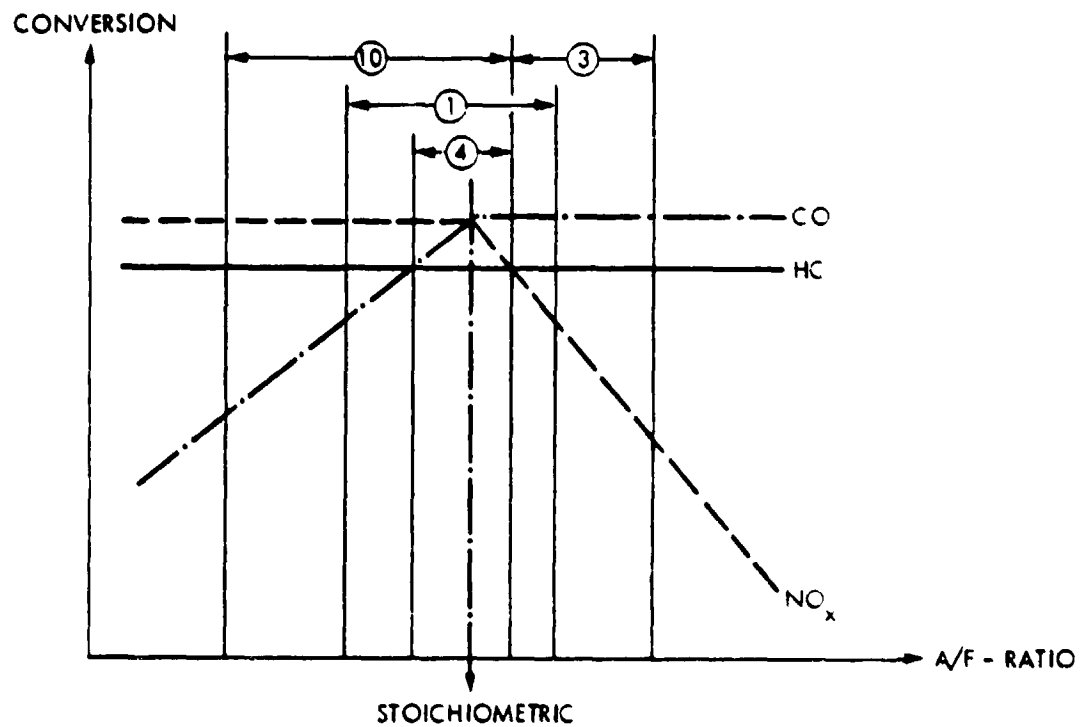
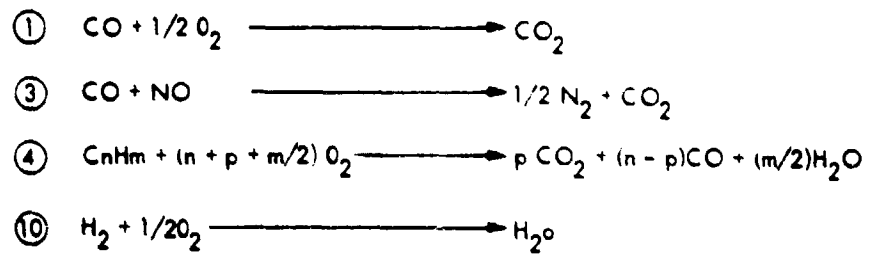


Figure 2-4. Air-Fuel (A/F) Ratio Effect on Reactions Within a Three-Way Catalyst (Ref. 5)

structural integrity, catalyst surface-supporting materials (stabilized gamma alumina appears to be superior) through special preparative procedure can be made to hold catalysts in such a way that interactions between active sites as well as with poisons are reduced. This helps prolong catalyst life and permits a reduction in the total catalyst loading needed to meet the durability standards (i.e., 50,000 miles). The support surface must, however, provide the active metal sites with enough exposure to exhaust gases to promote high activity at low temperatures, a condition necessary to maintain good carbon monoxide and hydrocarbon conversion (reactions 1, 2, 4, 5) during cold start operation of the engine.

Another factor which is important in extending the three-way catalyst operating range into the lean air-fuel ratio regime is the interference effect of excess oxygen on the carefully balanced rates of the interdependent reactions. If reactions 1, 4, and 10 become dominant in the oxidizing environment, NO_x reduction will not take place at a fast enough rate, if at all, resulting in inadequate NO_x control. To offset this, the engine could theoretically be constrained to run at stoichiometric or slightly rich conditions. An alternative means of reducing the oxygen content in the gas stream passing through the catalyst bed is to incorporate an oxygen getter into the catalyst bed. This could theoretically be accomplished by oxygen absorption into the support itself or by using an additional element or compound capable of being both oxidized and reduced when the air-fuel ratio changes from lean to rich. Whichever means is used, the need to respond rapidly under both oxidizing and reducing conditions and also the need to have sufficient capacity to compensate for large excursions is very critical. In addition, any added material must not hinder catalytic activity or react with the support and thereby reduce the effectiveness and durability of the catalyst. The utility of oxygen storage is not only necessary to extend the operating range into the lean side of stoichiometry, but also for supplying oxygen to permit reactions 1 and 4 to oxidize excess carbon monoxide and hydrocarbons generated during excursions into the rich region. Because of the catalyst size and relative rates and capacities of oxygen storage, rich or lean excursions must not be of long duration.

Among the transition metal possibilities for oxygen storage, perhaps the prime contender is rhenium oxide. The reasons for this are its rates of oxidation and reduction and its inertness relative to the alumina support and to sulfur poisoning. Rhenium availability does not appear to pose a problem but other candidates are also under investigation. The use of perovskites as three-way catalysts incorporates a built-in oxygen storage system. This results from the crystal structure participating in the oxidation reactions 1, 4, and 10. Excess oxygen would subsequently react with the oxygen vacancies in the lattice. Little data is available regarding the oxygen storage aspect of perovskites.

Although numerous transition metals catalyze the reactions previously listed, activity, susceptibility to poisoning by reactants, and non-reactivity toward the support are the three most important criteria which define the particular transition metals technically most desirable for a three-way catalyst. Of course, cost, availability, and safety enter into the actual catalyst selection. Activity is a term which refers basically to the activation energy which a particular transition metal must possess to

be catalytically active for a given reaction. Temperature is in fact the critical point here, because the lower the temperature of the gas stream at which a catalyst becomes efficiently active, the sooner the catalyst will become effective in reducing the level of pollutant from the exhaust. Although most catalysts become more comparable in their activity at higher temperatures, in general the noble metals, i.e., ruthenium, osmium, rhodium, iridium, palladium, and platinum, reach activity at lower temperatures, meaning they require a lower activation energy to perform catalytically. Because of this important point, noble metals have been the first choice for three-way catalysts. Another contributing factor is the relative inertness of noble metals for reacting with the retaining material, gamma alumina. Nickel and cobalt, two fairly active base metal catalysts, will react with alumina at high temperatures to form spinels (metal aluminates) which have relatively poor catalytic activity.

The three catalyst systems which have demonstrated the greatest potential for simultaneous control of HC, CO, and NO_x are platinum-rhodium (Pt-Rh), platinum-ruthenium (Pt-Ru), and various perovskites. While each system has certain advantages and disadvantages, the Pt-Rh catalyst combination has been shown to relate best to the oxidation catalyst expertise developed for automobiles and has therefore become the most widely accepted system at this time.

As stated earlier, a three-way catalyst must be able to activate a combination of reactions simultaneously at rates commensurate with the range of exhaust gas compositions, space velocities, and temperatures encountered in automotive exhausts. The Pt-Rh combination supported on washcoated monoliths or on pellets has been able to achieve this control over a narrow range of air-fuel ratios. The Pt is primarily responsible for maintaining high reaction rates for oxidation reactions 1 and 4, while Rh maintains a relatively high rate for reactions 3 and 7 with moderate selectivity of 7 over 8 in this air-fuel ratio range. Separate tests have shown that Rh is also very active in promoting reaction 5 and that Pt may contribute slightly to enhancing reaction 2. Other proprietary components may be included in the catalyst formulation but are not delineated here. The purpose of these added components would be to help speed the rates of reactions 2 and 5 as well as to store oxygen for aiding the Rh activity by oxygen uptake on the lean side and for aiding the Pt activity by oxygen release on the rich side.

Perhaps the greatest disadvantage of the Pt-Rh combination is the amount of Rh necessary to meet the most stringent emissions standards (0.41 g/mi HC, 3.4 g/mi CO, 0.4 g/mi NO_x) versus the amount available from free-world mines. The most durable Pt-Rh catalysts used in vehicle tests are those containing 3/1 to 7/1 Pt/Rh ratios with total loadings in the range of 0.08 to 0.095 troy ounces. The present total loading of noble metals (Pt and Pd) in oxidation catalysts is approximately 0.05 troy ounces/vehicle. A serious problem is apparent when the Pt-Rh ratios of 3/1 to 7/1 are compared to mine ratios of approximately 19/1. If it is necessary to equip more than a small percentage of all new vehicles with three-way catalysts, this Pt-Rh ratio must be increased or a substitute for a complement to Rh must be found and implemented.

The primary reason for the low Pt-Rh ratio on vehicles is the durability (i.e., 50,000 miles) performance which is required to meet the emissions standard. Although catalysts with Pt-Rh ratios of 19/1 have performed well while fresh, the NO_x conversion activity cannot be adequately maintained. This reduction in activity appears to be due to (1) sintering of the surface on which the catalyst is held, (2) poisoning from fuel additives, and (3) a Pt-Rh interaction (metal crystallite sintering). The Pt-Rh interaction is of particular concern because it is a problem which was not present in oxidation catalysts. Reports on Pt-Rh catalysts show that after exposure to hot oxidizing conditions, the Rh migrates to the surface of the Pt-Rh crystallites and is subsequently oxidized, thereby decreasing its activity to reduce NO_x . One method of solving this interaction problem is to separate the Pt and Rh by preparing different monolith segments for each noble metal or different pellets for each noble metal before mixing the pellets in the catalyst bed. The former "split-bed" approach has shown substantial improvement in catalyst activity. The alternative, of course, is to "fix" or bond the Pt and Rh in a superior way to the surface of the same catalyst bed.

Additional progress needs to be made in the CO conversion of the Pt-Rh system. Because of the location of the "window" in which NO reduction is not greatly inhibited by the oxygen content, the CO becomes a major problem. In Figure 2-5 the relative amounts of H_2 , CO, and CO_2 are shown for various air-fuel ratios. The level of CO at stoichiometry (air-fuel ratio ~14.5) and slightly richer without oxygen (or very little oxygen) requires a very rapid release of adequate quantities of oxygen from an oxygen storage component or a very active catalyst for reaction 2 above.

Early investigations for selective catalysts which would convert NO to N_2 with little conversion to NH_3 in rich conditions indicated ruthenium (Ru) to be the best choice. Ru was also observed to be active at a lower temperature (~100°C lower) than Rh. However, Ru undergoes oxidation to the volatile tetroxide under lean air-fuel ratios, which creates a health hazard in addition to a loss of NO conversion activity. A Pt-stabilized Ru catalyst could provide a viable alternative to the Pt-Rh catalyst; however, as yet all efforts to stabilize Ru such that virtually no RuO_4 would be lost have not succeeded. The market availability of Ru appears to be roughly twice that of Rh.

The use of perovskites for three-way catalysts has been attempted. Perovskites are commonly oxides of the lanthanide and transition metals having a cubic crystalline structure known as the perovskite structure. The solid-state properties of the compounds have been shown to be important in the reduction of NO via both molecular and dissociative chemisorption of NO on the surface. Oxidation of CO and HC are assumed to take place on the surface through reaction with lattice oxygen atoms. However, recent suggestions indicate that Pt on the perovskite surfaces, not in the lattice, are the primary oxidation sites. Considerably more work is needed to prove the merit of perovskites as three-way catalysts, although the wide variety of transition metal formulations and solid-state data indicate some potential exists.

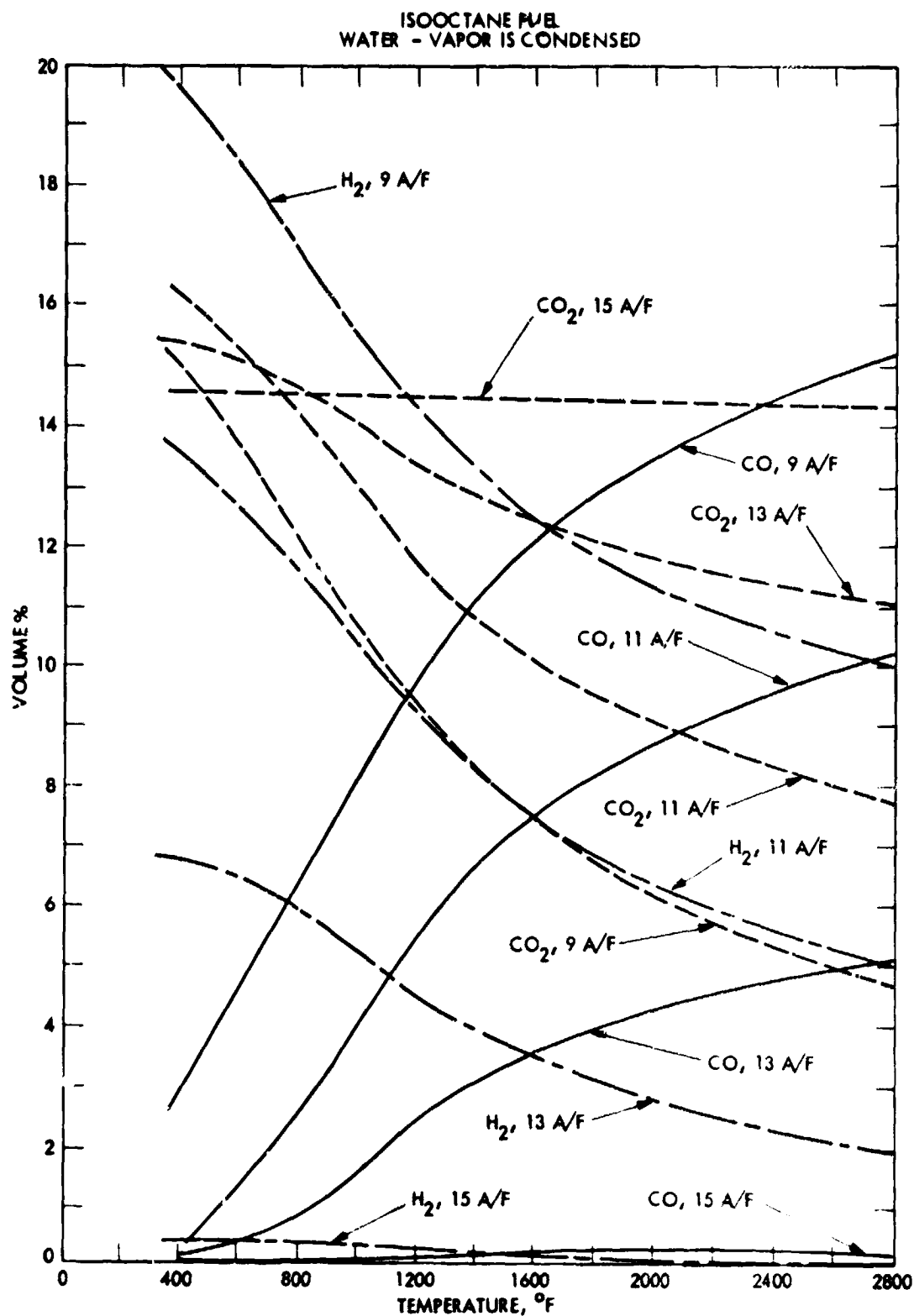


Figure 2-5. Amounts of H_2 , CO and CO_2 for Various Air-Fuel Ratios (Ref. 5)

Perhaps one of the most important contributors to the three-way catalyst activity in a vehicle is the control system. Most three-way catalyst vehicles have closed-loop feedback control. By rapidly modulating (1 Hz) the air-fuel ratio (± 1 air-fuel ratio unit) of the mixture supplied to the engine, the resulting exhaust gases also fluctuate between rich and lean conditions. This oscillation has been shown to result in widening of the operational air-fuel ratio window of the catalyst.

One of the most important reasons for the promising activity that the Pt-Rh catalyst has shown is due to the reduced level of lead and phosphorus in the fuel. Using 1975 certification fuel, three-way catalysts performed very poorly, and based on those early tests, little hope was offered for three-way catalysts to ever become a viable option. With the 1977 certification fuel, however, the Pt-Rh system has proved successful enough to be implemented on production vehicles. Comparisons of 1975 and 1977 certification fuel analyses are shown in Table 2-1. It can be seen that lead and phosphorus reduction constitutes the greatest change. All tests so far have shown that sulfur does not affect the activity of noble metals because of the instability of the sulfur products at the temperatures at which the catalysts normally operate ($> 400^{\circ}\text{C}$). With base metal catalysts, however, the operating temperatures are not high enough to prevent inactive sulfur compounds from forming, thus the catalyst is poisoned as a result. This is one of the greatest barriers to the use of base metals as substitutes for noble metals. Some test results indicate that combination base-noble metal catalysts are not as susceptible to sulfur poisoning as the base metal alone. Poison effects on perovskites are not well defined. Some work has indicated that lead and sulfur are not poisons for the Pt- and Ru-substituted catalysts.

Table 2-1. Typical Fuel Analysis

	1975 EPA Certification Fuel	1977 EPA Certification Fuel
Lead	0.03 (0.02-0.04) g/gal	0.006 (0.001-0.008) g/gal
Phosphorous	0.0027 (0.002-0.005) g/gal	0.0003 (0.0002-0.0008) g/gal
Sulfur	0.017 (0.04 Max.) g/gal	0.010 (0.04 Max.) g/gal

The removal of lead from automotive fuels has led to a search for a suitable antiknock agent to replace lead. Methylcyclopentadienyl manganese tricarbonyl (MMT) has been identified as the most logical choice; however, questions remain unanswered concerning its effect on three-way catalyst system performance and durability. With fuels containing MMT, manganese oxides are formed in the engine cylinder during combustion. The accumulation of manganese oxide deposits in the catalyst bed will result in increased engine backpressure and could adversely affect catalyst activity. Similar deposits on the oxygen sensor could significantly alter its operating characteristics. Fleet test results (Ref. 6) for automobiles with oxidation catalysts indicate that engine-out HC emissions increase linearly with fuel MMT content, as shown in Figure 2-6, and that MMT results in an enhancement of catalyst efficiency.

Vehicle tests with three-way catalysts indicate that neither ammonia (NH_3)ⁿ or hydrogen cyanide (HCN) constitute any health hazard as new pollutants formed by Pt-Rh catalysts. During some operations, small amounts may be formed but even gross malfunctions of the engine have not demonstrated any health hazards in EPA tests. This information is not available for other three-way catalyst systems. However, Ru has been shown to be lost from perovskite catalysts. The inclusion of Ru in perovskites is one method of stabilizing it under lean conditions. Because of the volatility and toxicity of ruthenium tetroxide, the use of Ru in perovskite catalysts is therefore still questionable.

Sulfate emissions from the Pt-Rh catalyst on various vehicles has been investigated. The use of a three-way catalyst has been shown to produce no more sulfates than a production oxidation catalyst vehicle with an air pump. A vehicle equipped with a hybrid of these two systems emits slightly higher sulfates.

The earliest successful demonstration of Pt-Rh three-way catalysts was in four-cylinder, in-line engines with fuel injection. The complications of implementing three-way catalyst systems increases greatly for larger engines with more cylinders, V-type engines, engines with less accurate fuel-metering systems, and engines with less accurate control systems. To offset these problems, other three-way catalyst systems have been developed and implemented. Dual catalyst beds containing a three-way catalyst followed by an oxidation catalyst is one approach. However, the catalysts involved are primarily the same three-way catalyst formulations discussed previously, and a conventional oxidation catalyst. These systems usually have exhaust gas recirculation (EGR) and an air pump. Another system uses a reducing catalyst with an oxidation catalyst, similar to the old "dual bed" catalyst system. A third approach, using progressive air injection, is basically a modified dual bed catalyst; the catalyst bed is divided into segments into which progressively more air is injected to compensate for the rich air-fuel ratio used in the engine. This catalyst is also comprised of Pt-Rh, being richer in Rh at the front. Both of the latter two approaches suffer by restricting engine operation to rich conditions and therefore resulting in a reduction of fuel economy.

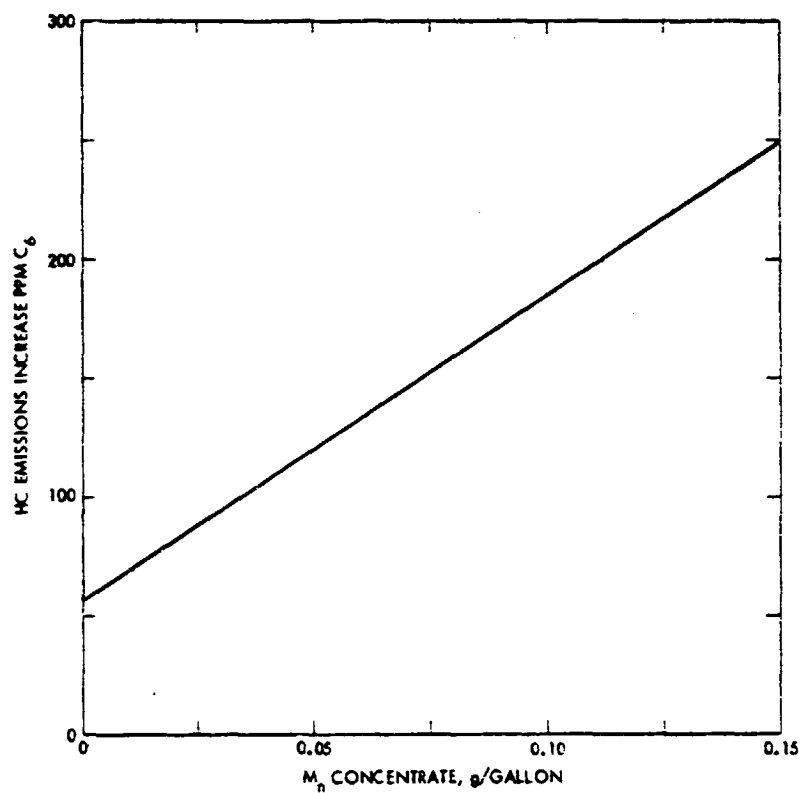


Figure 2-6. Effect of Fuel MMT Content on Engine-Out HC Emissions (Ref. 6)

The positioning of the catalyst in the exhaust system is a result of evaluating four interdependent factors; light-off temperature of the catalyst, maximum operating temperature which the catalyst can withstand, most-efficient operating range of the catalyst, and the temperature gradient of the engine exhaust. As mentioned earlier, noble metals have a light-off temperature which is lower than base metals. In order to commence and maintain a high level of activity, an ideal catalyst would light-off at a low temperature within approximately 50 to 60 seconds after engine ignition, then operate at temperatures within which the catalyst would not suffer thermal degradation. This degradation takes place through sintering (i.e., the catalyst being covered or blocked by thermal changes in the washcoat or pellet surface) and by catalyst crystallite growth. Commonly, the most active catalysts are also damaged at lower temperatures. Positioning of a catalyst in the exhaust stream, therefore, requires consideration of the activity and thermal stability of the catalyst and the characteristics of the engine (i.e., cold-start emissions, maximum exhaust gas temperature under load, and engine control about stoichiometric air-fuel ratio). It is these interacting factors which make a three-way catalyst vehicle require not only a unique three-way catalyst but also a well-integrated vehicle system.

2.2.2 Oxygen Sensor

An oxygen sensor (Refs. 7-11) provides an active signal which the electronic control unit of a closed-loop three-way catalyst control system can use to maintain engine air-fuel ratio near stoichiometric conditions. A typical oxygen sensor is shown in Figure 2-7. The thimble-shaped sensor body consists of a zirconium oxide (ZrO_2) ceramic of high mechanical strength, stabilized with yttrium (Y_2O_3). The advantages of Y_2O_3 stabilization over calcium oxide (CaO) stabilization are lower activation energy, higher conductivity, and about $100^\circ C$ lower starting temperature. The inner and outer electrodes consist of platinum (Pt) layers approximately $10\text{-}\mu$ thick. The outer electrode, which is exposed to exhaust gases, is protected against corrosion and erosion by a $100\text{-}\mu$ thick spinel coat and a slotted shield. Air makes contact with the inner electrode through holes in the protective sleeve which, along with the silicone protection cap, prevents water from contacting the ceramic body.

In operation, the oxygen sensor is mounted in or near the exhaust manifold where the outer electrode is exposed to exhaust gases and the inner electrode is exposed to ambient air. When heated by the exhaust gases, the sensor generates a galvanic potential between the two electrodes which depends on the oxygen partial pressure in the exhaust gases. The equilibrium oxygen partial pressure over an active catalyst surface in a rich exhaust is about 10^{-16} atmospheres at $800^\circ C$, giving a theoretical rich sensor voltage output of 830 Mv. Under lean conditions, the oxygen partial pressure is about 10^{-2} atmospheres at $800^\circ C$, giving a sensor output voltage of 70 Mv. This steep change in sensor voltage occurs sharply at or near the stoichiometric air-fuel ratio, providing a good voltage switch as the air-fuel ratio passes through stoichiometric conditions. This voltage switching is used as a feedback signal to the electronic control unit which controls the fuel metering system to maintain air-fuel ratios near stoichiometry.

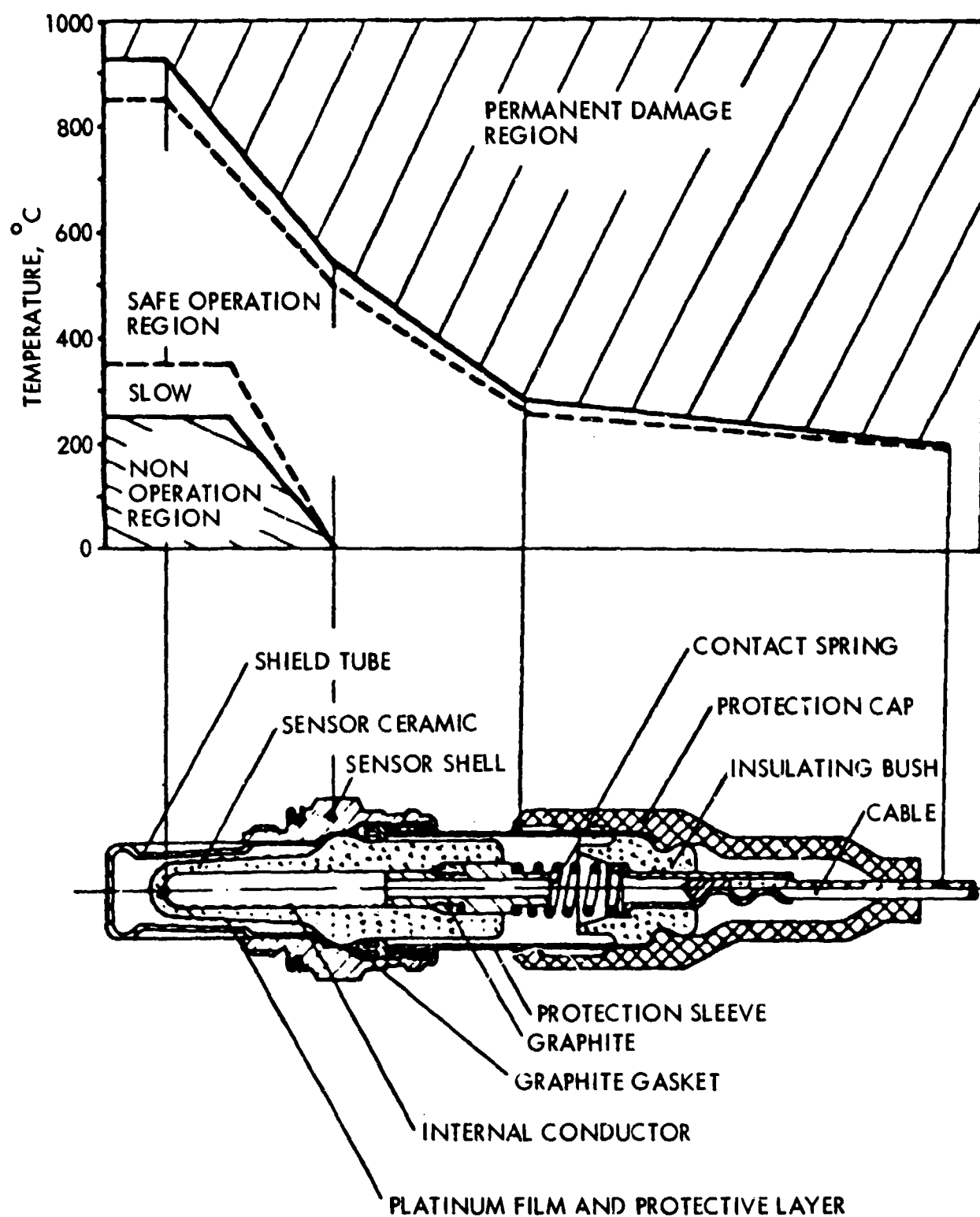


Figure 2-7. Schematic Design and Temperature Limits of Bosch Zirconia Sensor (Ref. 7)

Sensor characteristics which are desirable for effective closed-loop control of air-fuel mixtures are (1) high and stable rich voltage output with a sharp and large voltage change at the stoichiometric air-fuel ratio, (2) fast voltage switching in response to exhaust gas variation, and (3) low sensor internal resistance. A high and stable rich voltage output is necessary to ensure that the threshold voltage selected for closed-loop control is always near stoichiometry. Fast switching response is desirable for effective control of air-fuel ratio. Low internal resistance is necessary for extending the sensor operating temperature toward lower temperatures. Sensor characteristics are sensitive to many parameters including operating temperature, temperature gradients, control frequency, aging, deposits and fuel lead content. The effects of some of these parameters will be discussed in the following paragraphs.

To provide the signal needed for proper air-fuel control, the sensor must be designed and located in the exhaust system in such a way that it operates at the appropriate temperature. The recommended operating temperature ranges for a typical oxygen sensor are given in Figure 2-7. The recommended temperature for the sensor tip ranges from 350°C to 850°C; however, it can be operated up to 930°C for short periods of time. Sensor operation at high temperatures (>900°C) for long periods of time leads to splitting of the spinel protection layer and destruction of the thin-film outer electrode. The silicone protection cap has a maximum allowable temperature of about 250°C. When the temperature of the sensor is too low, the resistance of the ZrO₂ ceramic increases and the catalytic activity of the Pt electrode decreases. This leads to a reduction in sensor signal and a rapid increase in its response time. Also, sensor operation at low temperatures (300°C-500°C) leads to the formation of heavy deposits on sensor surfaces. In addition to temperature level, temperature gradients (°C/sec) must be kept below about 50°C/sec due to the limited thermal shock resistance of the ZrO₂ ceramic; however, this does not appear to be a severe limitation for automotive applications.

The response characteristics needed by the oxygen sensor are somewhat dependent on the control frequency used by the fuel metering system. With respect to control frequency, fuel injection systems used with single-bed three-way catalysts are considerably different from carburetor systems used with dual bed catalysts, air injection, and EGR. Shown in Figure 2-8 are the control frequency characteristics for two systems having similar temperature conditions at the oxygen sensor location. Over the entire engine speed range, fuel injection systems have a control frequency two or three times that of the carburetor systems. This indicates that the response speed of oxygen sensors has a much greater effect on three-way catalyst systems with fuel injection than on systems with carburetors. Thus, proper operation of three-way catalyst systems with fuel injection should be more sensitive to factors which degrade oxygen sensor response, such as deposits on sensor surfaces.

In single-bed three-way catalyst systems which require precise control of air-fuel ratio, it is important that the oxygen sensor have a well defined, precise voltage output characteristic. Static sensor voltage characteristics for both a new and aged sensor are shown versus lambda (normalized air-fuel

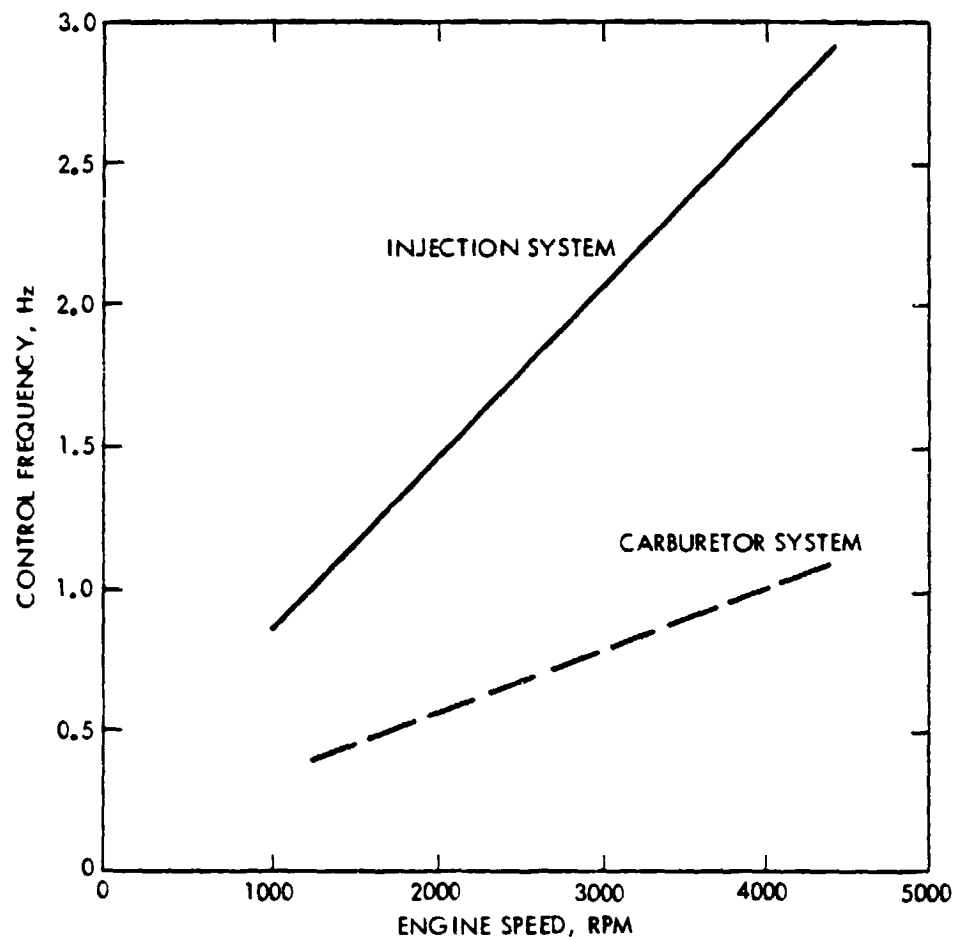


Figure 2-8. Control Frequency of New Sensor in Closed Loop Fuel Injection and Carburetor Systems with Four Cylinder Engine (Ref. 7)

ratio) in Figure 2-9. These sensor characteristics were measured using synthetic exhaust gases and slowly increasing lambda from 0.96 to about 1.05 at a scan rate of approximately 0.12 per hour. Note that for the new sensor the sharp voltage change occurs for a slightly lean air-fuel ratio. At a sensor voltage of 500 Mv, this lambda shift is typically $\Delta\lambda = 0.0055$ for new sensors ($\lambda \approx 1.0055$ at 500 Mv) at a 500°C operating temperature. The lean shift of the curve is a result of diffusion enrichment on the outer electrode resulting from the hydrogen contained in the exhaust gas. The degree of lean shift depends on hydrogen concentration in the exhaust and the pore structure of the protective coating used to prevent corrosion and abrasion of the outer electrode. For new sensors, the standard deviation of the lambda value at 500 Mv and 500°C is less than 0.0022 indicating good control during production of units. The aged sensor characteristic shows a typical rich shift of the characteristic of $\Delta\lambda = 0.0002$ at 500 Mv compared with the new sensor. This shift is due to the formation of microcracks in the protective coating caused by thermal loading imposed by vehicle operation. The catalytic activity of this normally aged sensor is only slightly less than that of a new sensor. The steepness of the characteristic curve at 500 Mv and the sensor voltage at $\lambda = 1.0$ are good indicators of the catalytic activity of the outer electrode.

Aging of oxygen sensors produces some changes in the rich and lean voltage outputs as shown in Figure 2-10. A typical characteristic for a new sensor is included for comparison purposes. The aging was accomplished in vehicles with closed-loop, three-way catalyst systems. The data show a decrease in rich voltage over the whole temperature range, particularly at temperatures below 400°C.

The switching response of new oxygen sensors is given as a function of electrolyte tip temperature in Figure 2-11. These data were taken on a propane gas burner test fixture maintained normally in a rich condition with $\lambda = 0.95$. A solenoid was used to quickly introduce air to switch the exhaust to a lean condition with $\lambda = 1.05$, and then return it to $\lambda = 0.95$ by cutting off the additional air. The response times for switching from rich to lean (R-L) operation are seen to differ significantly from the times for switching from lean to rich (L-R) operation. Both (R-L) and (L-R) response times increase gradually as the temperature is lowered from 800°C to around 350°C and increase rapidly below 350°C. For temperatures above 350°C, response time is affected by exhaust gas velocity transport time from combustion location to sensor position, and gas reaction kinetics. Below 350°C, the gas reaction kinetics over the Pt catalytic electrode are the dominant factor affecting switching response. Similar switching response curves are given in Figure 2-12 for sensors which were aged for about 50,000 miles in vehicles with closed-loop three-way catalyst systems. The results are similar to those for new sensors; however, the (L-R) response time has slowed considerably. This behavior can be explained by a possible reduction in the CO absorption affinity on the outer electrode as the sensors age.

The dynamic and static sensor voltage characteristics of both a new sensor and an aged sensor are given in Figure 2-13 for various exhaust gas change frequencies and an operating temperature of 350°C. The test data

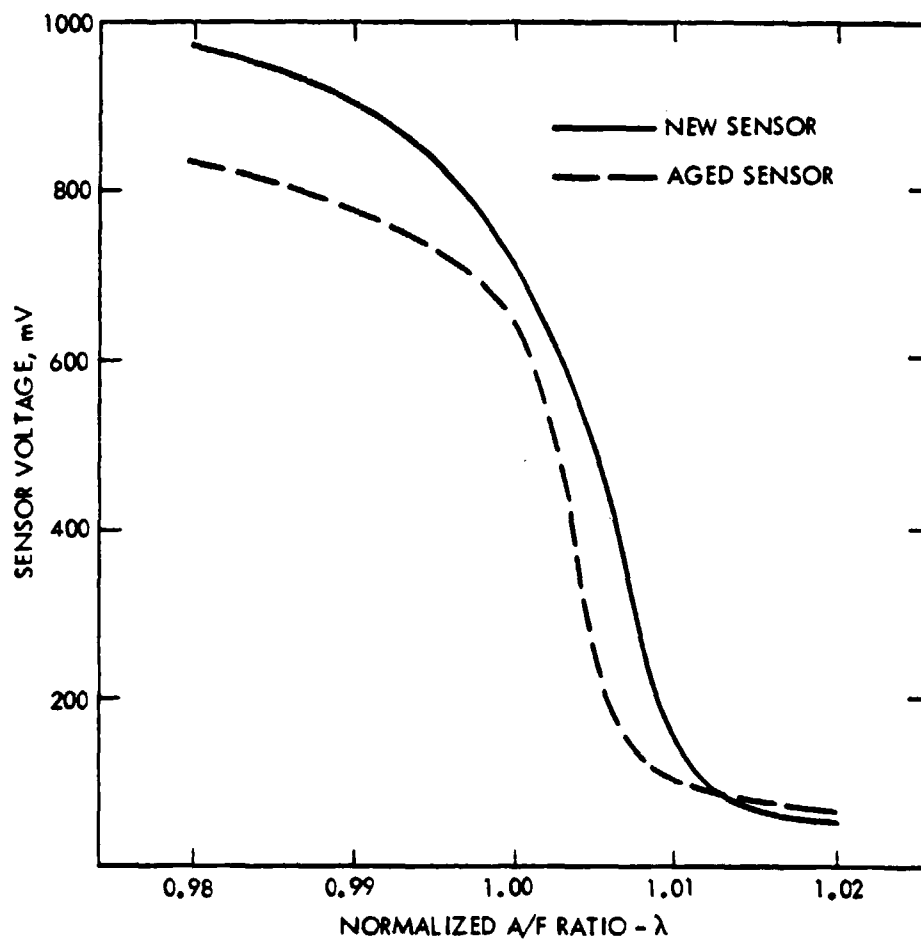


Figure 2-9. Static Lambda Characteristics at 550°C of New and Aged Sensor (48,000 km In Common Application In Medium Temperature Field) (Ref. 7)

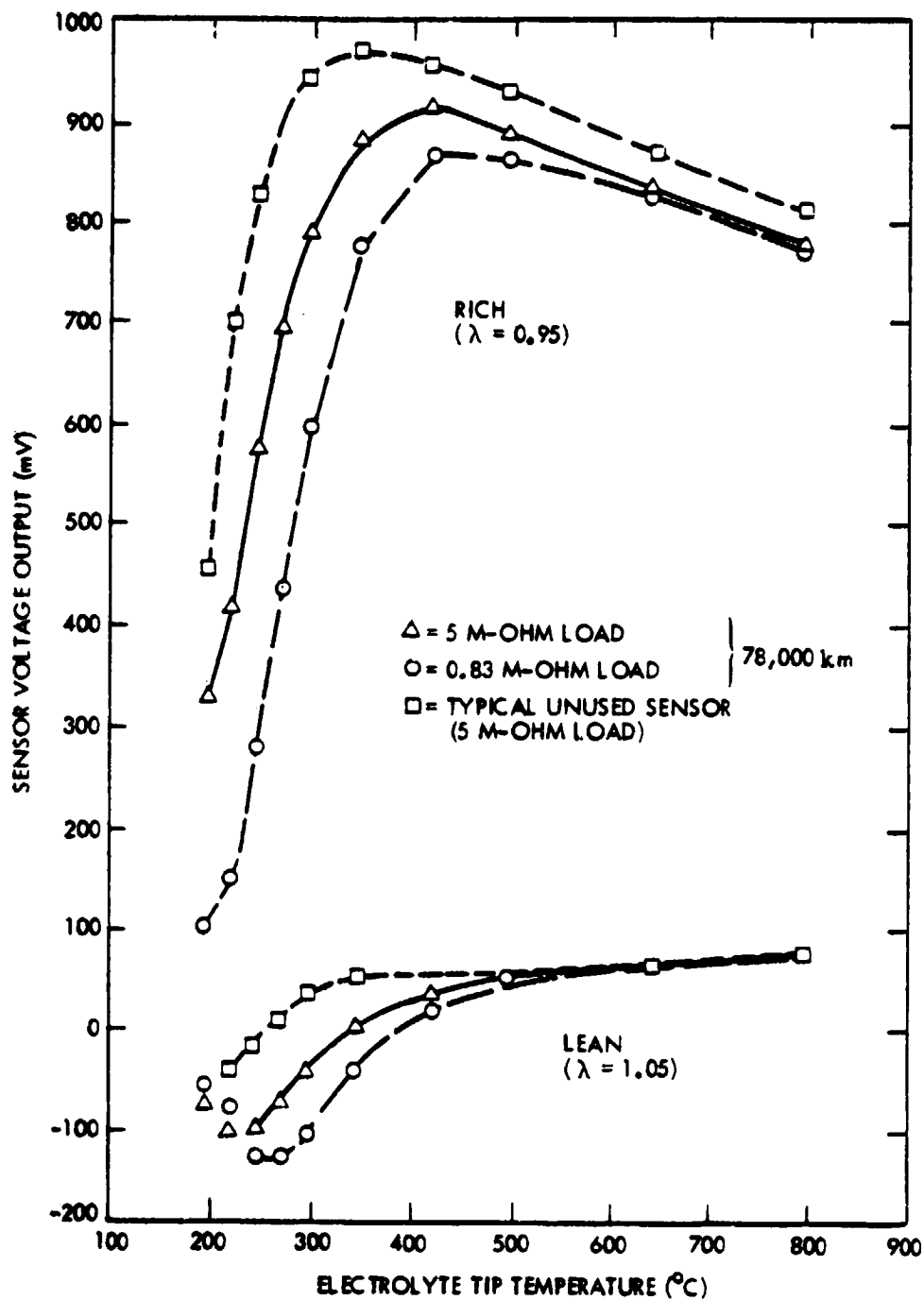


Figure 2-10. Averaged Output Voltages of Three Sensors Versus Electrolyte Tip Temperature After 78,000km Closed-Loop Vehicle Test. Typical Voltage Curves of Unused Sensors are Included for Comparison (Ref. 8)

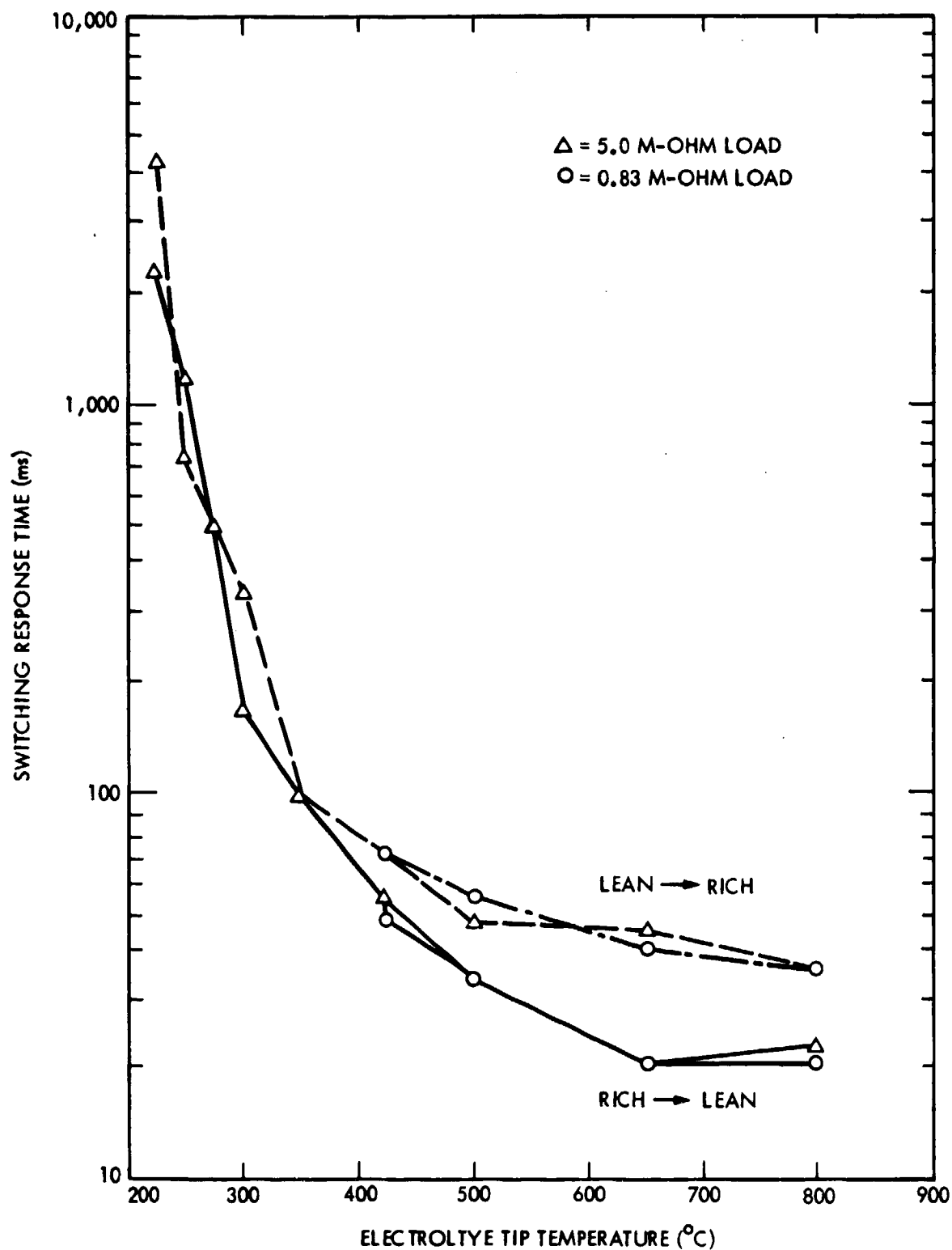


Figure 2-11. Averaged Voltage Switching Response Time of Six Unused Sensors Versus Electrolyte Tip Temperature (Ref. 8)

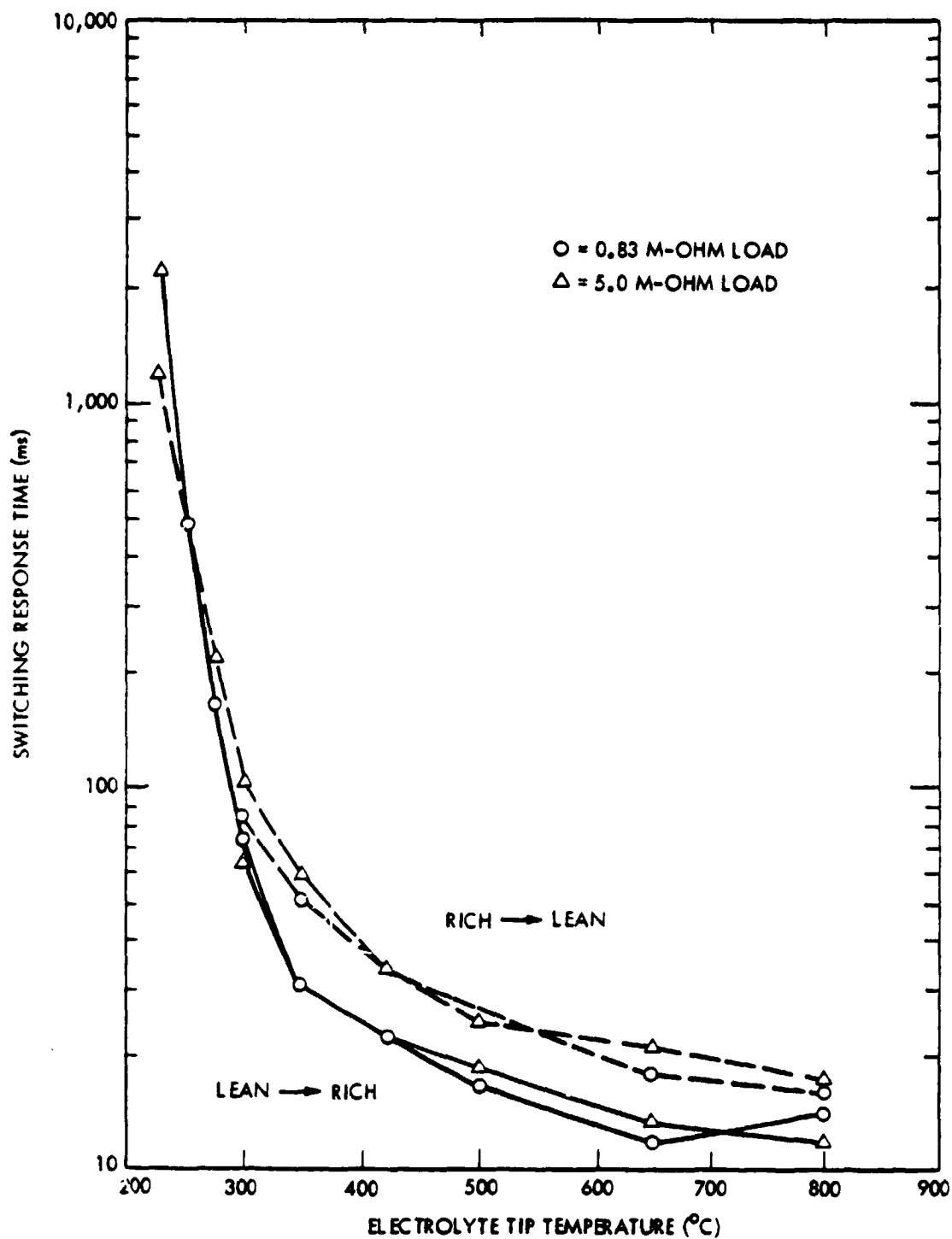


Figure 2-12. Averaged Voltage Switching Response Time of Three Sensors as a Function of Electrolyte Tip Temperature After 78,000 km Closed-Loop Vehicle Test (Ref. 8)

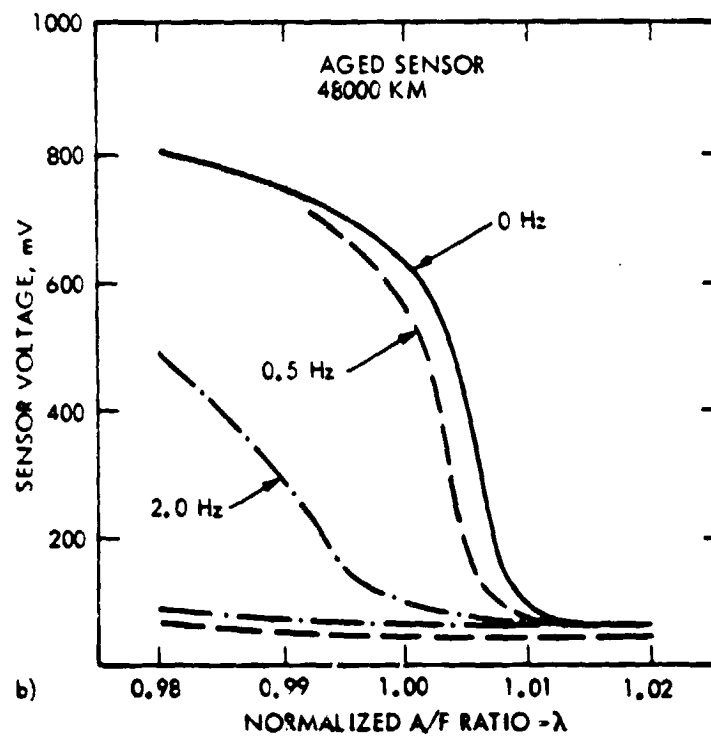
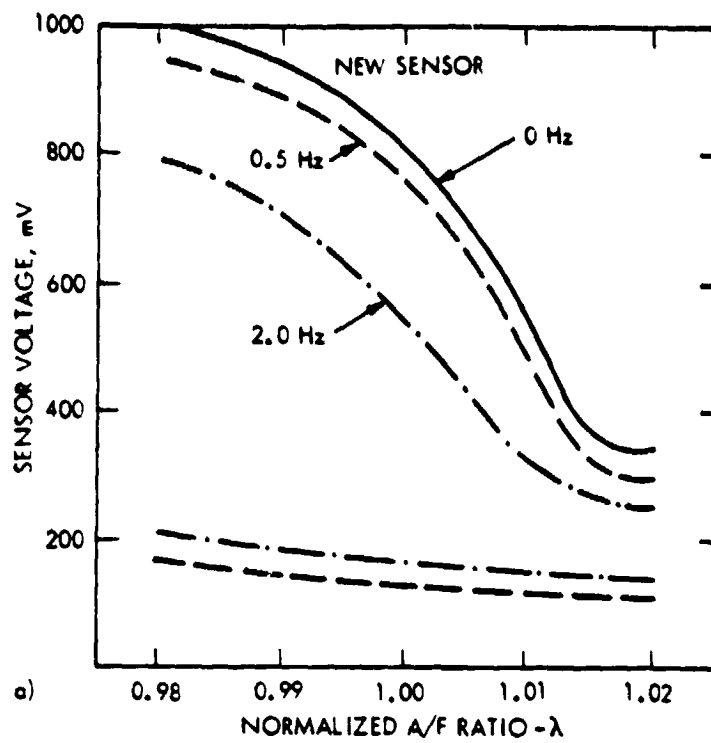


Figure 2-13. Dynamic Lambda Characteristics at 350°C of New and Aged Sensor (48,000 km in Common Application with Medium Temperature Field, Ref. 9)

were taken using synthetic exhaust gases and slowly increasing lambda from 0.96 to 1.05 at a scan rate of approximately 0.12 per hour. To determine the dynamic behavior of the sensor, short pulses of air were introduced at a given frequency. This resulted in a lambda value varying about the mean value with a defined amplitude of $\Delta\lambda = \pm 0.05$. The result is the dynamic characteristic curve represented by the maximum and minimum sensor voltage during one cycle of oscillation. Consider first the curve for the new sensor at an exhaust gas change frequency of 2 Hz, where the drop in sensor voltage following a rich to lean oscillation is fast and complete. On the other hand, when the exhaust gas returns from lean to rich, the sensor voltage does not return to the static curve within half an oscillation period. Thus, in a very rapid control system (>1.5 Hz), such as that used with fuel injection systems, a dynamic rich shift of exhaust gases is expected, especially at high engine speeds. At low sensor temperatures ($<400^\circ\text{C}$), sensor response times are of the same magnitude as the dead times in the vehicle closed-loop control circuit (gas transit times and dead times of final controlling elements). Curves for the aged sensor show a definite increase in the rich shift. Due to sensor aging, the asymmetry of the sensor switching times and the total switching time increase. This leads to somewhat lower control frequencies in rapid fuel injection systems, and as a general result, an increase in CO and NO_x emissions. Table 2-2 gives typical sensor aging characteristics with common sensor locations and operating conditions.

With change-out mileages for sensors being increased, the role of sensor deposits becomes more important. Factors which influence the formation of heavy deposits are engine oil consumption, oil type, main temperature and temperature range of sensor tip, and exhaust flow conditions at the sensor. Deposits can be a significant problem for sensors which are located relatively far from the engine and have a low operating temperature ($<500^\circ\text{C}$) but have some conditions where sensor tip temperature exceeds 650°C . In this case, oil ashes condense on sensor surfaces during low temperature operation and then melt during the high temperature operation to form a glaze on the sensor which prevents exhaust gases from passing through. This leads to much longer response time for the sensor over the entire temperature range. If the temperature never exceeds the glazing temperature, sensors with thick deposits can maintain good control efficiency. Table 2-3 shows functional values for a sensor with heavy deposits. The reduced rich voltage indicates a reduced catalyst activity on the outer electrode. The dynamic response of sensors with heavy deposits are reduced due to their gas-storage effect and the longer diffusion effect.

Excessive lead content in fuel can damage oxygen sensors after lengthy periods of service. Vehicle data (Ref. 9) obtained after using two tanks of fuel with 0.15 g/liter of lead on a system with low sensor tip temperatures ($<575^\circ\text{C}$) yielded no deterioration of the static lambda characteristic at 350°C but significant deterioration at 545°C (much flatter characteristic). When this lead-contaminated sensor was operated at the same low temperature with lead-free gasoline, the sensor regenerated itself. However, if the lead-contaminated sensor is operated for a short period at over 700°C , the lead-contaminated sensor can be fully inoperative. Endurance tests with leaded fuel at high sensor operating temperatures ($>700^\circ\text{C}$) show that lead contamination of the sensor starts after 50 hours compared with 15 hours when operated at low temperature ($<575^\circ\text{C}$). In high temperature operation with lead-free gasoline, the sensors can easily be regenerated.

Table 2-2. Typical Sensor Aging Characteristics with Common Sensor Locations and Operation Conditions, Functional Values in Test Burner at 350°C

Burner Values	New Sensor (Typical Values)	Field Sensor after 48,000 km
Rich output (mV)	900	804
Lean output (mV)	40	26
Internal resistance (k Ω)	20	49
Response times for 600 mV/300 mV		
t ₂ : R-L (ms)	200	130
t ₄ : L-R (ms)	30	40

Table 2-3. Functional Value in Test Burner at 350°C of a Sensor with Heavy Deposits

Burner Values	New Sensor (Typical Values)	Field Sensor 48,000 km with Heavy Deposits
Rich output (mV)	900	770
Lean output (mV)	40	-30
Internal resistance (k Ω)	20	37
Response times for 600 mV/300 mV		
t ₂ : R-L (ms)	200	670
t ₄ : L-R (ms)	30	600

2.2.3 Fuel/Air Mixture Preparation

Good fuel/air mixture preparation involves metering the required amounts of fuel and air, vaporizing or finely atomizing the fuel, mixing the fuel and air into a homogeneous mixture, and delivering equal mixtures to each engine cylinder. The metering and atomization is accomplished with either a carburetor or fuel injection system, while the mixing and distribution is done by the intake manifold.

As previously discussed in the three-way catalyst section of this report, good conversion efficiencies of all three gaseous emissions (HC, CO and NO_x) require that the fuel-metering system maintain close control of air-fuel ratio near stoichiometric conditions for a range of engine operating conditions from idle to wide-open-throttle. The degree of air-fuel control required depends on the type of three-way catalyst system used (i.e., single-bed catalyst or dual bed system with air injection). To make the air-fuel control job more difficult, the automotive engine is frequently operated under dynamic conditions due to vehicle accelerations and decelerations. In addition, the fuel-metering system must function properly over a range of ambient conditions of temperature, pressure, and humidity. The problems of providing a good stoichiometric mixture and maintaining acceptable vehicle driveability are exaggerated during cold start conditions by the increased friction of a cold engine and the fuel condensation in a cold intake manifold.

Control approaches for the fuel-metering element include (1) accurate precalibration of a unit with built-in compensation features, and (2) active adjustment of the metering element by means of a closed-loop feedback control system. Single-bed three-way catalyst systems require the use of a closed-loop feedback control system for adequate air-fuel control. As emissions standards have become more stringent, most control work has concentrated on the closed-loop feedback control approach. In addition to providing air-fuel ratio control, the fuel-metering system must provide good vehicle driveability, be reliable and maintenance-free, and achieve these characteristics at a reasonable cost. Recently, new regulatory requirements have made the fuel-metering job more difficult. California Air Resources Board has introduced an "anti-tampering" regulation requiring that the idle mixture adjustment on 1980 models be made inaccessible. In addition, the allowable maintenance on certification durability vehicles was reduced for 1980 (Table 1-2).

Even when overall air-fuel ratio is maintained near the stoichiometric ratio by the fuel-metering system, considerable cylinder-to-cylinder air-fuel ratio variations can exist as a result of poor atomization and poor distribution in the intake manifold. The influence of this maldistribution on three-way catalyst performance has not been systematically evaluated.

The most successful applications of three-way catalyst emissions control systems have utilized fuel injection (Refs. 12, 13 and 14) for fuel/air mixture preparation. Much of the fundamental work on fuel injection systems for automotive applications has been done by the Bendix Corporation (Ref. 13) and the Robert Bosch Corporation (Ref. 14). The systems are generally designated as electronic fuel injection (EFI) or mechanical fuel injection (MFI) depending upon whether electrical or mechanical means are used to

control the injection process. Fuel-injection systems have been developed for both intermittent and continuous operation. In intermittent injection systems, the injectors can be operated in groups or sequentially, with the amount of fuel injected being controlled by varying the injection pump stroke or the length of injection time.

In general, fuel-injection systems offer increased engine torque and power compared with that of an engine with a single carburetor. This results from the improved cylinder-to-cylinder fuel distribution of a fuel-injection system and the fact that intake manifolds for fuel-injection application can be more effectively designed to take advantage of the ram-effect to improve the air-charging efficiency of the intake manifold because the manifold transports only air to the cylinders. The potential pay-off for designing the intake manifold to utilize resonance effects for air charging is shown in Figure 2-14.

In Otto cycle engine applications of fuel injection, port injection is the common method of introducing the fuel. The fuel is normally injected into the intake manifold just upstream of the intake valves. The injector valves are designed to spray fuel into the manifold to promote better atomization.

To provide control of air-fuel ratio, the systems either measure air flow directly or infer air flow from other engine parameters such as engine speed, intake manifold pressure, and ambient temperature. Various compensation techniques have been used with fuel-injection systems to account for cold start operation, warm-up, and full load enrichment. Typical fuel enrichment curves are given in Figure 2-15 for a fuel-injection system when operated over a typical vehicle driving cycle. The fuel-air mixture is first enriched time-dependent and then temperature-dependent. There is an individual enrichment curve for each starting temperature. For the normal range of starting temperatures (-20°C to $+20^{\circ}\text{C}$), the starting enrichment factor (1.5 to 2.5) decreases to produce no enrichment after the first 2 to 4 minutes of engine operation. Acceleration enrichment curves are shown superimposed on the base enrichment curves.

Use of fuel injection can result in significant fuel economy improvements if the fuel injection system is properly matched to the engine and if the engine is designed to take full advantage of the characteristics of the fuel injection system. The good fuel distribution characteristics of fuel injection can, in general, permit an increase in engine compression ratio before engine knock occurs. This higher compression ratio would result in an increase in fuel economy. Fuel injection systems offer significant advantages when looking at some of the advanced concepts being considered for fuel economy improvements (e.g., fuel cutoff during deceleration). In the fuel cut-off concept, the fuel supply is completely switched off during deceleration and then switched on again when engine speed reaches approximately 1200 rpm. Deceleration cut-off is a method of improving fuel economy 3-7%, depending on vehicle, driving cycle, and transmission used. Fuel-injection systems offer good characteristics because driveability is not seriously affected by the fuel cut-off. In carburetor systems, drying-out

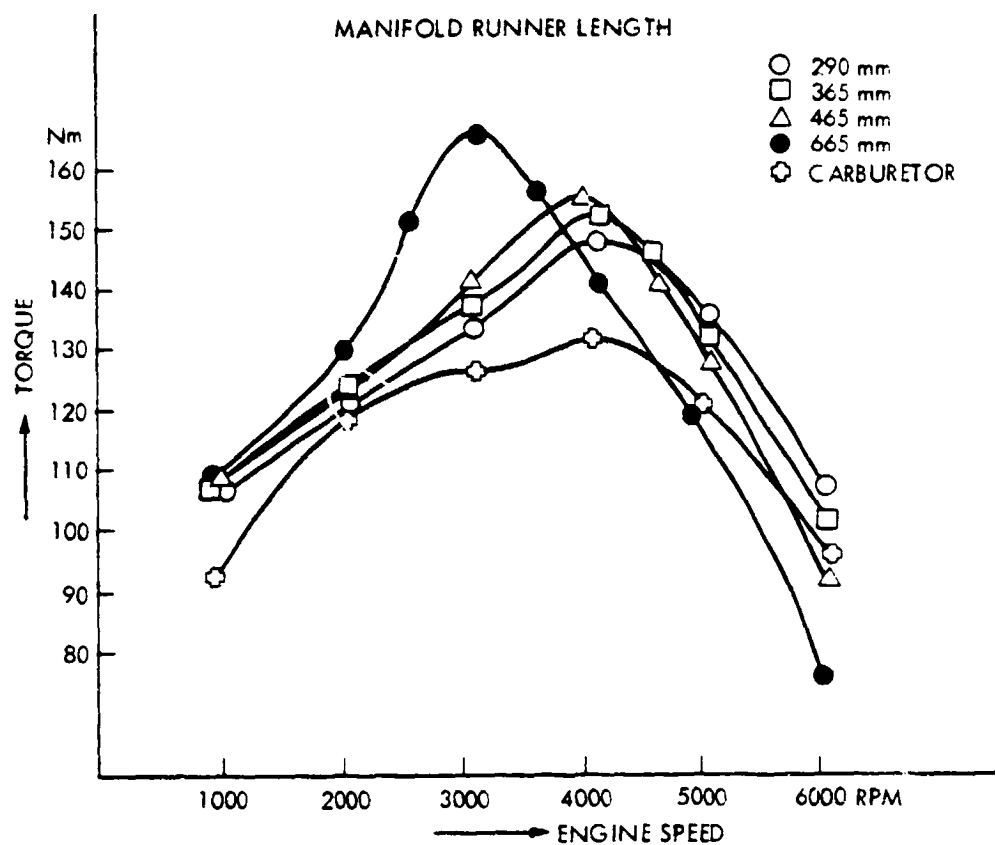


Figure 2-14. Torque as a Function of Manifold Runner Length (Ref. 12)

ENRICHMENT FACTOR

- ① WARM UP ENRICHMENT
- ② AFTERSTART ENRICHMENT
- ③ ACCELERATION ENRICHMENT

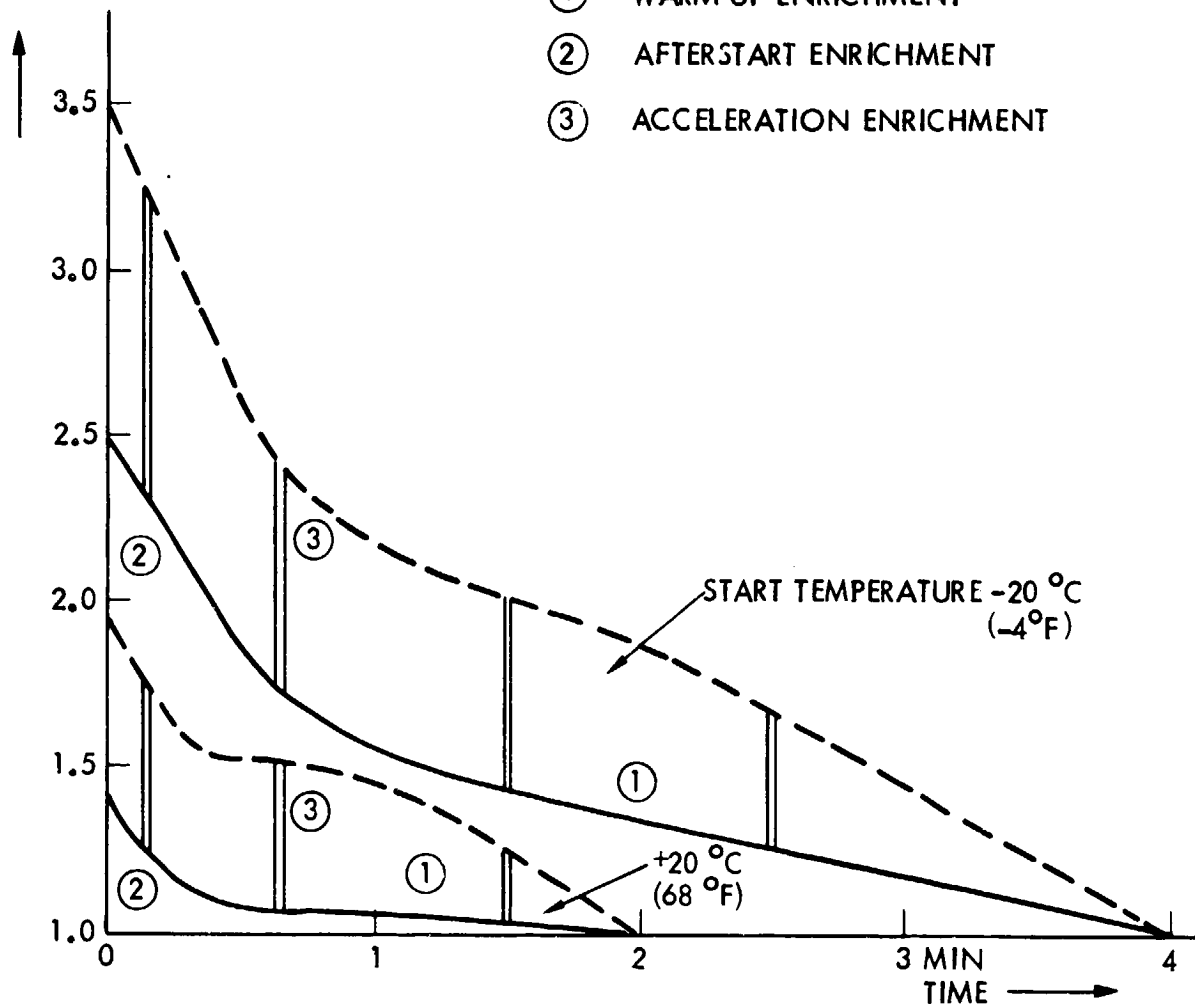


Figure 2-15. Enrichment Factor During Warmup for a Typical Driving Cycle (Ref. 12)

of the intake manifold and the delayed supply of fuel after switching on the fuel again create significant driveability problems.

The first production vehicles to use a three-way catalyst emissions control system were the 1977 Volvo and Saab vehicles introduced in California. Both vehicles used the Bosch K-Jetronic fuel injection system. Up through the 1980 model year, the Volvo and Saab have continued to yield the lowest exhaust emissions of any production vehicles. Therefore, the fuel-injection system used in the Volvo will be described in more detail.

The Bosch K-Jetronic fuel-injection system (Ref. 12), shown in Figure 2-16, is a mechanical, driveless, air-flow metering, continuous-injection system. The system continuously injects fuel in front of the intake valve with the spray pattern oriented toward the valves. This means that three-fourths of the fuel required for any given engine cycle is being stored temporarily in front of the intake valves, while one-fourth of the fuel is injected during the intake stroke.

Air-flow metering is done by a circular measuring plate mounted in a conical venturi. Movement of the air-measuring plate provides a measure of air-flow rate. A mechanical lever transfers air-measuring plate travel to the fuel-control plunger in the fuel distributor. The position of the fuel-control plunger determines the cross-section of small rectangular fuel-metering slits, providing a linear relationship between plunger position and fuel-flow rate.

There is one slit for each engine cylinder. Each slit leads to a differential-pressure valve, which regulates the pressure drop across the slit to a precise, constant value of 0.15 bar (2 psi), so that the fuel supplied is insensitive to changes in supply-pump pressure and injector opening pressure. Accurate fuel-metering slits and precise adjustment of differential-pressure valves ensure uniform proportioning of the fuel.

Control pressure acts on the fuel-control plunger to counteract the force resulting from the air flow acting on the air-measuring plate. By changing this control pressure, the air-fuel ratio of the mixture can be changed. For example, reducing control pressure leads to increased travel of the measuring plate for a given air-flow rate. This, in turn, leads to an increase in the cross-sectional area of the fuel-metering slits and a richer mixture.

The fuel metered in the fuel distributor is then fed to the injection valves. The needle in the fuel nozzle vibrates at a high frequency, leading to fine atomization of the fuel spray, even for small fuel quantities.

Mixture enrichment during engine warmup is controlled as a function of temperature and time by the warmup regulator. When the engine is cold, a bimetallic strip presses against the spring in the warmup regulator to reduce the control pressure. After starting, a heating resistor heats up the bimetallic strip, resulting in an increase in control pressure and a decrease in fuel enrichment with time. With the engine at operating temperature, the control pressure is kept constant and the warmup regulator is not used.

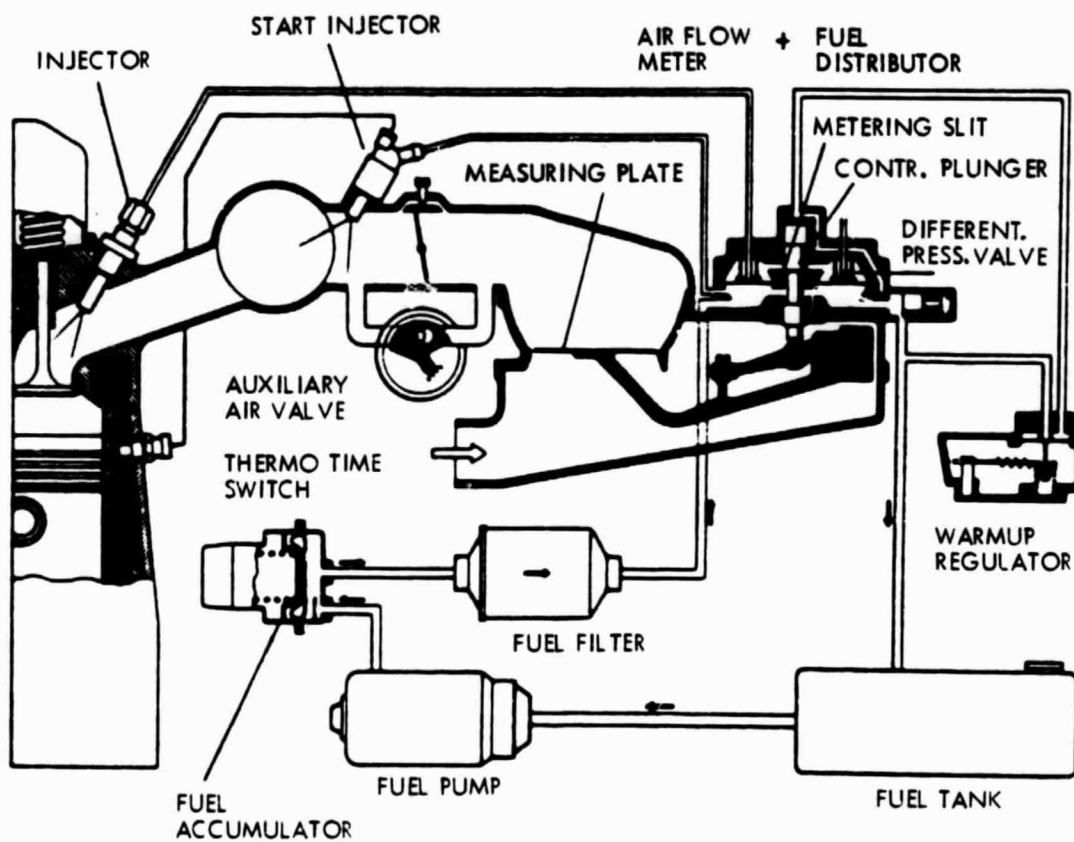


Figure 2-16. Bosch K-Jetronic Fuel Injection System (Ref. 12)

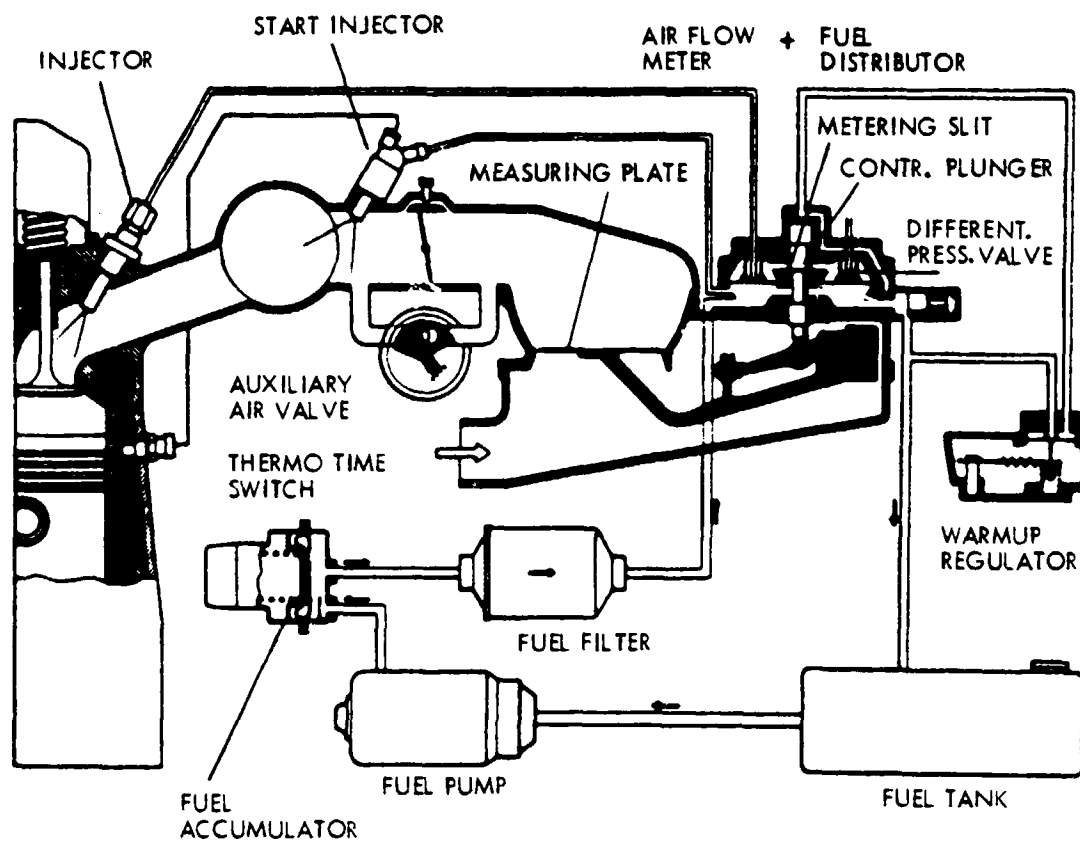


Figure 2-16. Bosch K-Jetronic Fuel Injection System (Ref. 12)

When used with three-way catalyst emissions control systems, a special hydraulic arrangement and a synchronized solenoid valve are used to vary the differential pressure at the control slits to alter the amount of fuel injected. The K-Jetronic system is particularly adaptable to the introduction of additional control signals.

Rather than the continuous, mechanical fuel-injection approach just described, other systems are based on electronically controlled injection with the fuel being injected intermittently. One such system is the Bosch speed-density system, the D-Jetronic, which is shown in Figure 2-17. This system is similar to the Bendix system used by Cadillac. In such a system, the basic parameters used for fuel metering are engine speed and intake manifold pressure. Many corrections provided by auxiliary signals (e.g., throttle movement, coolant temperature, intake-air temperature, etc.) are required in such speed-density systems to provide accurate control. In the D-Jetronic system, the electromagnetically-operated injectors form two groups. Practically, the injectors adjacent to each other in the firing order are grouped together. This arrangement causes one injector out of each group to inject into an open intake valve while the fuel from the other injectors is temporarily stored in front of the intake valves. The pulse diagram for such a system is given in Figure 2-18 for a 6-cylinder engine.

Considerable effort has been made to apply closed-loop feedback control techniques to conventional fixed-venturi carburetors for use with three-way catalyst emissions control systems (Refs. 15, 16 and 17). A definite economic advantage over fuel-injection systems could be realized in this case, as conventional carburetors and induction system hardware could be employed with minimum modifications.

Carburetor systems have been developed which apply feedback control to venturi air bypass loops, main and idle air-bleed circuits, main fuel-metering rods, and fuel-bowl pressure level. As a typical example of this type of fuel-metering approach, the Carter feedback-controlled carburetor (Ref. 16) will be discussed in more detail.

Figure 2-19 shows operation of the carburetor's two basic fuel subsystems, the main (high-speed) circuit and the idle (low-speed) circuit. In the Carter carburetor, each circuit has its own feedback control by means of an auxiliary air bleed. In the main circuit, fuel flow into the venturi nozzle is limited by means of a tapered metering rod. When the throttle is opened, a partial vacuum draws fuel through the nozzle where it is atomized in the venturi. The auxiliary air bleed for the main circuit is located immediately upstream of the nozzle opening. By varying the vacuum acting on the fuel nozzle, the air bleed adjusts the amount of fuel supplied to the carburetor venturi.

The idle circuit is required for those engine operating modes in which there is insufficient vacuum at the main circuit fuel nozzle. After leaving the main fuel jet, fuel is supplied to the idle circuit by the idle jet. This fuel is then mixed with air from a fixed idle bleed, accelerated through a channel restriction, and mixed with additional air from a second air bleed before being discharged through idle ports at throttle level. The auxiliary

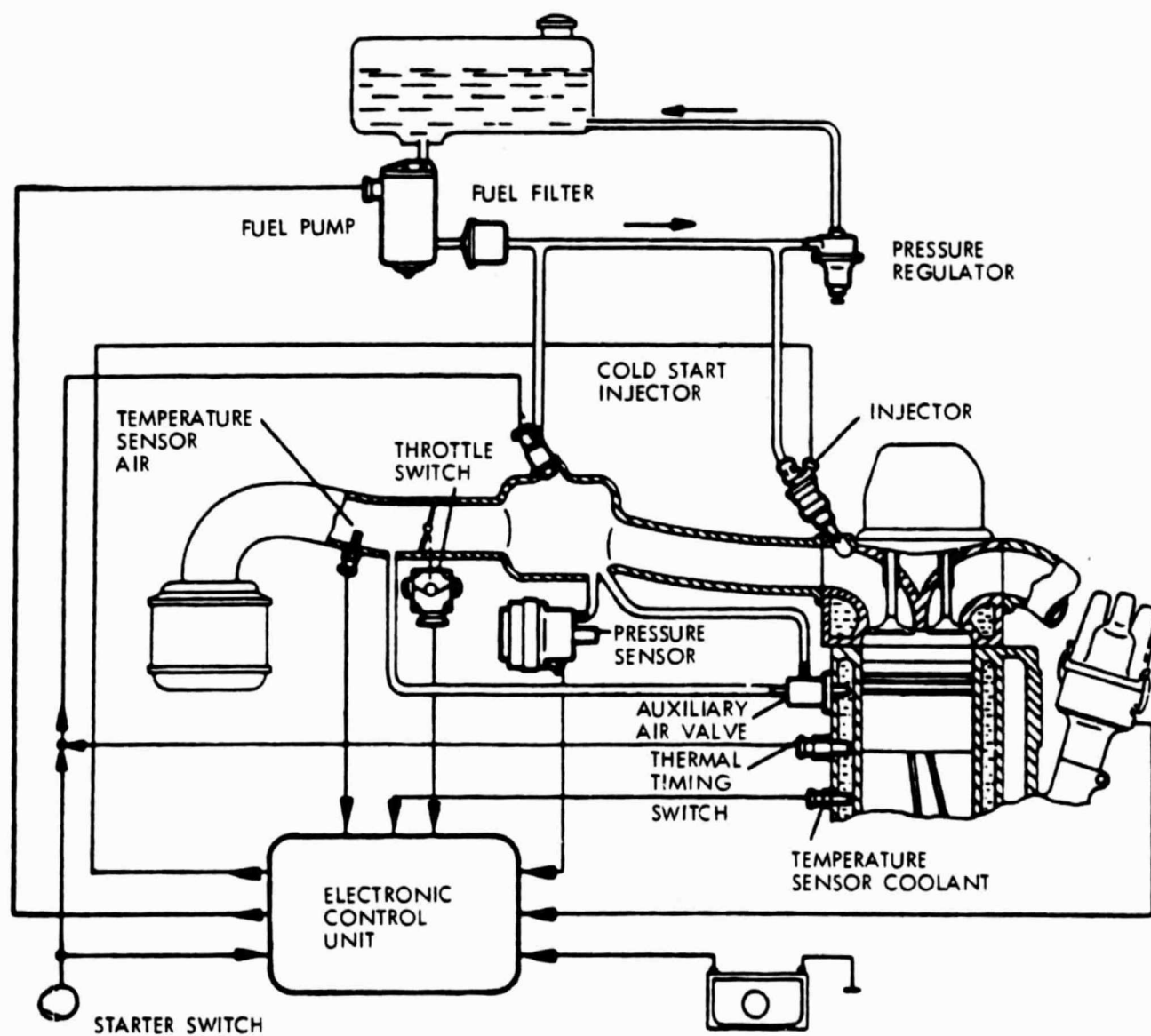


Figure 2-17. Bosch D-Jetronic Speed-Density Fuel Metering System (Ref. 12)

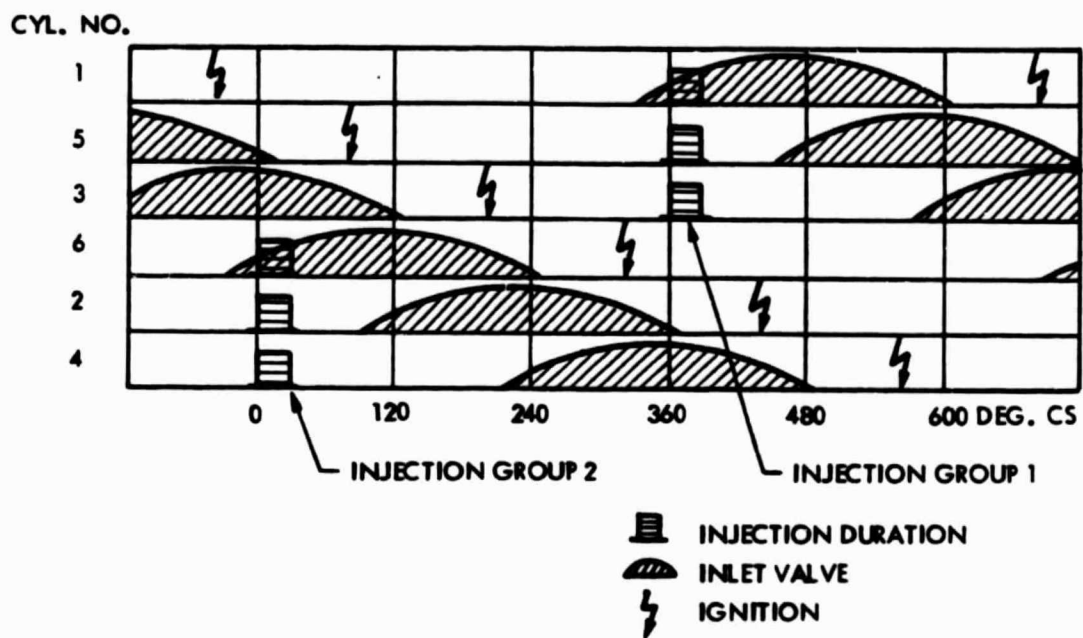


Figure 2-18. D-Jetronic Pulse Diagram, 6-Cylinder (Ref. 12)

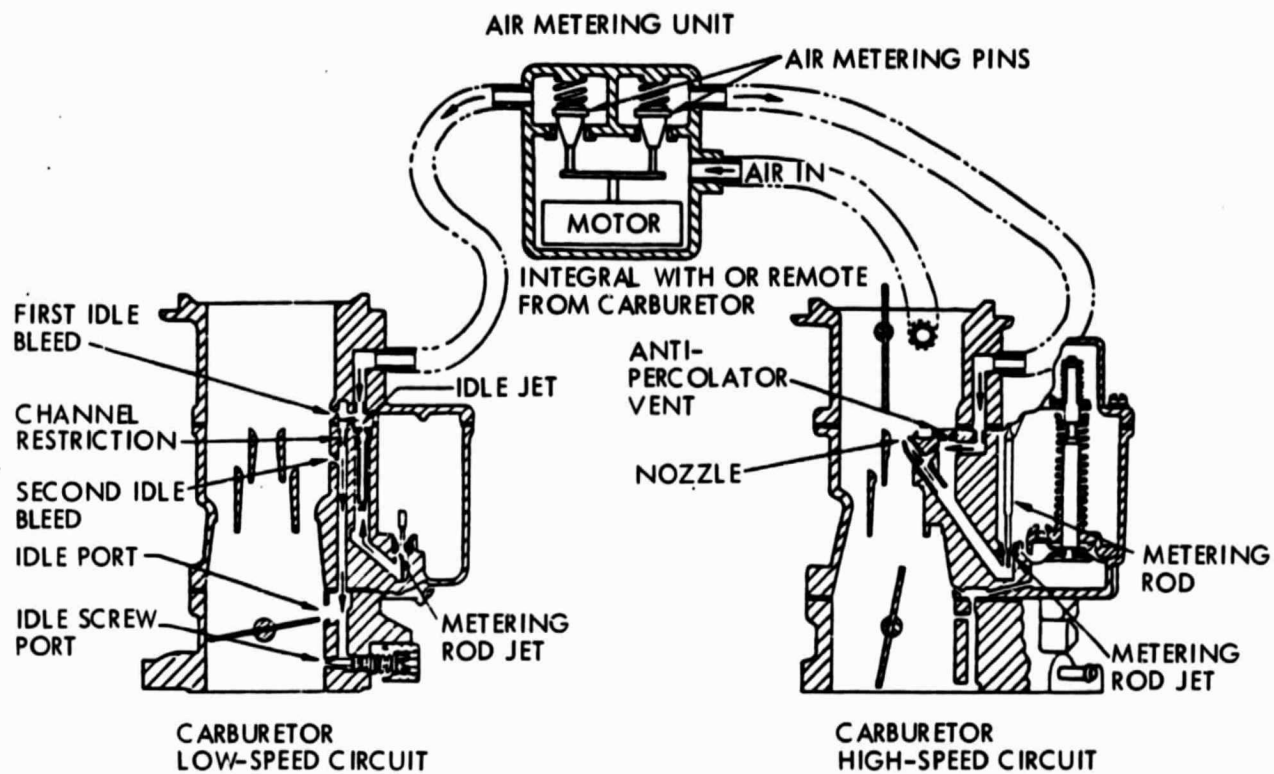


Figure 2-19. Carburetor Fuel Circuits (Ref. 16)

air bleed for the idle circuit is located between the first idle bleed and the channel restriction. This added air changes the vacuum signal on the idle jet, thus changing the amount of fuel delivered to the idle circuit.

The amount of air bled into the main and idle circuits is controlled by tapered metering pins that are positioned in orifices in the air-metering unit. The pin movement is controlled by a linear solenoid receiving its signal from an electronic control module. The solenoid has two coils that position the armature in response to an applied voltage at each coil. With zero voltage applied, the armature is at its central position, calibrated for a stoichiometric air-fuel ratio at sea-level. The pins can move relative to the central position to provide a four-unit variation in air-fuel ratio (A/F from 12.7 to 16.7). Digital logic of the system partitions this range of pin movement into 32 increments. In some cases, a stepper-motor can be used rather than a linear solenoid to provide control for the tapered metering pins.

The system incorporates two special modes of operation: a fast rate and an open-loop mode. The fast rate mode is used for those engine operating conditions requiring rapid adjustment of air-fuel ratio. The open-loop mode is used in response to wide-open-throttle operation, cold start, or other predetermined conditions.

Utilization of closed-loop feedback carburetors as the fuel-metering element in three-way catalyst emissions control systems has been primarily in the dual-bed catalyst approach with air injection and EGR. These systems were first introduced in limited-production vehicles for California in 1978.

Conventional fixed-venturi carburetors have from one to four fixed venturis through which air flows before mixing with the fuel. Maintaining precise air-fuel ratio control and good atomization and mixing is difficult, as most of the fuel enters the air stream in the venturi area where air velocity varies considerably over the engine operating range. Development is continuing on variable-venturi carburetor concepts which provide continuous adjustments to the throat area of the venturi to promote high air velocities for improved atomization, especially at low loads.

Ford first introduced a variable-venturi carburetor on a limited production vehicle introduced in California in 1977 (Ref. 18). The venturi throat area is controlled by a venturi valve which responds to changes in engine speed and load. The fuel flow is controlled by tapered metering rods that are inserted into the main metering jets and linked mechanically to the venturi valve. Any change in throttle-plate opening causes a corresponding change in venturi valve and fuel-metering rod position. This variable-venturi concept has apparently performed satisfactorily in the California application.

Work is continuing on the development of a sonic carburetor, which is a special kind of variable-venturi design (Ref. 19). Attempts to improve fuel-air mixture quality are made by maintaining sonic air flow through the carburetor throat. Most sonic carburetor designs continue to accelerate the flow to supersonic values downstream of the throat and then return to subsonic flow through a shock wave. Atomization is enhanced as the fuel

interacts with the sonic air flow and passes through the shock wave. In addition to better atomization, sonic designs should improve cylinder-to-cylinder air-fuel ratio distribution, yield more precise fuel metering, and improve compatibility with electronic controls. Sonic designs have no downstream throttle plates to disturb the flow and have no chokes in a conventional sense.

One of the most well-known developments of sonic carburetors has been the work of Dresser Industries (Ref. 19). The Dresserator carburetor has passed through several design iterations. One of the more recent designs uses a sliding jaw configuration to vary the throat area. The sliding jaw varies the length of a grooved fuel rod which meters the fuel. This model uses a differential pressure controller for air-fuel ratio control. This sonic concept has been evaluated on a vehicle at stoichiometric conditions with EGR and a three-way catalyst (Ref. 18). Results indicate that the sonic carburetor failed to show any cylinder-to-cylinder, air-fuel ratio distribution advantage over a conventional carburetor and did not yield a fuel economy advantage over the urban driving cycle. Without feedback control, the vehicle with sonic carburetor was not able to meet the 0.41 HC/3.4 CO/1.0 NO_x standard, even though it was capable of controlling air-fuel ratio to ± 0.25 (2 σ) over the driving cycle.

Much of the prior work on sonic carburetors has indicated advantages for sonic fuel preparation when applied at lean air-fuel ratios. When used with a closed-loop fuel control system and three-way catalyst under stoichiometric conditions, the potential application for sonic carburetors is not clear. These carburetors may be more compatible with the control concepts which evolve for three-way catalyst vehicles.

The need for precise air-fuel ratio control and control flexibility in an air-fuel metering system with mechanical simplicity and low cost has led U.S. automotive manufacturers to develop throttle-body injection (TBI) for application with three-way catalyst emissions control systems. The TBI system (Ref. 20) developed for some 1980 Cadillac passenger car models will be discussed as an example of this recent technology. The new TBI system, which on its 1980 introductory version operates in the open loop mode, replaces the port electronic fuel injection (EFI) system used on the 1976-1979 Cadillac models. The port EFI system had an on-board electronic control-unit, eight fuel injectors, and high pressure (39 psi) fuel requirements, and was considered a premium electronic fuel-control system. Throttle-body injection introduces a low pressure (10 psi) fuel-injection system that offers the fuel scheduling flexibility of port EFI while reducing complexity to establish a more cost-effective package.

The TBI system achieves its cost reduction objective by operating successfully a low pressure (10 psi) while meeting the hot fuel performance tests required of production vehicles. The required pressure is developed by a single in-tank pump, eliminating the precision high pressure fuel pump needed with port EFI systems. Many design provisions are built into the design to properly handle hot, low-pressure fuel. These include provisions for vapor tolerance at the injector, quick vapor purging of the system at turn-on, minimizing heat transfer to the fuel, eliminating subatmospheric pressure in the fuel-delivery system, and cooling of critical fuel hardware.

The earlier EFI injectors provided a long, dead-headed, high-surface-area path for the fuel to reach the metering orifice. Thus, any vapor formed due to hot soak was forced out the metering orifice. To eliminate this vapor delivery, the TBI injector provides a low resistance path for low-velocity fuel delivery to the metering tip. When vapor is present, buoyancy carries it up into the chamber surrounding the metering tip. To further ensure that liquid fuel is available at the injector, the fuel passages are arranged to purge stagnant vapor through the unit, as shown in Figure 2-20. Once past the injector, the fuel enters the regulator and passes through the return line to the tank. Continuous flow of fresh fuel past the injectors also helps to provide additional cooling. Intake air flowing over the fuel body assembly, as shown in Figure 2-21, provides more cooling. To minimize heat transfer from the intake manifold, a thick gasket insulates the throttle body assembly from the hot intake manifold.

Smoothing the fuel pulses over time is accomplished by proper design and placement of the injector assembly above the throttle bore walls and throttle blades. This design concentrates the fuel in a sheet directed toward the annular opening around the throttle blades, as shown in Figure 2-21. The sheet of fuel is then sheared off at the throttle opening.

The design of a TBI system to provide the necessary flow rate range within the time available presents a significant design problem. A comparison of the injector pulse timing and synchronization for EFI port injectors and TBI injectors is given in Figure 2-22. TBI systems generally have two fuel injectors which alternate in supplying fuel pulses for the successive cylinders in the engine firing order. Thus, the maximum open time for the fuel injector per pulse is 180 crankangle degrees. In the corresponding EFI port injection system, there is one injector per cylinder. The injector has a maximum open time per pulse of 720 crankangle degrees; however, typical injectors are limited to about 325 crankangle degrees. This indicates that TBI injectors must be sized to deliver about twice the flow rate of comparable EFI injectors. This maximum flow rate constraint can be easily met; however, the TBI injectors must also have the same nominal dynamic range. Thus, under light load conditions, the TBI injector must produce a repeatable 1- to 2-millisecond pulse width, which is a very difficult technical problem for the electromagnetic injectors. Comparative injector flow characteristics for typical TBI and EFI injectors are shown in Figure 2-23. Note that EFI injectors operate nominally in the 2-millisecond pulse width range and higher.

Considerable technical work (Ref. 20) has improved the TBI injector response characteristics to make TBI systems practical. The injector driver has two operating modes: an initial turn-on mode, when full system operating voltage is applied for fast pull-in, and a second hold-current mode, giving a low energy state for the pulse duration.

In 1980, Cadillac's TBI system obtained the base fuel pulse width by using the speed density control concept illustrated in Figure 2-24. The concept depends on an electronic control module (ECM) with preprogrammed look-up calibration tables and inputs from engine sensors (manifold absolute pressure, manifold absolute temperature, and engine speed) to calculate the fuel-pulse width. The speed density control approach does not accurately

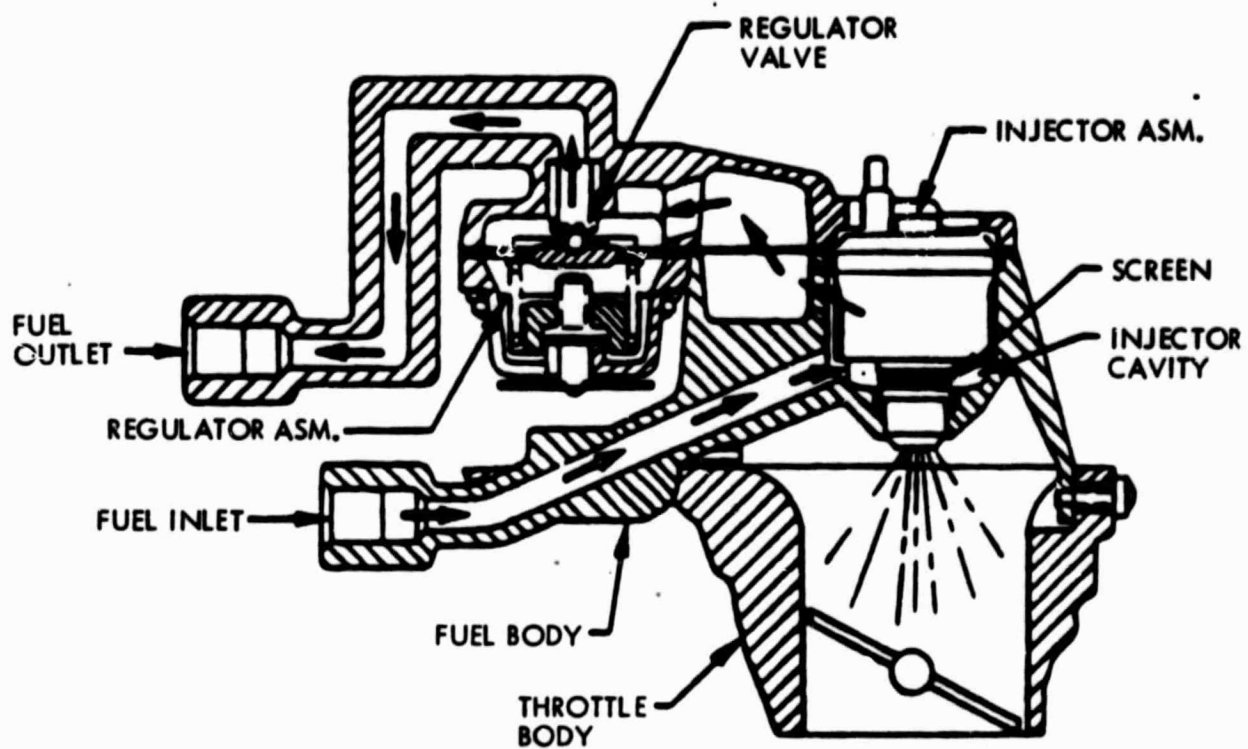


Figure 2-20. Fuel Body Assembly Showing Fuel Flow Path, Injector Mounting and Pressure Regulator (Ref. 20)



Figure 2-21. Fuel Body and Throttle Body Assembly Mounted on Dual Plane Manifold with Insulation Gasket (Ref. 20)

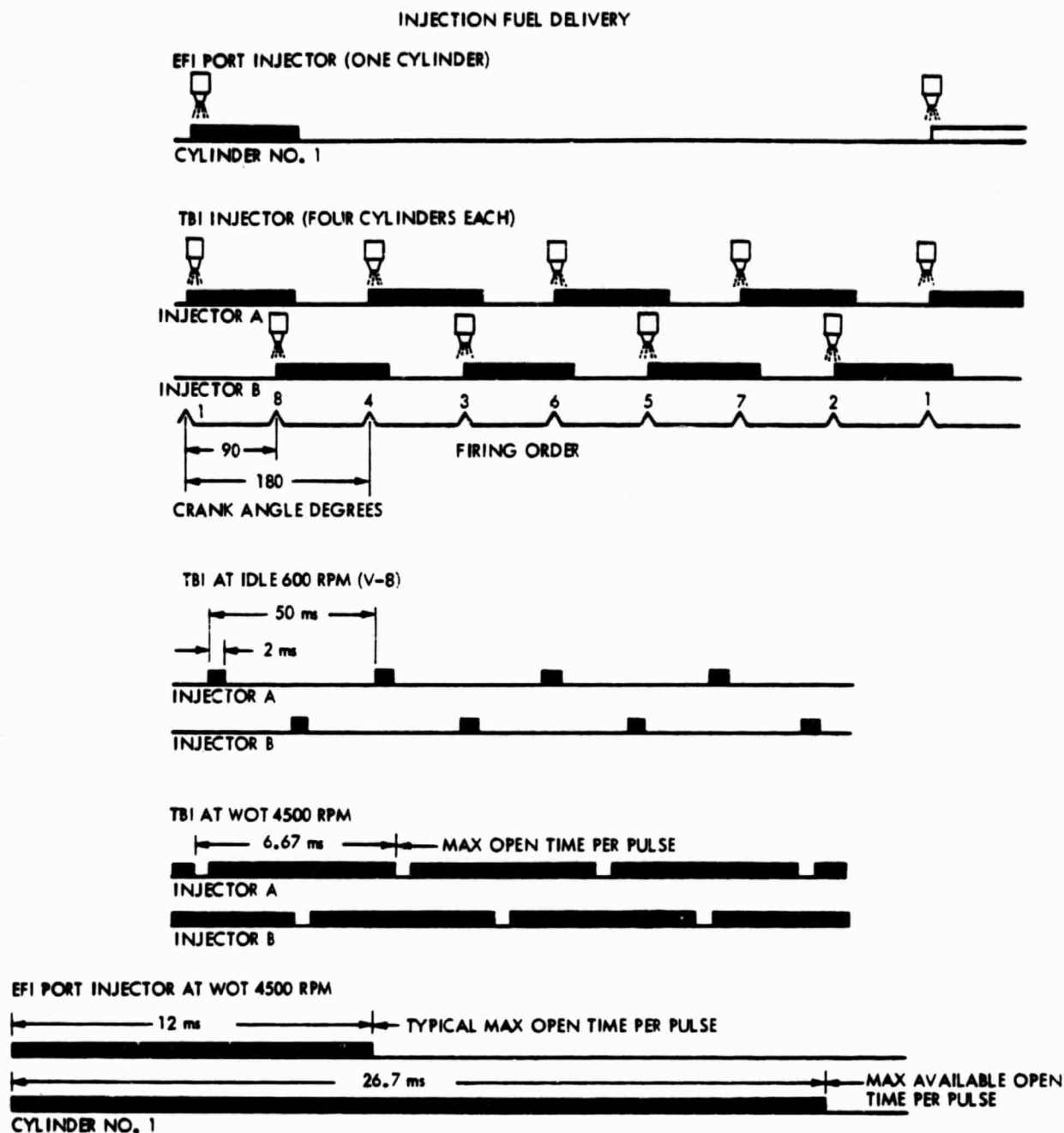


Figure 2-22. Injector Pulse Timing and Synchronization for Port EFI and Throttle Body Injectors (Ref. 16)

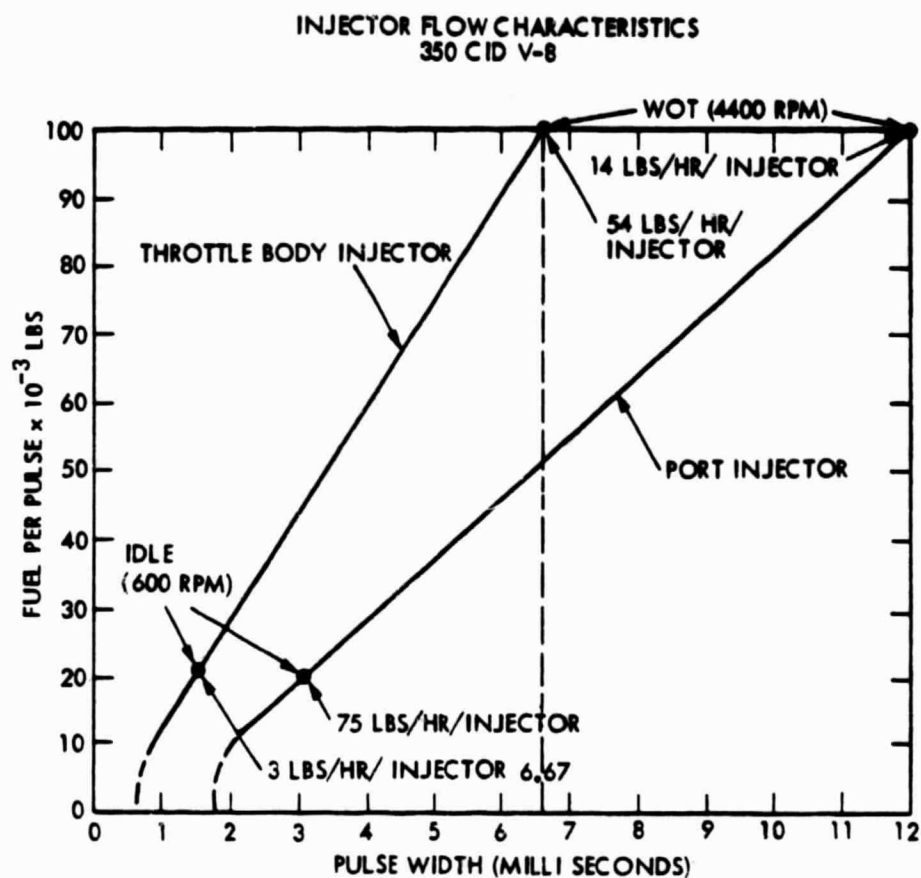


Figure 2-23. Injector Flow Characteristics for Typical TBI and EFI Units (Ref. 20)

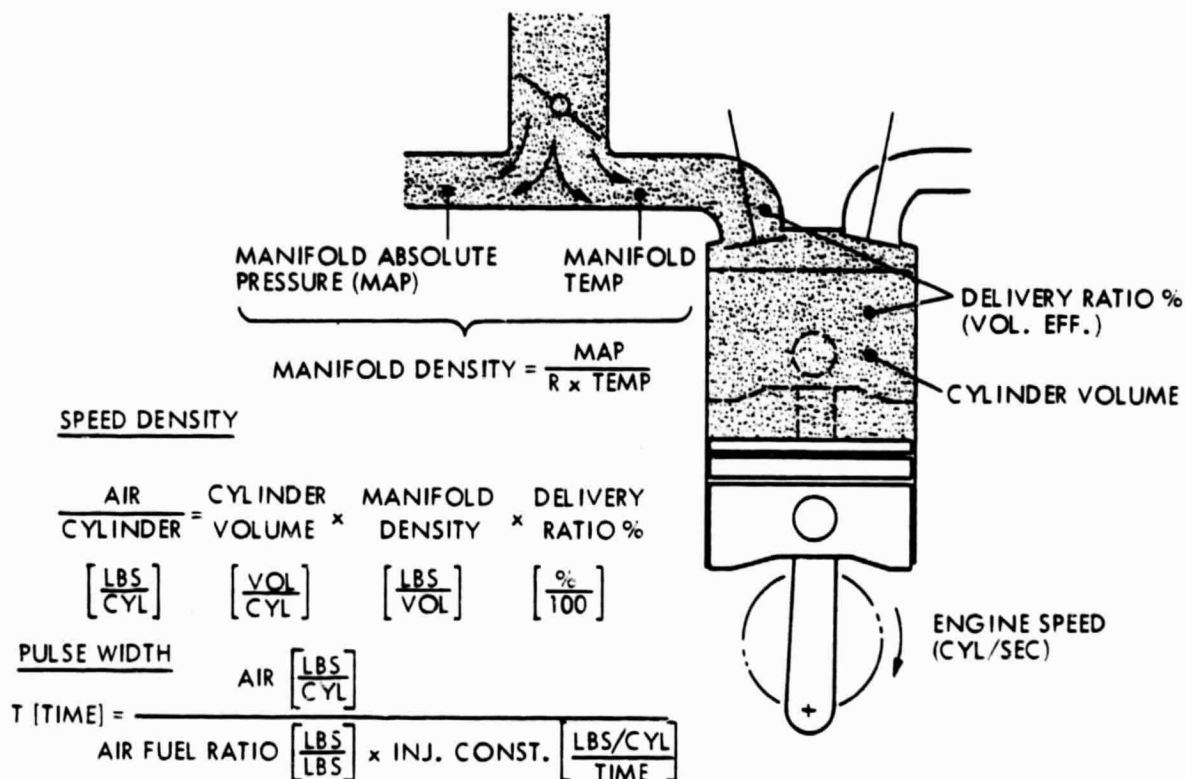


Figure 2-24. Speed Density Control Concept Diagram Illustrating the Generalized Approach to Obtaining the Base Fuel Pulse Width (Ref. 20)

handle fuel transient conditions, such as rapid acceleration demands. This transient fuel requirement is handled by the ECM through preprogrammed tables and sensor input signals.

2.2.4 Control Systems

The control function (Refs. 21-26) for a three-way catalyst emissions control system is provided by an electronic control module (ECM). The ECM processes oxygen sensor data, as well as data from other engine sensors, and produces an output signal that controls the fuel-metering system in a way that enhances overall system performance over that of the baseline open-loop system. This signal processing is often referred to as the control algorithm or strategy, and can be very simple or complex, depending on system complexity and control requirements.

The control problem can generally be defined as follows, with the degree of control required being more severe for the single-bed three-way catalyst system than for the dual-bed approach: The control system must maintain the accuracy of fuel-mixture preparation within 1 percent during continuous transient engine operating conditions to ensure that the exhaust gas entering the three-way catalyst is always within the very narrow composition band required to effectively reduce all three major pollutants (HC, CO and NO_x). This requirement is especially difficult because a high degree of accuracy is required under all engine operating conditions. The internal combustion engine is a very complex and nonlinear device which requires a rather sophisticated control algorithm to handle all contingencies over the entire operating range. In addition, because of its high nonlinearity, the engine does not easily lend itself to classical or modern control theory techniques. Control strategies are generally developed through a trial-and-error process. One common control strategy has been to use an integral controller whose output varies the fuel quantity linearly with the system error signal.

The system error is the difference between the commanded air-fuel ratio and the oxygen-sensor signal. Because of the system transport lag (the time for an air-fuel ratio alteration to pass through the engine and to the oxygen sensor), this type of control law will exhibit control oscillations or limit cycle characteristics even under steady-state conditions. The frequency of the oscillation is a function of integration time constant and transport lag (Ref. 27). Because transport lag is a predictable function of engine speed and load, additional compensation can be introduced to alleviate its effects. In addition, compensation is generally included to handle sensor aging, idling, large transients, temperature variations, and cold starts. It has also been found that by varying the set point around stoichiometry (i.e., dithering the air-fuel ratio command), the three-way catalyst window is effectively widened, resulting in less stringent accuracy requirements. The effective increase in window width is a function of dither amplitude and frequency, with common values being ± 0.5 air-fuel ratio units for a 1-Hz dither frequency.

An adaptive control feature has been added to some of the more recent systems (Ref. 22) to further enhance the closed-loop operation. The adaptive control algorithm stores a time-weighted function of the fuel-metering system

control signal in the electronic control module memory, while the engine is operating in a defined area of engine speed and load. When the engine-operating area changes via an engine speed or load change, the adaptive memory assigned to the new operating point is used to initiate the integrator and thereby the control signal for the fuel-metering system.

2.3 VEHICLE SYSTEMS

2.3.1 General Description

The characteristics and limitations of the major components which comprise a three-way catalyst emissions control system have been discussed in the previous section. The successful development of the three-way catalyst concept for a particular engine/vehicle combination requires a systems approach because of the strong interactions between components. The total engine/vehicle emissions control system must be optimized to achieve the best compromise in the areas of emissions, fuel economy, driveability, and cost. Factors which enter into the development of a three-way catalyst emissions control system include catalyst selection, oxygen sensor location, type of fuel-metering system, actuator type, cold-start systems, and various compensation systems. The interplay among these factors must be carefully considered with the realization that they are not independent of the engine being used.

Volvo was the first automobile manufacturer to successfully develop the three-way catalyst emission control system for production automobiles with their 1977 Volvo Model B21 for the California market. This initial application of the three-way catalyst concept was on the 130 CID, in-line, 4-cylinder, fuel-injected engine. The Volvo system used a single-bed, three-way catalyst unit without either EGR or AIR and was highly successful in achieving low emissions and good fuel economy. A year later, Saab introduced a similar emissions control system on their California automobiles. The Volvo and Saab continue today to be two of the more successful vehicle applications, especially from an emissions point of view.

In 1978, U.S. automobile manufacturers entered into production of three-way catalyst vehicles; however, all vehicles were equipped with carburetors and gave only marginally better emissions results than previous technology. Since that time, all manufacturers have been forced to develop three-way catalyst emissions control technology as the most logical technology for meeting the more stringent emissions standards. The transition to three-way catalyst systems was almost complete for the 1980 model year in California, and a similar transition is expected for the other 49 states in the 1981 model year.

The types of three-way catalyst systems which have been developed vary greatly both in approach and complexity. The systems generally can be grouped into the following two categories; (1) systems using a single-bed three-way catalyst and having neither EGR nor AIR, and (2) systems using both a three-way catalyst and oxidation catalyst and having both EGR and AIR. Table 2-4 gives some of the system characteristics of production vehicles with three-way catalyst emissions control systems.

Table 2-4. Characteristics of Production Vehicles with Three-Way Catalyst Emission Control Systems

Vehicle	Engines	Cal	49 State	Catalyst System	Control System	Oxygen Sensor	Mixture Prep.	Other
1980 Ford's Mercurys	5.0L	X		3-way light-off catalyst and oxidization catalyst	EEC-III (Same as above)	Oxygen Sensor	Feedback Carburetor	EGR, AIR, cooled EGR
1980 Ford's Mercurys	5.0L	X	X	3-way light-off catalyst and oxidization catalyst	EEC-III (Same as above)	Oxygen Sensor	Feedback Carburetor	EGR, AIR cooled EGR
1980 Cadillac	6.0L		X	3-way catalyst	Digital micro-process or inputs include manifold absolute pressure, amb. barometric pressure, engine coolant temp., intake manifold mixture temp. eng. speed and throttle position, controls electronic spark timing, fuel metering, idle speed-open loop control system	None	Digital electronic fuel injectors (DEFI)-2 pulse type fuel injectors integral with throttle body-in tank electric turbine type fuel pump injectors operate at 10 psi (Olds 88 injector system used 34 psi)	EGR, AIR
1980 AMC Vehicle	6-cylinder engines		X	Main catalyst is a dual bed unit upstream bed (1.5L) is Pt-Rh and downstream bed (1.3L) is Pt-Pd	Microprocessor feedback control	Oxygen Sensor	Feedback carburetor-stopper motor actuates pair of tapered fuel metering plus-trims A/F ratio within ± 0.1 ratio	Air injected between 2 catalyst beds
1980 AMC Vehicle	6-cylinder engines	X		Dual bed catalyst upstream 3-way unit (1.5L) and downstream oxidizing unit (1.5L)-additional 3-way (0.8L) unit used as start catalyst near engine	Microprocessor feedback control	Oxygen Sensor	(Same as above)	(Same as above)
1980 AMC Vehicles	4-cylinder engines	X		Single 3-way catalyst Pt-Rh	Microprocessor feedback control	Oxygen Sensor	Feedback carburetor cycling on-off solenoid regulates fuel flow according to percentage	EGR and air pump

2.3.2 Systems with Fuel Injection

Because it was the first three-way catalyst system certified on a production automobile and is still being sold in essentially the same form, the Volvo system (Refs. 21 and 24) will be described in more detail. The emissions control system, shown in Figure 2-25, uses a single-bed three-way catalyst, Bosch oxygen sensor, Bosch continuous mechanical fuel-injection (MFI) system and a closed-loop feedback control system.

Briefly, the operation of the Volvo system is as follows. The oxygen sensor, located at the outlet of the exhaust manifold, detects the oxygen content of the exhaust. Using this as an indication of air-fuel ratio, the sensor transmits a continuous nonlinear electrical signal to the electronic control module (ECM) which converts it into a signal for the continuously oscillating on/off frequency valve. When the on/off bias time is altered, the frequency valve changes the differential pressure across the metering slots in the fuel distributor to control the fuel injected, as shown in Figure 2-26. This control system attempts to maintain the composition of the exhaust gas entering the three-way catalyst unit within a narrow band to promote a high conversion efficiency for all three major gaseous pollutants.

The three-way catalyst used in the Volvo system is an Engelhard monolith Pt-Rh catalyst with a volume of approximately 100 in³. The Pt-Rh ratio of the catalyst is 5:1 with a total precious metal loading on the catalyst unit of 0.095 troy ounces. Both the Bosch oxygen sensor and the Bosch continuous MFI system have been described in the component section of this report and will not be discussed here. The logic of the electronic system is shown in Figure 2-27. Generally, the oxygen sensor signal is compared with an electronic reference signal to produce the integrator output. The resulting integrator characteristic, shown in Figure 2-28, causes the air-fuel regulation system to oscillate continuously around stoichiometric conditions. As previously mentioned, the air-fuel regulation system consists of an electromagnetic frequency valve which corrects the fuel flow by influencing the pressure drop over the fuel metering slots in the fuel distributor.

Regulation speed is the slope of the regulation curve in Figure 2-28, and ideally it should vary with the total system response time. Because the response time of the fuel system remains approximately constant, the total response time of the system is determined by the transport time (i.e., the time taken for an air-fuel ratio alteration to pass through the engine and down the exhaust manifold to the oxygen sensor location. Thus, response time depends largely on engine speed and load conditions. Regulation speed could be compensated for engine speed and load to match the response time. The good performance of the three-way catalyst in the Volvo system permitted a constant regulation speed to be used while still maintaining good conversion of gaseous pollutants.

Some component characteristics and overall system considerations resulted in modifications to the simple triangular regulation curve given in Figure 2-28. During development of the oxygen sensor, the changes in sensor output voltage characteristic with aging and scaling of the outer platinum electrode were solved by modifying the method of platinum application and adding a thicker spinel protection layer. The thicker layer caused an in-

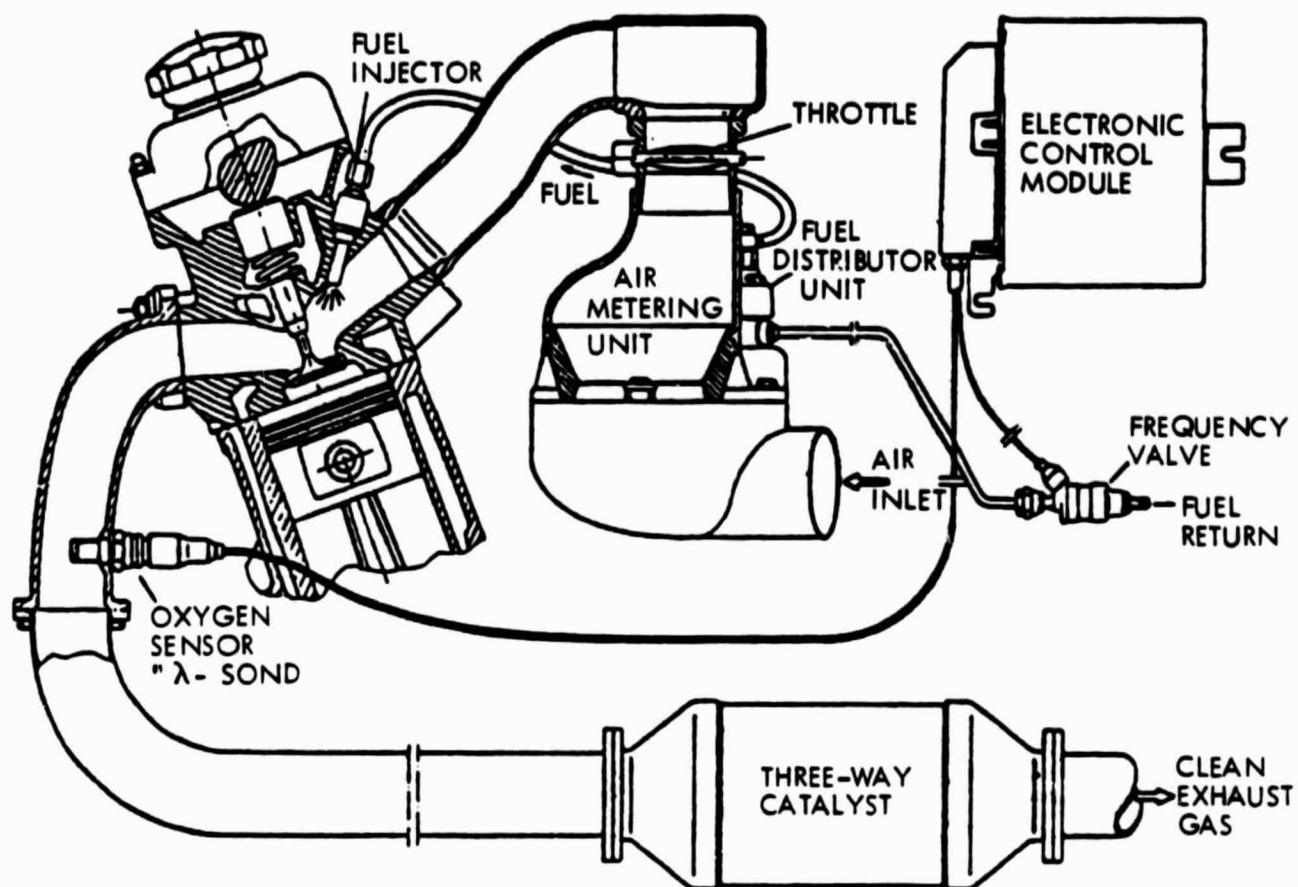


Figure 2-25. Volvo Lambda-Sond System (Ref. 24)

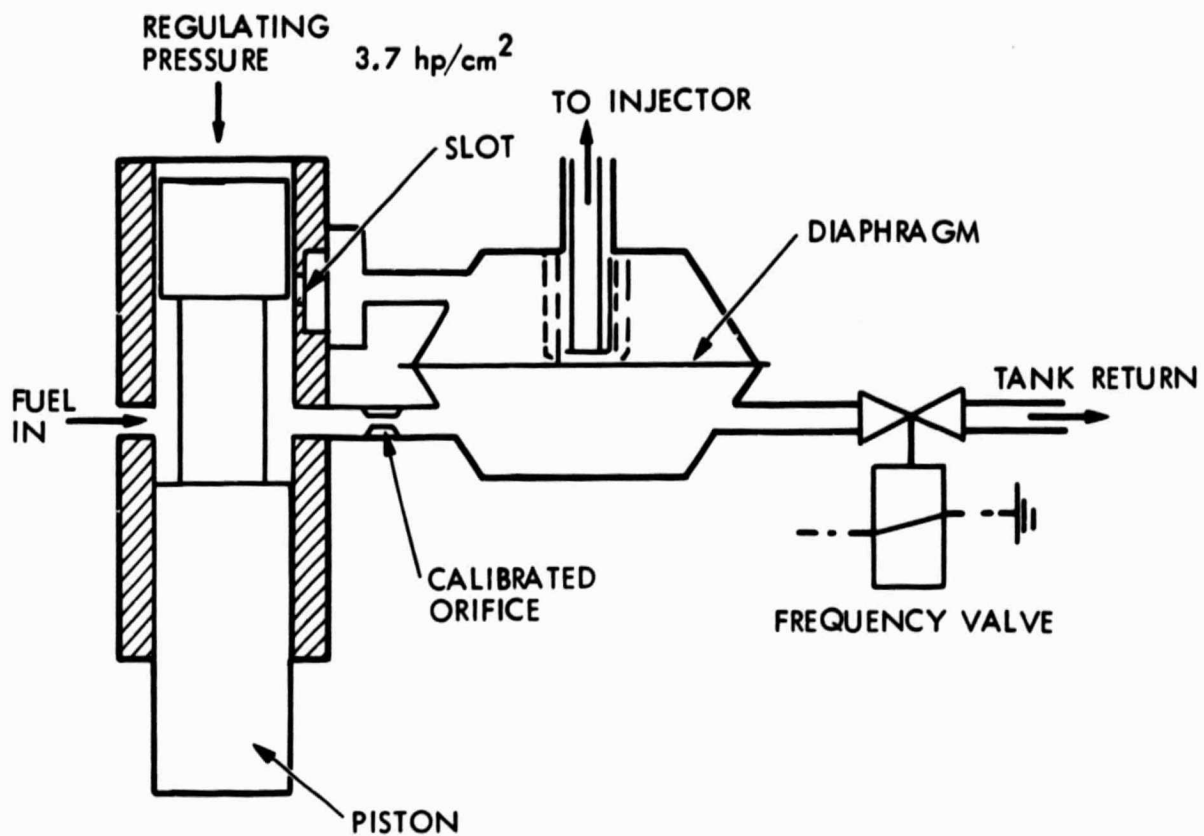


Figure 2-26. Principle of Fuel System Pressure Regulation

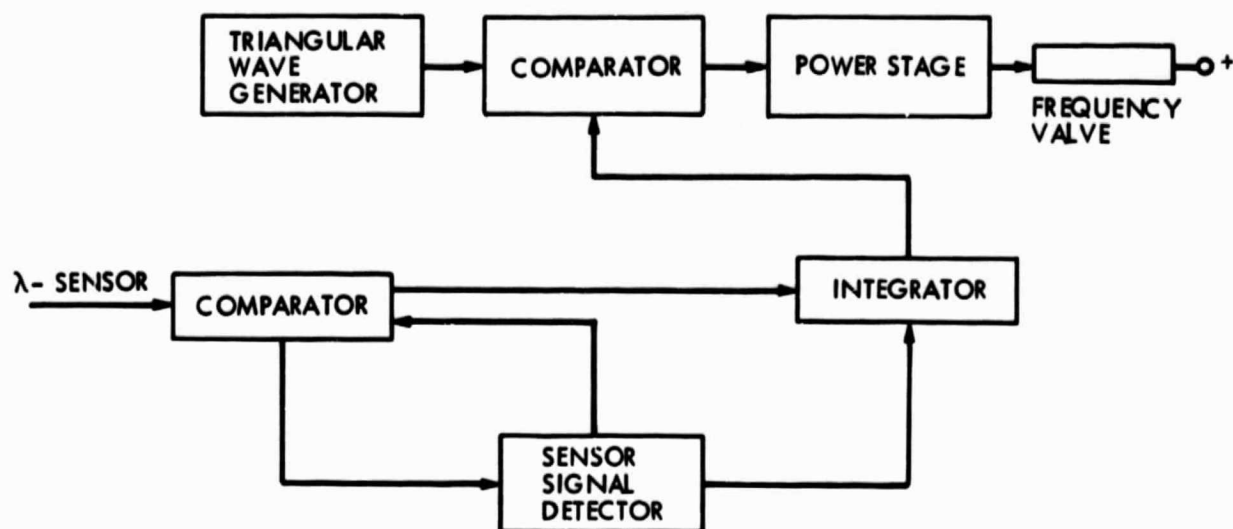


Figure 2-27. Electronic Logic System (Ref. 24)

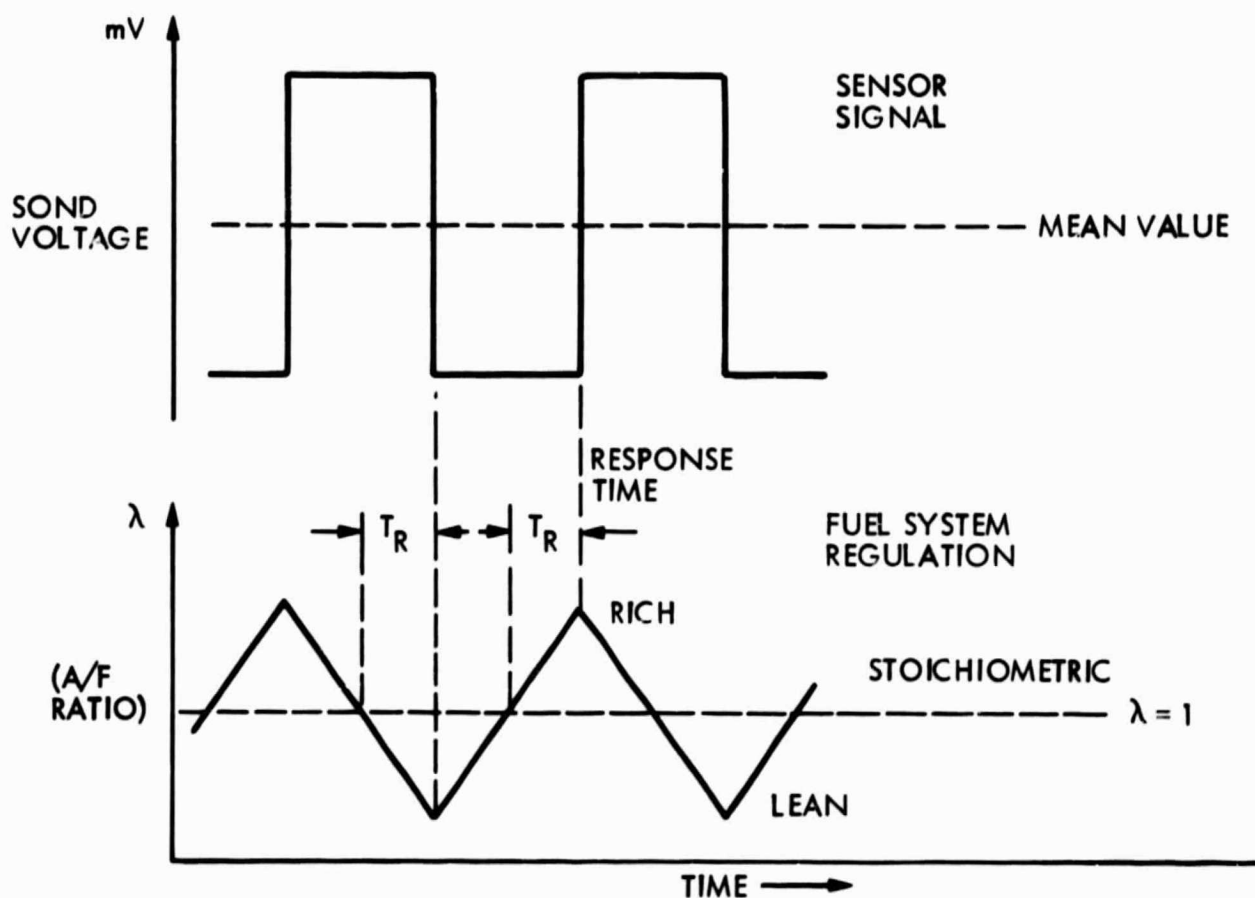


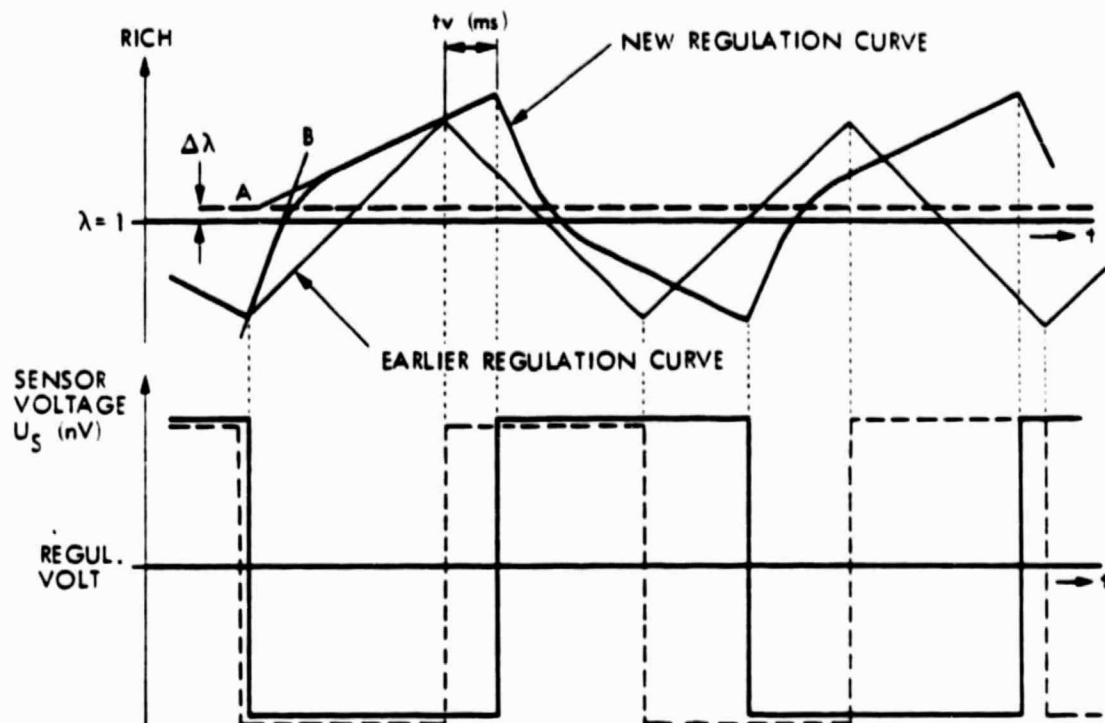
Figure 2-28. Sensor Signal and Integrator Characteristic (Ref. 24)

crease in sensor output voltage at stoichiometric conditions ($\lambda = 1.0$). To further minimize sensor drift with aging, the switching voltage for the sensor was left at 500 mV. This caused the system to run lean by an amount. A compensating correction was made by adding a time delay (t_V), to the enrichment pulse of the integrator regulation curve shown in Figure 2-29. This compensation raised the average air-fuel ratio by an amount ($\Delta\lambda$) toward the rich side. It was also found that additional benefits could be obtained by changing the regulation curve to one based on two straight lines of different slopes, as shown in Figure 2-29. Thus, at high engine speeds with short response times, the steeper part of the regulation curve leads to a slight power enrichment and a more rapid engine response under transient operating conditions, and at low speeds the longer response time ensures that the flatter part of the regulation curve prevents excursions over the rich and lean limits which can cause poor catalyst performance and erratic engine idling.

Another fuel-injection-based system (Refs. 23 and 26) which has been developed and marketed in Japan by Nissan Motor Co., Ltd., is called the electronic concentrated engine control system (ECCS). The system employs a microprocessor to electronically control fuel injection, spark timing, exhaust gas recirculation (EGR), and air intake during idling and deceleration. The combination of idle-speed control (ISC) and spark-timing control not only reduces maintenance but also makes idle speed and spark timing tamper-proof because they cannot be changed. This built-in control would also make it easier to meet the new California "anti-tampering" regulation and the reduced maintenance schedule allowed on certification vehicles.

The ECCS system installation is shown in Figure 2-30. This system is based on the Bosch L-Jetronic fuel injection system (Ref. 12). There are a number of sensors which provide the necessary input information to the microprocessor. The air-flow sensor is of the same flap type as used in the L-Jetronic fuel injection system. The ECCS is also equipped with a crankshaft position sensor. The resolution ability of the crankshaft position sensor not only influences the accuracy of the spark timing but also determines the measurement of engine speed and fuel-injection timing. A magnetic pickup is used to sense the gear teeth on a toothed disk attached to the crankshaft. A crankshaft position signal is provided for each degree of crankshaft movement. Other signals sent to the microprocessor include engine coolant temperature, catalyst temperature, battery voltage, and oxygen-sensor output voltage. Several on/off signals are also employed.

A number of actuators receive information from the microprocessor and carry out the desired control function. The fuel supply is controlled by the pulse duration during which current flows the fuel injector. A vacuum modulator (VCM) unit controls both the EGR and auxiliary air control (AAC) valves. By modifying the on/off ratio of the output pulse train from the microprocessor control unit to the VCM unit, the solenoid valve in the VCM unit acts as a variable orifice and changes the leakage between atmospheric pressure and a constant depression source. This modulated vacuum moves the EGR and AAC valves as shown in Figure 2-31. The ECCS has a control unit which uses an 8-bit CPU and a custom-designed LSI HD46506 for input/output.



THE NEW REGULATION CURVE IS MADE UP OF TWO LINES (A AND B) WITH DIFFERENT SLOPES
 t_v - DELAY TIME, DETERMINES THE SHIFT OF THE CENTER LINE FROM $\lambda = 1$
 $t_v = 0$ GIVES A CENTER LINE OF $\lambda = 1$

Figure 2-29. Modifications to Regulation Curve (Ref. 24)

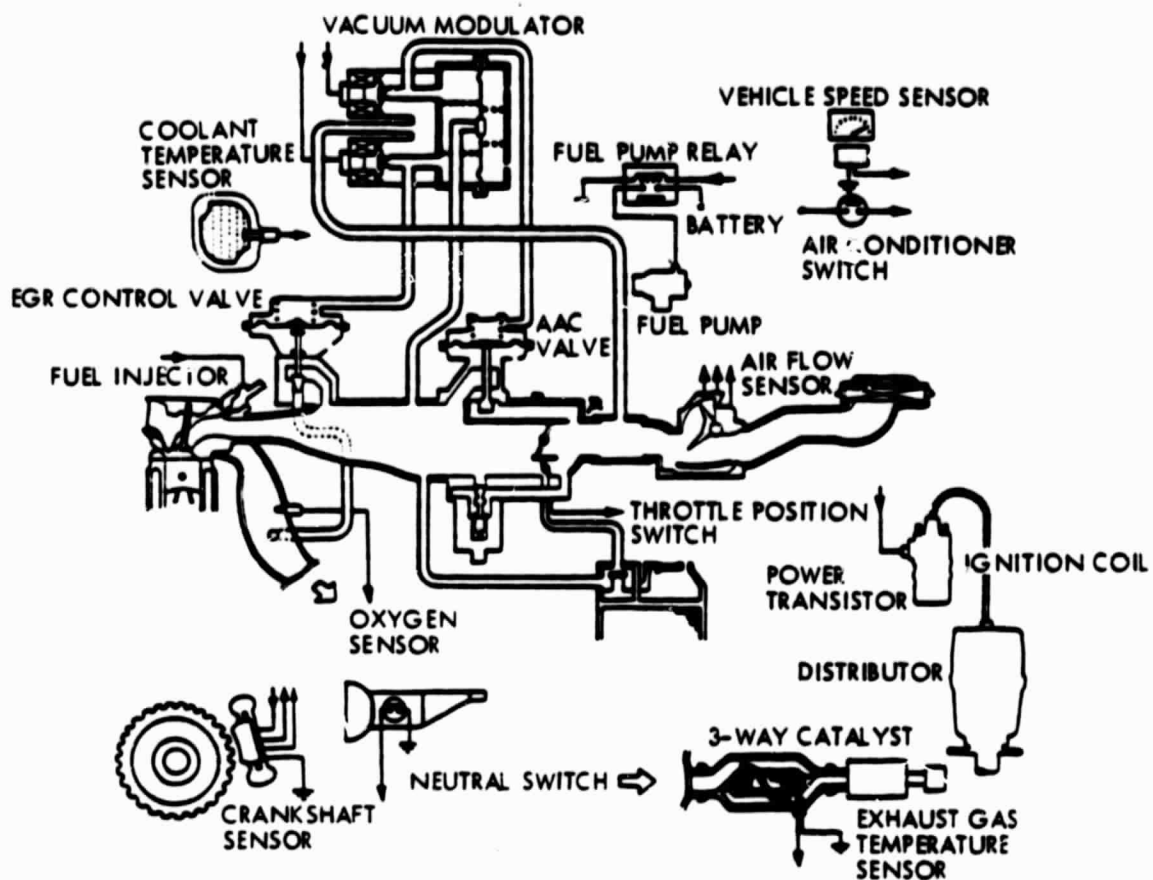


Figure 2-30. ECCS System Installation (Ref. 23)

The ECCS provides much flexibility in controlling air-fuel ratio, spark timing, EGR, and idle air-flow. By optimum calibration, tests have shown a 10% improvement in fuel consumption in the standard 10-mode Japanese driving cycle test. Control by the microcomputer system has improved performance, driveability, and exhaust emissions levels in transient conditions (e.g., engine warmup, gear shifts, standing start accelerations, low temperature starts, and high temperature restarts).

2.3.3 Systems with Carburetors

Development of three-way catalyst emissions control systems by U.S. automobile manufacturers have concentrated primarily on systems using carburetors as the fuel-metering element. One reason for this is the significantly lower cost of carburetors when compared with most fuel injection systems. Another reason is that U.S. automobile manufacturers have in the past used carburetors almost exclusively as the fuel-metering device on their automobiles and have close ties with the carburetor supply industries. Switching over to fuel-injection systems on their high-volume production models would require a large capital investment.

Carburetors, in general, provide less accurate control of air-fuel ratio than do fuel-injection systems. For this reason, three-way catalyst emissions control systems using carburetors frequently use a dual-bed catalyst system with EGR and air injection to achieve the necessary emissions levels. The tremendous recent advances in the use of microprocessors for engine control have helped make carburetor systems more practical because more engine variables can be monitored and controlled. Figure 2-31 details an idle speed control system.

Although a number of carburetor-based systems are in various stages of development, the General Motors Computer Controlled Catalytic Converter (C-4) system (Ref. 22) will be described here in more detail as a typical example of such a system. This carburetor C-4 system was first introduced on a limited number of 1979 California models and then extended to all California models with spark-ignition engines in 1980. An extended version of this system was introduced in 1981 to meet the more stringent emissions requirements.

The C-4 system provides a closed-loop carburetor control (CLCC) system to maintain air-fuel ratio near stoichiometry. The C-4 system has been used with both single-bed and dual-bed catalyst units. The first systems introduced included secondary air management control (SAMC). Expanded C-4 system capabilities include electronic spark-timing (EST), idle-speed control (ISC), controlled-canister purge (CCP), torque-converter clutch control (TCC), on/off control of exhaust gas recirculation (EGR) and early fuel evaporation (EFE), and system self-diagnostics (SSD). The evolution of the C-4 system and its utilization on various models is shown in Figure 2-32.

The C-4 system has been implemented on production vehicles with the dual-bed three-way catalyst units which use the first bed for reduction of exhaust gases (NO_x conversion) and the second bed with injected air for

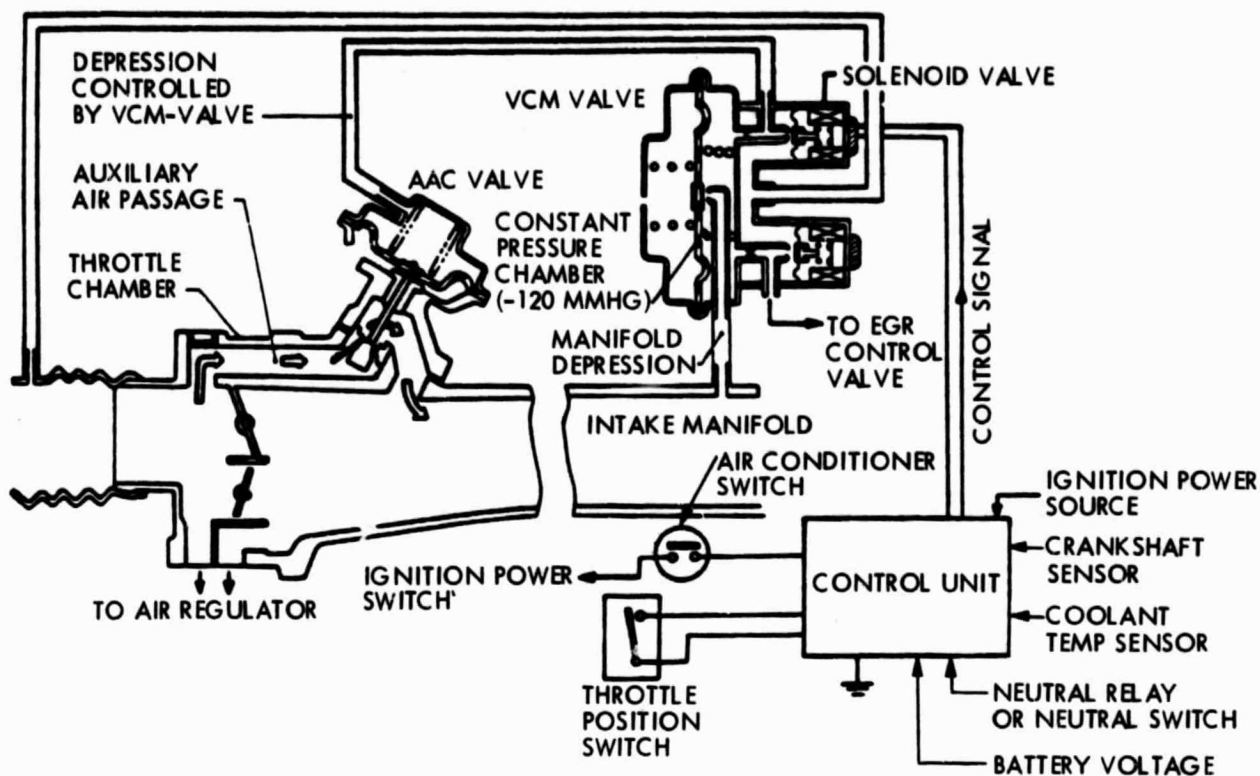


Figure 2-31. Cutaway View of Idle Speed Control System (Ref. 23)

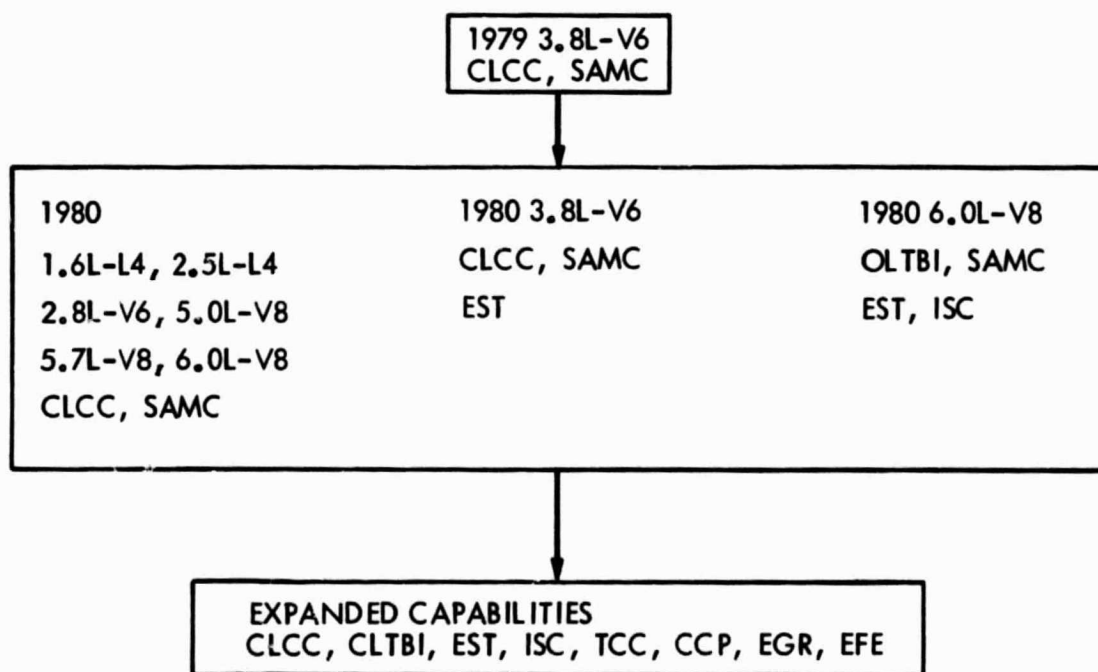


Figure 2-32. C-4 System Evolution (Ref. 22)

further oxidation of exhaust gases (CO and HC conversion). The dual-bed system has a more extensive air management system, with secondary air being switched between the catalyst unit and the engine exhaust manifold.

The basic C-4 control system is shown in Figure 2-33. Its operation is quite similar to that previously discussed for systems with fuel injection. The oxygen sensor sends a signal to the electronic control module (ECM) indicating whether the exhaust mixture is rich or lean. The ECM then generates and sends an appropriate corrective signal to the carburetor which adjusts the air-fuel ratio. As long as a rich or lean mixture is indicated, the carburetor control signal integrates in the corrective direction at a fixed rate. When the oxygen sensor indicates a change in the mixture (rich to lean or lean to rich), the control signal from the ECM to the carburetor steps in the opposite direction of the previous signal and begins to integrate in the new corrective direction, as illustrated in Figure 2-34.

As previously discussed, the regulation curve (i.e., integrator and step calibrations) should vary with total system response time. The total system response time is determined primarily by the transport time, which is a function of engine speed and load. To provide this compensation, the C-4 system includes the capability for two levels of gain scheduling (integrator and step) with engine speed, as shown in Figure 2-35, with expansion up to 16 levels as a function of engine speed and load inputs (indicated by manifold pressure or throttle position).

An additional feature of the C-4 system is adaptive control. The adaptive control algorithm stores a time-weighted function of the carburetor control signal in ECM memory, while the engine is operating in a defined speed-load area. When the engine operating area changes via an engine speed or load change, the adaptive memory function assigned to the new operating point is used to activate the integrator and thereby the carburetor control signal.

This form of closed-loop control produces a carburetor control signal oscillation or limit cycle about stoichiometry. The amplitude and frequency of the limit cycle are determined by engine transport delay time and system calibration. The C-4 system compensates for this condition by using variable gain scheduling as a function of engine speed and load so that the limit cycle amplitude can be minimized.

In addition to closed-loop operation, the C-4 system also operates in the open-loop enrichment and inhibit modes under certain conditions. The inhibit mode is used during engine starting to turn off ECM outputs and let the carburetor provide a rich mixture to the engine. The enrichment mode provides a richer mixture at high engine loads. The open-loop mode provides a transition between the inhibit and closed-loop modes by providing carburetor control-signal scheduling as a function of coolant temperature, engine speed, and engine load.

The ECM has the additional capability of providing a continuously-powered memory (CPM) which retains the carburetor control signals calculated by the adaptive control feature even after the ignition is turned off. The CPM is

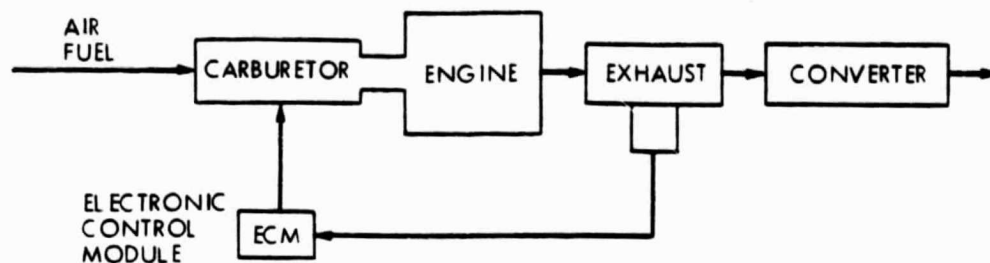


Figure 2-33. Computer-Controlled Catalyst Converter (C-4) System (Ref. 22)

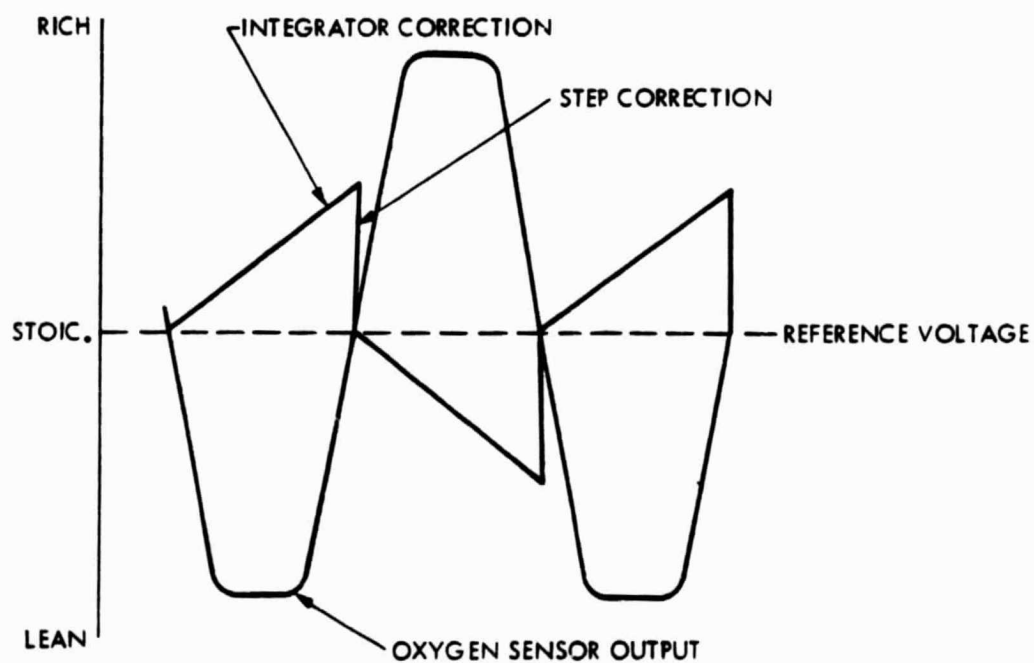


Figure 2-34. Integrator and Step Correction - Carburetor Control Signal (Ref. 22)

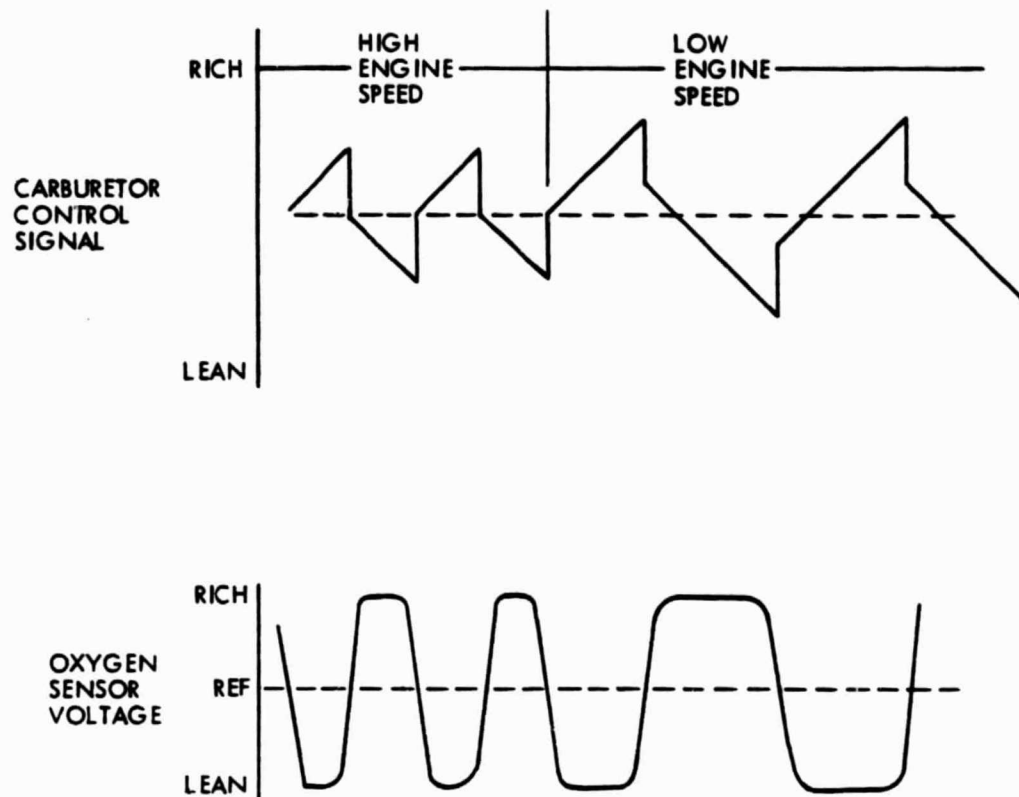


Figure 2-35. Gain Scheduling Feature (Ref. 22)

powered directly from the vehicle battery. The ECM in the C-4 system is a microprocessor-based control module containing input, processing, and output sections. The input section transforms the sensor signals into a format understood by the processing section. The input section interfaces both discrete (on/off) and analog signals with the processor area. The processor section consists primarily of a Central Processor Unit (CPU), a Program Memory - Read Only (ROM), a Calibration Memory - Programmable Read Only (PROM) and an Operational Memory - Random Access Memory (RAM). The central processor operates on instructions stored in the program memory. Input data and intermediate results are stored in the random access memory, as directed by the CPU. User-specified calibration constants are stored in the calibration memory for use by the CPU. The output section of the ECM uses primarily discrete outputs (on/off) except for the pulse-width modulated carburetor control signal and the electronic spark-timing signal in the expanded C-4 system.

The C-4 system carburetor is a modification of a previously available open-loop carburetor. A pulse-width modulated solenoid controls the carburetor fuel-metering function. As the pulse-width modulated control signal drives the solenoid from stop to stop, an average air-fuel ratio is generated based on the ratio of solenoid on-time to total pulse width period. The oxygen sensor and most other sensors in the C-4 system are similar to those previously described.

The basic C-4 system provides control of the secondary air used in the converter unit. The secondary air is directed to the engine exhaust manifold during open-loop operation via an ECM output to a control valve. During closed-loop operation, the air is directed to the dual-bed converter or into the air cleaner for silencing. The EGR system is controlled only in an on/off way. Once the engine is running, the EGR is enabled based on coolant temperature and engine load. The EGR will be enabled if coolant temperature is greater than a specified level and if the load is less than a specified level.

The C-4 system provides the flexibility for control of torque converter lock-up on those transmissions having this feature. First, the system checks coolant temperature, engine load and vehicle speed against a specified table of constraints to be sure that the necessary conditions are satisfied before engaging the transmission clutch.

An idle-speed control function is also provided with the C-4 system. The desired engine speed is specified as a function of coolant temperature, with some modification when the transmission is in park or neutral and when the battery voltage is low. The throttle is controlled during vehicle deceleration using available system information. Another condition covered is anticipation of the air conditioning and park/neutral-to-drive load changes. When there is an electrical indication that these loads are being applied to the engine, an anticipate pulse is issued to compensate for the effect of the change in load on engine speed.

The fully expanded C-4 system being developed by General Motors is given in Figure 2-36.

Toyota has developed a closed-loop secondary air (CSA) control system (Refs. 28 and 29) that differs from other three-way catalyst emissions control systems. In this CSA system, which was introduced in some 1981 models, the air-fuel ratio is not controlled in the engine intake mixture but instead in the exhaust. A block diagram of the CSA system is shown in Figure 2-37. The carburetor is conventional except the air-fuel ratio is adjusted slightly richer than stoichiometric. An oxygen sensor monitors the exhaust air-fuel ratio and adjusts an air control valve (ACV) through an electronic control unit (ECU) and a vacuum-switching valve (VSV) to inject secondary air to adjust the exhaust air-fuel ratio to stoichiometric. This produces a short control loop which results in a high oscillation frequency and a rapid correction ability for maintaining the air-fuel ratio at stoichiometric conditions. This gives the CSA system a higher conversion efficiency for the gaseous pollutants, as shown in Figure 2-38, which gives the conversion characteristics of a three-way catalyst for various oscillation frequencies and amplitudes. The slightly richer intake air-fuel ratio used in the CSA system results in better vehicle driveability and lower NO_x emissions, but with some loss in fuel economy.

The secondary air control mechanisms of the CSA system are shown in Figure 2-39. When the exhaust air-fuel ratio is richer than stoichiometric, the ECU activates the VSV according to the oxygen sensor output. When the VSV is in the "on" position, intake manifold vacuum is supplied to the ACV and the diaphragm lifts the valve which increases the flow of secondary air into the exhaust. When the oxygen sensor detects a lean air-fuel ratio in the exhaust, the VSV is switched to the "off" position, and atmospheric air is supplied to the ACV. The valve then closes and the flow of secondary air into the exhaust is reduced.

The air-fuel ratio oscillation frequency, as represented by oxygen sensor output voltage, is higher on the CSA system than for a corresponding closed-loop air-fuel ratio control system (fuel injection). The reason for the higher air-fuel ratio oscillation frequency is explained in Figure 2-40. In the CSA system, the shorter oxygen sensor response time (T_1) and shorter transit time (T_7) result in a shorter total response time than for a fuel injection system. The shorter oxygen sensor response time results from the wider air-fuel ratio amplitude of the CSA system. The resultant higher air-fuel ratio oscillation frequency more than compensates for the wider air-fuel ratio amplitude and gives higher catalyst conversion efficiencies (Figure 2-38). The oxygen sensor response time and the ACV delay time of the CSA system comprise the bulk of the total system response time and hence determine the air-fuel oscillation frequency.

2.3.4 Systems with Throttle-Body Injection

To meet the more stringent emissions standards, most automobile manufacturers are going to three-way catalyst emissions control systems with closed-loop feedback control. In such systems, throttle-body injection provides a measure of better air-fuel ratio control than carburetor systems

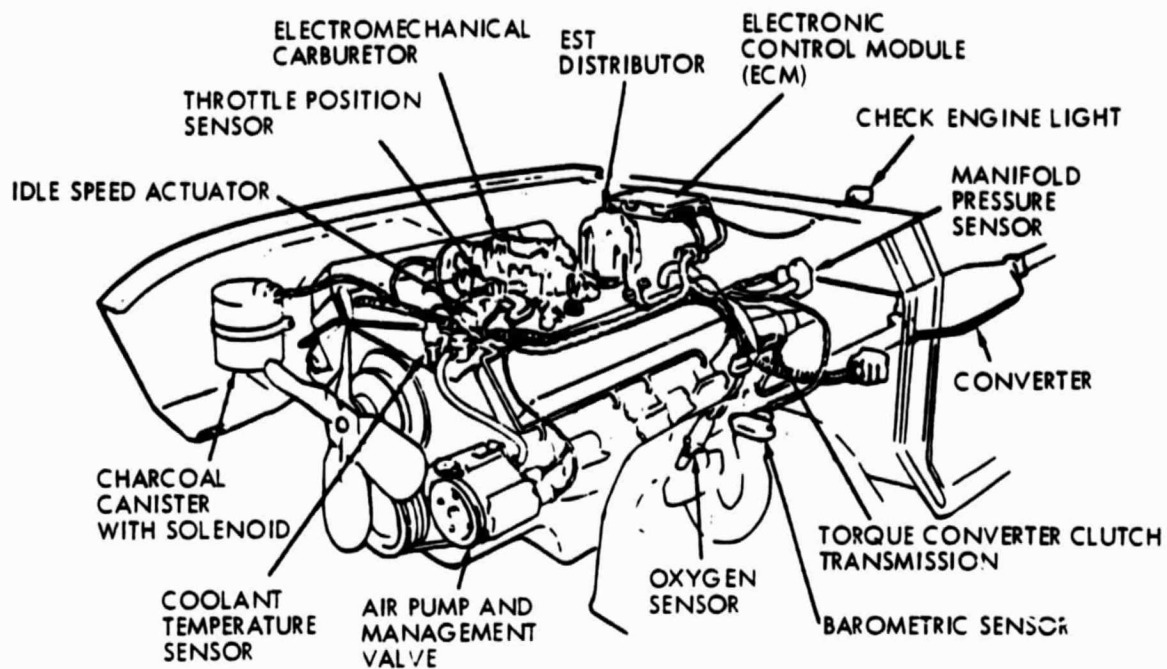


Figure 2-36. Fully Expanded C-4 System (Ref. 22)

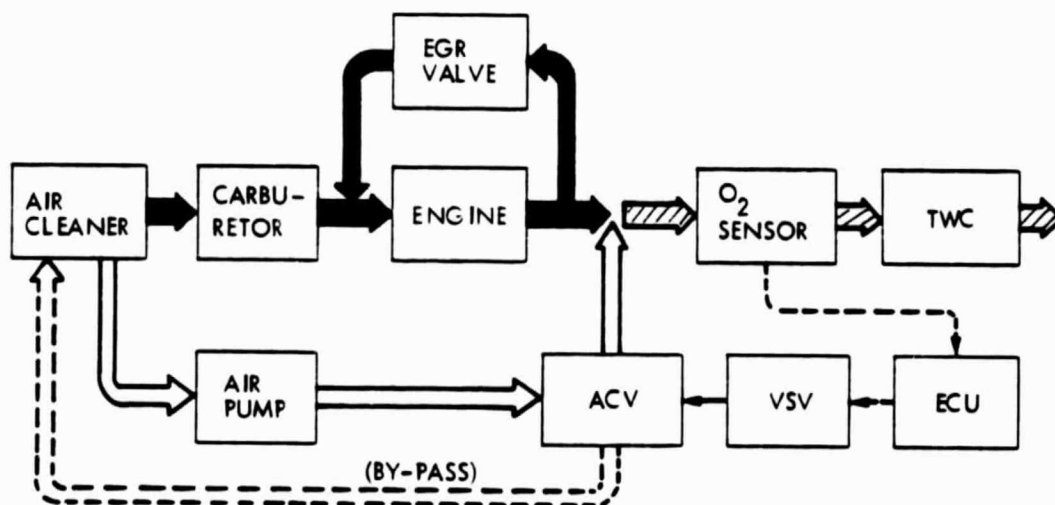


Figure 2-37. Block Diagram of Closed-Loop Secondary Air Control Three-Way Catalyst System (USA System, Ref. 26)

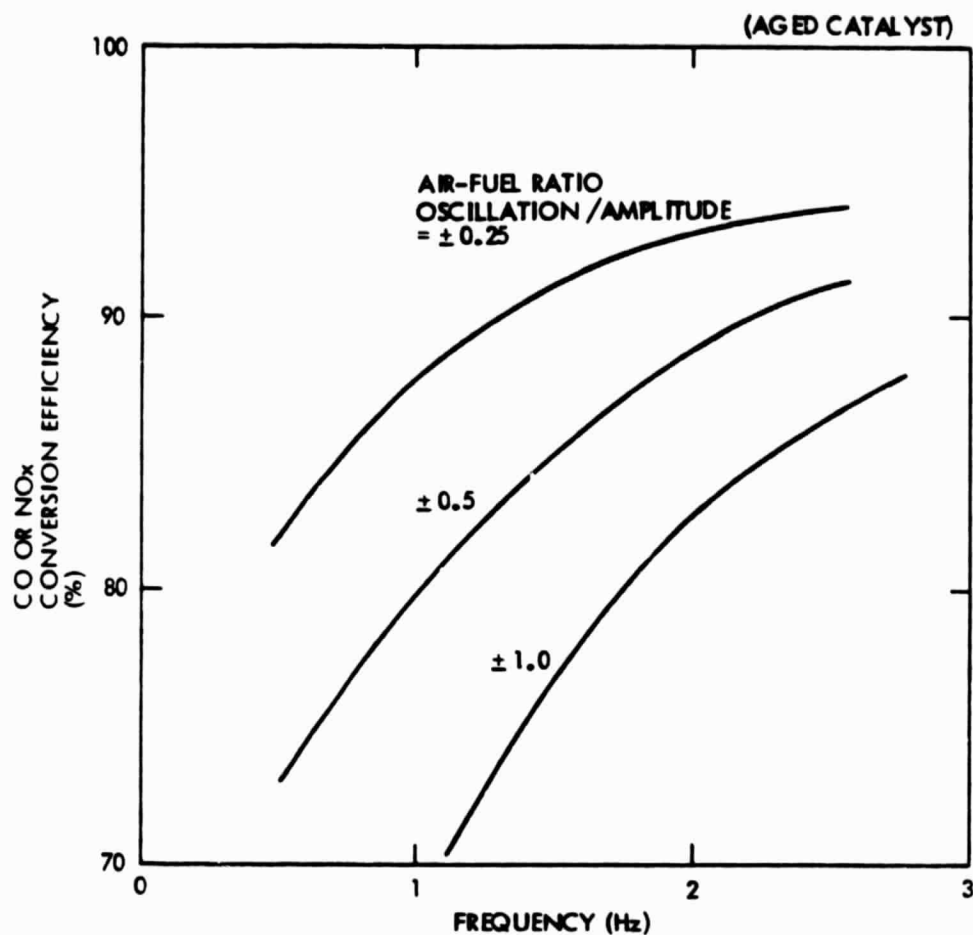


Figure 2-38. Relation Between Three-Way Catalyst Conversion Efficiency and Oscillation Frequency of Air-Fuel Ratio with Three Cases of Oscillation Amplitude (Ref. 28)

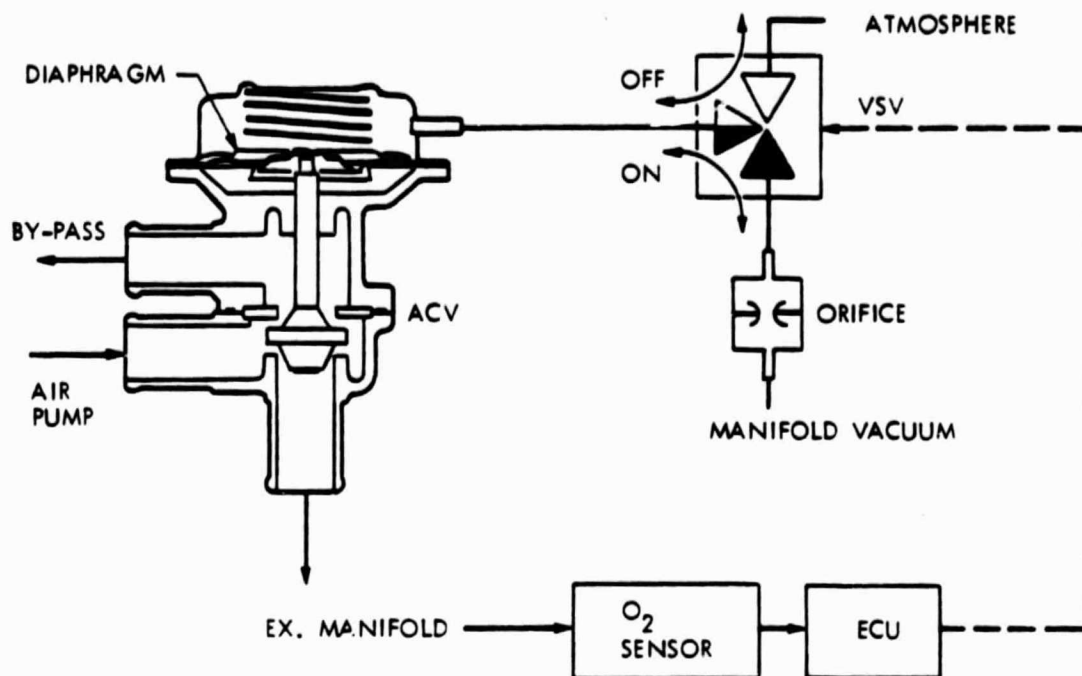


Figure 2-39. Secondary Air Control Mechanisms of CSA System (Ref. 28)

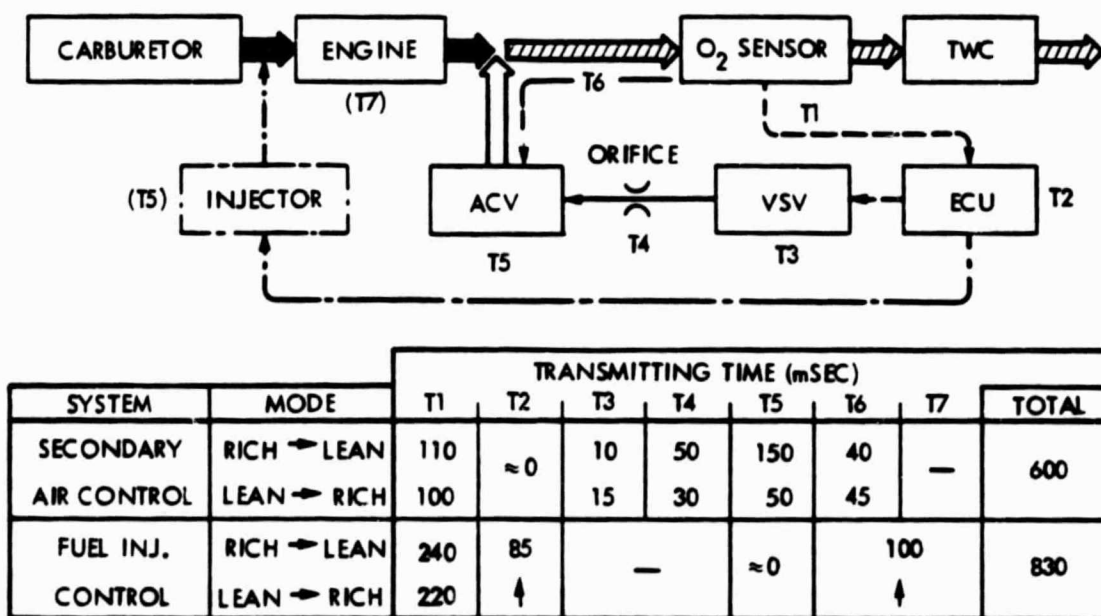


Figure 2-40. Signal Transmitting Time of Each Component at 40 km/h (Ref. 28)

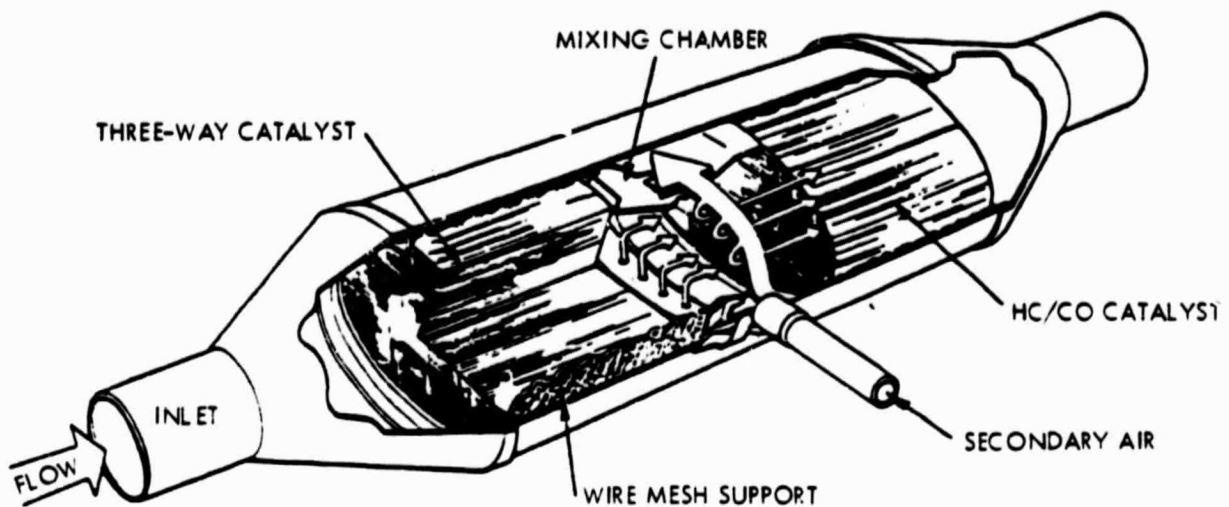
and is also more easily adapted to closed-loop control Throttle-body injection (TBI) systems are considerably less expensive than the individual-cylinder, high-pressure, port-injection systems used on some engines.

The TBI system introduced on 49-state Cadillac Eldorados and Sevilles in 1980 was discussed in the section on fuel/air mixture preparation. In 1981 models, the TBI system (Refs. 20 and 30) is standard on all Cadillacs equipped with the new variable displacement V-8-6-4 engines. As previously discussed, the Cadillac TBI system is a speed-density system which uses a throttle-body assembly with two electronically-pulsed fuel injectors operating at low pressure (10 psi). Each injector feeds four cylinders of the engine. A digital microprocessor provides all the computational capability for engine controls, including spark-timing, fuel metering, and idle speed. When the microprocessor receives information from the engine sensors, it computes the spark timing and air-fuel ratio required, then controls the amount of fuel delivered by the two pulse-width injectors.

As a pilot program, central fuel injection (CFI) was introduced on 1980 Lincolns (Ref. 31) for all 50 states. The fuel metering is controlled by Ford's third-generation electronic engine control (EEC-III) system (Ref. 32). Sensors monitor manifold absolute pressure, barometric pressure, coolant temperature, throttle position, EGR valve position, crankshaft position, and oxygen content in the exhaust stream. Sensor signals are assimilated by the microprocessor which uses table lookup and interpolation to compute optimal settings of spark advance, EGR flow, secondary air, and air-fuel ratio.

Emissions are controlled by a single converter operating in two distinct catalytic modes, as shown in Figure 2-41. A three-way catalyst bed lies immediately upstream of a conventional oxidizing catalyst unit, with the two separated by a secondary air injection port and mixing chamber. An oxygen sensor in the right-bank exhaust manifold gives input to an air-fuel ratio feedback control of the CFI system. The CFI system has two electrically-actuated fuel-metering injectors, which spray fuel into the engine's intake air stream when energized, as shown in Figure 2-42. Fuel is supplied from the tank by an electric pump, and fed to the injectors through a regulator which maintains supply pressure at a constant 39 psi. Excess fuel is returned to the tank through a return line. The fuel injectors are mounted above the throttle plates, within an air-throttle body. The amount of fuel injected is determined by the pulse length or the amount of time the injectors are energized. Frequency of injection is constant at four pulses per engine revolution, so only the pulse length is varied.

Chrysler introduced an electronic fuel injection (EFI) system (Ref. 30) on the 1981 Imperial models. This system is significantly different from the other two systems described in that the Chrysler system uses a continuous flow method of EFI, and incorporates both air-flow and fuel-flow sensors. The EFI system, which is shown in Figure 2-43, includes three major assemblies; (1) the fuel supply assembly, which includes an in-tank electric turbine pump and check valves, (2) the air cleaner, which carries the air flow sensor and the metering and ignition electronic control module, and (3) the throttle-



Note: Converter combines three-way catalyst bed, mixing chamber with secondary air injection, and downstream oxidizing catalyst. Three-way unit contains platinum/rhodium; oxidizing unit, platinum/palladium.

Figure 2-41. Three-Way Catalyst Bed Converter (Ref. 32)

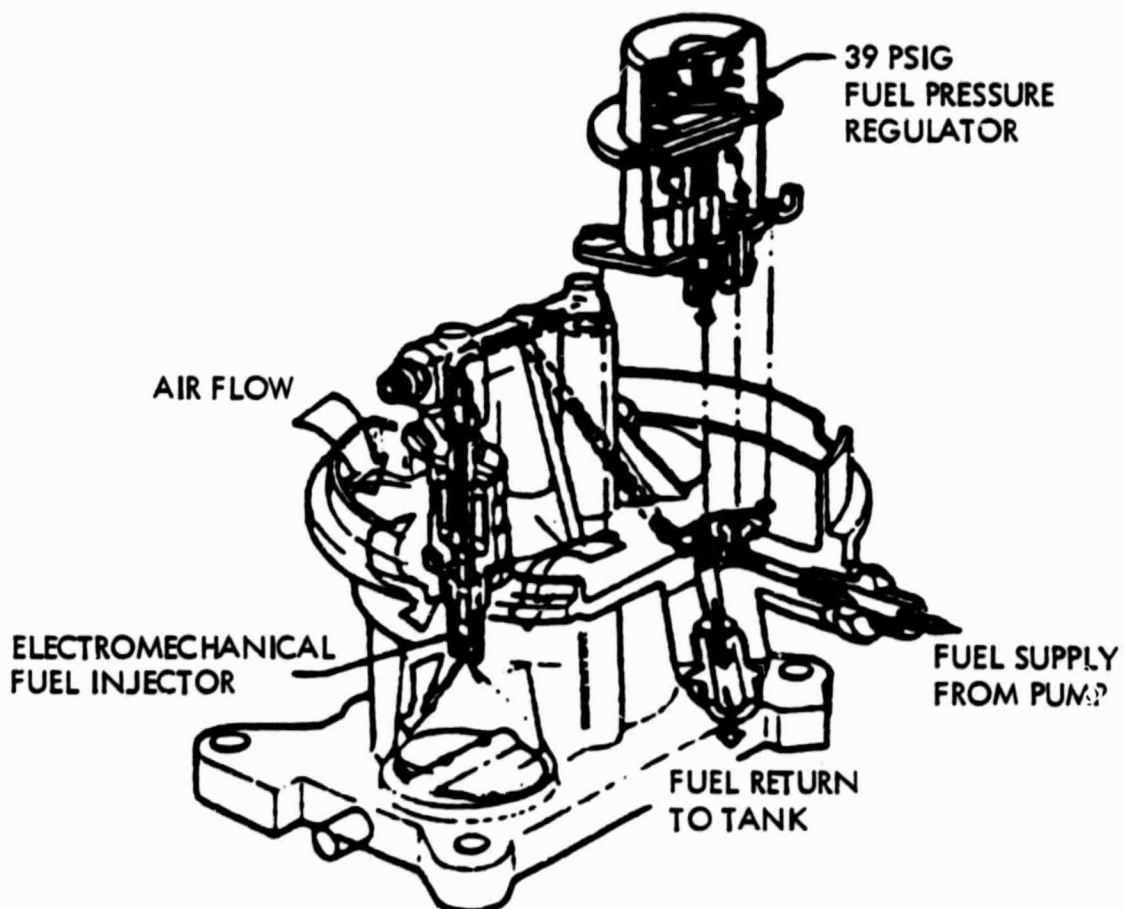
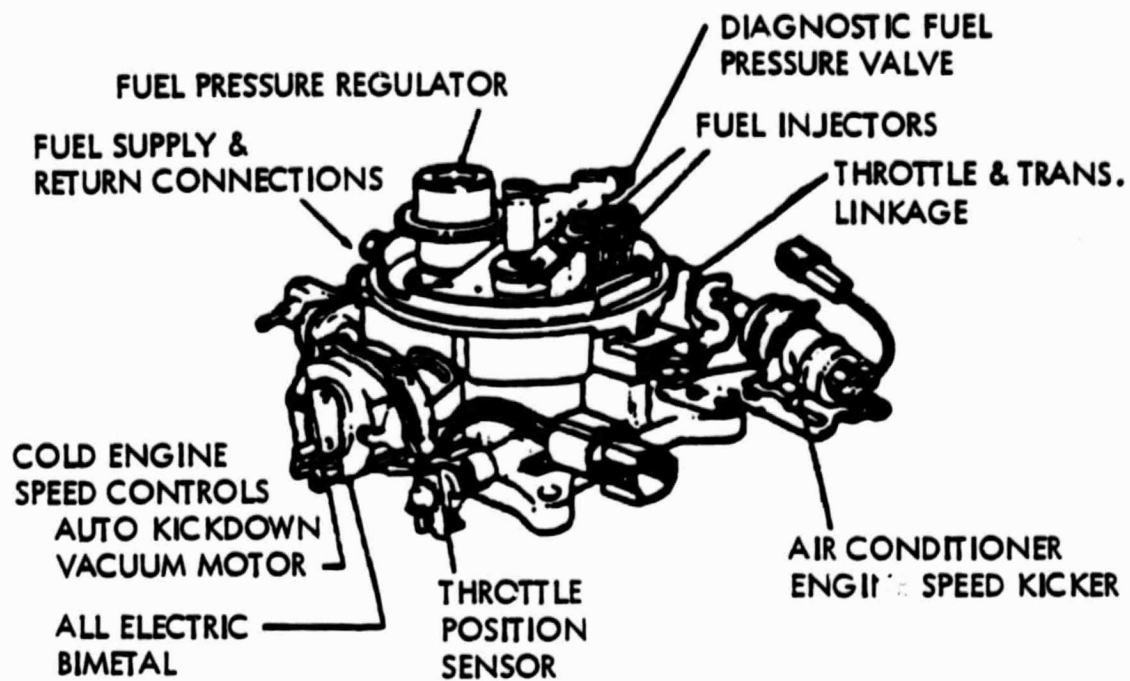
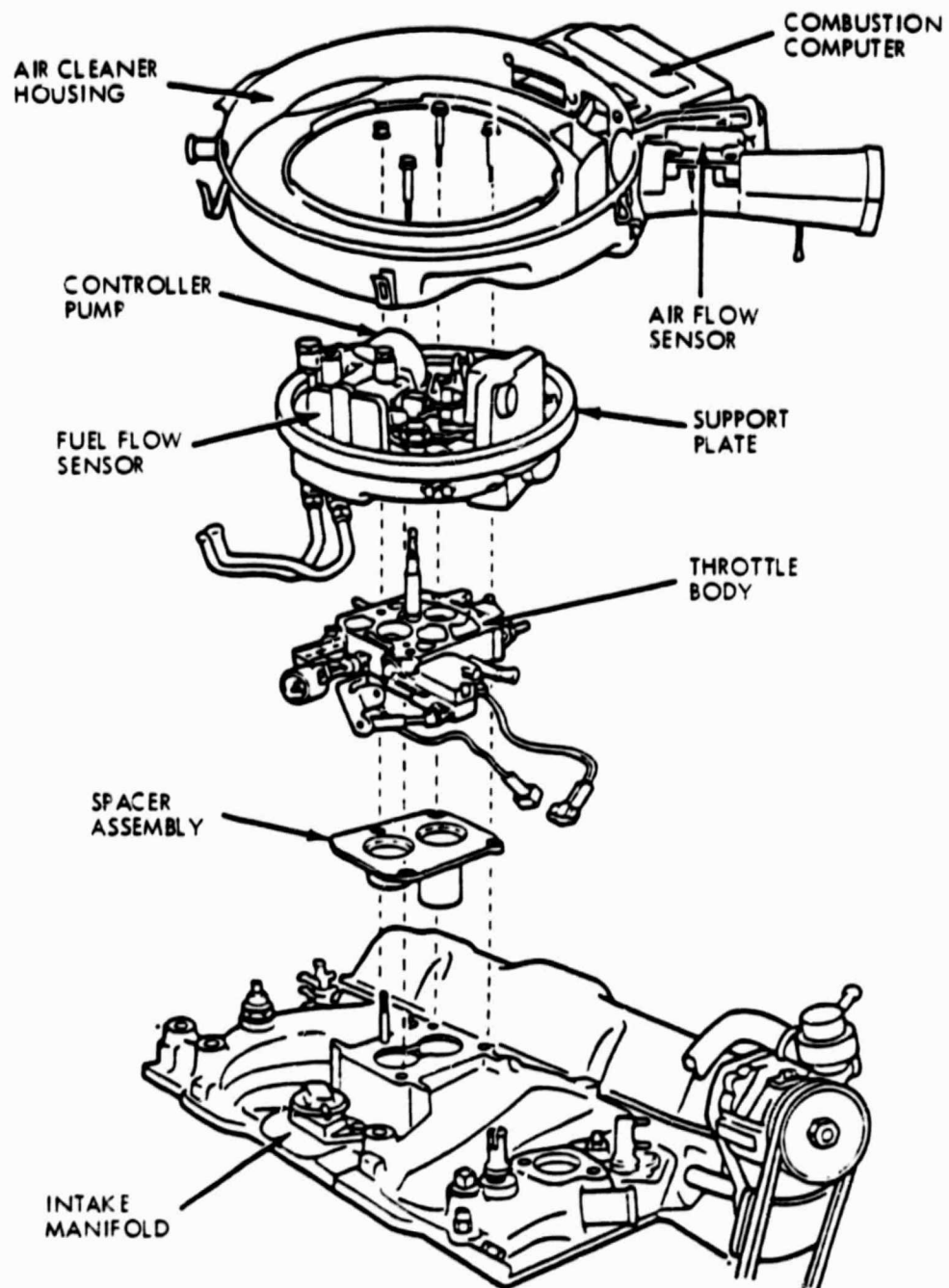


Figure 2-42. Electrically-Actuated Fuel-Metering Injectors for a CFI System (Ref. 31)



ELECTRONIC FUEL INJECTION

Figure 2-43. 1981 Chrysler Electronic Fuel Injection System (Ref. 30)

body and fuel-controller assembly, which includes the control pump, fuel-flow sensor, pressure-regulating valves, fuel spraybars, and automatic idle-speed motor.

The EFI and electronic spark-control functions are coupled with the Chrysler combustion-computer system, as shown in Figure 2-44. After receiving signals from the air-flow, fuel-flow, and oxygen sensors, the computer compares these signals to an ideal calibration. When any of the signals differ from the calibration, the computer sends a corrective signal to the control pump to supply more or less fuel. The control pump takes part of the fuel supplied by the in-tank pump and delivers it at 21 psi at idle through the fuel flow sensor and lower-pressure regulator valve, into the spraybar. Because the fuel openings in the spraybar are fixed, supply pressure is varied to increase fuel flow. At maximum speeds, the control pump delivers fuel at 60 psi. The main features of fuel metering element of the EFI system are shown in Figure 2-45. All fuel is introduced above the throttle blades. There are two fuel spraybars above each intake port, a primary bar for low fuel flow and a power bar for staged high fuel flow. The conventional butterfly throttle blades have a fuel film spreader mounted above the blades and a mixture deflector mounted below. An additional mixture deflector and mixing ring are located below the throttle blades to improve the cylinder-to-cylinder air-fuel mixture. The air-flow and fuel-flow sensors measure volumetric flow rate, and therefore three additional sensors supply the combustion computer with the information required to convert the volumetric readings to mass readings. Some comparative characteristics of the three throttle-body injection systems discussed above are summarized in Table 2-5. It is expected that other systems similar to these will be introduced if the field experience with these pilot systems is good.

Table 2-5. Comparative Characteristics of Throttle-Body Injection Systems

Vehicle	System Control	Injector Type	Fuel Flow Rate Control	Fuel Supply Pressure
Cadillac	Open Loop	Pulse	Pulse Length	10 psi
Lincoln	Closed Loop	Pulse	Pulse Length	39 psi
Imperial	Closed Loop	Continuous	Supply Pressure	21-60 psi

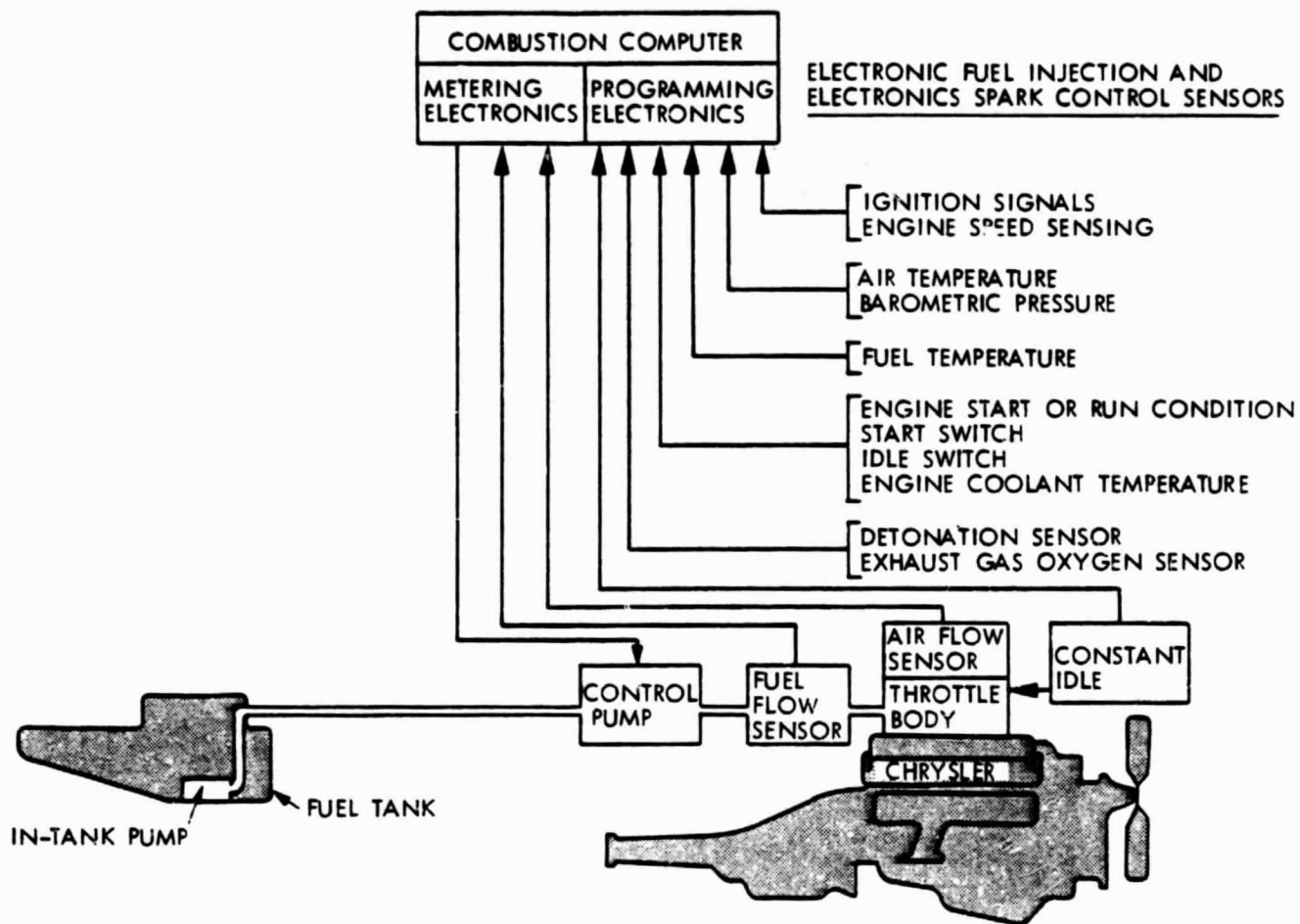


Figure 2-44. 1981 Chrysler Combustion Computer with Electronic Fuel Injection and Spark Control (Ref. 30)

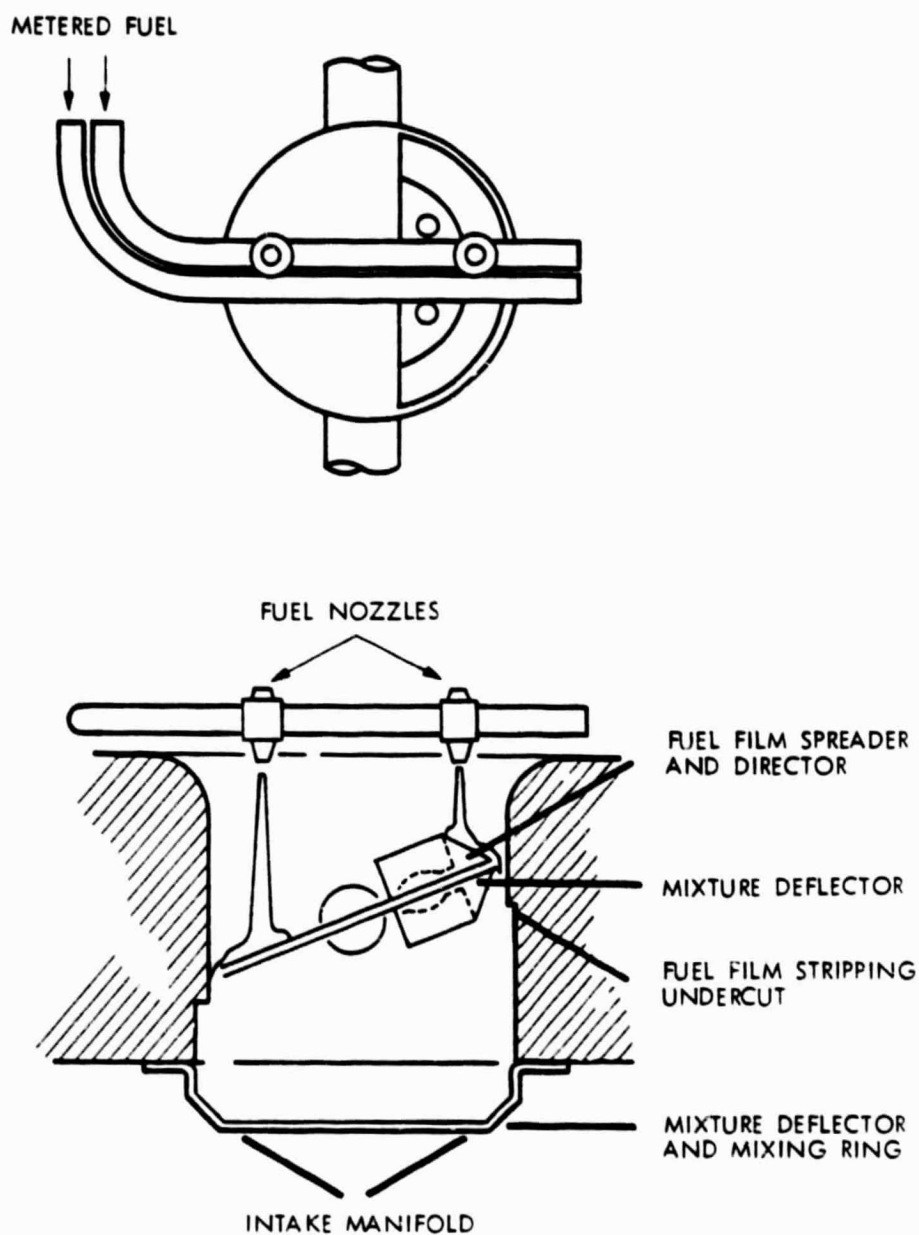


Figure 2-45. Main Fuel Metering Elements of 1981 Chrysler EFI System (Ref. 30)

2.4 VEHICLE FUEL ECONOMY AND EMISSIONS RESULTS

This section covers the fuel economy and emissions results for current production vehicles which use three-way catalyst emissions control systems. The data is taken from EPA certification and fuel economy data for the 1980 model year in California. California data is used because California emissions standards are felt to be more representative of future emissions requirements for all states.

Fuel economy over the urban (city) driving cycle is given in Figure 2-46 as a function of vehicle inertia weight. Data scatter is partially due to the fact that the data represent vehicles with 4-speed manual, 5-speed manual and automatic transmissions, as well as those with a range of rear axle ratios. The solid lines which represent the bounds for this data set are referred to later for comparison purposes. Similar fuel economy data for the highway driving cycle is shown in Figure 2-47. In this case, there is considerably more data scatter than for the urban cycle results. The difference in transmission type becomes more important in the highway cycle, with vehicles equipped with 5-speed manual transmissions showing significantly higher highway fuel economy than vehicles with other transmissions. Also, note that highway fuel economy is a stronger function of vehicle inertia weight than is the urban fuel economy. Composite fuel economy results are given in Figure 2-48 for California vehicles with three-way catalyst emissions control systems. The composite fuel economy is based on the harmonic average of urban and highway cycle mileages with weighting factors of 55% for the urban cycle and 45% for the highway cycle. Bounding lines are again drawn around most of the data. Data from California vehicles not using three-way catalysts for emissions control are shown in Figure 2-49. The bounding curves for three-way catalyst data from Figure 2-48 are included for comparison purposes. Where three-way catalyst systems are used on vehicles of all inertia weight classes, other emissions control approaches tend to be used primarily on lighter-weight vehicles. In lighter-weight vehicles, some vehicles without three-way catalysts show somewhat higher composite fuel economy than systems with three-way catalyst controls.

The previous discussions did not attempt to distinguish between vehicles having different levels of performance; however, this is an important consideration in making vehicle comparisons. Figures 2-50 through 2-53 show the previous fuel economy data expressed as inertia weight times MPG plotted versus horsepower divided by inertia weight (IW). In these figures, inertia weight is expressed in tons. Fuel economy in $IW \text{ (ton)} \times \text{MPG}$ is indicative of engine efficiency, and horsepower/IW (ton) provides a first-order indication of performance. These data show a significant spread in fuel economy at any given performance level. The solid lines again bound the data for vehicles using three-way catalyst emissions control and will be used later for comparison purposes.

Emissions characteristics for California vehicles with three-way catalyst emissions control are shown in Figures 2-54 and 2-55. Solid lines in the figures represent the 1980 California emissions standards and the Federal NO_x emissions research goal of 0.4 g/mi. These results indicate that 1980 California vehicles with three-way catalyst emissions control have controlled

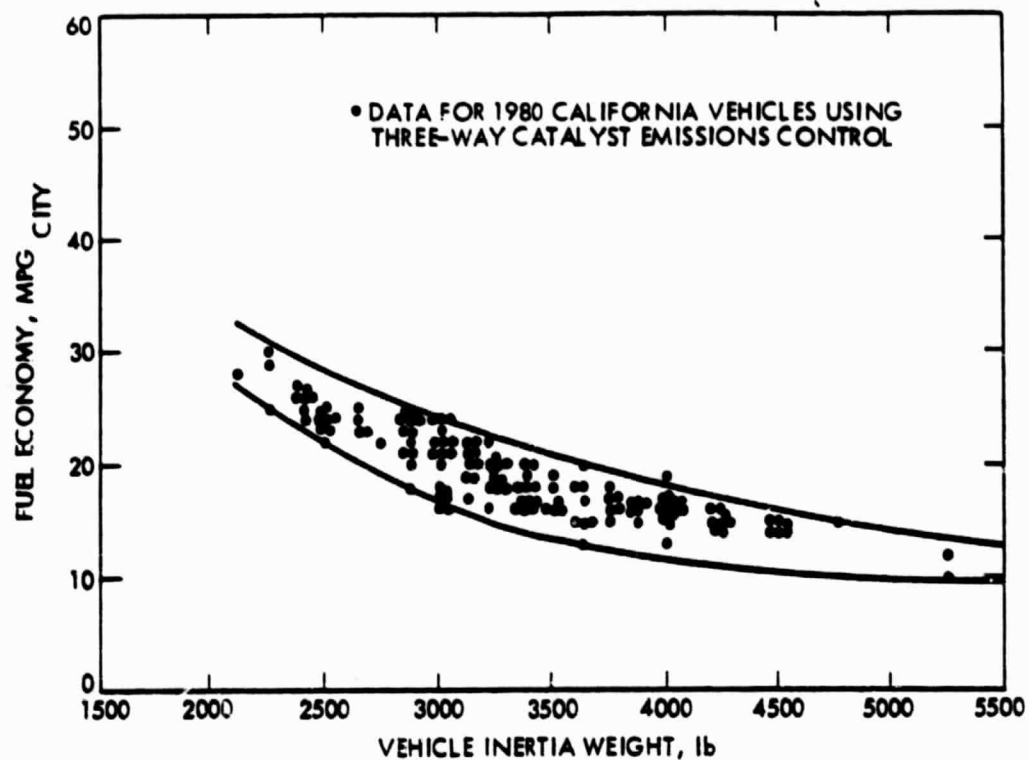


Figure 2-46. City Fuel Economy for Vehicles with Three-Way Catalyst Emissions Control Systems

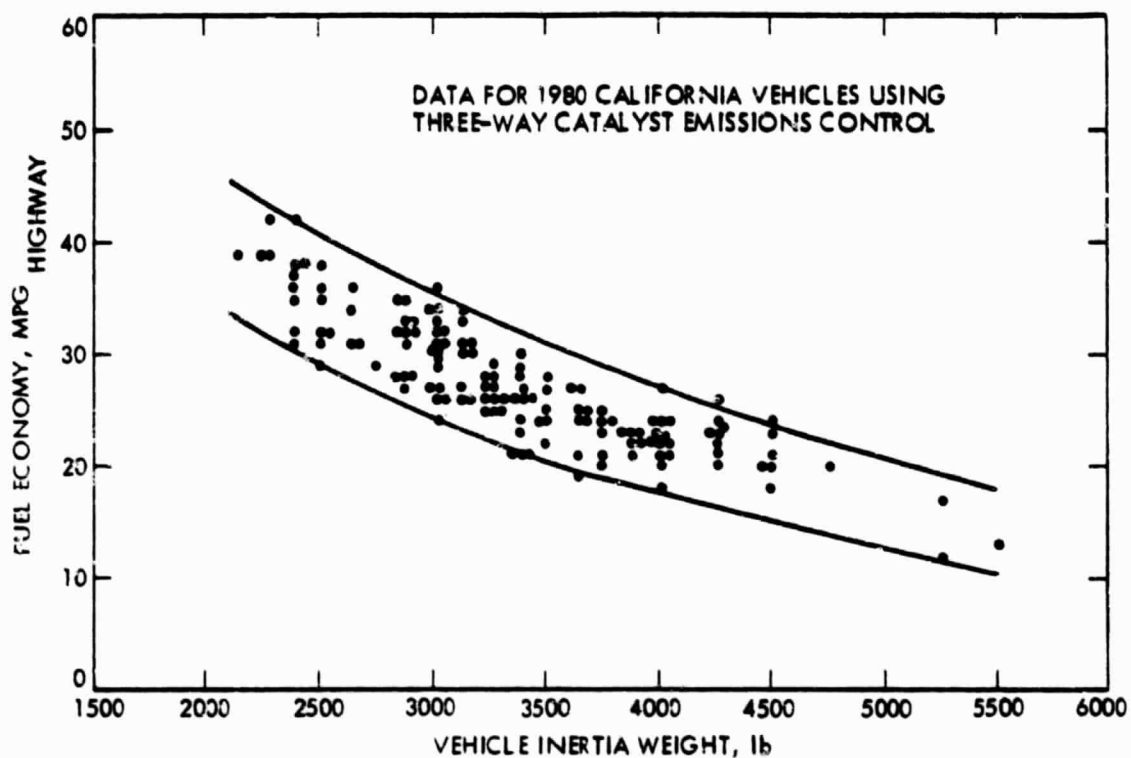


Figure 2-47. Highway Fuel Economy for Vehicles with Three-Way Catalyst Emissions Control Systems

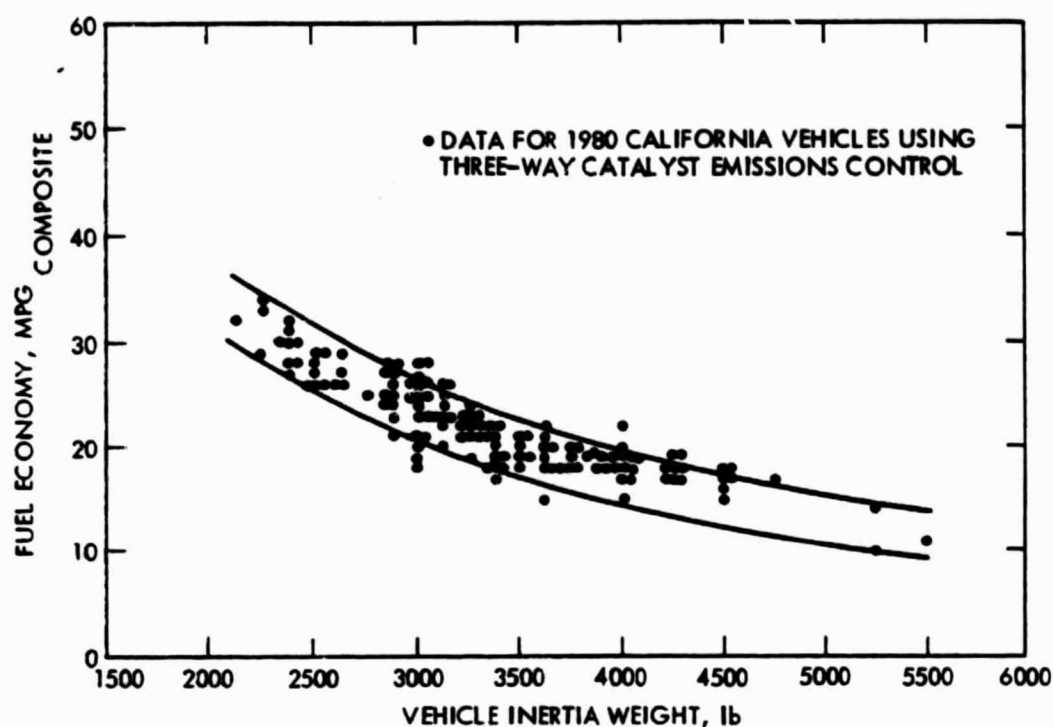


Figure 2-48. Composite Fuel Economy for Vehicles with Three-Way Catalyst Emissions Control Systems

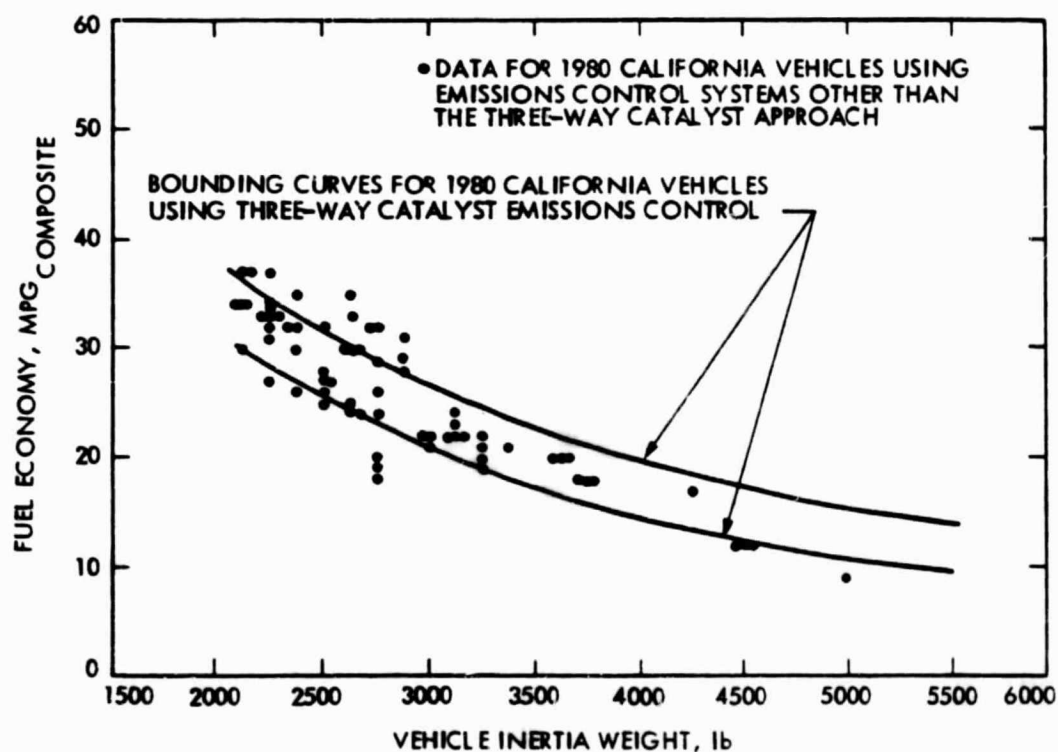


Figure 2-49. Composite Fuel Economy for Vehicles Without Three-Way Catalyst Emissions Control Systems

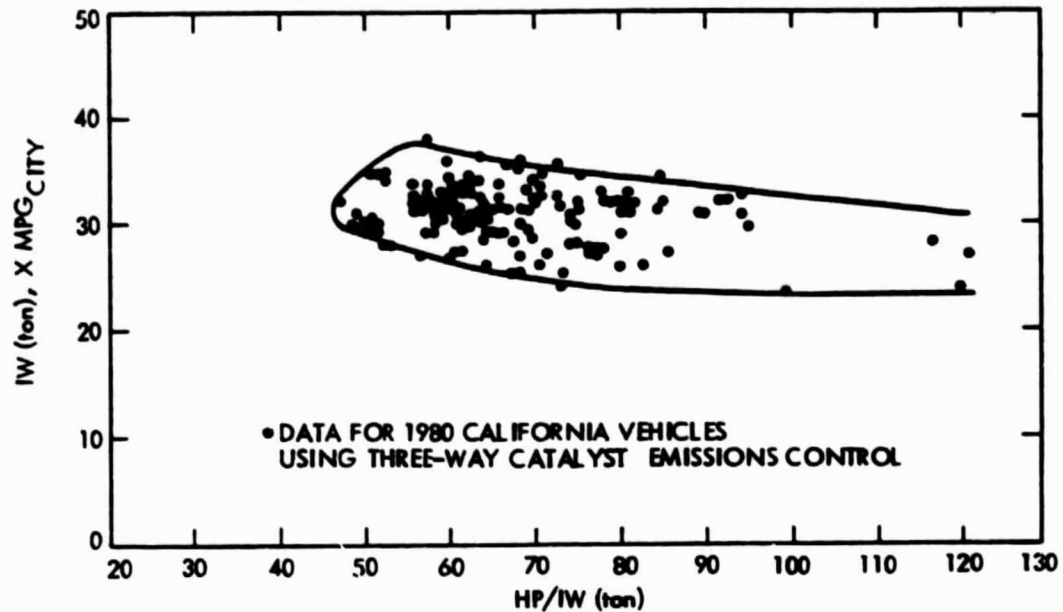


Figure 2-50. City Fuel Economy of Three-Way Catalyst Vehicles

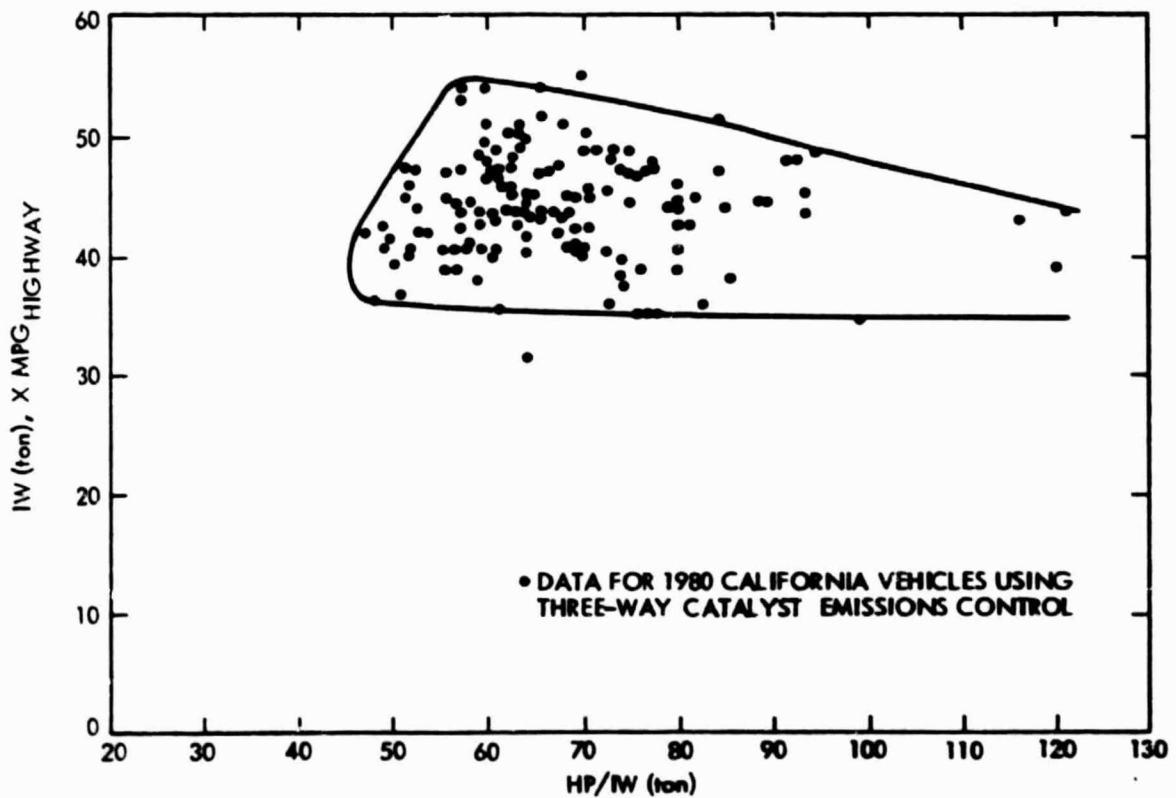


Figure 2-51. Highway Fuel Economy of Three-Way Catalyst Vehicles

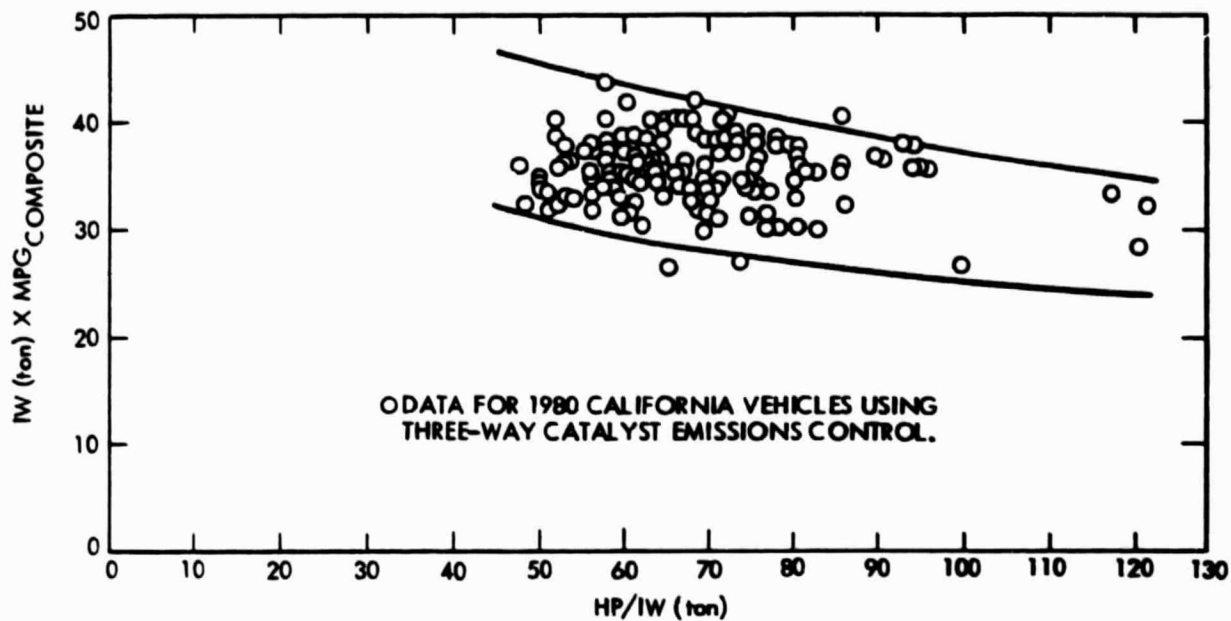


Figure 2-52. Composite Fuel Economy of Three-Way Catalyst Vehicles

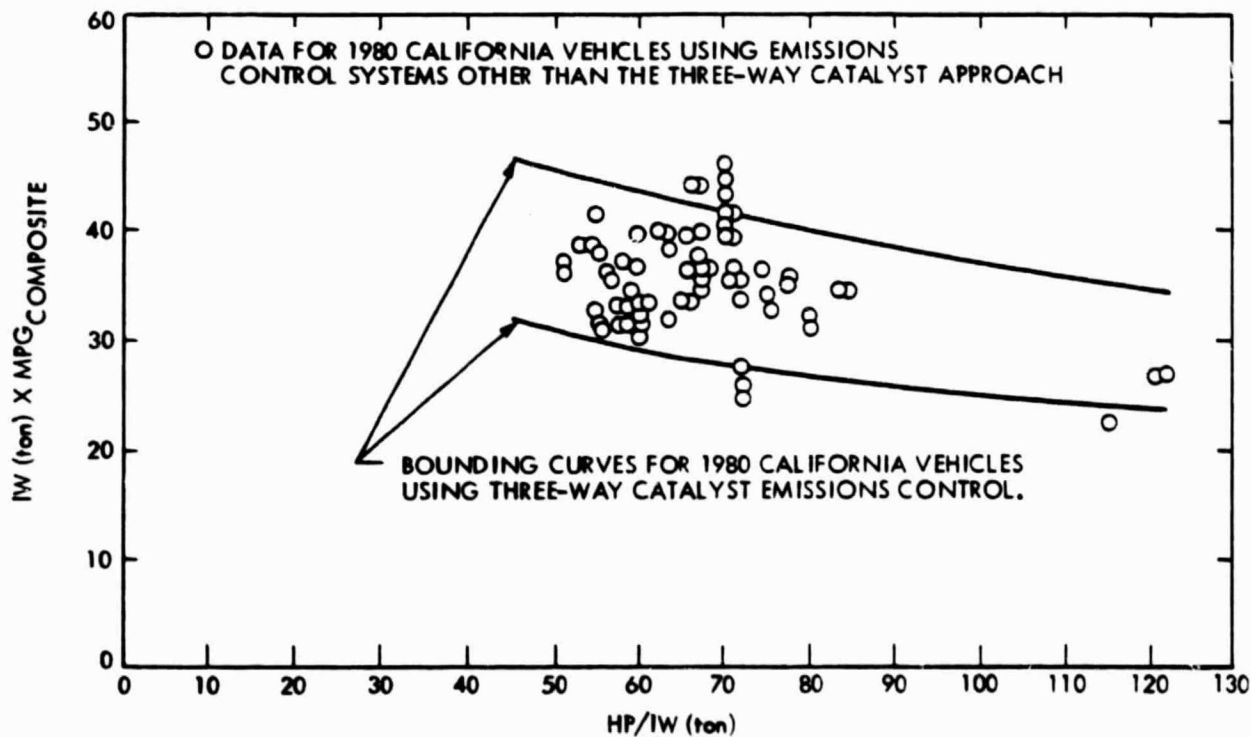


Figure 2-53. Composite Fuel Economy for Vehicles Without Three-Way Catalyst Emissions Control

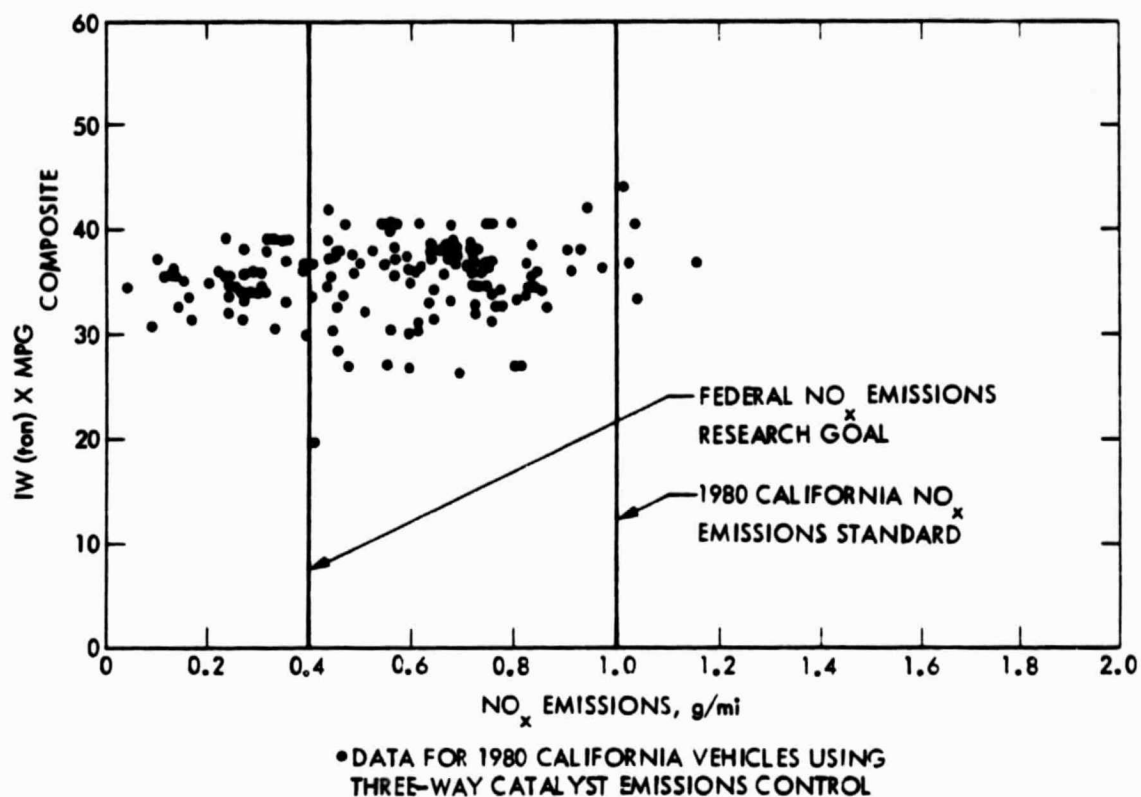


Figure 2-54. Fuel Economy Versus NO_x Emissions for Vehicles with Three-Way Catalyst Emissions Control

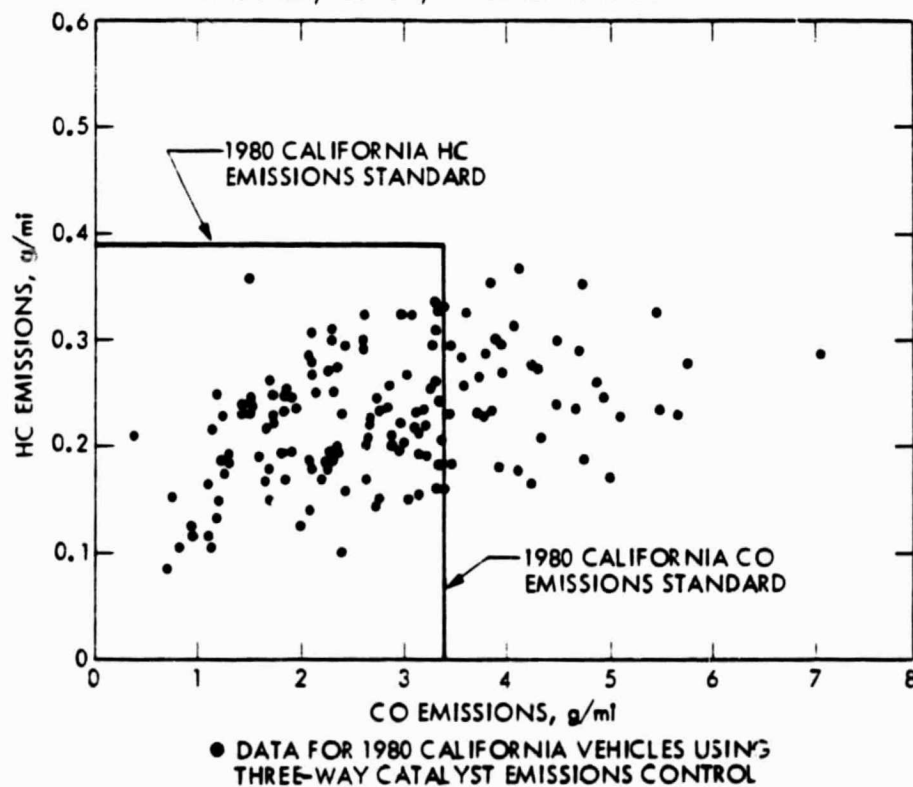


Figure 2-55. HC and CO Emissions Characteristics for Vehicles with Three-Way Catalyst Emissions Control

NO_x emissions from 1.2 g/mi down to 0.1 g/mi with no noticeable penalty in engine efficiency. It is important to note that most of the vehicles achieving NO_x emissions less than 0.4 g/mi had fuel-injected 4-cylinder engines and vehicle inertia weights of 3000 lb or less. The plot showing the HC and CO emissions characteristics does not imply any relationship between HC and CO emissions, but merely serves as a convenient means of presenting the data.

Fuel economy and emissions comparisons for California vehicles with three-way catalyst emissions control and 49-state vehicles with oxidation catalysts are given in Table 2-6 and Figures 2-56 through 2-58. Examination of these data show that vehicles with three-way catalyst systems calibrated to meet the more stringent California emissions requirements do not always suffer a fuel economy penalty relative to the 49-state versions with oxidation catalyst systems. In most instances the lower NO_x emissions in the California vehicle are accompanied by higher CO emissions than the 49-state vehicle. In Figure 2-58, the effects of an automatic overdrive (AOD) transmission with lock-up are shown. This transmission shows a slight fuel economy advantage on the highway cycle and no advantage on the urban cycle test based on this very limited data.

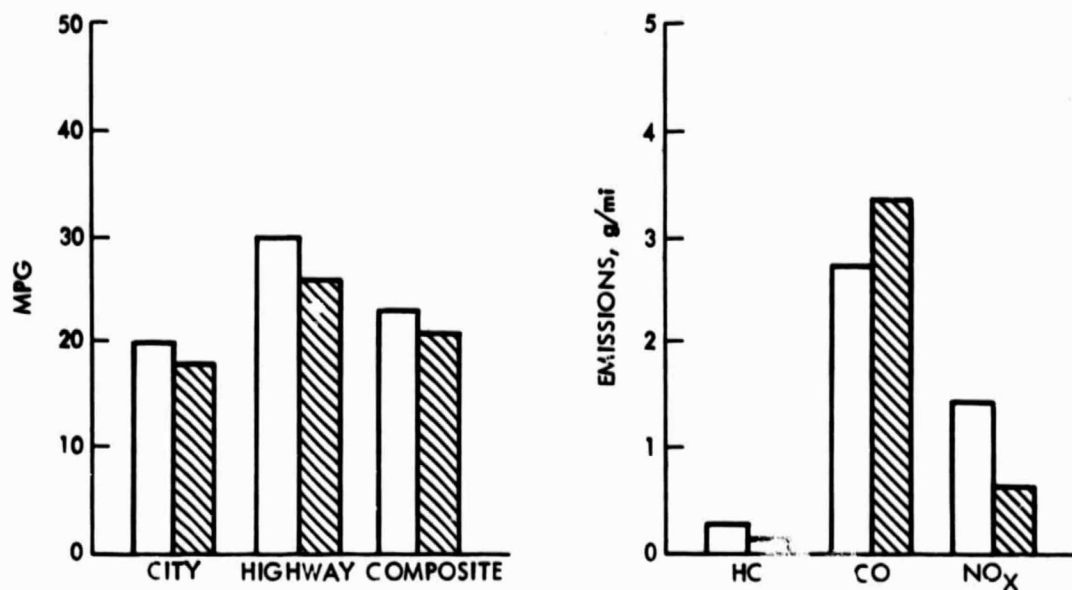
Three-way catalyst systems using fuel injection are compared in Figures 2-59 through 2-62 with those using carburetors for fuel-air preparation. Examination of these results shows no clear advantage of either fuel-air preparation system from a fuel economy standpoint. For those systems included on 1980 production automobiles, systems using fuel injection provide lower NO_x and CO emissions than carburetor-based systems. Some fuel economy penalty would be expected, in most cases, if carburetor systems were calibrated to achieve the lower NO_x and CO emissions levels which are presently being met by fuel injection systems.

Fuel economy and emissions results for the 1980 California Volvo vehicles are compared with the results for all 1980 California vehicles using three-way catalyst emissions control in Figures 2-63 through 2-66. This comparison is especially interesting because Volvo was the first automobile manufacturer to introduce the three-way catalyst emissions control system on a production vehicle. Examination of the fuel economy results indicates that the fuel economy of the Volvo vehicles is about equal to the average fuel economy for all vehicles using the three-way catalyst emissions control approach. The NO_x and CO emissions results for the Volvo vehicles are better than many other vehicles using three-way catalysts, with all but one Volvo vehicle meeting the 3.4 g/mi CO emissions requirement and well over one-half of the Volvo vehicles meeting the 0.4 g/mi NO_x research goal. Thus, the Volvo vehicles have some emissions control advantages, but no fuel economy advantages, over other three-way catalyst-equipped vehicles in California.

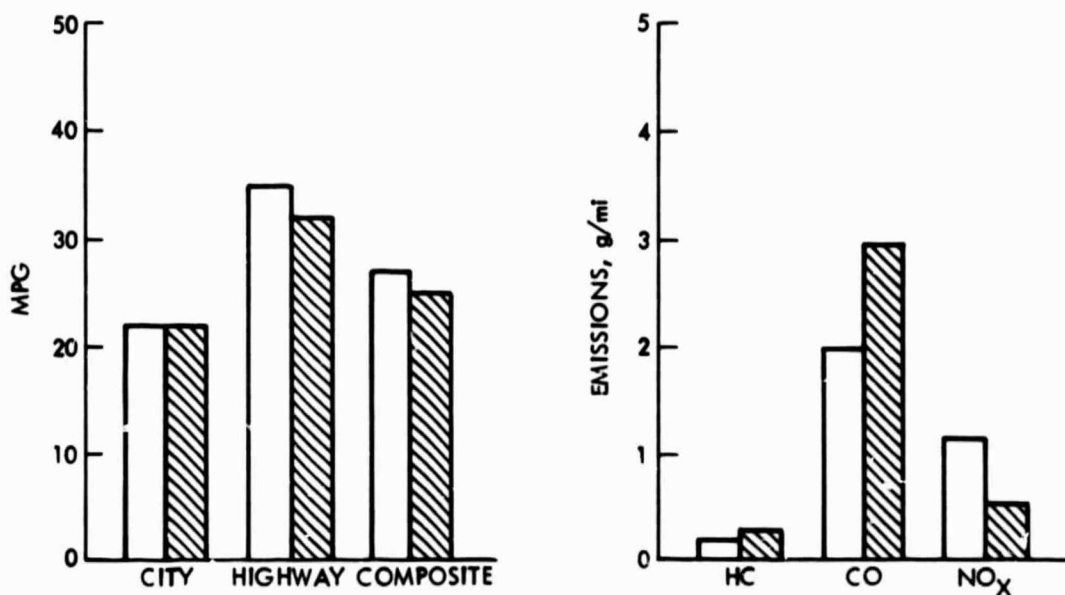
It is generally agreed that a closed-loop feedback control system is needed to provide the fuel-air ratio control needed for three-way catalyst systems to meet the most stringent emissions requirements. However, Mazda sold several 1980 California vehicles with three-way catalysts and open-loop carburetor fuel-air preparation systems. Fuel economy and emissions results for these Mazda vehicles are given in Figures 2-67 through 2-70. Notice that all of these vehicles are small, with a vehicle inertia weights less

Table 2-6. Comparison of Some California and 49-State Vehicle Characteristics

MFG	Car Line	CID	Carb. FI	Comp. Ratio	HP	Emission	Trans	Weight	Axle	City	Highway	Comb	HC	CO	NO _x	Ton x MPG Comb	HP/1W (ton)
Dodge	Chevy Citation (Cal)	173	C-2	8.5	115	EGR/PLS/ 3MY/CLS	A3-1	3000	2.84	18	26	21	0.160	3.40	0.64	31.50	76.67
	Chevy Citation (49-State)	173	C-2	8.5	115	EGR/PLS/ OXD	A3-1	3000	2.84	20	30	23	0.268	2.78	1.43		
	Chevy Citation (Cal)	151	C-2	8.2	90	EGR/3MY/ CLS	A3-1	2875	2.84	22	32	25	0.222	2.93	0.48	35.94	62.61
	Chevy Citation (49-State)	151	C-2	8.2	90	EGR/PLS/ OXD	A3-1	2875	2.84	22	35	27	0.142	1.96	1.11		
	Buick Riviera Turbo (Cal)	231	C-4	8.0	185 (Turbo)	EGR/PMF/ CLS	A3-1	4000	2.93	16	24	19	0.358	1.49	0.90	38.00	92.50
	Buick Riviera (49-State)	231	C-4	8.0	185 (Turbo)	EGR/PMF/ OXD	A3-1	4000	2.93	16	23	19	0.350	3.39	1.20		
Chrysler	Plymouth Horizon (Cal)	105	C-2	8.2	65	EGR/PMF/OXD/ 3MY/CLS	M4-1	2500	3.37	24	36	29	0.235	4.67	0.72	36.25	52.00
	Plymouth Horizon (49-State)	105	C-2	8.2	65	EGR/PMF/ OXD	M4-1	2375	3.37	23	33	26	0.227	4.61	1.25		
	Plymouth Horizon (Cal)	105	C-2	8.2	65	EGR/PMF/ 3MY/CLS	A3-1	2500	3.48	23	32	26	0.168	1.86	0.86	32.50	52.00
	Plymouth Horizon (49-State)	105	C-2	8.2	65	EGR/PMF/ OXD	A3-1	2500	3.48	24	31	27	0.178	3.32	1.21		
Ford	Ford LTD (Cal)	302	C-2	8.4	135	EGR/PMF/OXD/ 3MY/CLS	A3-1	4000	2.26	15	21	17	0.251	1.86	0.28	34.00	67.50
	Ford LTD (49-State)	302	C-2	8.4	135	EGR/PMF/ OXD	A3-1	4000	2.26	17	24	20	0.150	2.28	1.64		
	Ford LTD (49-State)	302	C-2	8.4	135	EGR/PMF/ OXD	L4-2	4000	3.08	17	26	20	0.222	3.46	1.25		
	Ford LTD (49-State)	302	C-2	8.4	135	EGR/PMF/ OXD	L4-2	4000	3.08	17	26	20	0.222	3.46	1.25		
Volvo	Rabbit (Cal)	97	F1	8.2	76	3MY/CLS/ FI/EGR	M5-2	2375	3.90	26	42	32	0.133	1.19	0.52	38.00	64.00
	Rabbit (49-State)	97	F1	8.1	76	OXD	M5-2	2375	3.90	25	42	31	0.148	1.41	1.35	36.81	64.00
Volvo	Sedan (Cal & 49-State)	130	F1	9.3	107	3MY/CLS	A3-1	3375	3.73	20	26	22	0.212	3.15	0.10	37.13	63.41
	Sedan (Cal & 49-State)	174	F1	8.8	130	3MY/CLS	A3-1	3375	3.54	16	21	18	0.188	1.59	0.33	30.38	77.04



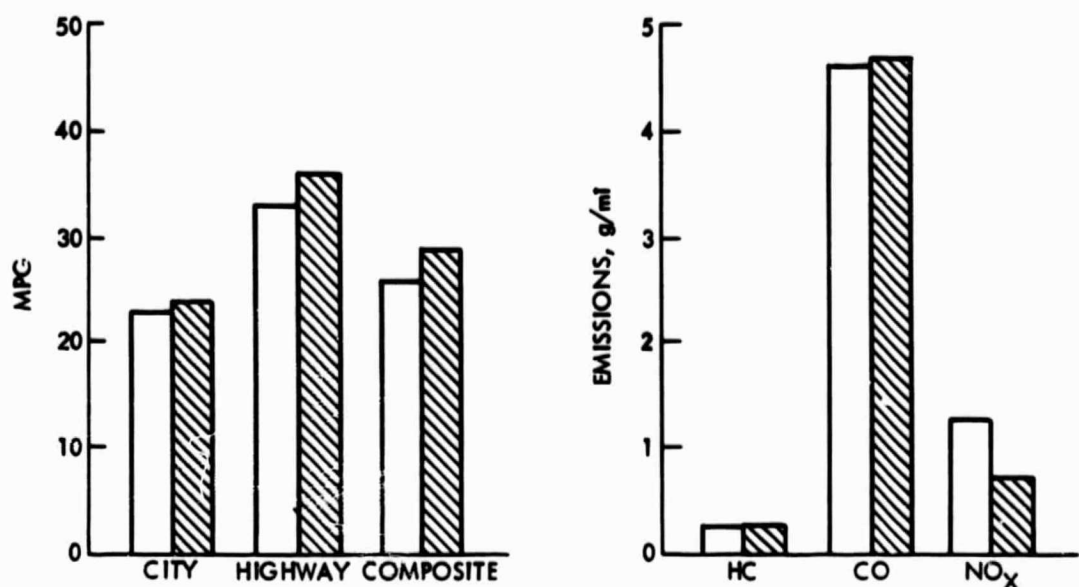
FUEL ECONOMY AND EMISSIONS COMPARISONS FOR CALIFORNIA AND 49-STATE VEHICLES CHEVROLET CITATION (173 CID ENGINE)



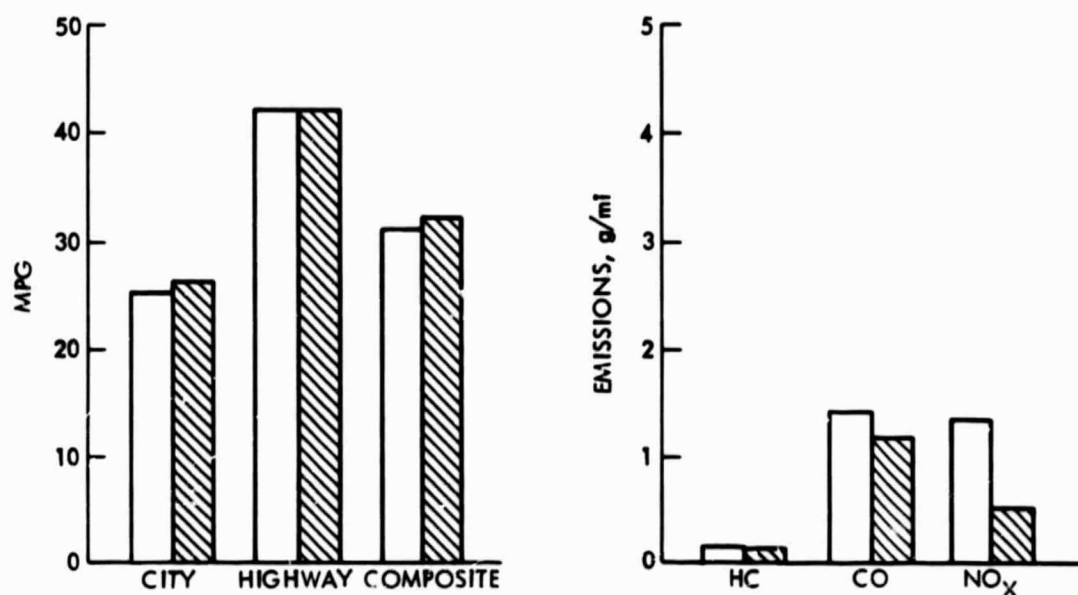
FUEL ECONOMY AND EMISSIONS COMPARISONS FOR CALIFORNIA AND 49-STATE VEHICLES CHEVROLET CITATION (151 CID ENGINE)

 CALIFORNIA
 49-STATE

Figure 2-56. Fuel Economy and Emissions Comparisons for California Vehicles with Three-Way Catalyst Emissions Control and 49-State Vehicles with Oxidation Catalyst Systems



FUEL ECONOMY AND EMISSIONS COMPARISONS FOR CALIFORNIA AND 49-STATE VEHICLES
PLYMOUTH HORIZON (105 CID ENGINE)



FUEL ECONOMY AND EMISSIONS COMPARISONS FOR CALIFORNIA AND 49-STATE VEHICLES
VW RABBIT (97 CID ENGINE)

 CALIFORNIA
 49-STATE

Figure 2-57. Fuel Economy and Emissions Comparison for California Vehicles with Three-Way Catalyst Emissions Control and 49-State Vehicles with Oxidation Catalyst Systems

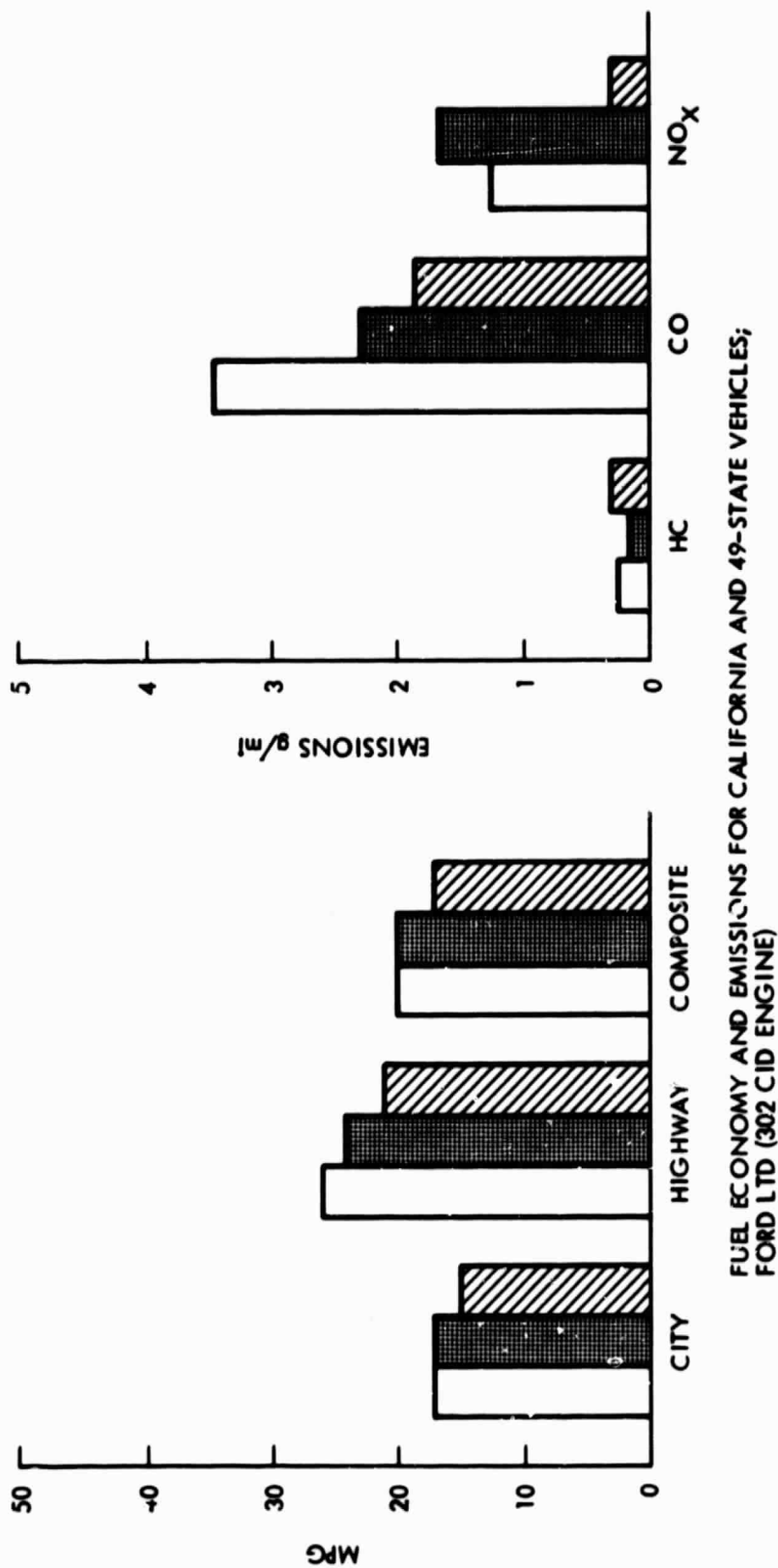


Figure 2-58. Fuel Economy and Emissions Comparisons for California Vehicles with Three-Way Catalyst Emissions Control and 49-State Vehicles with Oxidation Catalyst Systems

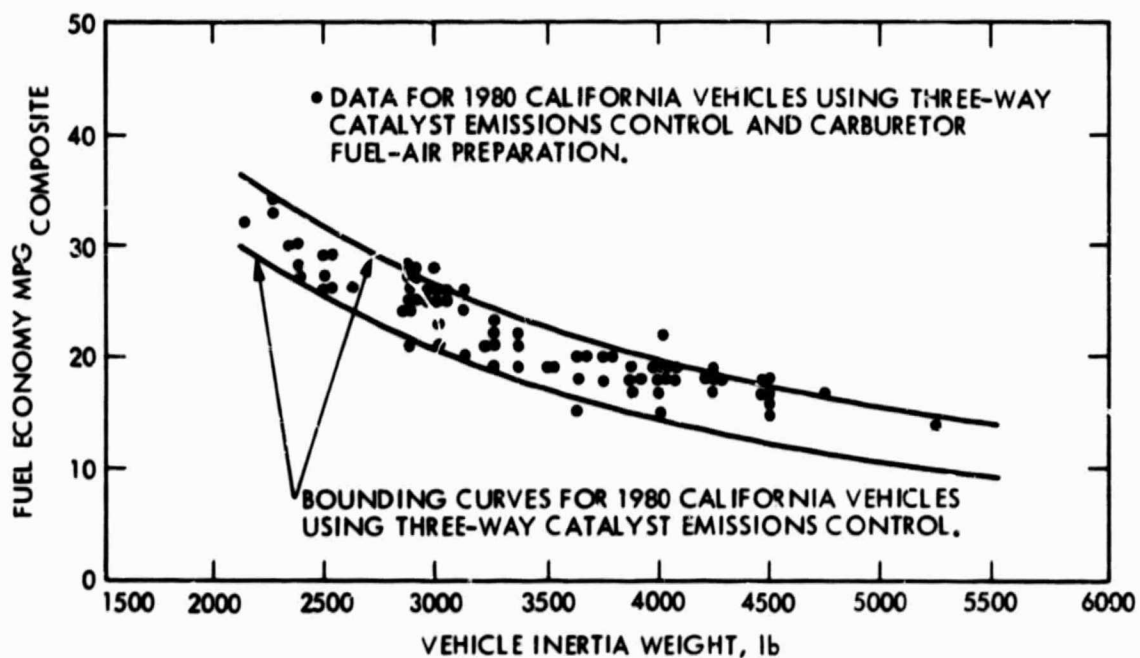
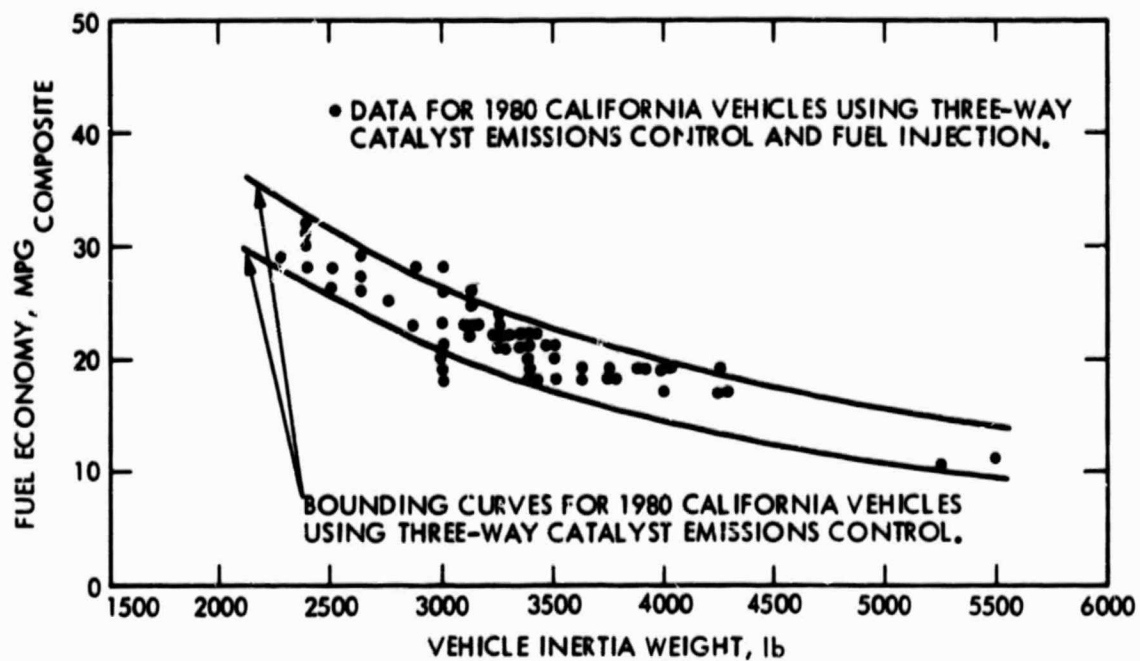


Figure 2-59. Composite Fuel Economy Characteristics for Fuel Injection and Carburetor Fuel-Air Preparation Systems

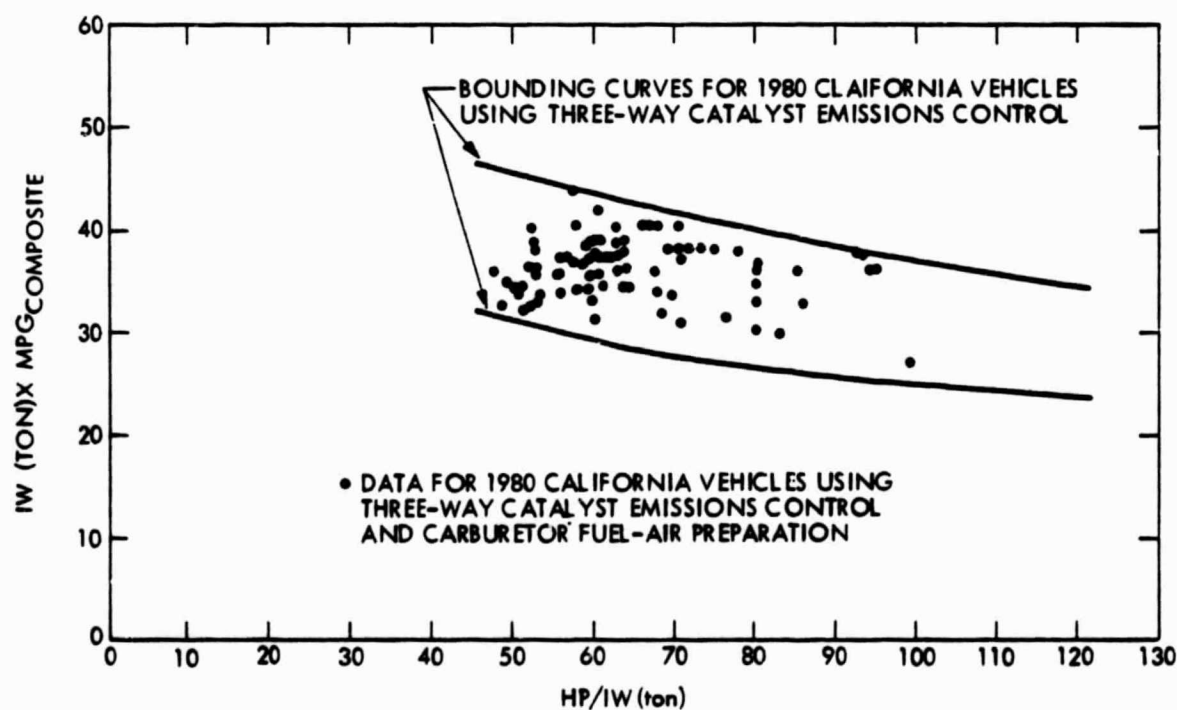
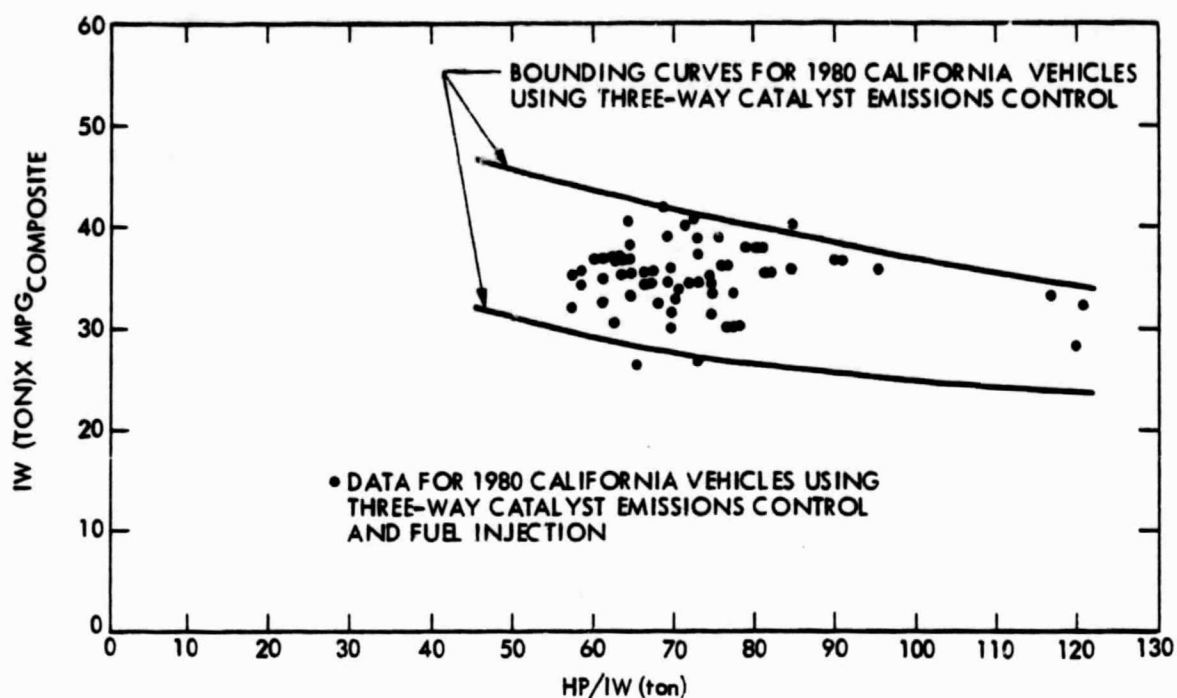


Figure 2-60. Fuel Economy and Performance Characteristics for Fuel Injection and Carburetor Fuel-Air Preparation Systems

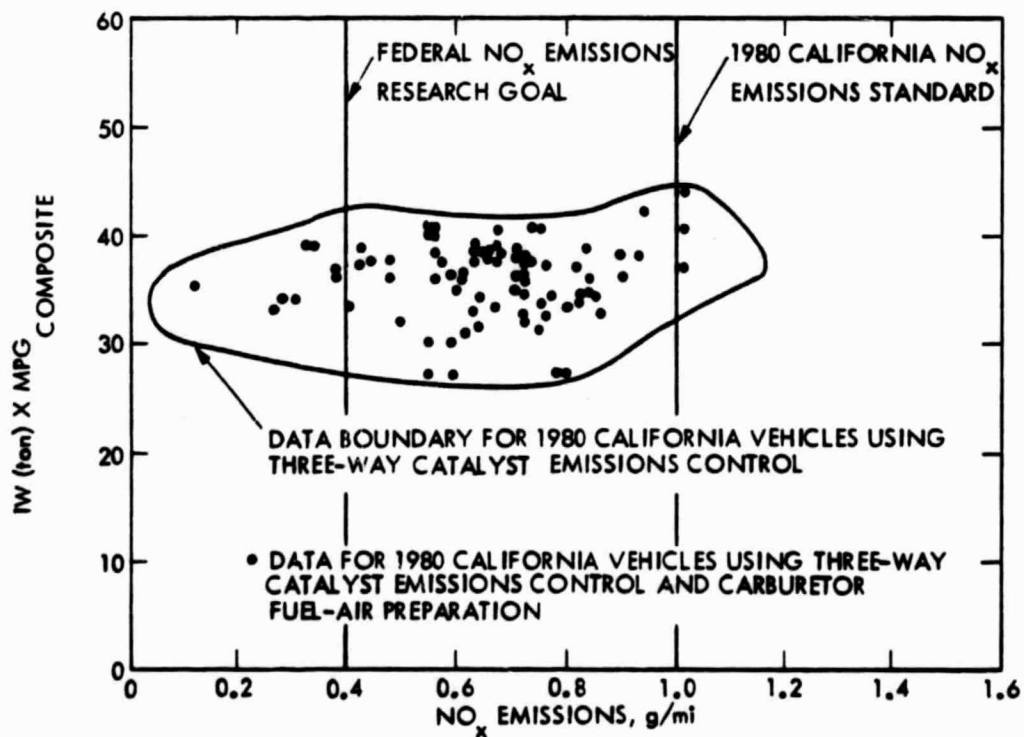
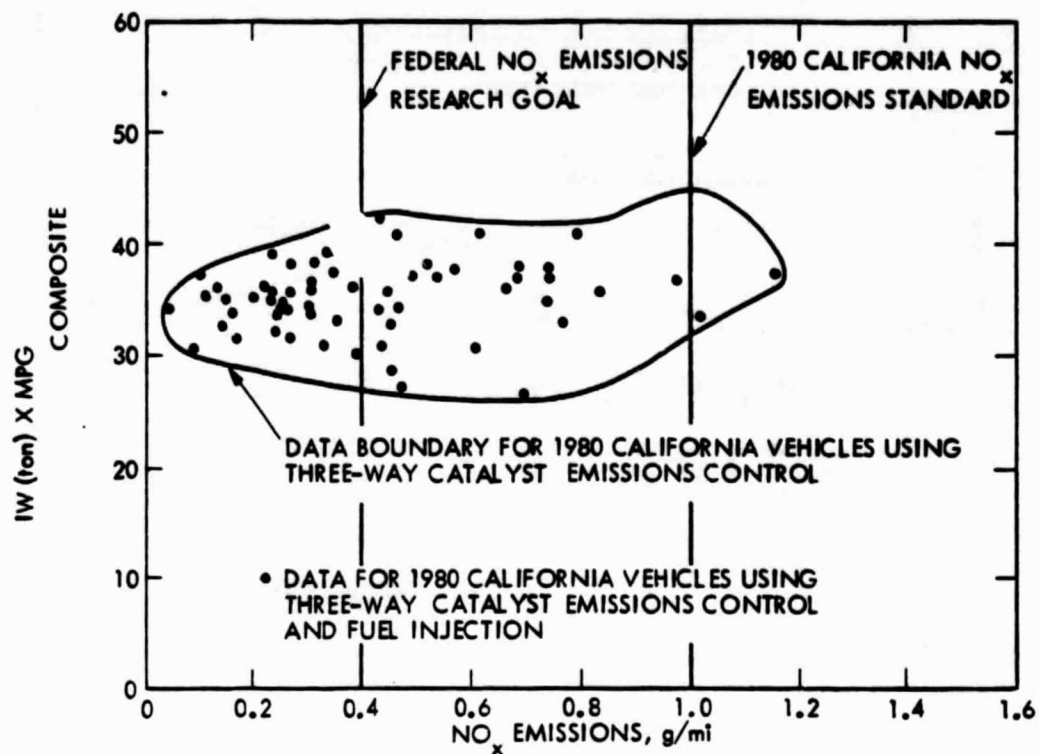


Figure 2-61. NO_x Emissions Characteristics for Fuel Injection and Carburetor Fuel-Air Preparation Systems

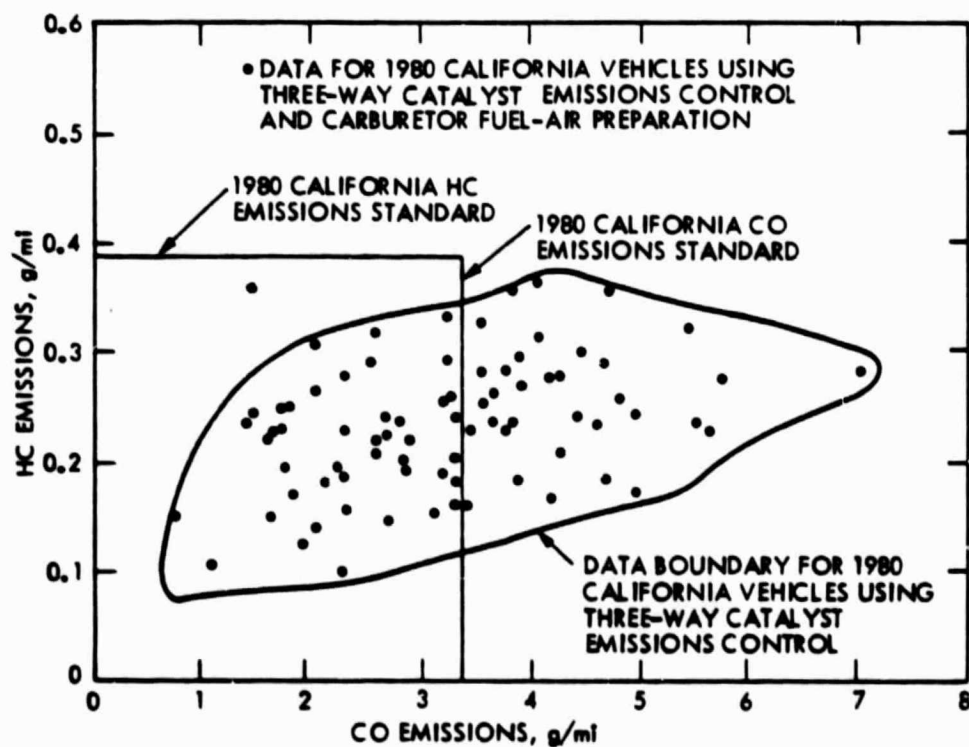
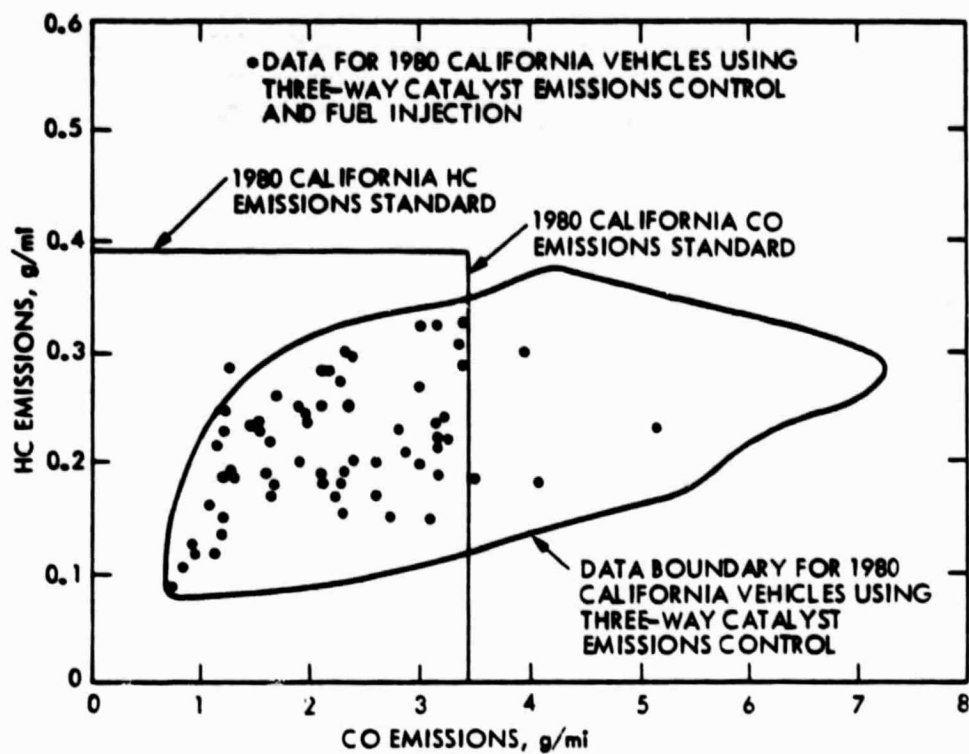


Figure 2-62. HC and CO Emissions Characteristics for Fuel Injection and Carburetor Fuel-Air Preparation Systems

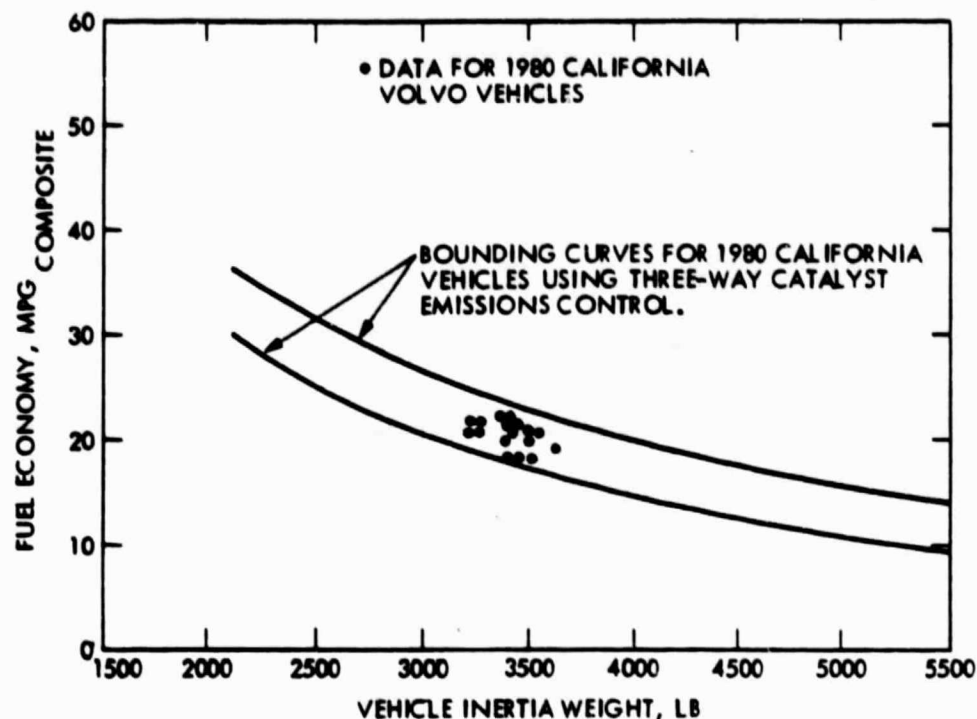


Figure 2-63. Composite Fuel Economy for Volvo Vehicles

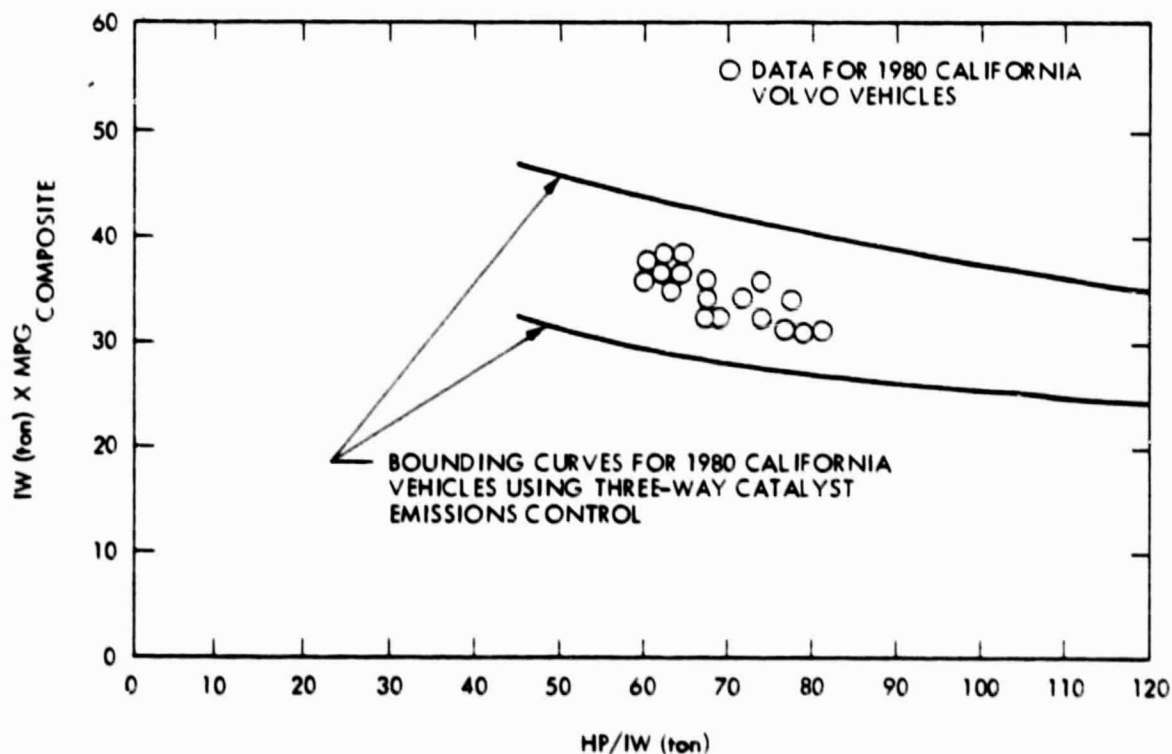


Figure 2-64. Fuel Economy Characteristics for Volvo Vehicles

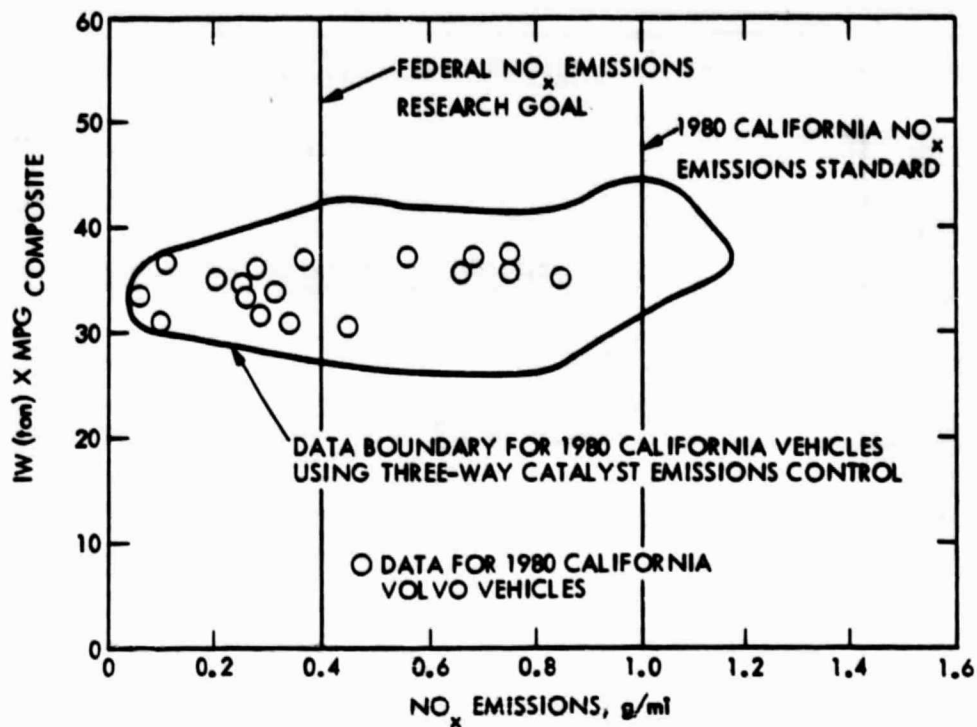


Figure 2-65. NO_x Emissions Characteristics for Volvo Vehicles

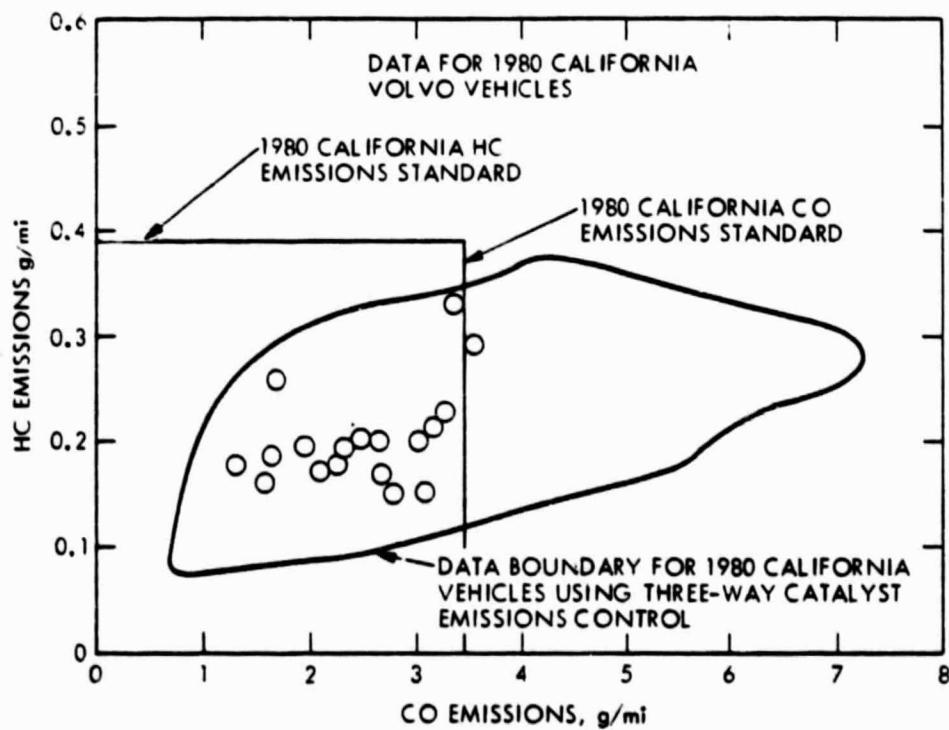


Figure 2-66. HC and CO Emissions Characteristics for Volvo Vehicles

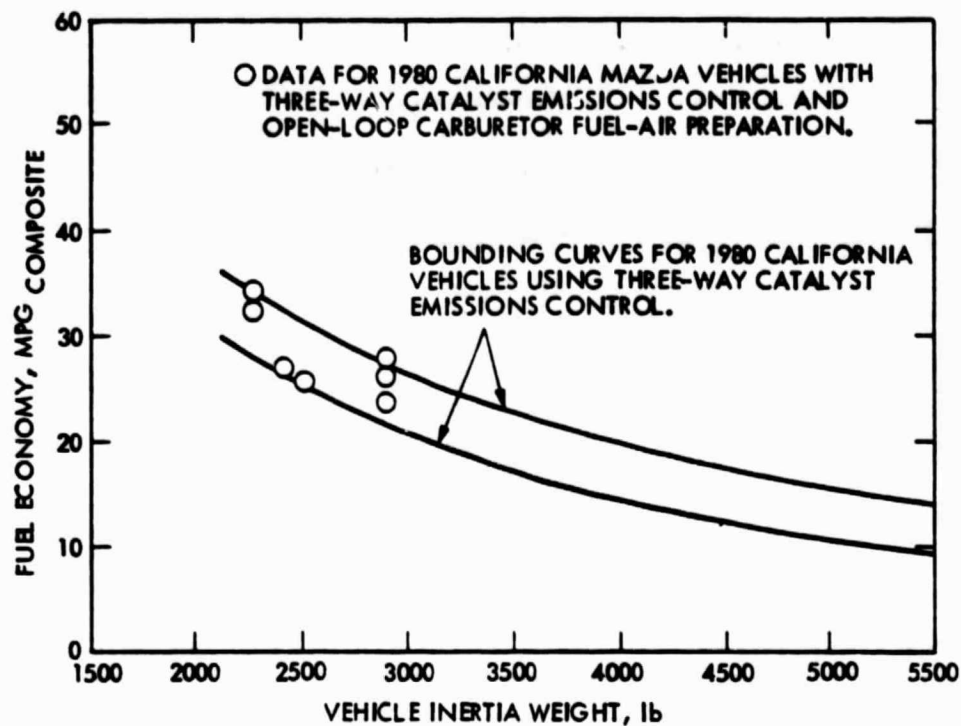


Figure 2-67. Composite Fuel Economy for Mazda Vehicles

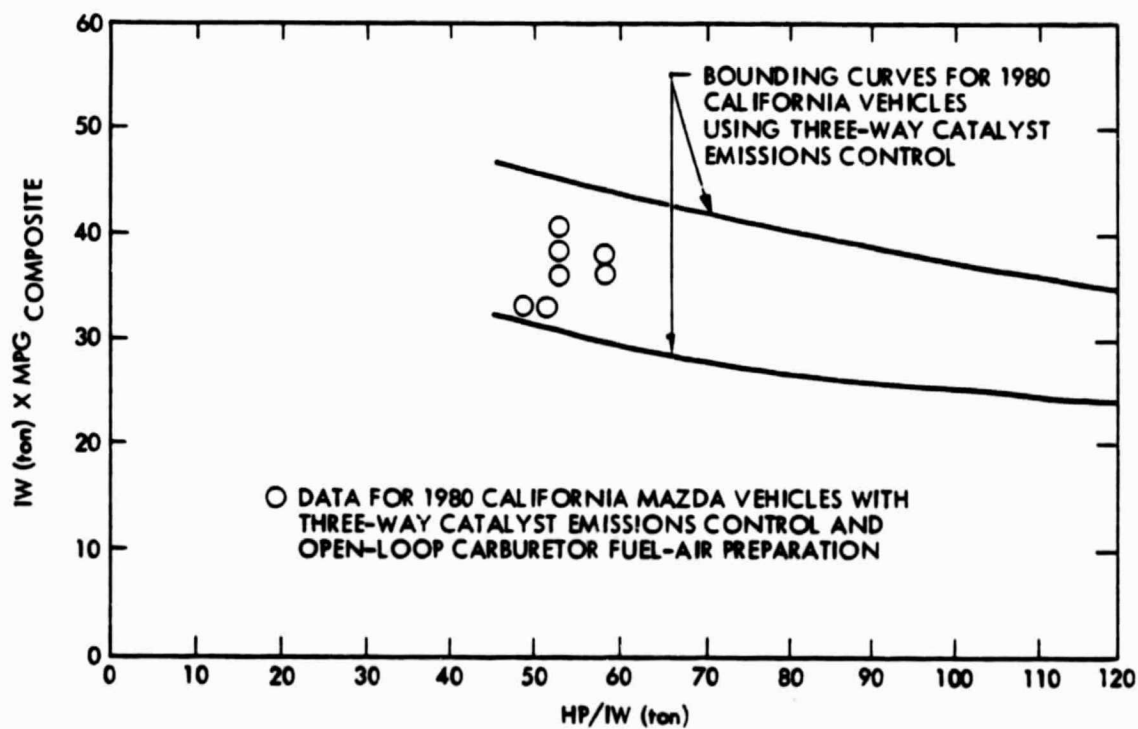


Figure 2-68. Fuel Economy Characteristics for Mazda Vehicles

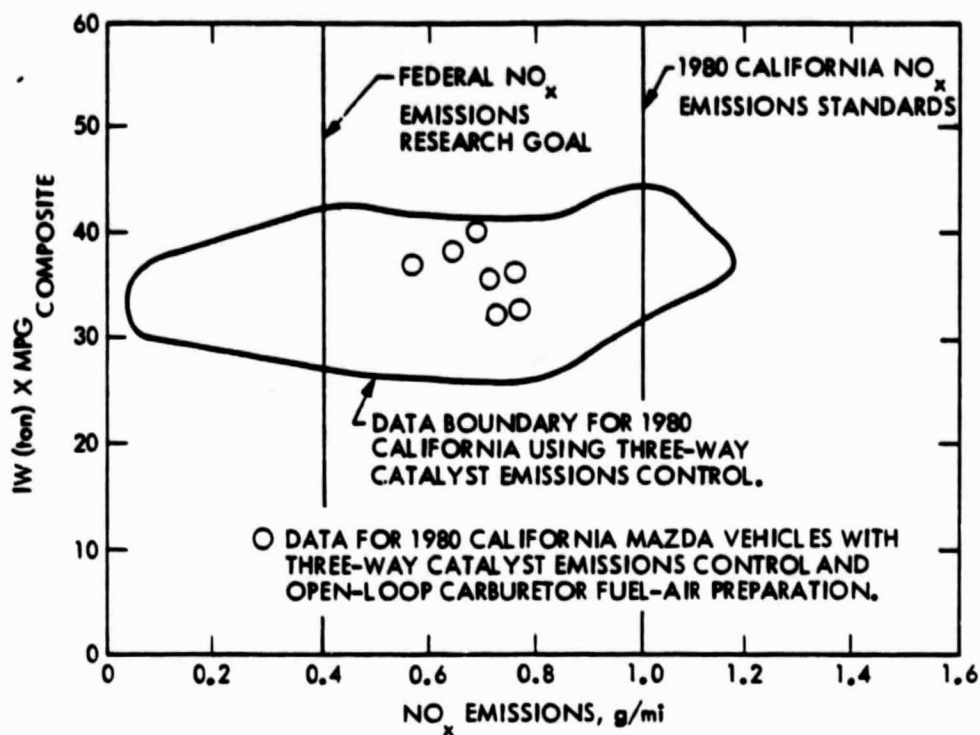


Figure 2-69. NO_x Emissions Characteristics for Mazda Vehicles

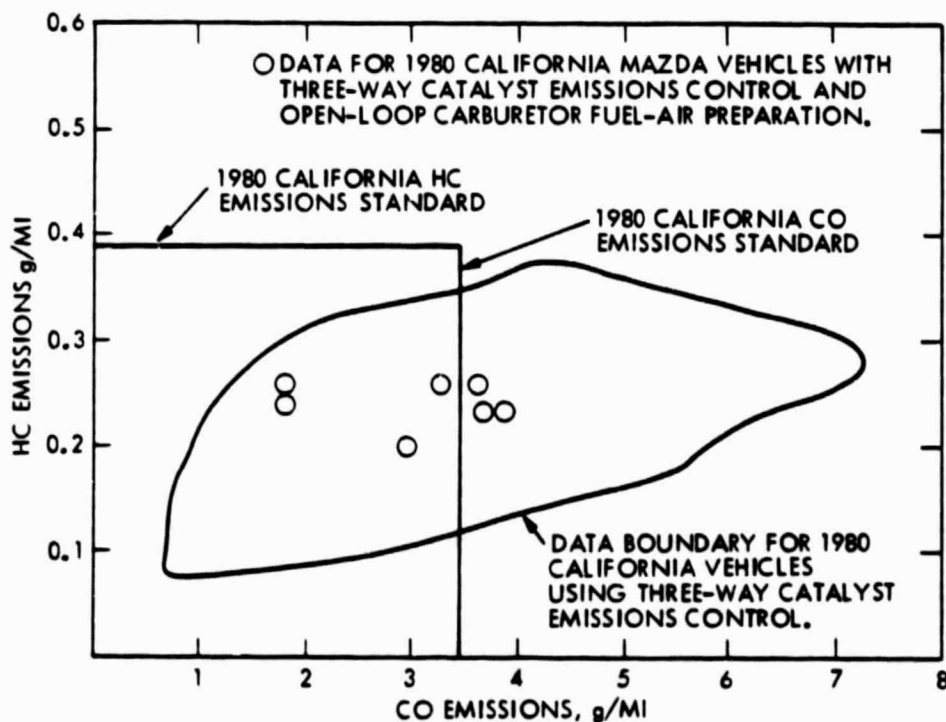


Figure 2-70. HC and CO Emissions Characteristics for Mazda Vehicles

than 3000 lb. As shown in Figure 2-68, the efficiencies of these vehicles, as indicated by the (IW X MPG) parameter, are generally less than the average for all California vehicles with three-way catalysts. Note also that the Mazda vehicles have low (HP/IW) values. The HC and CO emissions are good and the NO_x emissions fall between 0.6 g/mi and 0.8 g/mi. Reducing NO_x emissions would result in further reduction of the efficiency of this system. Thus, closed-loop feedback control systems appear to offer better fuel economy potential, especially for systems calibrated to meet a low NO_x emissions requirement.

Three manufacturers have introduced throttle-body fuel injection (TBI) for use with their three-way catalyst emissions control systems. As previously mentioned, the throttle-body fuel injection concept is being developed to provide better fuel-air control than carburetor systems, and at a lower cost and complexity level than current fuel injection systems. The three TBI systems have been introduced in the relatively low volume luxury car market segment to gain field experience with these systems. Fuel-economy and emissions results for vehicles using TBI are given in Figures 2-71 through 2-74. Note that the Cadillac and Chrysler data are based on 1981 EPA test results, because the TBI systems were only introduced on the 1981 models. The Cadillac TBI system is used on the variable displacement V-8-6-4 engines. As shown in Figure 2-72, the efficiencies of these vehicles, as indicated by the (IW X MPG) parameter, are higher than the average efficiency for all California vehicles with three-way catalysts. The HC and CO emissions are very low, being well below the California standards. The NO_x emissions are quite low, considering the fact that these vehicles all have inertia weights greater than 4000 lb. The 1981 Chrysler Imperial achieved a NO_x emissions level below the 0.4 g/mi research goal. If the TBI systems work well in field use, their use will probably spread to other vehicle models in future years. Comparisons of the fuel economy and emissions characteristics of the California and 49-state versions of these vehicles with the TBI systems are given in Table 2-7 and Figure 2-75. Only the Chrysler Imperial suffers a significant fuel economy penalty in the California version.

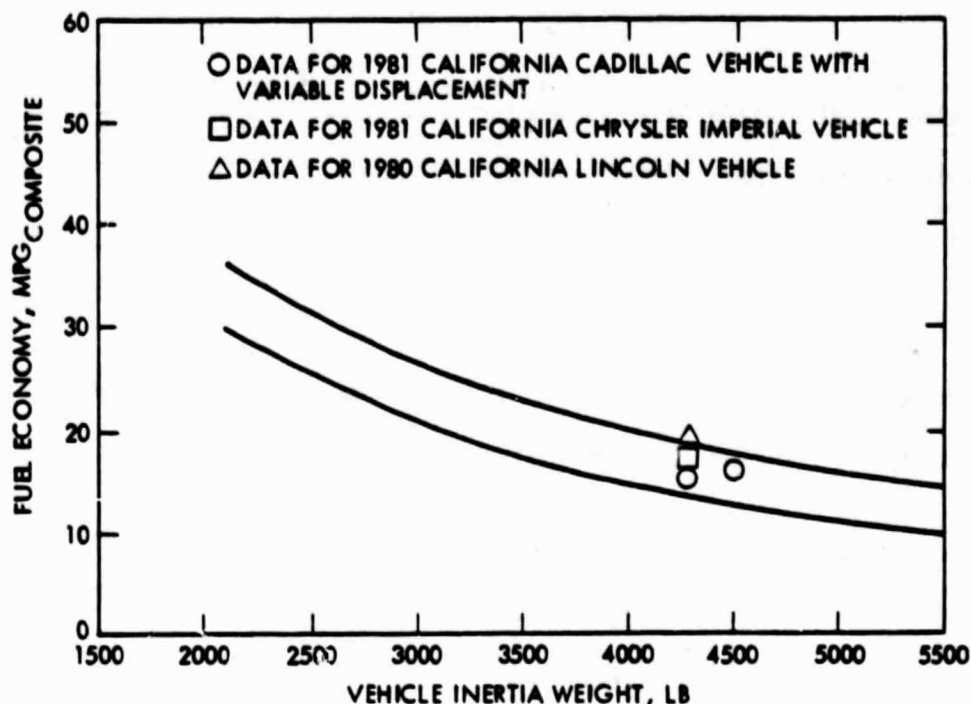


Figure 2-71. Composite Fuel Economy for California Vehicles Using Throttle-Body Injection

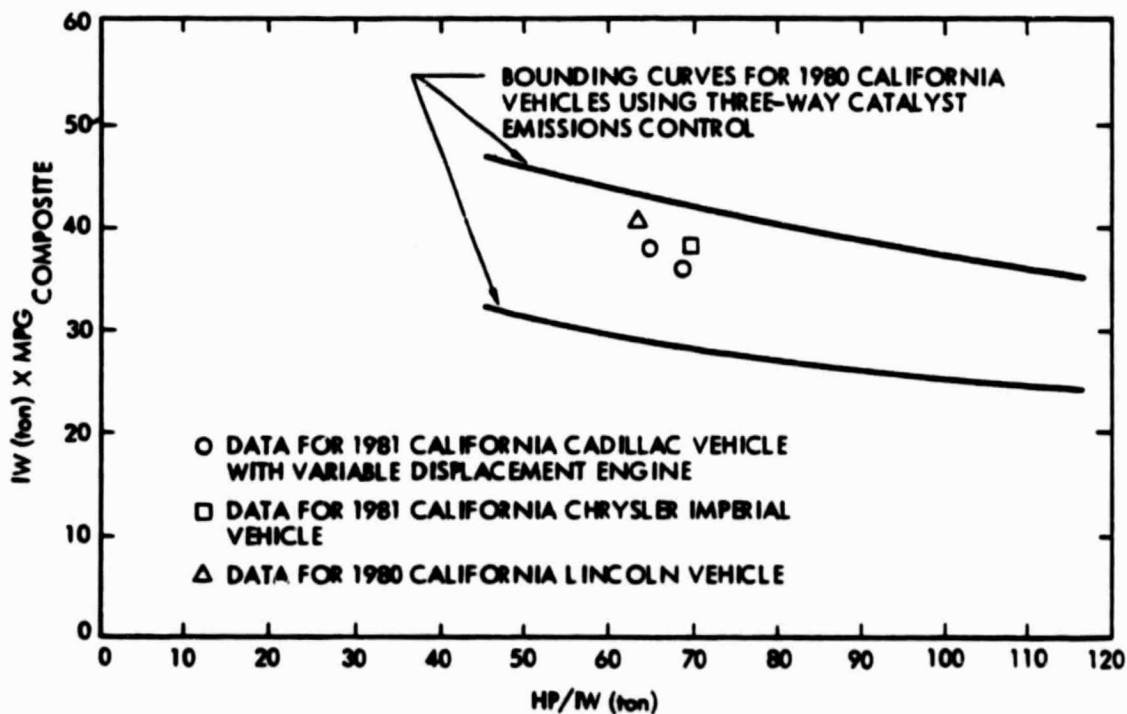
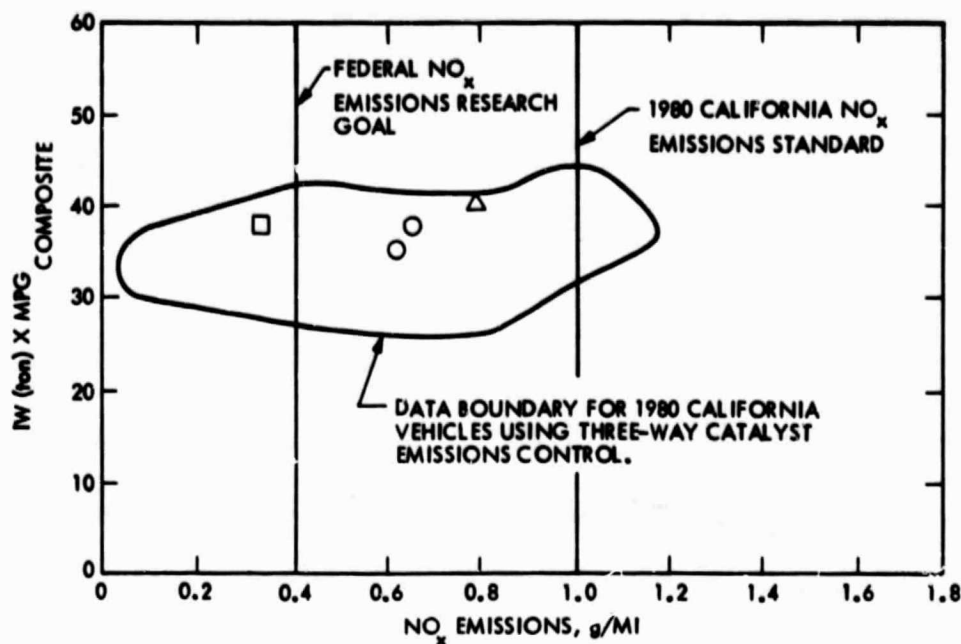
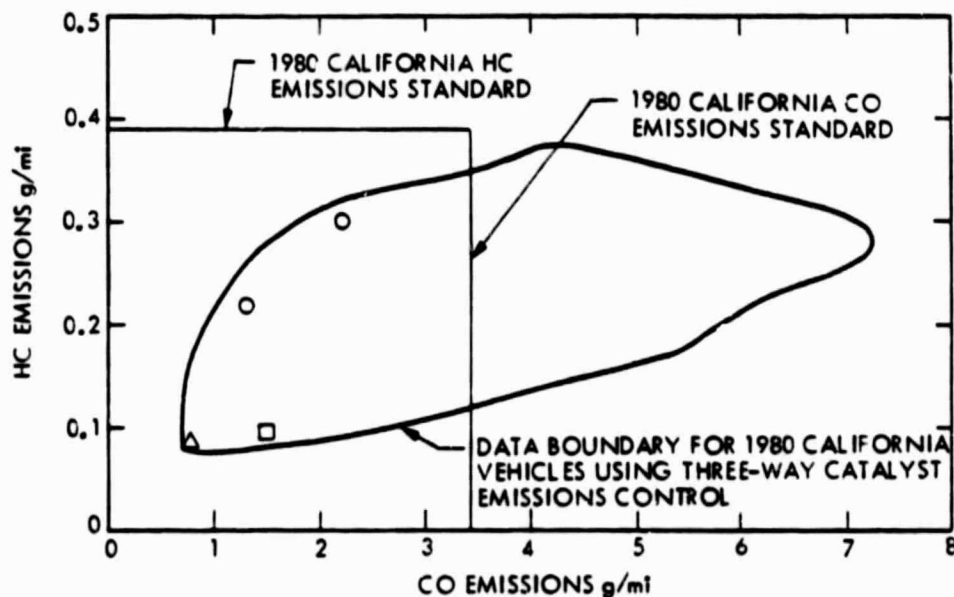


Figure 2-72. Fuel Economy Characteristics for California Vehicles Using Throttle Body Injection



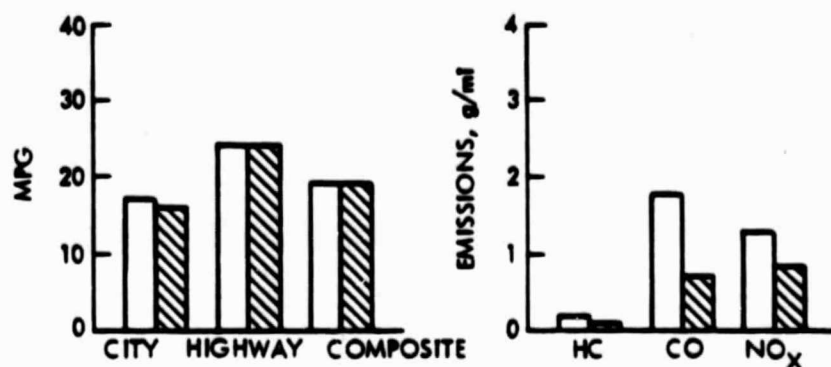
- DATA FOR 1981 CALIFORNIA CADILLAC VEHICLE WITH VARIABLE DISPLACEMENT ENGINE.
- DATA FOR 1981 CALIFORNIA CHRYSLER IMPERIAL VEHICLE
- △ DATA FOR 1980 CALIFORNIA LINCOLN VEHICLE

Figure 2-73. NO_x Emissions Characteristics for California Vehicles Using Throttle-Body Fuel Injection

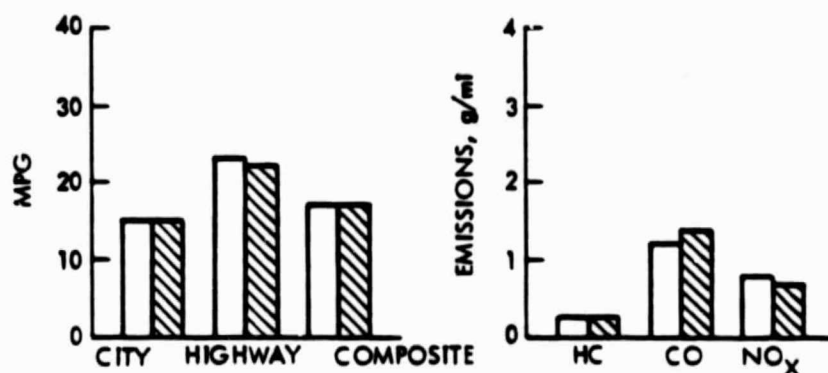


- DATA FOR 1981 CALIFORNIA CADILLAC VEHICLE WITH VARIABLE DISPLACEMENT ENGINE
- DATA FOR 1981 CALIFORNIA CHRYSLER IMPERIAL VEHICLE
- △ DATA FOR 1980 CALIFORNIA LINCOLN VEHICLE

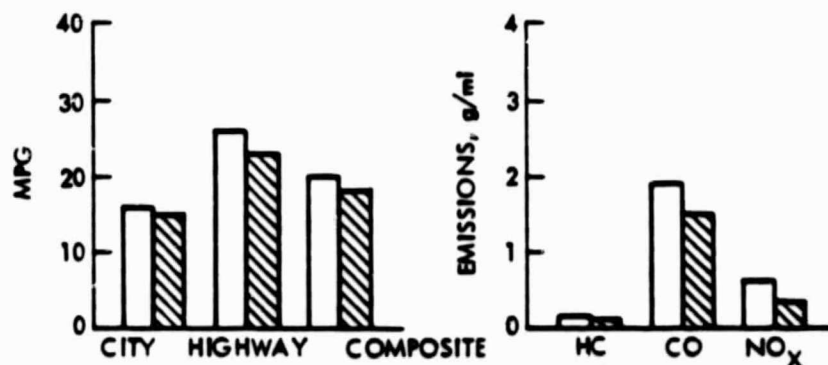
Figure 2-74. HC and CO Emissions Characteristics for California Vehicles Using Throttle-Body Fuel Injection



FUEL ECONOMY AND EMISSIONS COMPARISONS FOR CALIFORNIA AND 49-STATE VEHICLES
1980 LINCOLN (302 CID ENGINE)



FUEL ECONOMY AND EMISSIONS COMPARISONS FOR CALIFORNIA AND 49-STATE VEHICLES
1981 CADILLAC DEVILLE (368 CID ENGINE)



FUEL ECONOMY AND EMISSIONS COMPARISONS FOR CALIFORNIA AND 49-STATE VEHICLES
1981 CHRYSLER IMPERIAL (318 CID ENGINE)

 CALIFORNIA
 49-STATE

Figure 2-75. Fuel Economy and Emissions Comparisons for California and 49-State Vehicles Using Throttle-Body Injection

Table 2-7. Comparison of Some California and 49-State Vehicle Characteristics

MFG	Car Line	CID	Carb FI	Comp. Ratio	HP	Emission	Trans	Weight	Axle	City	Highway	Comb	HC	CO	NO _x	Ton x MPG Comb	HP/1W (Ton)
Ford (1981)	Continental Mark VI (Cal)	302	F1	8.4	135	EDR/AIR/ OXY/3WY/CLS	L4-2	4250	3.08	16	24	19	0.084	0.68	0.79	40.38	63.53
	Continental Mark VI	302	F1	8.4	135	EDR/AIR/ OXY/3WY/CLS	L4-2	4250	3.08	17	24	19	0.180	1.73	1.26	40.38	63.53
	(49-State) Continental Mark VI	302	F1	8.4	135	EDR/AIR/ OXY/3WY/CLS	L4-2	4250	3.08	17	24	19	0.163	1.13	1.06	40.38	63.53
Chrysler (1981)	Imperial (Cal)	318	F1	8.6	148	EDR/AIR/ OXY/3WY	L3-1	4250	2.24	15	25	18	0.093	1.49	0.32	38.25	69.64
	Imperial (49-State)	318	F1	8.6	148	EDR/AIR/ OXY/3WY	L3-1	4250	2.24	16	26	19	0.121	1.81	0.71	40.38	69.64
	Imperial	318	F1	8.6	148	EDR/AIR/ OXY/3WY	L3-1	4250	2.24	16	26	20	0.104	1.89	0.59	42.50	69.64
	(49-State)					OXY/3WY											
GMC (1981)	Deville (Cal)	368	F1	8.2	145	EDR/AIR/ OXY/3WY	A3-1	4500	2.41	15	22	17	0.221	1.33	0.64	38.25	64.44
	El Dorado (Cal)	368	F1	8.2	145	EDR/AIR/ OXY/3WY	A3-1	4250	2.41	14	23	17	0.299	2.20	0.61	36.13	68.24
	Deville (49-State)	368	F1	8.2	145	EDR/AIR/ OXY/3WY	A3-1	4500	2.41	15	23	17	0.228	1.15	0.74	38.25	64.44
	El Dorado (49-State)	368	F1	8.2	145	EDR/AIR/ OXY/3WY	A3-1	4250	2.41	15	22	18	0.226	1.59	0.72	38.25	68.24

SECTION 3

LEAN BURN (FAST BURN) CONCEPTS

3.1 INTRODUCTION

In the early 1970's when reducing automobile fuel consumption became equally important as meeting the more stringent emissions standards, there was renewed interest in lean burn engine technology as a near-term means for achieving these goals. This interest has continued even though most manufacturers have chosen the exhaust catalyst approach for meeting the emissions requirements. Recent engine developments in this field are generally referred to as fast burn concepts. The designation "fast burn" implies an attempt to reduce the burn time required to consume the fuel-air charge, whether or not the incoming mixture is lean. In general, fast burn approaches are beneficial for very lean (excess air) mixtures and mixtures with large amounts of exhaust gas recirculation (EGR).

The main benefits available from lean burn operation of an engine can be seen by examining some general analytical results (Ref. 33). Lean burn operation offers the potential for improved fuel economy by increasing engine thermal efficiency, as shown in Figure 3-1. The figure shows results for three effective combustion intervals. The effective combustion interval is defined as the time period from the first significant combustion pressure rise to the time when peak cylinder pressure is reached, expressed in crank-angle degrees. Equivalence ratio is defined as the fuel-air ratio of the mixture divided by the stoichiometric fuel-air ratio. Thermal efficiency is seen to increase as the equivalence ratio is decreased toward leaner mixtures. This increase in thermal efficiency results from the increase in specific heat ratio of the fuel-air mixture and the decrease in throttling losses with the leaner mixture. It can also be observed that higher thermal efficiency is achieved with the shorter combustion interval. If it were possible to maintain a constant combustion interval while lowering the equivalence ratio, then significant improvements in engine thermal efficiency could be achieved until the lean flammability limit of the fuel is reached. In most conventional engines, thermal efficiency begins to decrease rapidly well before reaching the lean flammability limit of the fuel because of reduced flame speed. The fuel economy benefits of lean operation in a particular engine configuration are limited by the equipment lean limit for the fuel being used. To achieve the potential of lean burn, it is necessary that the engine maintain a fast-burning charge for lean equivalence ratios. If EGR is used as the fuel-air mixture diluent rather than air, the thermal efficiency gain achieved by operating leaner (more air or more EGR) is reduced. EGR produces less of an increase in the specific heat ratio of the fuel-air mixture than that produced by the addition of air.

For constant equivalence ratio operation, the analytical results in Figure 3-1 indicate that thermal efficiency is increased by reducing the combustion interval. Reducing the combustion interval is one of the key objectives of fast burn concepts. Another key potential benefit of fast burn concepts is their ability to successfully utilize higher compression

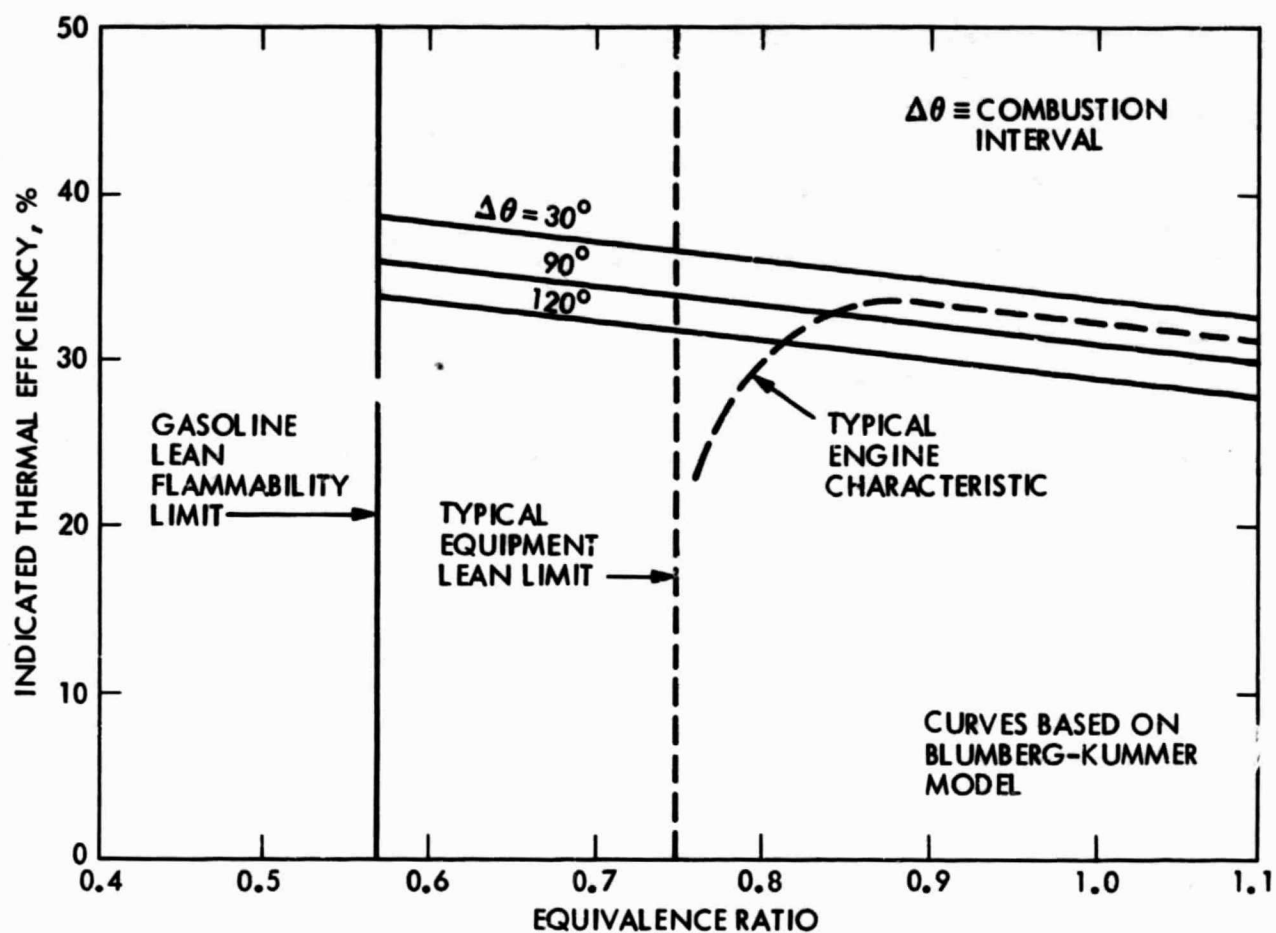


Figure 3-1. Thermal Efficiency Versus Equivalence Ratio Variance of Indicated Mean Effective Pressure (A/F Ratios 14.5:1, 1400 rpm, MBT, Ref. 33)

ratios which result in higher thermal efficiency. Alternatively, fast burn concepts of good design permit use of lower grade fuel (lower octane number) at the same compression ratio. These possible benefits of fast burn will be discussed further in the following sections of this chapter.

The lean burn concept also offers potential for controlling NO_x emissions, as shown in Figure 3-2. This analytical curve indicates that NO_x emissions reach a peak for an equivalence ratio of about 0.85; however, significant reductions in emissions can be achieved for leaner equivalence ratios. The goal of simultaneously achieving increased fuel economy and reduced exhaust emissions from lean burn operation depends on the success of making engine modifications which permit the efficient use of fuel at equivalence ratios which approach the lean flammability limit of the fuel. The amount of NO_x emissions formed in the combustion process depends on oxygen concentration in the mixture and the time spent above the NO_x formation temperature. For this reason, the use of EGR as a mixture diluent is better than air from the standpoint of NO_x emissions reduction. This is one reason why much of the fast burn engine work has concentrated on increasing the EGR tolerance of engines.

The control of unburned HC emissions has posed a problem for many lean burn concepts. As engines are made to operate near their lean limit, engine misfire and incomplete flame propagation occur with increasing frequency. These misfire and partial-burn cycles produce significant increases in HC emissions from the engine. Even before reaching the misfire limit or partial-burn limit, other factors influence the HC emissions produced in the lean burn operations. In general, lower exhaust temperature, a thicker quench layer, and lower HC density in the quench layer have been identified as consequences of progressively leaning a fuel-air mixture. The first two factors would tend to increase HC output; the last would favor HC control. The interaction of these factors and the degree of flame propagation are critical elements in the HC generation in lean burn engines. The use of large amounts of EGR rather than air tends to produce a negative effect on HC emissions control by reducing the oxygen available for oxidation of the fuel.

For a given fuel, it has generally been established that mixture quality, turbulence, and ignition system characteristics contribute toward an extension of the equipment lean limit (Refs. 34 and 35). The relative importance of these factors, however, may vary from engine to engine. Because of the complex interactions of flame initiation, turbulence, mixture homogeneity, and flame propagation, it is seldom possible to predict the performance improvement which will result from a single change to a particular engine. However, certain general characteristics have been found to be important for good lean burn operation.

Because a lean burn engine must operate efficiently near the lean flammability limit of the fuel to achieve the fuel economy and emissions benefits of lean burn, it is generally agreed that it is desirable to have a uniform, homogeneous fuel-air mixture equally distributed to each cylinder with a minimum of cycle-to-cycle variations. Sonic carburetors, fuel atomizers, heated manifolds, large mixing volumes, and various turbulence devices have demonstrated an ability to improve mixture distribution; however,

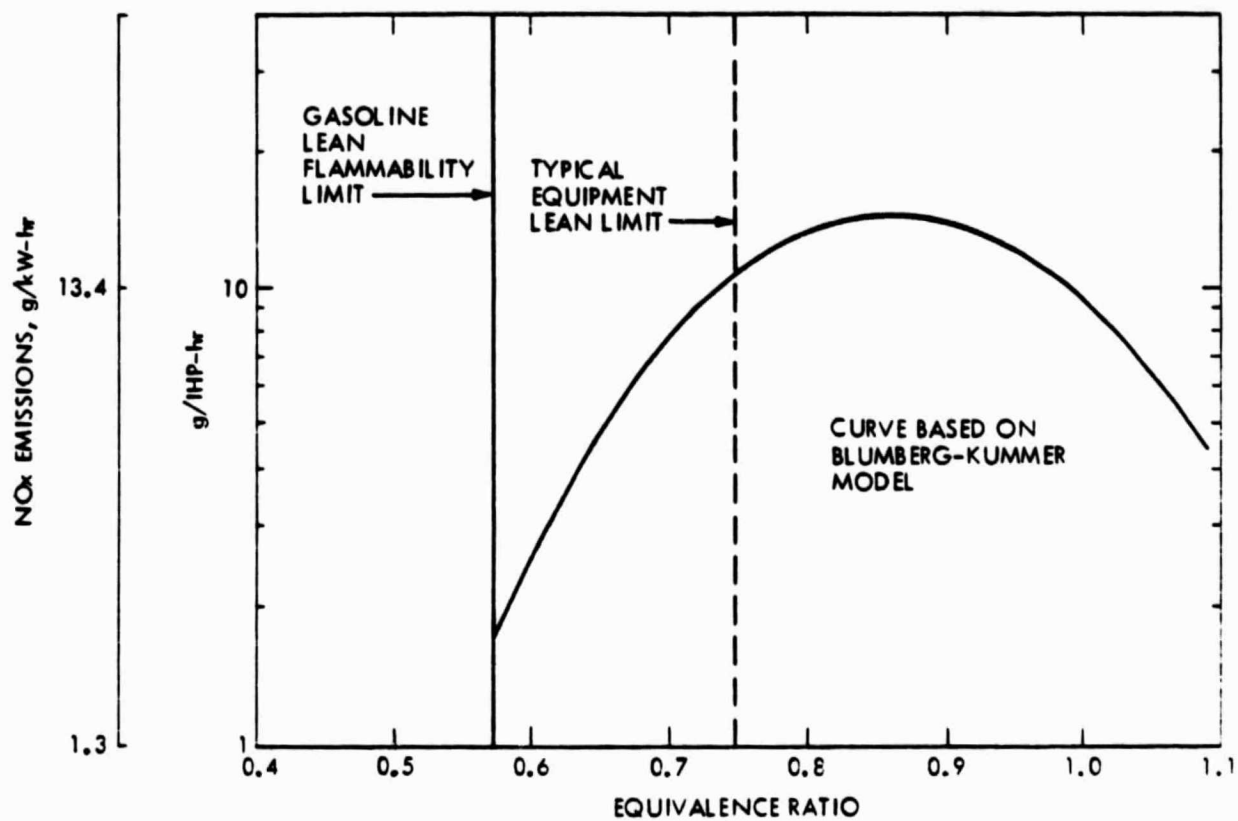


Figure 3-2. NO_x Emissions Versus Equivalence Ratio (Ref. 33)

many of these devices also have an associated volumetric efficiency penalty. Several induction systems which have been evaluated for improving mixture distribution and homogeneity are the Shell Vapipipe (Ref. 36), Ethyl Corporation lean reactor (Ref. 37), Dresserator (Ref. 38), and Autotronics (Ref. 37) systems.

Recent results by GM researchers (Ref. 39) indicate that the best mixture for lean combustion may not be the most highly atomized one. They found an injected fuel-air mixture even better than a prevaporized one in terms of lean limits, combustion pressure variations, and specific fuel consumption. The results of the GM work, which were obtained on a shrouded-valve Cooperative Fuel Research (CFR) engine, suggest that droplet size may be the most important factor. Around each droplet, there could be a "micro-stratification," one that would be insensitive to plug location, rpm, etc., as long as the number of droplets is sufficient. It is likely that an optimal size exists that gives better initiation and improved flame propagation in lean heterogeneous mixtures. This performance advantage for lean heterogeneous mixtures was removed when the tests were repeated without shrouded valves, which indicates that these results may be difficult to duplicate in a practical automotive engine.

Ignition system characteristics become more critical with lean operation. Lean mixture ignition is improved with a long-duration, high-energy spark discharging through an extended-reach spark plug having a wide spark gap (Ref. 38). For successful ignition to occur, it is necessary that the spark kernel, which is established by the spark discharge, interact with the local flow field and develop into a fully turbulent flame front. This flame front development can be inhibited or completely quenched by excessively high or irregular turbulence. For this reason, small-scale, uniform turbulence is desirable at the spark plug. Once the flame front has been established, uniform turbulence of relatively high intensity is needed in the combustion chamber to produce a fast flame speed through the lean mixture. Combustion chamber turbulence is difficult to control because it consists of the superimposed flow fields produced by intake charge flow, piston movement and combustion chamber shape. This is further complicated by the different kinds of turbulence needed for the development and propagation of a flame front in lean mixtures. Turbulator intake valves (Refs. 40 and 41) and the Heron or bowl combustion-chamber shapes (Ref. 41) have been reasonably successful in the lean mixture application. Other approaches being used to control turbulence in recent fast-burn concepts include the use of prechambers (Refs. 42 and 43) and air-injection valves (Ref. 44) connected to the main combustion chamber.

On fast burn concepts (Ref. 45), considerable attention has been given to combustion chamber geometry and spark plug location. The compact open chamber, with a more central spark plug, produces a faster burning charge. Some concepts have introduced two spark plugs per cylinder to further reduce the combustion time.

3.2 TECHNOLOGY DEVELOPMENTS AND VEHICLE SYSTEMS

Because only a relatively few lean burn systems are presently being used on production vehicles, much of the technology is contained in research studies and engine prototype developments. The results of some of the more important of these studies and engine developments will be reviewed to provide a basis for evaluating the potential of lean burn (fast burn) concepts.

Research efforts at General Motors (Refs. 46 and 47) have shown that two distinct lean-mixture limits exist for the internal combustion process, one related to problems of flame initiation and the other to incomplete propagation of the flame. The tests were conducted on a single-cylinder CFR engine using propane as a fuel and operated in a steady-state mode. The premixed propane-air mixture was preheated to 65.5°C before delivery to the engine. Pressure-time measurements of combustion chamber pressure were used to identify engine misfire.

The tests were conducted by adjusting the spark timing to the minimum spark timing for best torque (MBT) and varying the equivalence ratio from 1.2 to the lean misfire limit. "Misfire" was characterized by a pressure-time trace identical to a motoring trace. The lean misfire limit was defined as the leanest mixture at MBT spark timing for which stable engine operation was possible with a misfire frequency of 0.5-0.8% of the cycles. At each equivalence ratio, the limits of spark timing were probed until the start of combustion degradation.

The MBT spark timing was tested with both shrouded and nonshrouded intake valves. As expected, the leaner mixture required an increase in the MBT spark timing. The researchers postulated that this increase in MBT spark timing was the result of changes in flame propagation rather than those of flame initiation. Currently, the shrouded intake valves in the standard CFR engine impart a gross rotating motion to the incoming charge. Comparisons of the data for tests with shrouded and nonshrouded intake valves provide a measure of the effect of turbulence on timing parameters. The less turbulent charge is seen to require significantly more advance at any given equivalence ratio.

Experiments were run to determine the ignition-limited timing by advancing the spark timing from its MBT value until flame initiation failed to occur. These results indicated that the ignition-limited timing decreased as the mixture was leaned, as shown in Figure 3-3. This behavior can be understood by noting that an increase in spark advance results in a lower charge temperature and a higher turbulence level in the charge at the time of the spark. Both of these charge conditions hamper the ignition of lean mixtures. It was also found that a decrease in compression ratio shifted the ignition limit lines in the direction of lower spark timing. This shift is a result of the lower charge temperature and higher charge dilution by residual gases for the lower compression ratio configuration.

To study flame propagation, a spacer was fitted between the cylinder head and block of the CFR engine to permit on-gap measurements in the flame. Tests were made by retarding the spark timing from its MBT value

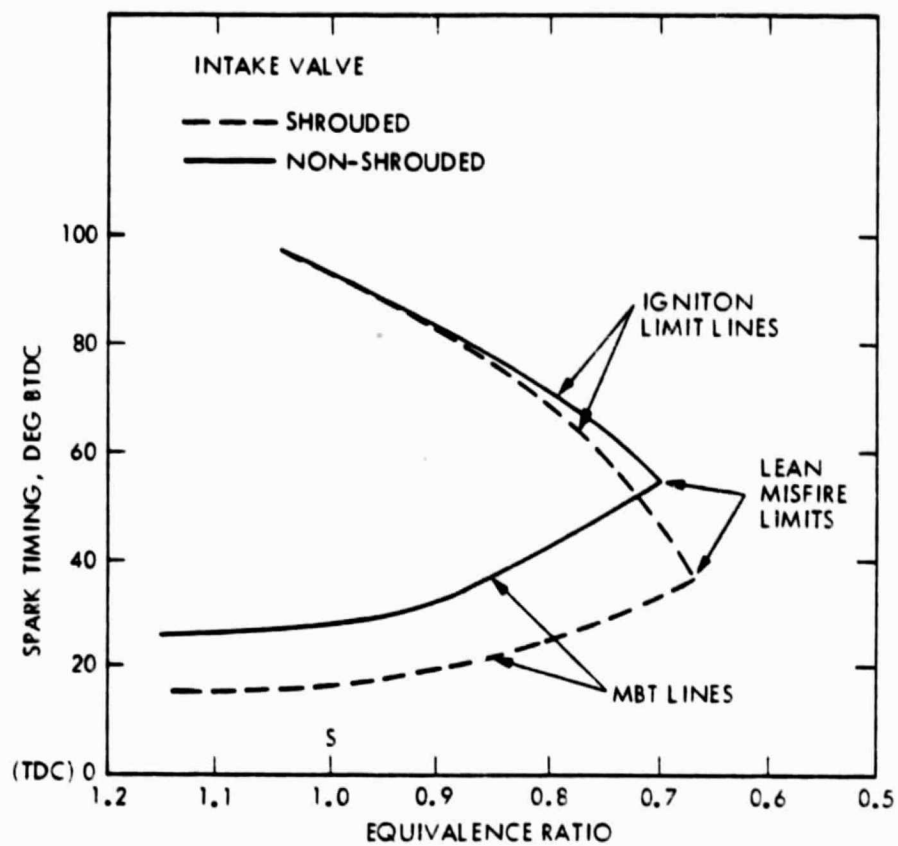


Figure 3-3. Ignition-Limited and MBT Timing, with Shrouded and Nonshrouded Intake Valve (Ref. 47)

until a "partial-burn" condition was reached. This partial-burn limit was defined as that spark timing at which incomplete flame propagation occurred in 2-4% of the cycles. Results of these tests confirmed that spark retardation could lead to flame quenching before the end gas was consumed. Complete propagation was achieved for rich mixtures; however, for equivalence ratios less than 0.83, the partial-burn limit increased with increasing leanness. The complete results obtained with the spacer-fitted CFR engine are given in Figure 3-4. These results differ somewhat from those in Figure 3-3 due to the effect of the spacer. The MBT spark-timing characteristic is seen to intersect the partial-burn limit line at an equivalence ratio of about 0.7.

Thus, there are two constraints on spark timing for stable operation with very lean mixtures, as shown in Figure 3-5. At spark-timing A, progressive leaning would lead to the onset of misfire at point B. Combustion would be degraded because of a failure to initiate the flame. At spark-timing E, a similar leaning would lead to point F, where the degeneration of combustion is a result of incomplete flame propagation. Finally, there would be some point C, from which progressive leaning would lead to the unstable point D, where the combustion degradation could result from either mechanism.

A series of additional investigations (Refs. 39 and 48) were performed at General Motors using a CFR engine fitted with a fuel injection system. The time of the fuel injection could be adjusted to vary the state of mixture preparation. For comparison, a steam-heated manifold was used in several tests to promote a completely vaporized charge. During the tests, injection timing and equivalence ratio were varied and the resulting changes in combustion were observed. Other parameters measured included peak cylinder pressure and its variation, ignition delay, combustion rate, specific fuel consumption, emissions, knock sensitivity, ignition limit, partial-burn limit, and lean-misfire limit. The partial-burn limit and lean-misfire limit were defined in the same way as in the earlier GM work. The ignition limit was defined as the leanest mixture at a given spark timing that gave stabilized operation with a 0.5-0.8% misfire frequency. In this series of tests, a flame ionization detector (FID) was used to monitor the HC emissions to help identify the partial-burn limit.

Results from these latest tests suggest that prevaporized charges are not necessarily optimal for lean combustion. By varying the time of fuel injection (and thus mixture preparation), identification was made of a mixture condition that gave substantial improvement in lean misfire limit (LML), even compared to that of the premixed charge, as shown in Figure 3-6. The leanest LML, an equivalence ratio of 0.55, corresponded to injection at the crank angle giving maximum intake valve lift. This point-giving optimal preparation was denoted best injection timing (BIT). By comparison, the LML for the premixed charged was 0.67. The point just after intake valve closing was chosen to be typical of other injection times and was identified as worst injection timing (WIT). It should be noted that fuel residence time in the intake system was shortest for BIT and longest with WIT.

In another test series, equivalence ratio was set at 0.9 while the injection timing was varied to identify the MBT spark timing for the different mixture preparations. The MBT timing for the BIT mixture was about 7 degrees

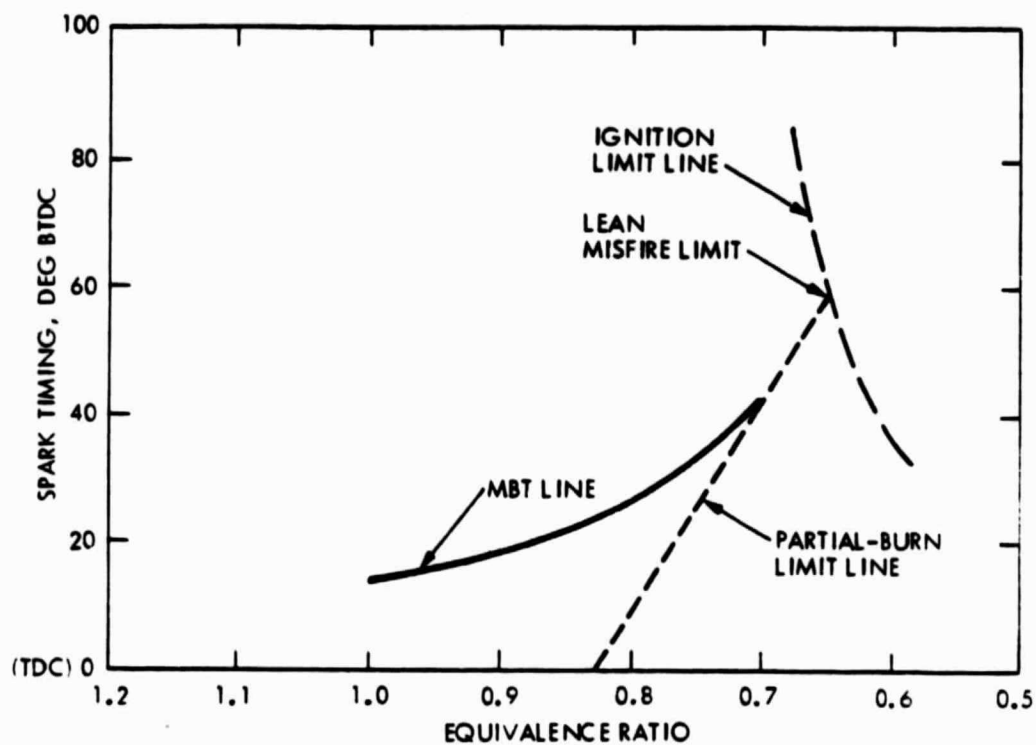


Figure 3-4. Partial-Burn Limit and MBT Timing. Spacer was Installed Between Head and Block (Ref. 47)

ORIGINAL PAGE IS
OF POOR QUALITY

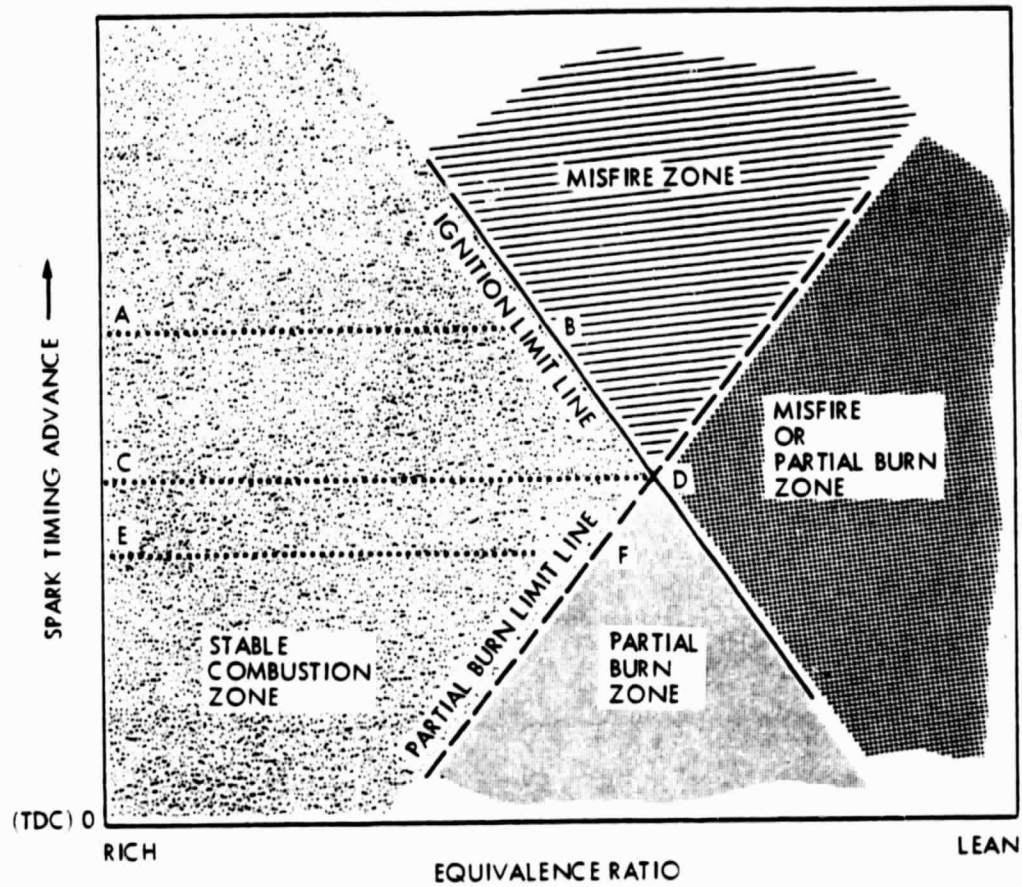


Figure 3-5. Combustion Degradation Through Progressive Leaning
(Ref. 47)

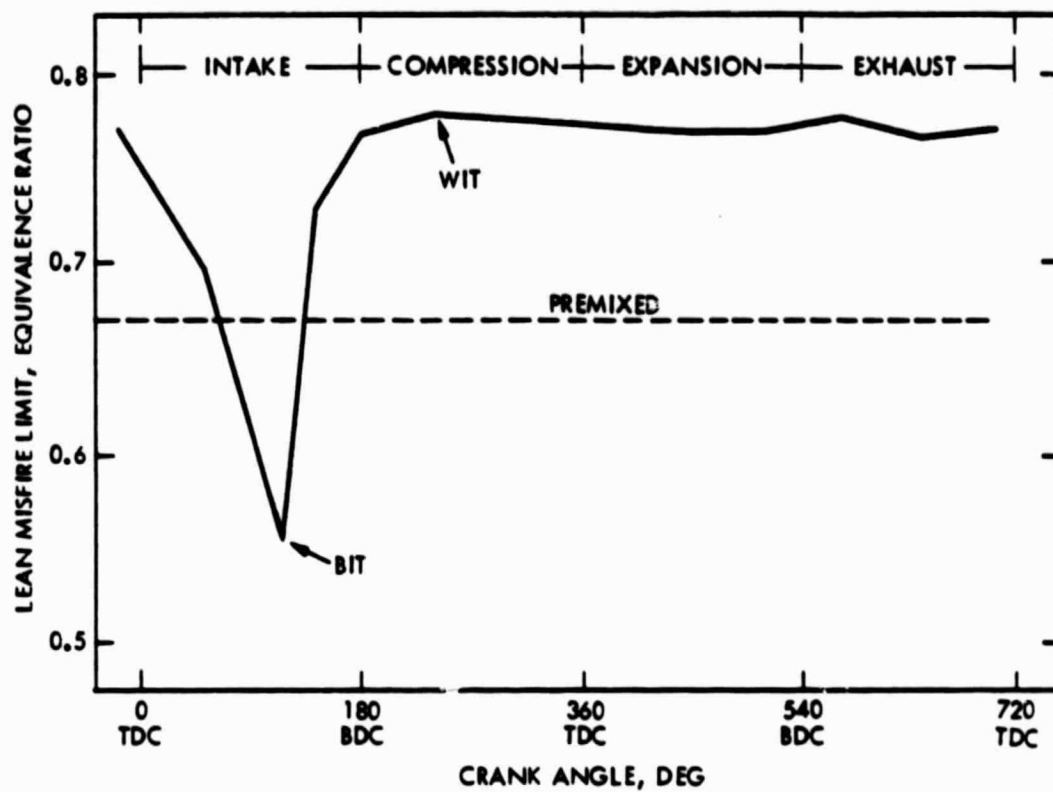


Figure 3-6. Heterogeneous Mixture (BIT) Runs Leaner at MBT than Even Prevaporized Charge — WIT is chosen as Typical of Other Heterogeneous Extrema (Ref. 48)

less than that for the WIT mixture, suggesting more rapid combustion for the BIT mixture, either in terms of quicker initiation, more rapid propagation, or both. These results are shown in Figure 3-7, which looks very similar to Figure 3-6.

Results of the ignition limit tests indicated that for any given spark timing, the BIT mixture would run leanest, followed by the prevaporized charge, with the WIT mixture being the richest. In general, the BIT mixtures would run almost 0.1 equivalence-ratio unit leaner than their prevaporized counterpart. The differences between BIT and WIT mixtures were in the range of 0.2 equivalence-ratio units.

Results of the partial-burn limit tests showed much smaller differences for the three mixture preparations. For example, at a spark timing of 30 degrees BTDC, partial-burn limits were 0.69, 0.72, and 0.79 for the BIT, prevaporized, and WIT mixtures, respectively. For the WIT mixtures, the partial-burn and ignition-limit curves coincided. Thus, for this mixture preparation, partial burns were accompanied by intermittent misfires; therefore, the BIT mixture preparation seemed to enhance spark initiation more than it did flame propagation, although it helped in both areas.

Variations in peak pressure were considerably less for the BIT mixture than for the WIT mixture. As equivalence ratios were leaned, BIT even had an advantage over the premixed charge. At an equivalence ratio of 0.86, for instance, the standard deviation for BIT was 4.7% of the mean, compared to 10.4% for WIT and around 6.7% for the prevaporized case.

A comparison of the ignition delay results for the three mixture preparation cases is given in Figure 3-8. The BIT mixture had the shortest ignition delay, especially for the leaner mixtures. A significant result is that, for a given equivalence ratio, the differences in ignition delay account for most of the MBT spark timing differences among the three mixture preparations. For example, at an equivalence ratio of 8.86, rapid combustion began at approximately the same crank angle for all three mixtures. Yet the MBT spark timing, measured in terms of crank angle degrees BTDC, varied from 18 degrees for BIT to 32 degrees for WIT.

With regard to specific fuel consumption, differences of up to 5% were observed for the three mixtures, with the BIT mixture consistently giving the lowest. Emissions results were mixed. CO emissions were essentially insensitive to mixture preparation. HC emissions were lowest for the BIT mixture and highest with the WIT mixture, with the prevaporized data falling between. NO_x emissions results showed a crossover at an equivalence ratio of 0.90. At an equivalence ratio leaner than 0.90, the BIT mixture generated the most NO_x, while for richer mixtures, the WIT and premixed preparations generated the most NO_x.

Tests were run to determine the knock-limiting compression ratios for the three mixtures. Contrary to expectations, the BIT mixture's limiting-compression ratio was 9.5:1, while the slower-burning WIT mixture's was 9.8:1.

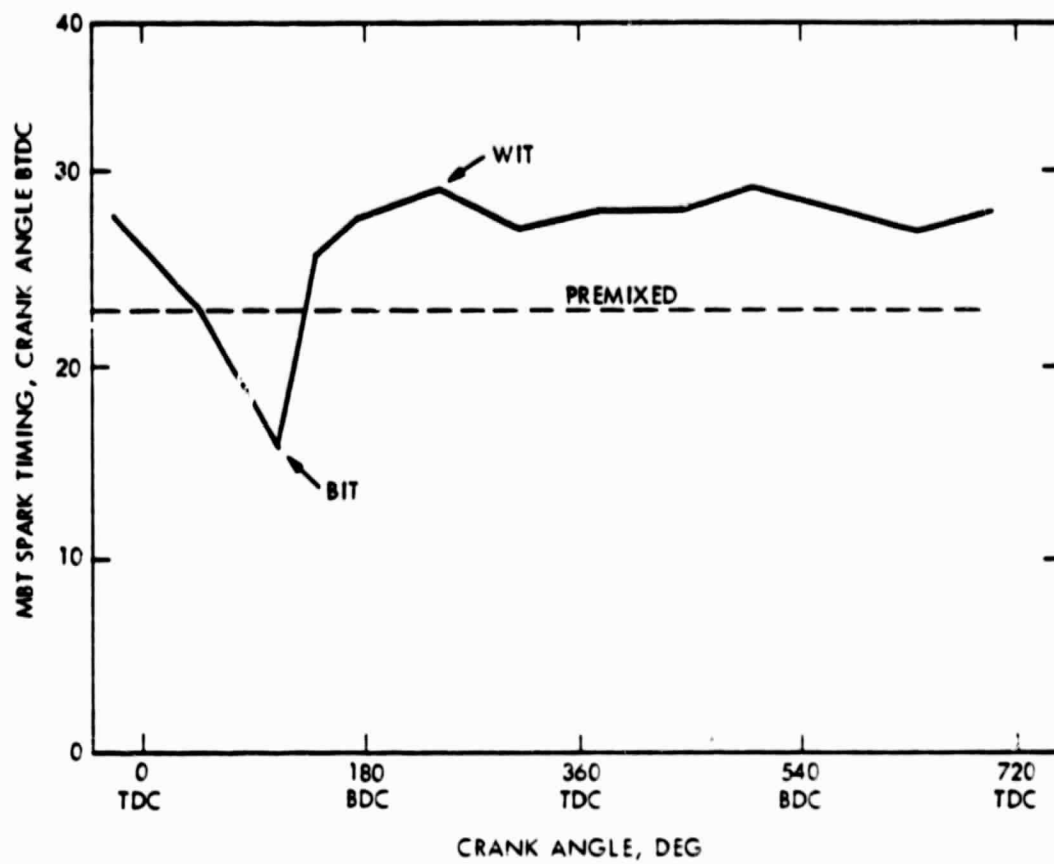


Figure 3-7. BIT Preparation Allows Smallest MBT Value at Fixed Equivalence Ratio, Suggesting More Rapid Combustion (Ref. 48)

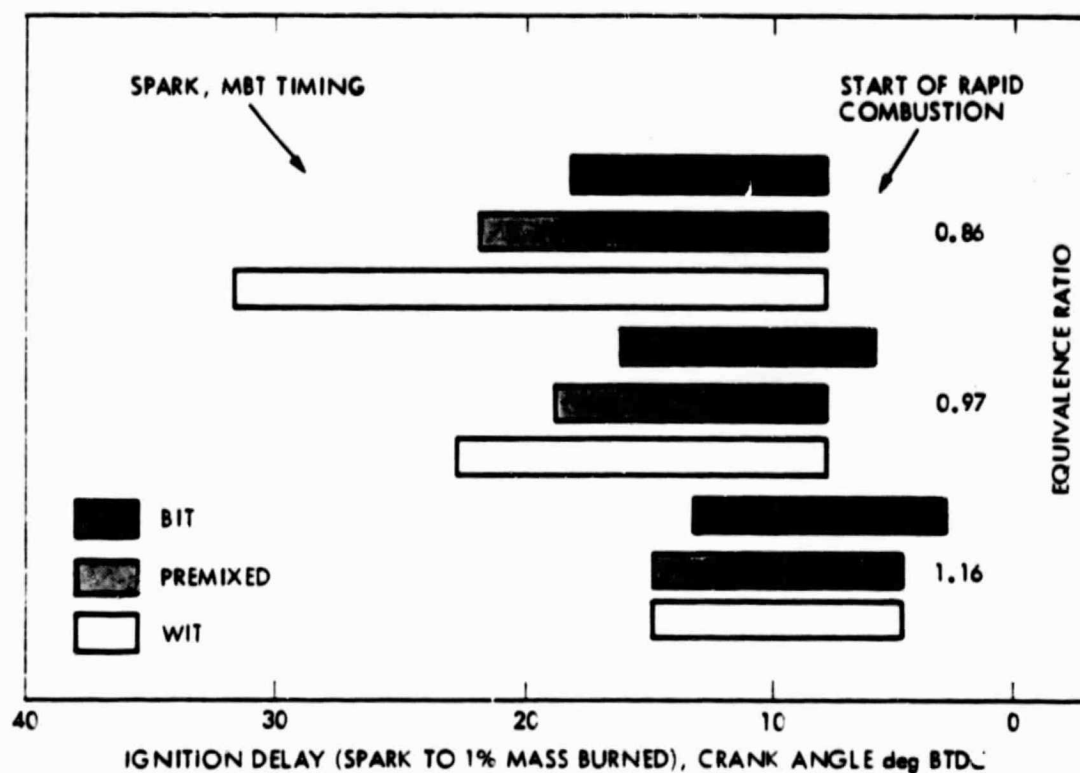


Figure 3-8. Ignition Delays May Explain Much of BIT's Advantage with Lean Mixtures - While Researchers Believe Both Propagation and Initiation are Enhanced, the Latter Seems to Profit More (Ref. 48)

The test results described so far were generated with the conventional CFR engine which has a shrouded intake valve. When the shrouded valve was replaced with an unshrouded valve, the lean mixture limit (LML) for the BIT mixture deteriorated by increasing from 0.55 to 0.76, but the LML of the WIT mixture improved by decreasing from 0.78 to 0.71. Two possible explanations for this result were expressed. One is that the shrouded valve brings about a beneficial bulk stratification of the charge which benefits the BIT mixture preferentially. The other reason, perhaps more plausible, is that the shrouded valve modifies the droplet size distribution to a more optimal size, which gives better initiation and improved flame propagation in lean heterogeneous mixtures.

Another set of investigations (Refs. 45 and 49) have been performed by General Motors to experimentally evaluate burning rate effects on engine behavior. The experiments were made on multi-cylinder spark-ignited gasoline engines which were converted for single-cylinder operation. Engine efficiency, emissions, cyclic variability of engine output power, roughness, and octane requirements were evaluated. The wedge and open combustion chambers shown in Figure 3-9 were extensively instrumented and tested to compare their combustion characteristics. The wedge chamber, with its off-set spark plug and resulting long flame-travel distance promotes relatively long burning times. On the other hand, the compact open chamber, with a more central spark plug location, is expected to produce faster burning.

The open chamber design did have faster burning, as measured by shorter combustion times and reduced MBT spark timing values. Comparisons of the net thermal efficiency and NO_x emissions characteristics of the two chamber designs is given in Figure 3-10. For engine operation with MBT spark timing, the open or faster burning chamber exhibits higher thermal efficiency. For each chamber design, the thermal efficiency increases for progressively higher EGR rates until reaching the dilution tolerance limit of each engine, after which the thermal efficiency decreases rapidly. Note the increased dilution tolerance of the faster-burning chamber. EGR rates as high as 28% can be accommodated with the open chamber, compared with 22% for the wedge chamber, before thermal efficiency drops significantly. Similar results hold when air is the diluent rather than EGR.

Also included in Figure 3-10 are index lines of constant NO_x emissions. Movement vertically downward from the MBT curve represents retarding the spark timing from its optimum value. Comparison of conditions at points A and B indicate that faster burning produces higher NO_x emissions. However, by adding a slight amount of EGR to the open chamber, as designated by point C, its efficiency advantage can be maintained while matching the NO_x emissions of the slower burning chamber. No significant effect of burning rate on HC emissions was found. Data indicate that engine operation at low EGR rates and retarded spark timing is an effective way to lower HC emissions, due to the higher exhaust temperature that results. In general, as thermal efficiency increases with faster burning, exhaust temperature decreases, resulting in a higher HC concentration at the exhaust port. However, the higher thermal efficiency means less total mass flow through the engine, which should more than compensate for the higher HC concentration. In addition to its potential for simultaneously achieving higher thermal efficiencies and lower NO_x emissions, fast burning also lessens cyclic variations

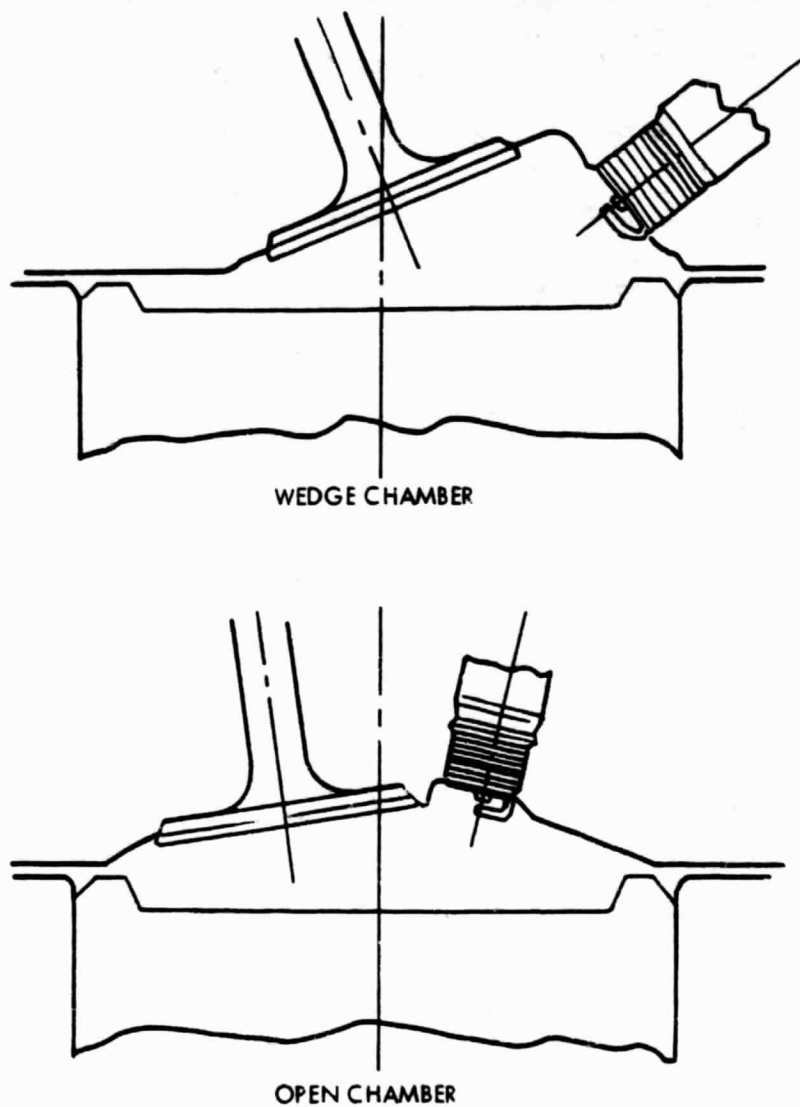
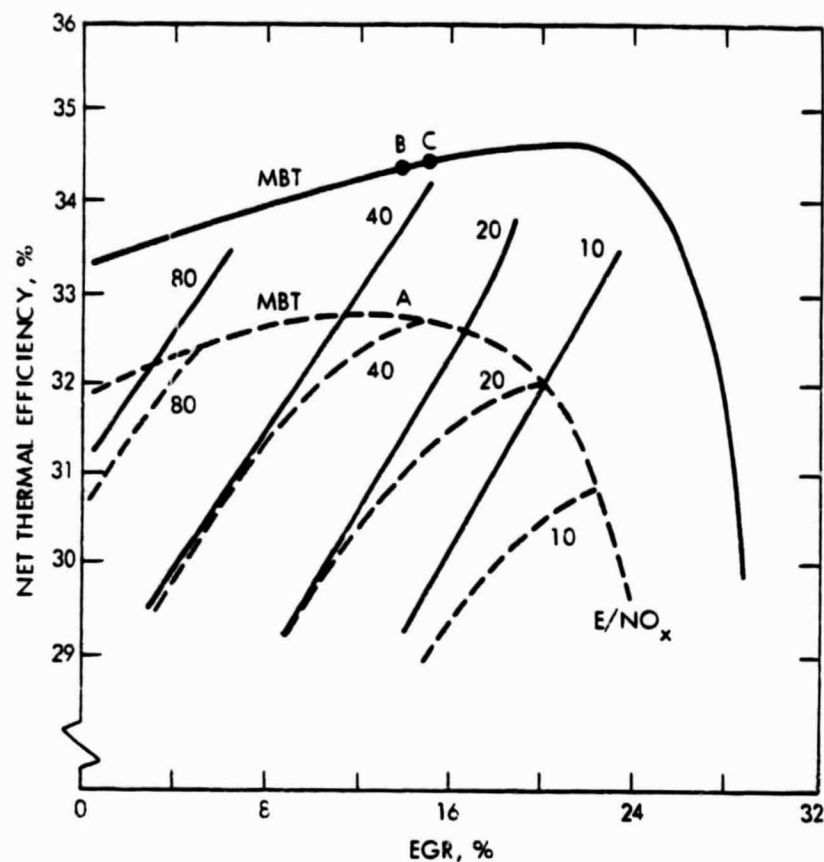


Figure 3-9. Combustion Chambers for Experimental Study Indicates Differing Volume Distributions of Wedge (Top) and Open Varieties (Bottom) (Ref. 49)



Note: MBT Varies with Amount of Exhaust Gas Recirculation for Open (Solid Lines) and Wedge (Dashed) Combustion Chambers. Emissions Index Figures are Expressed as Grams of Pollutant per Kilogram of Fuel. Fuel Input 23.0 mg/Cycle. A/F Ratio 16:1, 1900 RPM

Figure 3-10. Efficiency and NO_x Emissions (Ref. 49)

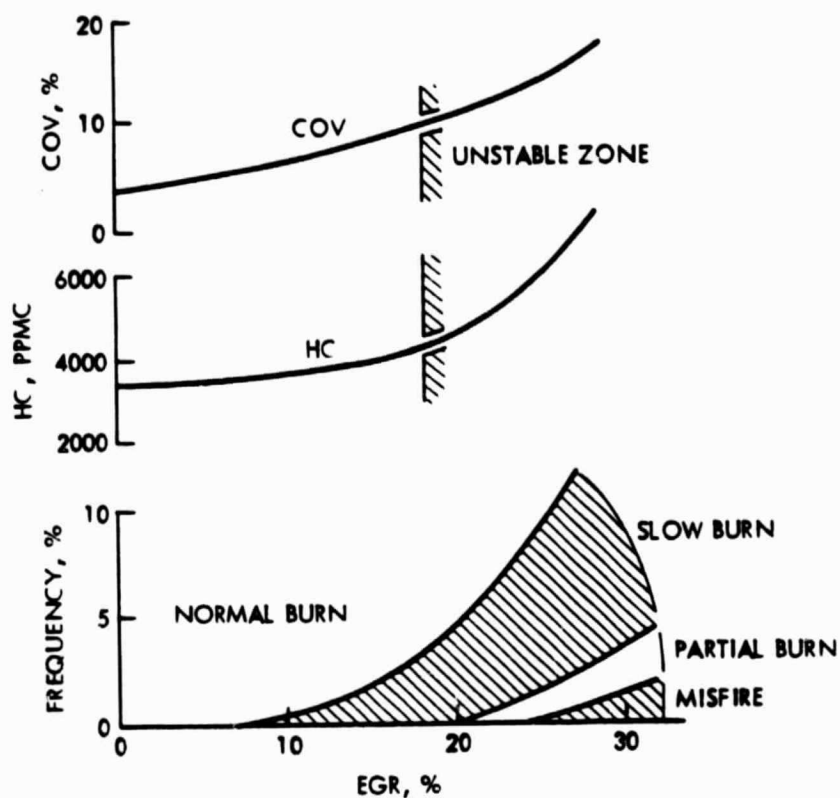
In engine power and thereby improves driveability. If cyclic variability is extreme, it can lead to vehicle surge. A measure of cyclic variability which can be used for comparison purposes is a coefficient of variance (COV) parameter, defined as the standard deviation of engine-indicated mean effective pressure (IMEP) divided by the average IMEP over a time period. A value of COV of about 10% marks the threshold of unacceptable vehicle stability.

As shown in Figure 3-11, increasing the amount of EGR, or correspondingly slowing down combustion, leads to greater cyclic variability. Four different regimes associated with additional EGR amounts have been identified: normal burn, slow burn, partial burn, and misfire. In the normal burn regime, flame propagates across the combustion chamber in a reasonable time. However, as more EGR is added, a slow-burn regime is entered, in which the flame barely gets across the combustion chamber in up to 5% of the engine cycles before the exhaust valve opens. In the partial-burn regime, some cycles may experience exhaust valve opening before the flame has completely propagated across the chamber. Finally, in the fourth regime, engine misfire occurs in some cycles with the addition of more EGR. The 10% threshold value of COV mentioned above is associated with the occurrence of slow-burn cycles at a frequency of 5%. Thus, for the engine operating condition in Figure 3-11, 20% EGR can be used without exceeding a COV of 10%.

An additional advantage of fast burning is that it lessens the knocking tendency of an engine and permits the use of higher allowable compression ratios which lead to further fuel economy advantages. Engine knock is caused by the instantaneous burning or detonation of a portion of the unburned gases ahead of the propagating flame. With the unburned mixture ahead of the propagating flame, the so-called end gas experiences an increase in both pressure and temperature during engine compression and a further increase caused by expansion of the burned gas behind the propagating flame front. In this increasing temperature environment, the end gas goes through a series of chain-branching chemical reactions which may lead to detonation under the right conditions. Two basic approaches have been taken to reduce engine knock; the use of fuel additives which inhibit the chemical reactions leading to detonation, and the use of combustion chamber design techniques which both reduce end-gas temperature and promote more rapid flame front propagation through the chamber.

Spark hooks indicating the minimum fuel octane numbers for knock prevention in slow-burn and fast-burn chambers are illustrated in Figure 3-12. These results show that the fast-burn chamber requires a fuel octane number of only 80 to operate at MBT spark timing. In contrast, the slow-burn chamber needs a fuel with a 97.5 octane rating at optimum timing. Alternatively, retarding the spark timing to allow an 80 octane fuel to be used in the slow-burn chamber would significantly reduce engine efficiency.

While fast burning of the mixture is a fundamental approach for reducing octane requirements, various engine design techniques are available for achieving it. Among favorable design features, from an anti-knock viewpoint, are a short flame travel distance, a concentration of chamber volume around the ignition point, generation of chamber turbulence, and provision of a large surface-to-volume ratio in the end-gas region.



NOTE: Rates Determine Frequencies of Various Burning Regimes, HC Concentrations, and Coefficient of Variance of Indicated Mean Effective Pressure (A/F Ratios 14.5:1, 1400 RPM, MBT)

Figure 3-11. EGR Rates (Ref. 49)

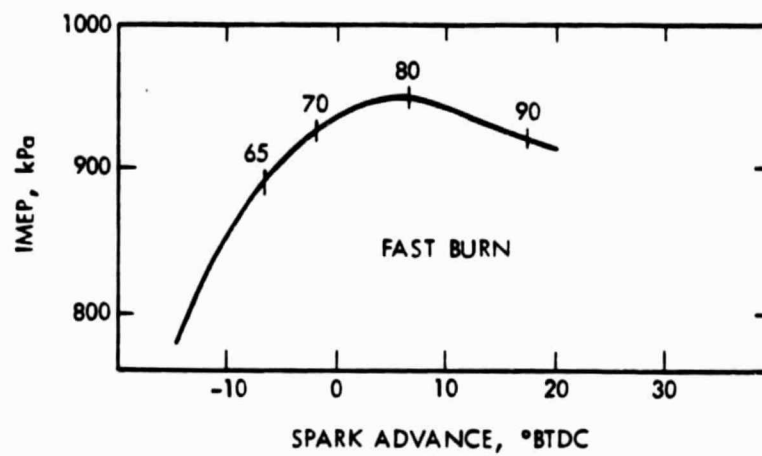
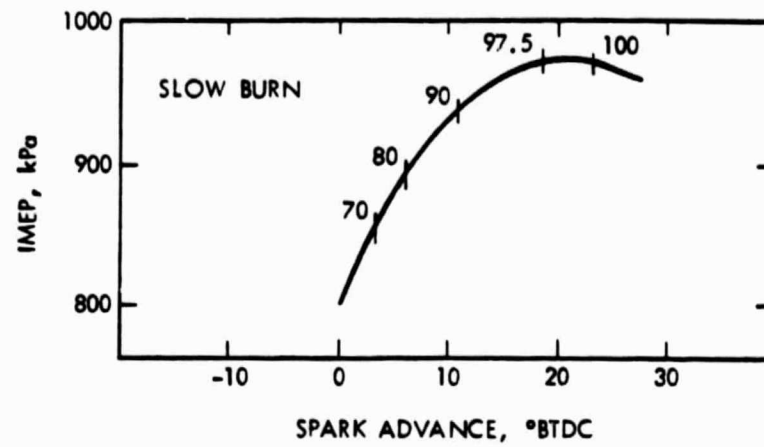


Figure 3-12. Spark Hooks Indicate Minimum Fuel Octane Numbers for Knock Prevention in Different Combustion Chambers (Ref. 49)

The effects of four engine design factors known to have significant influence on burning rate have been experimentally investigated. These design factors were spark plug location, intake-port charge velocity, swirl, and squish, as illustrated in Figure 3-13. Effects of these factors on ignition delay (0% to 10% mass-burned), combustion duration (10% to 90% mass-burned), and cyclic variability were examined by running each factor in combinations of the two levels given in Table 3-1. Results of these tests are shown in Table 3-2 in the form of percentage reduction for individually changing each factor from its lower to its higher value, while keeping the other factors at their lower levels. Test operating conditions were 1500 rpm, 70 psi IMEP, 14.2 air-fuel ratio, and MBT spark timing. As can be seen in the results, the effects of changing the four design factors are not additive for each of the three dependent parameters; strong interactions exist.

Design factors of spark plug location, chamber geometry, intake port or valve-flow velocity, swirl, and squish have been shown to have a strong influence on fuel-burning rates. There are many ways to integrate these factors into combustion chamber design to accomplish fast burning in engines.

Nissan researchers (Refs. 42 and 50) have evaluated the fast-burn concept with heavy EGR in a Datsun in-line four-cylinder 1.8 liter engine. A dual spark plug system was adopted to provide more rapid combustion in the engine cylinder. Combustion chamber shape and spark plug location were optimized experimentally to equalize flame propagation from both plugs. Engine displacement and compression ratio were unaltered.

Combustion duration and cyclic variability of the conventional and dual-spark plug, fast-burn engine were compared. Mass fraction of cylinder charge burned for each process was calculated by the average cylinder pressure trace of 400 consecutive cycles. With fast burn, combustion duration showed a marked decrease. With 20% EGR, combustion duration of the fast-burn engine was almost the same as that of the conventional engine with no EGR. Cyclic variability of the engines was represented by a coefficient of variance (COV) parameter defined as the standard deviation of engine IMEP divided by the average IMEP over a time period. A COV value of about 10% marks the threshold of unacceptable vehicle stability. For an air-fuel ratio of 14.5:1 and 20% EGR, the COV for the conventional engine reached 11%, well over the engine stability limit, while the COV for the fast-burn engine was about 4%, which is about the level for a conventional engine with no EGR.

Engine performance for various EGR rates is compared for the fast burn and conventional engines in Figure 3-14. Because combustion with heavy EGR is greatly improved by fast burn, the EGR rate at the engine stability limit is 33% compared with 18% for the conventional engine. At EGR rates below the engine stability limit for the conventional engine, NO_x emissions from the fast-burn engine are higher. At higher EGR rates, fast burn can significantly reduce NO_x emissions. At the same time, stabilized combustion decreases the HC emissions from the fast-burn engine compared with those from the conventional engine. The MBT spark timing for the fast-burn engine is more than 10 degrees below than that for the conventional engine because

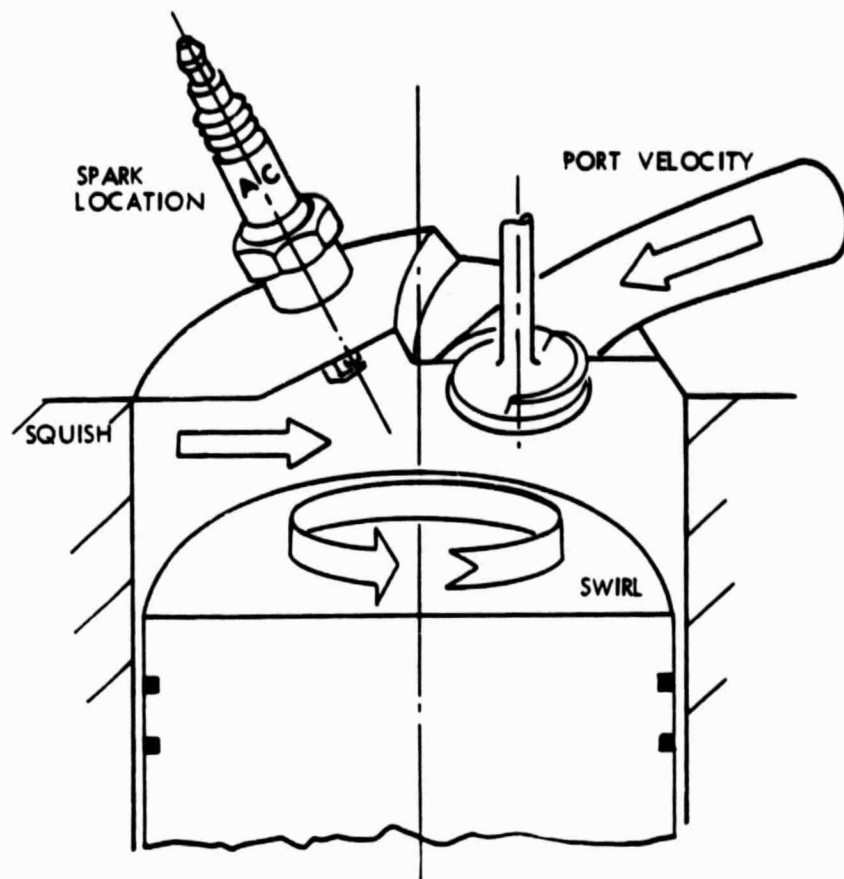


Figure 3-13. Four Major Design Factors Indicated Schematically
(Ref. 49)

Table 3-1. Experimental Design Factors

Factor	Change from Low to High Level
Spark Plug Location	17 mm off cylinder centerline to central location
Port Charge Velocity	25% increase ^a
Swirl	0 to 5000 rpm ^b
Squish	0% (open chamber) to 30% squish area

^aIntake port area was restricted so that flow was reduced 35% at 10-mm valve lift and 16.9 kPa (127-mm Hg) pressure drop on flow bench. Therefore, at given engine airflow, port velocity is increased.

^bBased on flow bench with 10-mm valve lift and 16.9 kPa (127-mm Hg) pressure drop.

Table 3-2. Percentage Reductions in Combustion Parameters

Factor	Ignition Delay	Combustion Duration	Cyclic Variation
Spark Plug Location	4.8	20	30.5
Port Charge Velocity	12.8	24	27.0
Swirl	33.2	24	50.5
Squish	6.4	11	16.8
Combination of all four factors	20	42	59

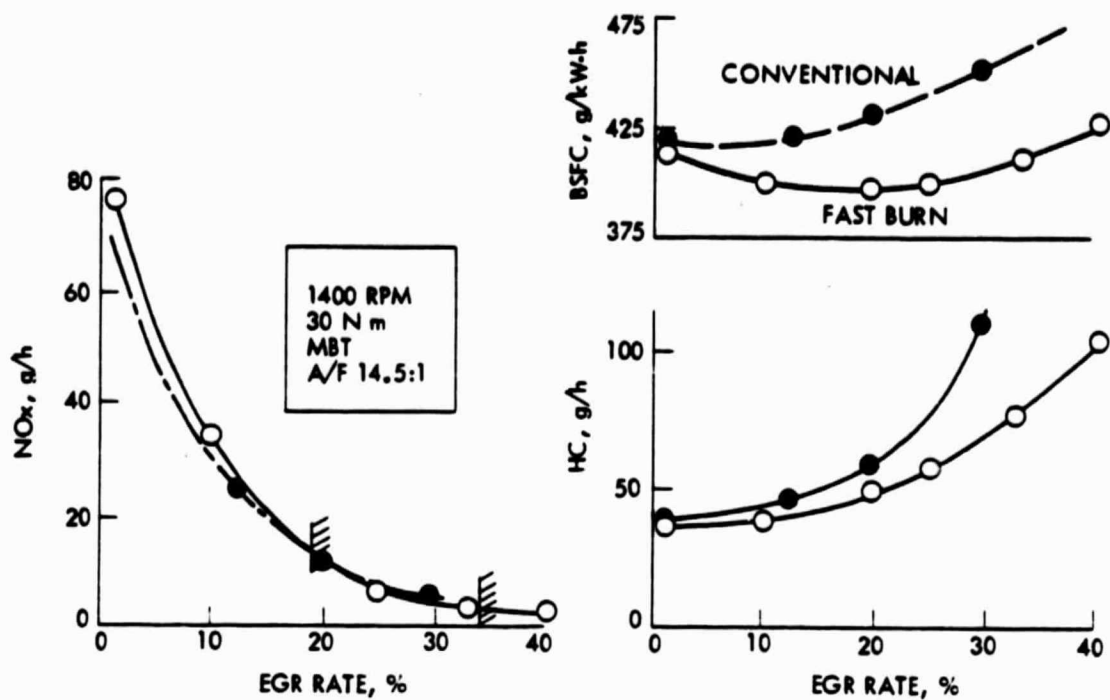


Figure 3-14. Fuel Economy and Emissions are Improved by Fast Burn Engine, with Greater Proportional Benefits at Higher EGR Rate (Ref. 50)

of the shortened combustion duration. Fuel economy was improved by fast burn, the improvement being larger with higher EGR rates.

The relationship between NO_x emissions and specific fuel consumption for the two engine types is given in Figure 3-15. The vertical portions of the two L-shaped curves were drawn from test results with MBT spark timing at various EGR rates. The hatched portions correspond to data from various spark timings retarded from MBT values and EGR rates at the engine stability limit. Engines can be operated in the zone above the L-shaped lines. These results indicate that the fast-burn engine can achieve a marked reduction in NO_x emissions while maintaining good fuel economy. As a result of these investigations, Nissan has introduced a fast-burn engine incorporating dual spark plugs (designated the NAPS-Z engine) in some of their 1980 California model vehicles. The combustion chamber configuration in the fast-burn engine is shown in Figure 3-16.

Another fast-burn concept which has been under development for several years is the May Fireball engine (Ref. 51). In this engine approach, the combustion chamber shape is designed to enhance a well-defined vortex or swirl motion in the charge, as shown in Figure 3-17. The combustion chamber is located below the exhaust valve in the cylinder head. A channel-like recess leads from the intake valve area to the combustion chamber. In combination with the approaching piston deck, this geometry forces a part of the charge to enter the combustion chamber in a substantially tangential manner, thereby creating a controllable swirl motion. This combustion chamber design concentrates the combustible mixture near the spark plug and promotes a charge motion with sufficient turbulence to obtain fast burning rates.

Fuel economy and emissions characteristics over the urban and highway driving cycles are given in Table 3-3 for a May Fireball 115 horsepower engine installed in a car of 1140 kilograms. The engine is a 4-cylinder, 2-liter, watercooled passenger car engine with a compression ratio of 14.6:1. The test was run using European premium fuel of approximately 97 research octane number (RON). The test was made without the use of catalysts, EGR, air injection, or other emissions control hardware.

Table 3-3. Engine-Out Emissions of a 115-hp and 1140-kg Vehicle in the U.S. SYS Test

Engine-Out		
HC	gr/mile	3,2
CO	gr/mile	2,9
NO_x	gr/mile	0,3
Consumptions		
City	miles/gallon	21
Highway	miles/gallon	35
Combined	miles/gallon	25

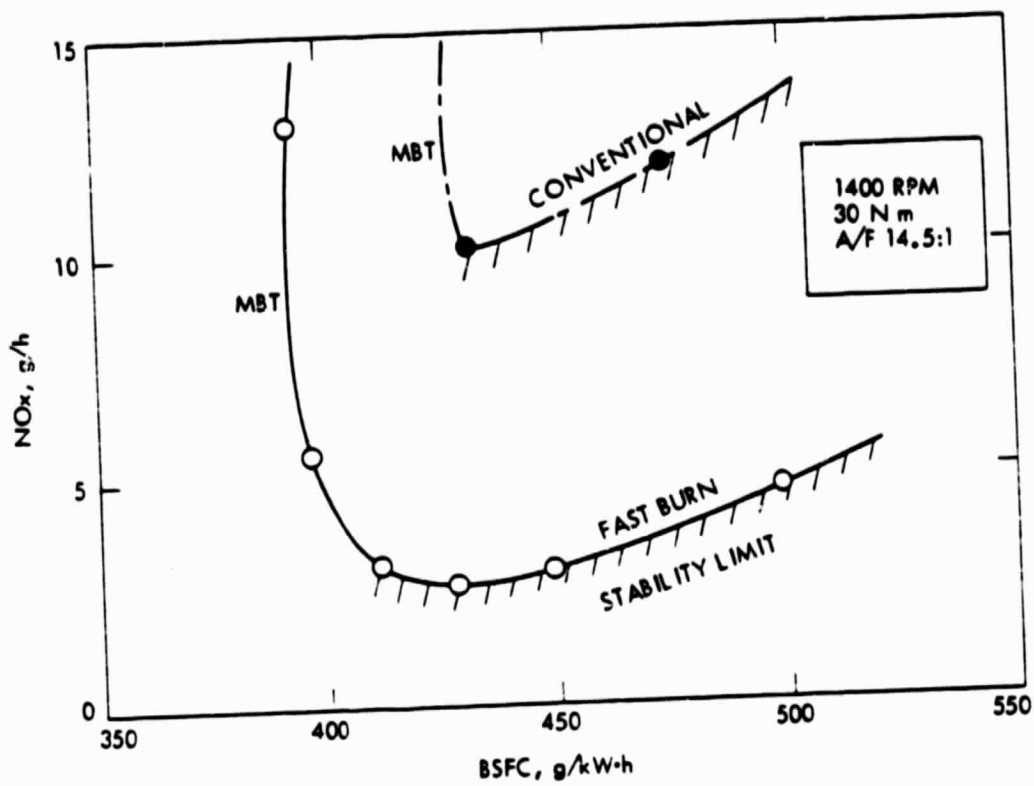


Figure 3-15. Brake-Specific Fuel Consumption versus NO_x Relationship Indicates Benefits of Fast Burn Engine (Ref. 50)

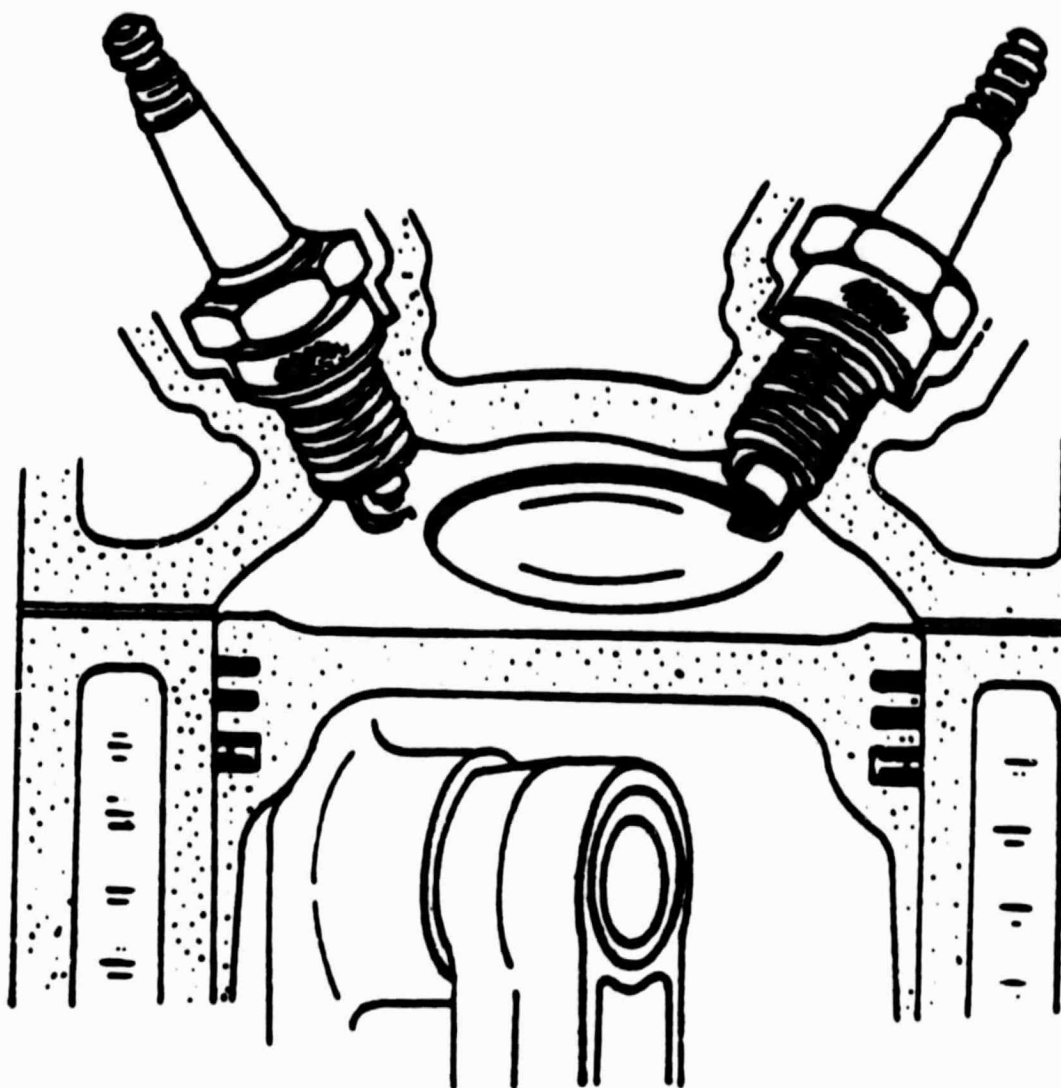


Figure 3-16. Configuration of Dual Spark Plugs Used
in Nissan NAPS-Z Engine (Ref. 42)

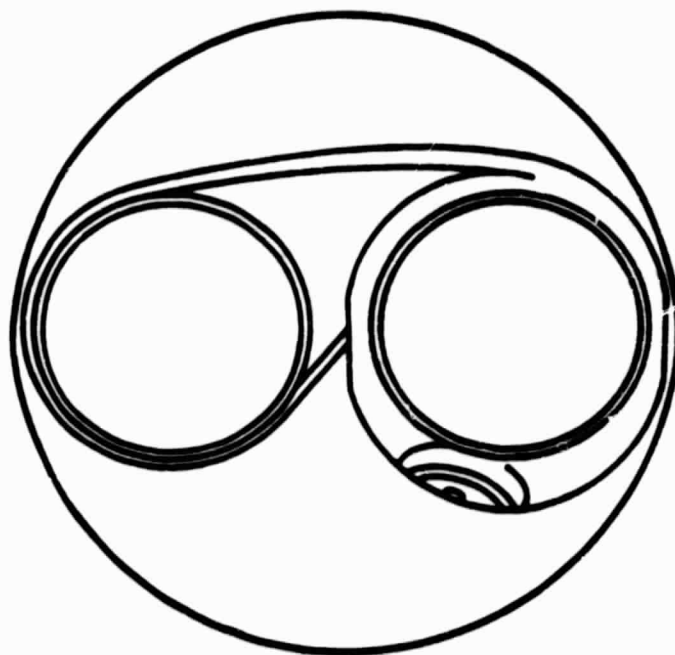
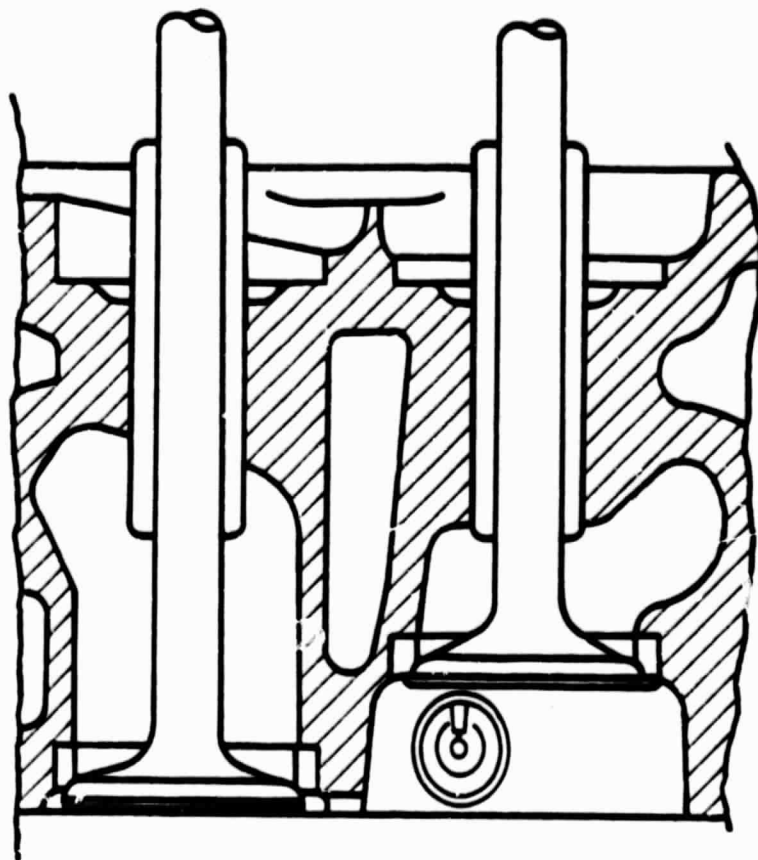


Figure 3-17. High Compression Lean Mixture Homogeneous Charge Combustion Chamber (Ref. 51)

Mitsubishi engineers have developed a combustion system (Refs. 4 and 44) (designated the MCA-Jet), that improves the low-speed light load operating modes typical of urban driving. Their MCA-Jet engine incorporates extra valves which induct air into the combustion chambers to generate carefully controlled turbulence. Flame propagation is promoted by this induced swirl which persists through both compression and expansion. MCA-Jet benefits include a substantial extension of the lean mixture limit, more stable combustion of EGR-deadened mixtures, and significantly improved fuel economy.

The integration of this concept into Mitsubishi's 4-cylinder overhead cam (OHC) engine is shown in Figure 3-18. Each cylinder has a small third valve, the jet valve, operated by the same rocker arm actuating the conventional intake valve. Below each jet valve lies an insert containing an orifice which directs the air toward the spark plug.

Jet valves are fed with either air or a super-lean mixture, whose source is adjacent to the carburetor throttle plate. Because of this location, jet-valve induction is sensitive to changes in throttle opening. However, the system is optimized to provide air to the jet valves mainly under light throttle conditions with little or no air supplied at idle or wide-open throttle (WOT) conditions.

The MCA-Jet system demonstrated fuel economy improvements in all operating modes. For example, at a 40 km/h road load, the MCA-Jet gave better than 10% improvement in fuel economy, compared to an engine running without jet air.

The MCA-Jet extended the engine lean mixture limit significantly. With timing at 30 degrees BTDC, for instance, the conventional engine started exhibiting unstable combustion with air-fuel ratios in the 20:1 range. With the same timing, MCA-Jet combustion remained stable to around 24:1.

To evaluate the MCA-Jet engine effect on EGR-controlled NO_x emissions, it was compared with a conventional engine with both engines controlled to a NO_x level of 10 parts per million (ppm). Each engine had optimal timing and a 40 km/h road load. Air induction rate on the MCA-Jet was 0.97 liter/sec. Test results showed that MCA-Jet gave about 10% improvement in fuel economy while running with equivalent NO_x control.

Comparison of the combustion characteristics of a conventional engine and MCA-Jet engine are shown in Figure 3-19. These results confirm the greater flame speed, improved combustion, and better fuel economy of the MCA-Jet engine.

The MCA-Jet system is standard in Mitsubishi's engine family which is used in small Plymouth and Dodge automobiles.

Several of the newer engine designs introduced in recent years have made use of the geometrical approach to fast burn. A cross-section of the General Motors, 2.8 liter, V-6 engine designed by Chevrolet is shown in Figure 3-20. This engine has a somewhat open chamber with a near-central spark plug location. Another geometrical approach to fast burn is shown in Figure 3-21, where the original shallow cavity of a flat-topped piston in

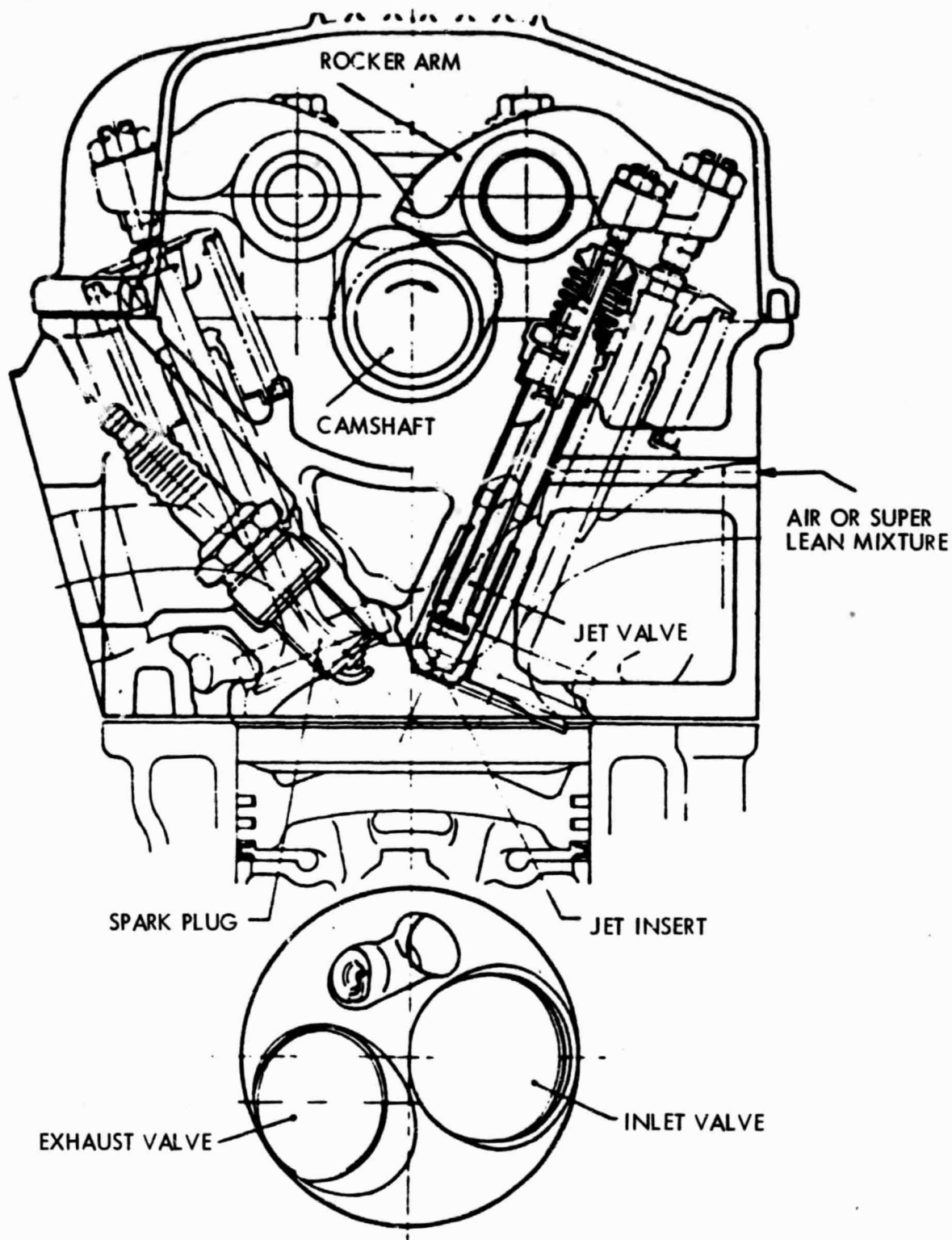


Figure 3-18. MCA-Jet Valve Operates Off Same Rocker Arm as its Adjacent Intake Valve. Orifice in Jet Insert Directs Air Toward Plug (Ref. 4)

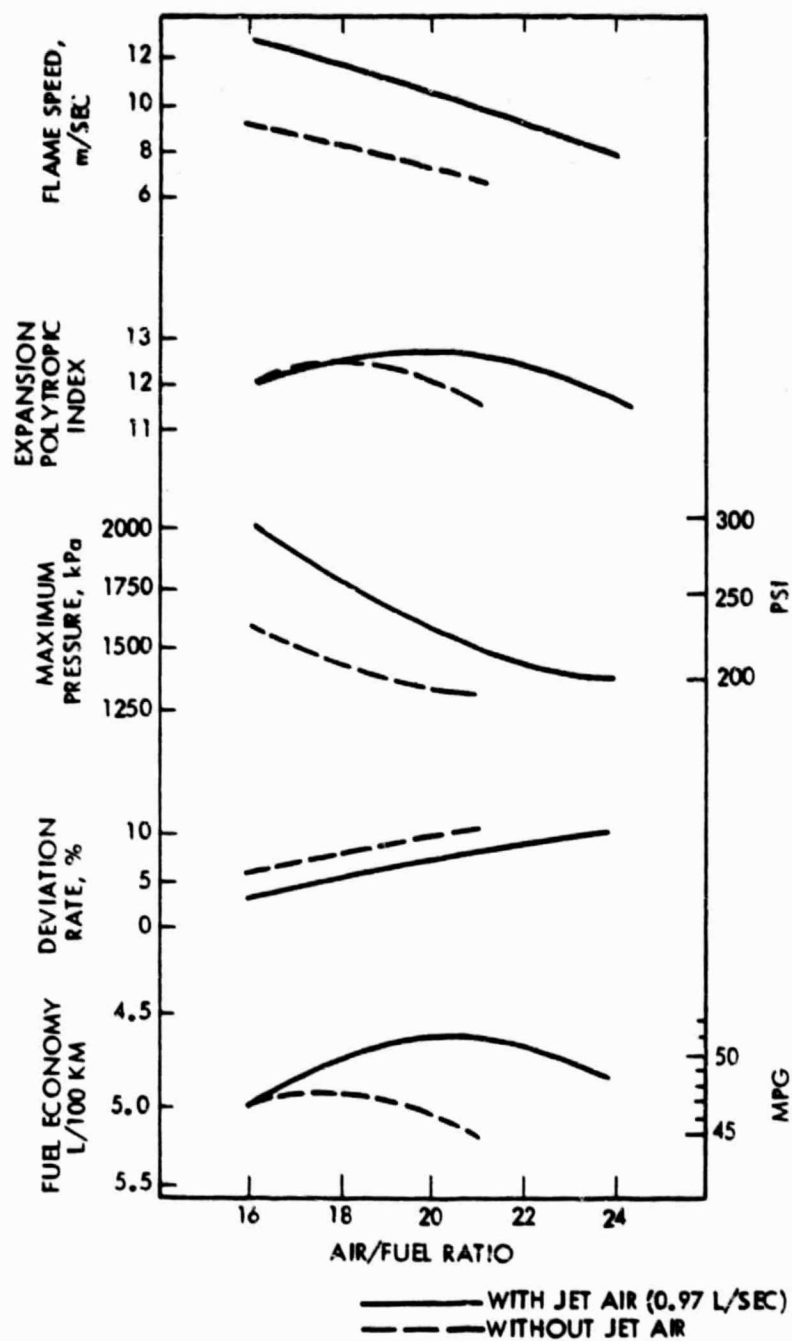


Figure 3-19. Combustion Analyses Confirm MCA-Jet's Greater Flame Speed, Improved Combustion, and Better Fuel Economy (Ref. 4)

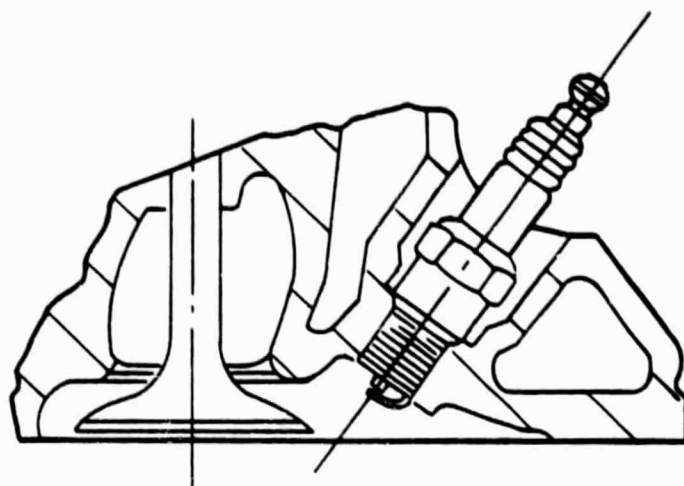


Figure 3-20. Combustion Chamber of GM's 2.8-L V-6 Engine Designed by Chevrolet (Ref. 49)

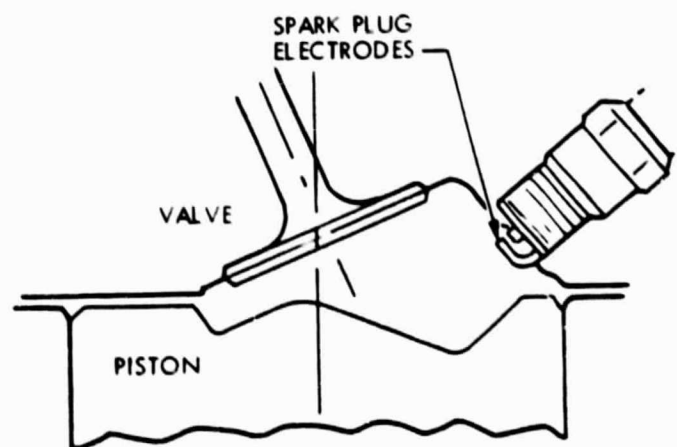


Figure 3-21. Modified Wedge Chamber Has Been Employed in Turbocharged Version of Pontiac 4.9-L V-8 Engine (Ref. 49)

a wedge-shaped chamber was redistributed to provide an off-set cavity. The original compression ratio was maintained. This off-set cavity provides a large frontal area to the propagating flame, while improving the fuel octane requirement by providing more effective end-gas cooling. This piston cavity approach is used in the turbocharged version of the Pontiac 4.9 liter, V-8 engine.

In the 1981 model year, Ford introduced an engine having a hemispherically-shaped combustion chamber for the new Escort automobile. This combustion chamber shape is similar to the Chrysler "hemi" engines of the early 1950's, as shown in Figure 3-22.

3.3 VEHICLE FUEL ECONOMY AND EMISSIONS RESULTS

This section covers the fuel economy and emissions results for current production vehicles which use lean burn (fast burn) engine technology. Only those vehicles which do not utilize three-way catalyst-emissions control systems are discussed. Only vehicles using the Nissan NAPS-Z engine and the Mitsubishi MCA-Jet engine meet these requirements. The data is taken from EPA certification and fuel economy data for the 1980 model year in California. California data is utilized because it is felt that California emissions standards are more representative of future emissions requirements for all states.

Fuel economy and emissions results for the 1980 California vehicles using the Mitsubishi MCA-Jet engine are compared with the results for all 1980 California vehicles using three-way catalyst emissions control in Figures 3-23 through 3-26. It should be noted that these are primarily small vehicles with inertia weights between 2000 and 3000 lb. As shown in Figure 3-24, the efficiencies of these vehicles, indicated by the (IW X MPG) parameter, are generally higher than the average for all California vehicles with three-way catalysts. Also, the MCA-Jet vehicles have HP/IW values, which should make them good performance vehicles; the HC emissions are very low, CO emissions on the average meet the 3.4 g/mi requirement, and NO_x emissions fall between 0.4 g/mi and 0.9 g/mi. Comparisons of the fuel economy and emissions characteristics of the California and 49-state versions of these vehicles are given in Table 3-4 and Figure 3-27. Examination of this data indicates that some fuel economy penalty is associated with meeting the low NO_x emissions level. This fuel economy penalty is substantial for the small (86 CID) MCA-Jet engine. Also, note that substantial increases in CO emissions result when the engines are calibrated to meet the lower NO_x requirement. These data indicate that the MCA-Jet engine system may have difficulty in meeting more stringent emissions requirements, especially without significant fuel economy penalties.

Fuel economy and emissions results for the 1980 California vehicles using the Nissan NAPS-Z engine are compared with the results for all 1980 California vehicles using three-way catalyst emissions control in Figures 3-28 through 3-31. These vehicles have inertia weights between 2500 and 3000 lb, and have HP/IW values around 70. As shown in Figure 3-29, the efficiencies of these vehicles, as indicated by the IW X MPG parameter, are as good as the best of all California vehicles with three-way catalyst emis-

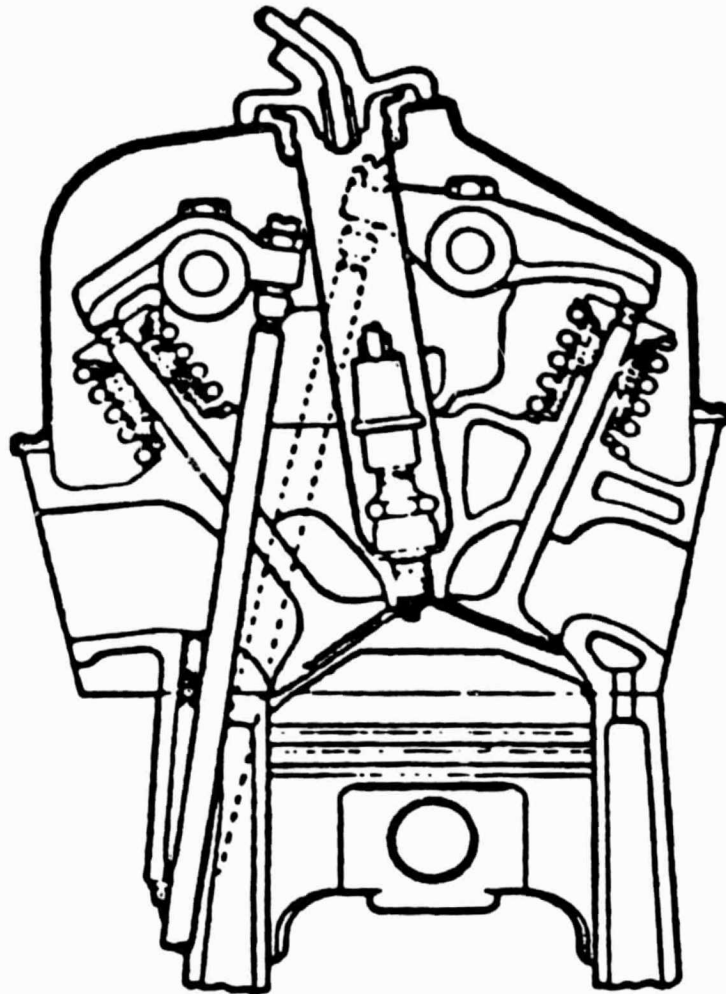


Figure 3-22. Chrysler's "Hemi" Head Style Chamber Adapted for Use in 1981 Ford Engine (Ref. 49)

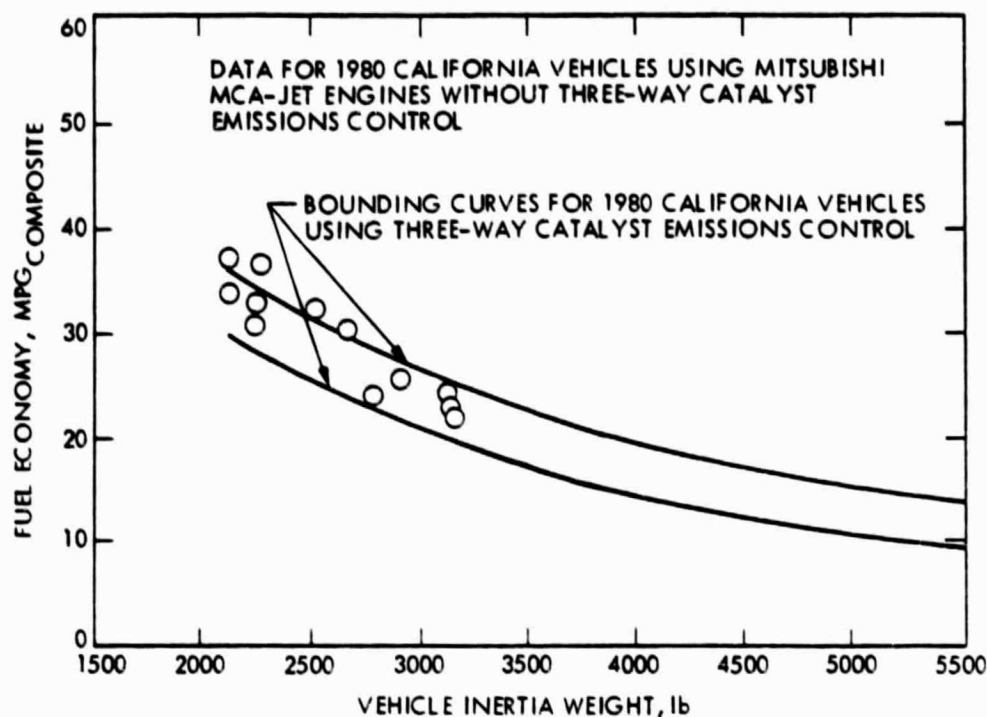


Figure 3-23. Composite Fuel Economy for California Vehicles Using the Mitsubishi MCA-Jet Engine

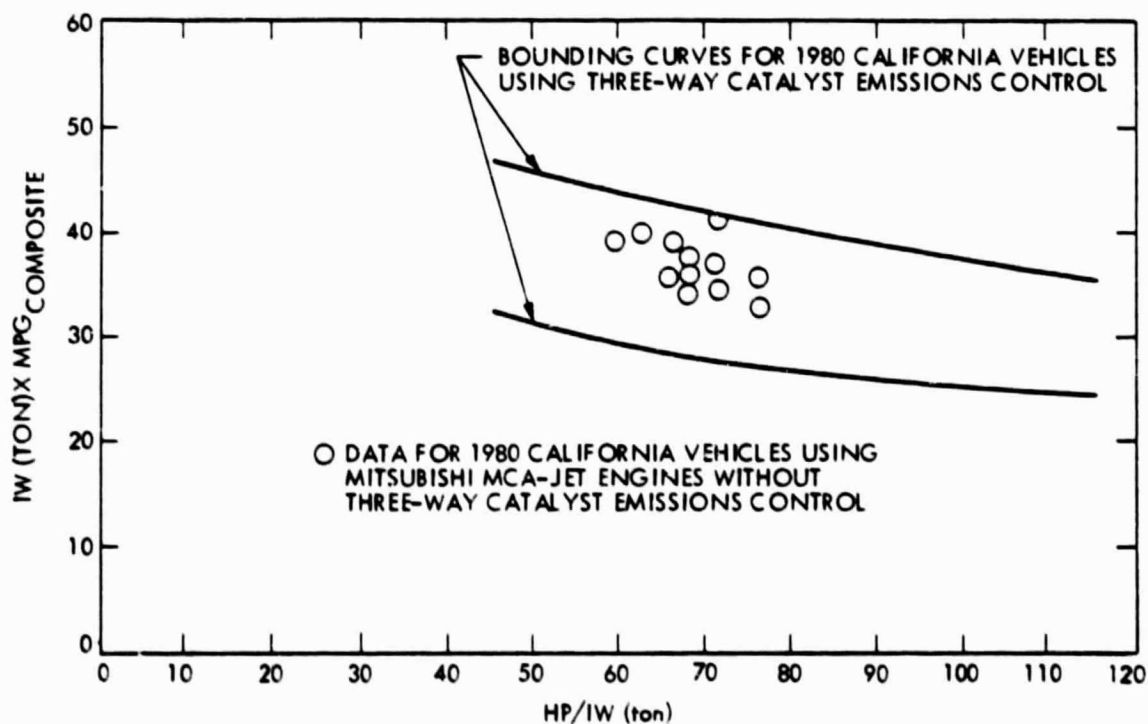


Figure 3-24. Fuel Economy Characteristics for California Vehicle Using the Mitsubishi MCA-Jet Engine

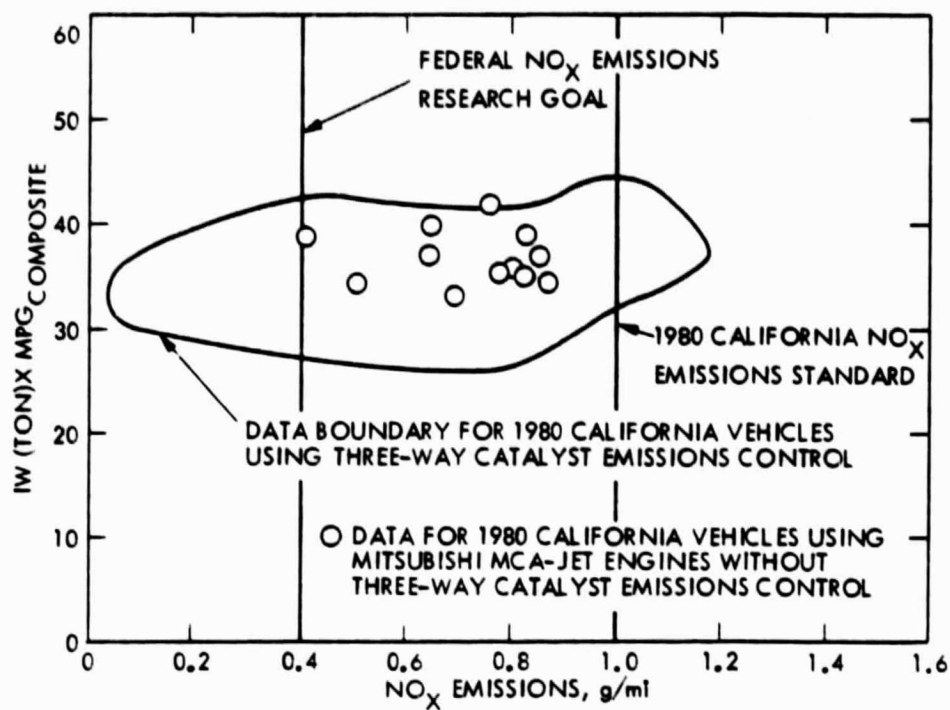


Figure 3-25. NO_x Emissions Characteristics for California Vehicles Using Mitsubishi MCA-Jet Engines

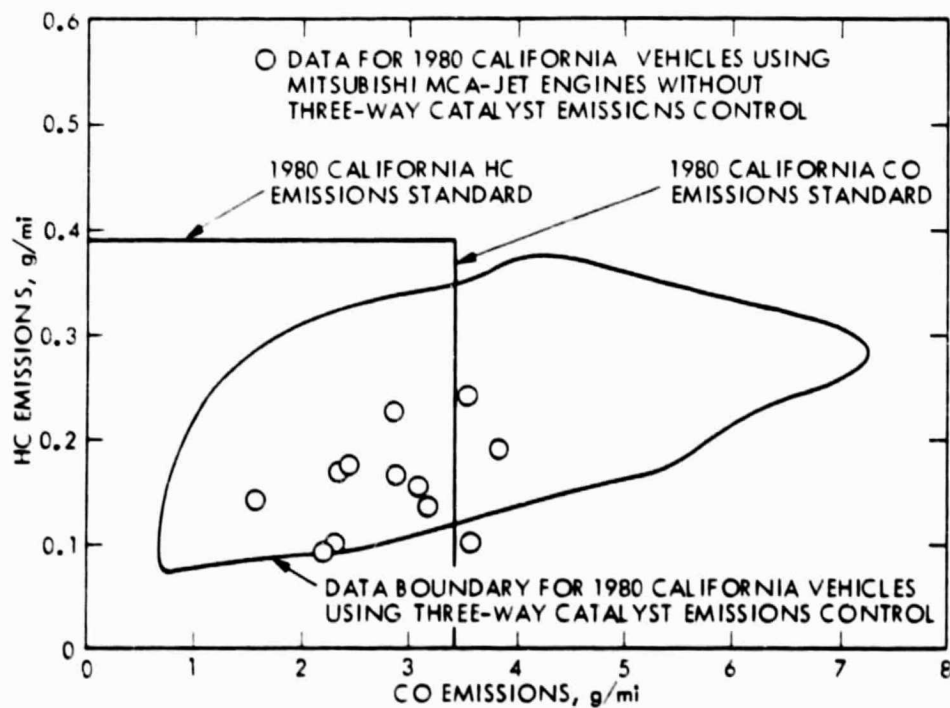
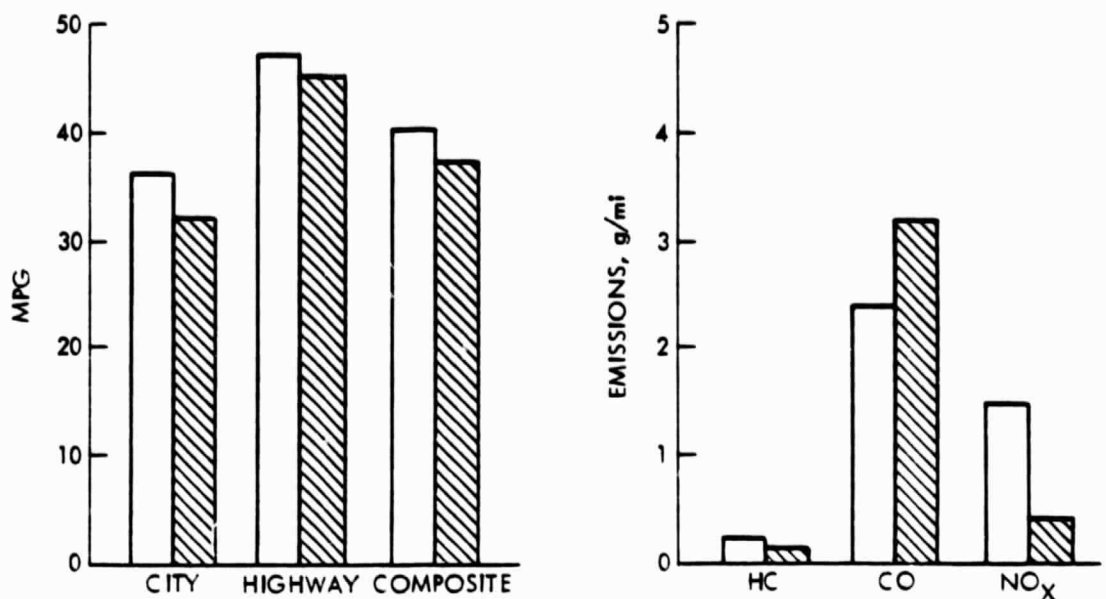


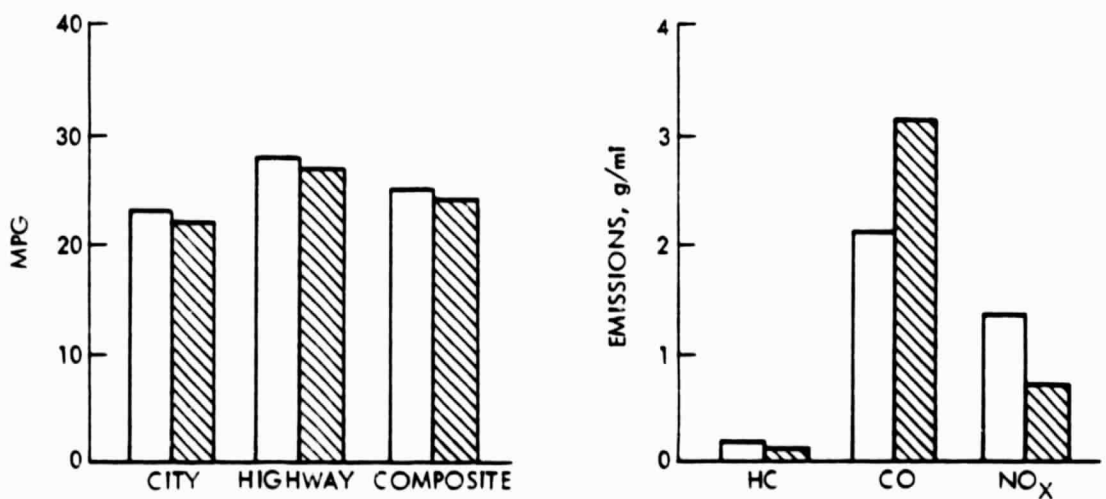
Figure 3-26. HC and CO Emissions Characteristics for California Vehicles Using Mitsubishi MCA-Jet Engines

Table 3-4. Characteristics of Mitsubishi MCA-Jet Engines in 1980 California and 49-State Vehicles

MFG	Car Line	CID	Carb Comp.		HP	Emission	Trans	Wt	Axle	City	Hwy	Comb	HC	CO	NOx	Ton x	
			FI	Ratio												MPG	Comb
Mitsubishi (Cal) (MCA-Jet)	Champ	86	C-2	8.8	70	EGR/PLS/OXD	D4-2	2125	3.47	32	45	37	0.136	3.15	0.04	39.31	65.88
	Champ						D4-1	2125	3.47	30	41	34	0.139	1.58	0.79	36.13	65.88
	Champ	86	C-2	8.5	80	EGR/PLS/OXD	A3-1	2250	3.17	29	35	31	0.183	2.42	0.83	34.88	71.11
	Arrow						A3-1	2625	3.54	27	35	30	0.170	2.90	0.81	39.38	59.43
	Champ						D4-2	2250	3.47	33	44	37	0.175	2.39	0.75	41.63	71.11
	Champ						D4-1	2250	3.47	29	39	33	0.088	2.21	0.63	37.13	71.11
	Arrow						M5-2	2500	3.91	27	40	32	0.098	2.27	0.64	40.00	62.40
	Arrow	156	C-2	8.2	105	EGR/PLS/OXD	A3-1	2750	3.54	22	27	24	0.152	3.12	0.69	33.00	76.36
	Colt Wg.						A3-1	3125	3.54	20	25	22	0.101	3.55	0.50	34.38	67.20
	Colt Wg.						A3-1	3125	3.54	21	26	23	0.189	3.84	0.79	35.94	67.20
	Arrow						M5-2	2750	3.54	22	34	26	0.221	2.88	0.81	35.75	76.36
	Challenger						M5-2	3125	3.54	21	30	24	0.240	3.52	0.83	37.50	67.20
Mitsubishi (49-St)	Champ	86	C-2	8.8	70	EGR/PLS/OXD	D4-2	2125	3.47	36	47	40	0.215	2.36	1.43	42.50	65.88
	Champ						D4-1	2125	3.47	33	43	37	0.187	1.81	1.61	39.31	65.88
	Champ						M4-2	2125	3.47	37	47	41	0.157	2.00	1.60	43.56	65.88
	Champ	98	C-2	8.5	80	EGR/PLS/OXD	A3-1	2250	3.17	30	36	52	0.119	2.12	1.00	36.00	71.11
	Arrow						A3-1	2625	3.54	29	36	31	0.195	2.94	1.73	40.69	59.43
	Champ						D4-2	2250	3.47	35	46	39	0.195	2.69	1.47	43.88	71.11
	Champ						D4-1	2250	3.47	31	40	34	0.176	1.15	1.63	38.25	71.11
	Arrow						M5-1	2500	3.91	29	41	35	0.154	2.14	1.35	41.25	62.40
	Arrow	156	C-2	8.2	105	EGR/PLS/OXD	A3-1	2750	3.54	23	28	25	0.182	2.09	1.34	34.38	76.36
	Colt Wg.						A3-1	3125	3.54	22	26	24	0.145	4.58	0.94	37.50	67.20
	Colt Wg.						A3-1	3125	3.54	22	27	24	0.145	4.47	0.86	37.50	67.20
	Arrow						M5-2	2750	3.54	22	34	26	0.220	1.55	1.73	35.75	76.36
	Challenger						M5-2	3125	3.54	21	32	25	0.257	3.48	1.59	39.06	67.20



FUEL ECONOMY AND EMISSIONS COMPARISONS FOR CALIFORNIA AND 49-STATE VEHICLES
MITSUBISHI CHAMP (86 CID ENGINE)



FUEL ECONOMY AND EMISSIONS COMPARISONS FOR CALIFORNIA AND 49-STATE VEHICLES
PLYMOUTH ARROW (156 CID ENGINE)

 CALIFORNIA
 49-STATE

Figure 3-27. Fuel Economy and Emissions Comparisons for California and 49-State Vehicles Using Mitsubishi MCA-Jet Engines

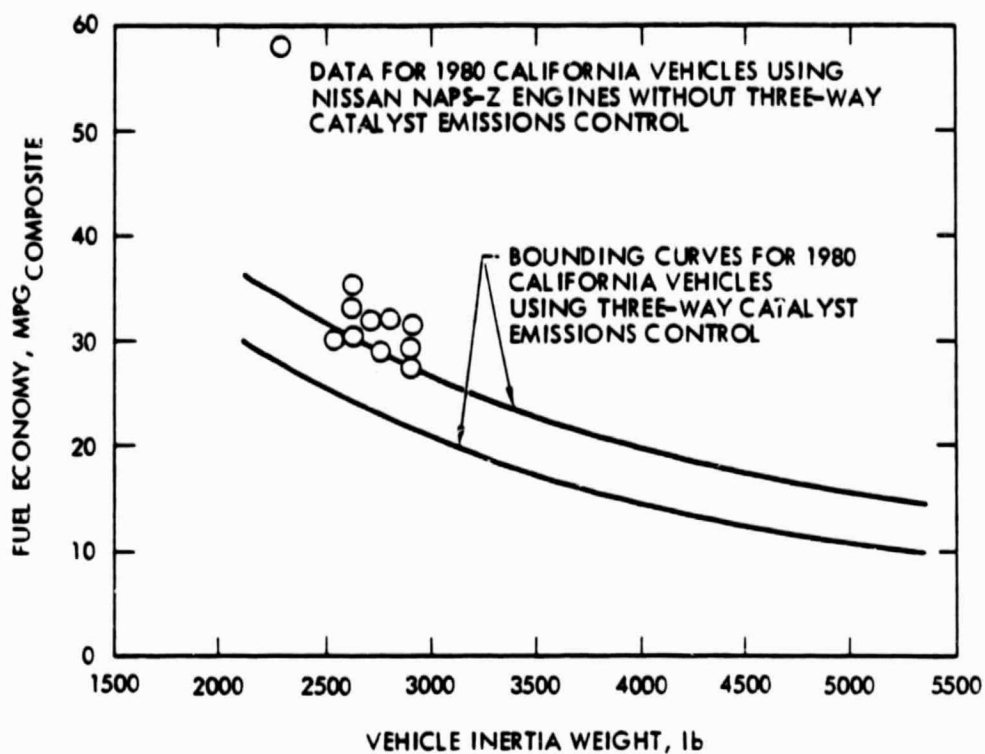


Figure 3-28. Composite Fuel Economy for California Vehicles Using the Nissan NAPS-Z Engine

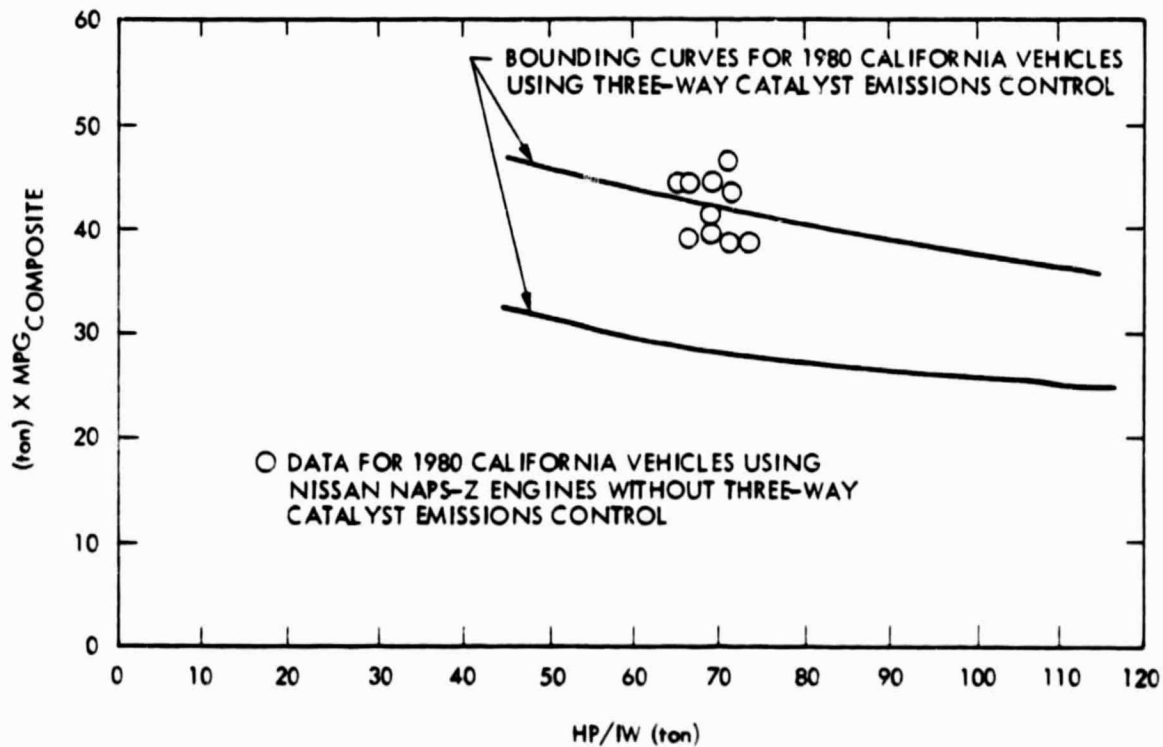


Figure 3-29. Fuel Economy Characteristics for California Vehicles Using the Nissan NAPS-Z Engine

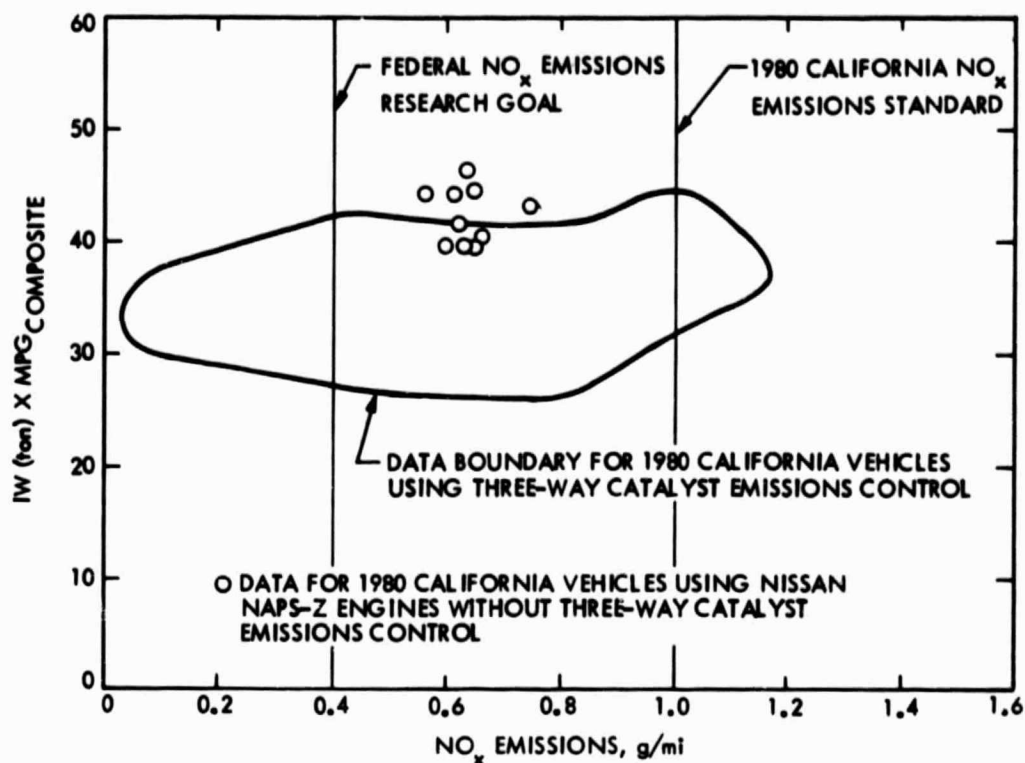


Figure 3-30. NO_x Emissions Characteristics for California Vehicles Using Nissan NAPS-Z Engines

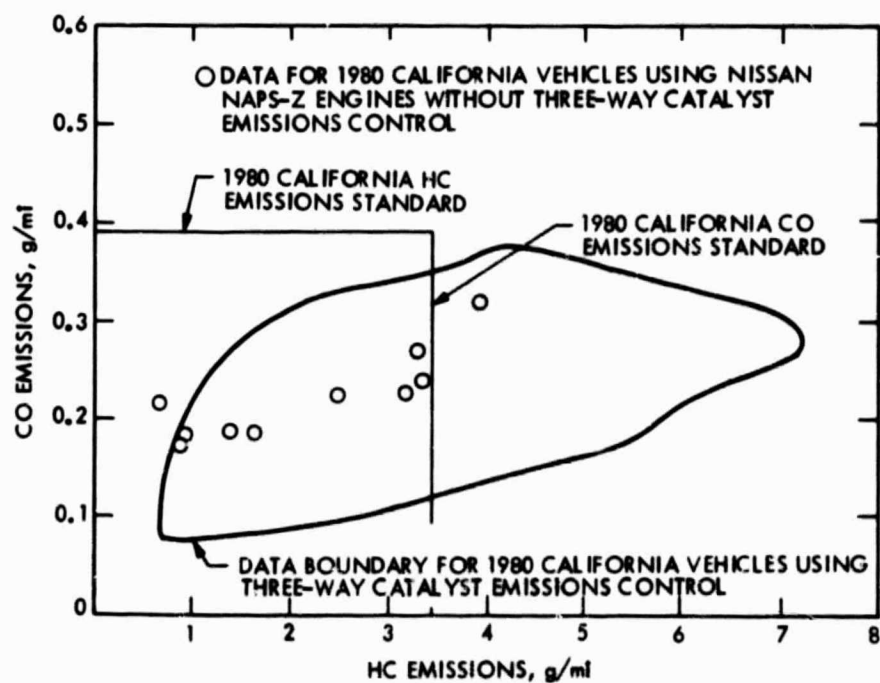


Figure 3-31. HC and CO Emissions Characteristics for California Vehicles Using Nissan NAPS-Z Engines

sions control. The HC and CO emissions are both good and the NO_x emissions are generally between 0.6 g/mi and 0.7 g/mi. The NAPS-Z system could suffer some fuel economy penalty if calibrated to meet lower NO_x emissions levels.

SECTION 4

STRATIFIED-CHARGE ENGINE CONCEPTS

4.1 INTRODUCTION

In the early 1970's, the need for higher efficiency and lower emissions from automotive powerplants led to an increased interest in the development of alternatives to the spark-ignition, uniform-charge Otto cycle engines used in most automobiles. In addition to having desirable efficiency and emissions characteristics, any alternative powerplant being considered for production had to also be acceptable from other standpoints (e.g., cost, manufacturability, maintenance, dependability, durability, driveability, response). The stratified-charge engine concept appeared to offer advantages over the other alternatives in these areas and as a result offered a better chance of reaching production status, because it was in many ways similar to existing production powerplants. However, the production development of the Ford PROCO stratified-charge engine appears to have been cancelled as a result of cost and manufacturability problems associated with the precise metering and control requirements of the fuel-injection system. Also, a factor in the the Ford decision was the recent trend to smaller vehicles and smaller engines, which invalidated much of the PROCO engine research and development that had been done on large V-8 engines.

The first true stratified-charge engine introduced in a production vehicle was the Honda CVCC engine offered in 1975 California models. The Honda CVCC engine was able to meet the 1975 emissions standards without the use of exhaust catalysts, EGR, or other emissions-control devices. The emissions control was aided only by the enlarged and insulated exhaust manifold which acted as a thermal reactor for the control of HC and CO emissions. As emissions standards have become more stringent, the Honda CVCC engines have started using catalytic converters for emissions control to achieve the best fuel economy while maintaining emissions standards levels. Catalytic converters were first introduced on Honda CVCC engines on the 1980 California models.

The Honda CVCC engine remains the only stratified-charge engine in a production vehicle. Although some interest continues in stratified charge engine research and development, most automobile manufacturers have chosen uniform charge engines with three-way catalyst emission-control systems for meeting the more stringent emissions requirements.

The distinguishing feature (Refs. 52 and 53) of stratified charge engines is the significant stratification of the fuel-air mixture which exists at the time combustion is initiated by the spark plug. The large variety of stratified-charge engine designs reflect the different approaches used to achieve and control this charge stratification over the range of engine speeds and loads required in an automotive engine. Basically, a rather rich charge is provided for ignition and flame kernel development, with the remainder of the charge being much leaner. Using this approach, stratified-charge engines can operate successfully at lower overall equivalence ratios than those which are possible in uniform-charge, spark-ignition engines.

In principle, charge stratification can be used to increase the engine thermal efficiency without sacrificing good engine response. The increase in efficiency is obtained in part from operating the engine at an overall lean equivalence ratio, especially for part-load operation. In stratified-charge engines having relatively low compression ratios, it is possible to utilize stoichiometric conditions for maximum power operation. However, under these conditions the advantages of charge stratification are lost. In some stratified-charge engine designs which are essentially knock-free, higher compression ratios can be utilized to further increase engine thermal efficiency.

The level of engine-out emissions produced by stratified-charge engines is very dependent on the effectiveness of the control of charge stratification during engine operation. The fraction of the charge which burns first must be relatively rich to provide reliable ignition and good flame development. It is likely that significant unburned HC and CO emissions originate during combustion of this first fraction of the charge. However, by effectively mixing the combustion products from this first fraction with the very lean remainder of the charge, the unburned HC and CO are further oxidized. As the last fraction of the charge becomes leaner, the amount of unburned HC emissions produced by flame wall quenching is also reduced. Low CO emissions are achieved if complete mixing of the charge is obtained rapidly after combustion of the first fraction of the charge. The requirement for a fast switch from the initial slow mixing (which is needed to maintain charge stratification) to the final fast mixing (which is needed to complete CO oxidation) is difficult to implement in engine hardware. These factors led Honda to use a thermal reactor on their early CVCC engines to promote further oxidation of CO and unburned HC emissions. Lower NO_x emissions are obtained in stratified-charge engines by properly selecting the equivalence ratio of the fraction of the charge which burns first and then controlling the mixing of its products with the remaining charge.

Engine knock is reduced by charge stratification because of the very lean mixture ahead of the flame. It is eliminated when only air is present away from the ignition source. When the fuel is injected directly into the combustion chamber, preignition can also be eliminated. Thus, some stratified-charge engine designs can readily operate with a large variety of fuels.

Implementation of the stratified-charge concept can be accomplished in several different ways. Some of these configurations are illustrated in Figure 4-1. In general, charge stratification is accomplished through one of two approaches; divided chamber or open chamber. The divided chamber approach is represented by sketches A1 and B1 in Figure 4-1. The two fuel-air charge fractions in the two chambers are both uniform but at different equivalence ratios. Whether the fuel is introduced by a carburetor or a fuel-injection system, each chamber has a uniform composition at the time of ignition. The open chamber approach, represented by sketch C1, accomplishes charge stratification by controlling the fuel-air mixing process through fuel injection and air motion. Thus, the equivalence ratio varies continuously from point to point within the combustion chamber.

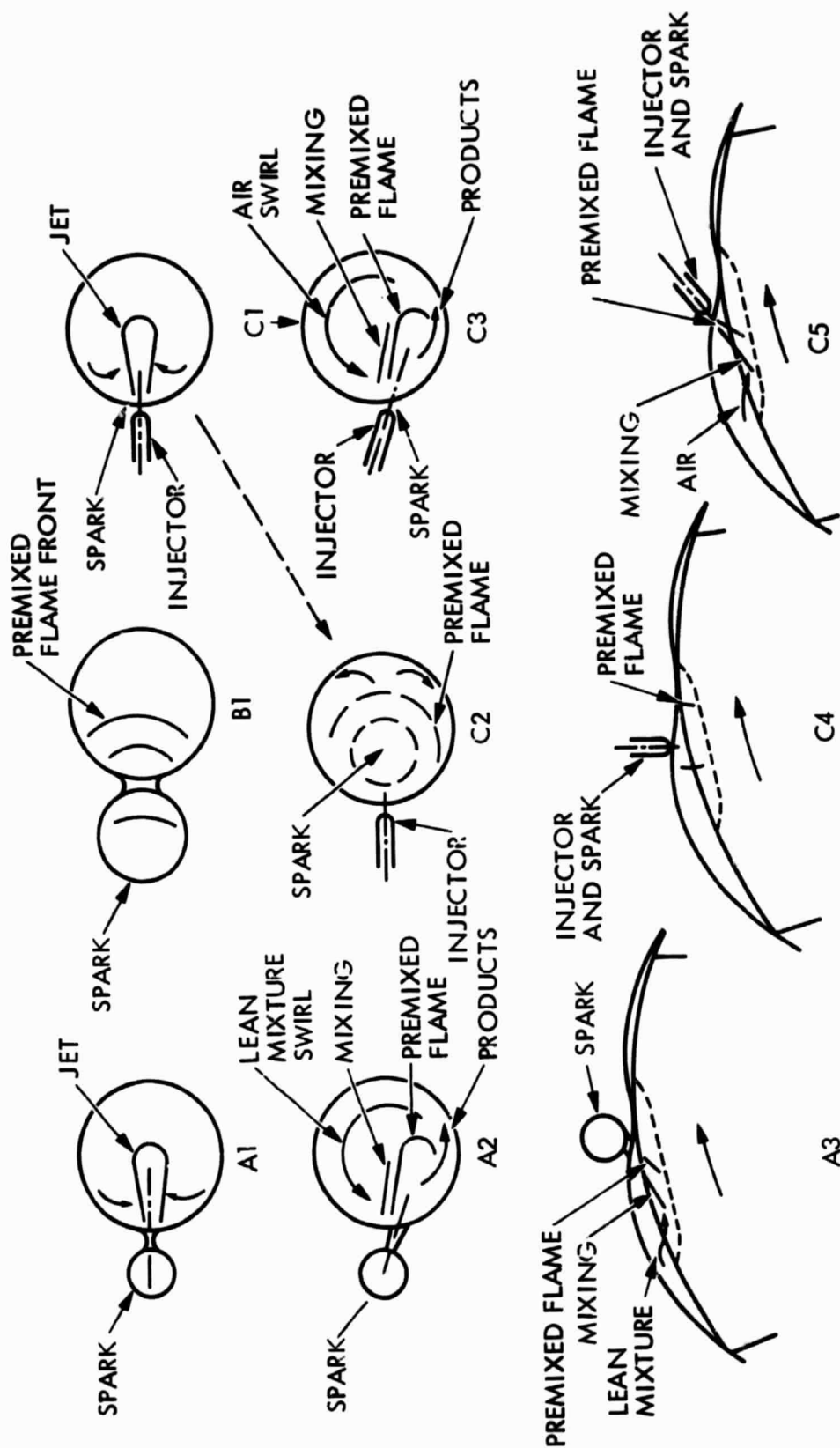


Figure 4-1. Stratified-Charge Concepts (Ref. 53)

Divided chamber approaches to charge stratification are easier to implement than open chamber approaches, but there are several inherent limitations in the divided chamber approach. Although it is more efficient to vary engine load by varying the overall equivalence ratio, most divided chamber designs are forced to accomplish load variations by throttling the incoming charge. This throttling is necessary to maintain the equivalence ratio in the proper range; high enough to obtain complete combustion of the uniform mixture and low enough to avoid combustion harshness. Furthermore, when the two chambers are of comparable size, as in sketch B1 (Figure 4-1), there is a tradeoff to be made in sizing the interconnecting orifice between the two chambers. The orifice must be small enough to promote adequate charge stratification, yet large enough to permit adequate mixing of the two subcharges after combustion of the rich fraction of the charge. The higher surface-to-volume ratio of divided chamber designs results in higher wall heat transfer losses and limits their ultimate efficiency potential.

On the other hand, open chamber approaches to charge stratification permit variations of load to be accomplished by varying the overall equivalence ratio through changes in the fuel injection schedule. However, charge stratification in open chamber designs is obtained only by very precise control of fuel injection and air motion. This control is very difficult to achieve over the range of speed and load conditions required in automobile engines. At first, it is desirable that turbulent diffusion be slow in order to maintain charge stratification, but later it should be fast to burn efficiently and mix combustion products with residual air.

There are some important similarities among the combustion processes in these different configurations. In configuration A1 of Figure 4-1, the small chamber contains a small fraction of the total charge and is connected to the large chamber through a small orifice. When the small charge burns, a pressure difference is established across the orifice. This pressure difference generates a high-speed jet made up mostly of combustion products which entrains and ignites the premixed fuel-air mixture (which is too lean to sustain its own premixed flame) in the main chamber. In configuration B1, the sizes of the two chambers are comparable and the interconnecting orifice is relatively large. Thus, some mixing of the two charges occurs prior to ignition, and combustion occurs in a turbulent premixed flame front. In configuration C1, stratification is achieved by controlled, direct fuel injection. The resulting high speed jet penetrates and entrains the surrounding air so that combustion occurs primarily via diffusion flames along the edges of the jet, after being initiated by the spark.

Two alternative stratified-charge configurations which incorporate swirling motions in their main chambers are shown as sketches A2 and C3 in Figure 4-1. Although the swirling motion produces some benefits, a penalty is paid to generate these motions in reciprocating engines. In configuration A2, the lean mixture in the main chamber enters a region where it is mixed with the hot combustion products from the small chamber. At the end of this mixing region, the charge temperature is high enough for combustion to occur. In configuration C3, there is a fuel-air mixing region followed by a premixed stationary flame, originally initiated by a spark, and followed by combustion products. Higher loads are achieved by longer fuel injections.

Still another alternative stratified-charge configuration is shown as sketch C2 in Figure 4-1. In this case, swirl is eliminated in the main chamber, and fuel is injected directly, but not as it burns. The fuel and air motion are coordinated to generate a premixed mixture in part of the chamber, around the spark location, at ignition time. In order to minimize midair flame quenching, the fuel concentration should decrease sharply at the boundary between the air and fuel-air regions of the charge. In this configuration, combustion times can be shorter than for configuration C3 because most mixing is achieved before ignition, and combustion occurs via premixed flames.

4.2 TECHNOLOGY DEVELOPMENTS AND VEHICLE SYSTEMS

Because only one stratified-charge engine, the Honda CVCC design, is currently used on production vehicles, much of the technology is contained in research studies and engine prototype developments. The results of some of the more important of these studies and engine developments will be reviewed to provide a basis for evaluation the potential of stratified-charge concepts.

The Honda Controlled Vortex Combustion Chamber (CVCC) engine, shown in Figure 4-2, is based on the divided chamber concept (Refs. 54 and 55). The auxiliary combustion chamber is placed where the spark plug is located in the conventional engine. A special carburetor, separate intake passage, and separate intake valve are provided to supply the auxiliary combustion chamber with a rich fuel-air mixture. The auxiliary combustion chamber has a spark plug and is connected to the main combustion chamber by a torch opening. Upon combustion of the rich mixture in the auxiliary combustion chamber, a hot jet of combustion products passes through the torch opening into the main combustion chamber and promotes the combustion of the very lean mixture supplied to the main chamber through the main intake valve. The CVCC engine was designed to keep the maximum combustion temperature as low as possible for reduction of NO_x generation, and at the same time to maintain the mean combustion gas temperature considerably higher than conventional engines for a long duration over the expansion stroke for promoting oxidation of CO and HC. Further developments (Refs. 56 and 57) of the CVCC engine have resulted in improvements in the fuel consumption and emissions characteristics of the engine relative to the original CVCC engine. A new combustion chamber, shown in Figure 4-3, was developed to produce stable combustion of lean mixtures over a wide range of engine loads. The auxiliary combustion chamber is located closer than before to the center of the main combustion chamber and the torch opening is modified to incorporate five openings, so that the torch flame spreads rapidly throughout the main combustion chamber. These engine modifications have improved the knock characteristics of the engine and permitted use of a compression ratio of 9.0. To further enhance the fuel economy, a catalyst unit was added to lower the CO and HC emissions. This new 1.5-liter CVCC engine was introduced in some vehicle models in 1980.

Comparison tests were conducted using the new CVCC engine and a conventional engine with the same wedge-type combustion chamber as the CVCC engine, (shown in Figure 4-4). The conventional engine had the same intake

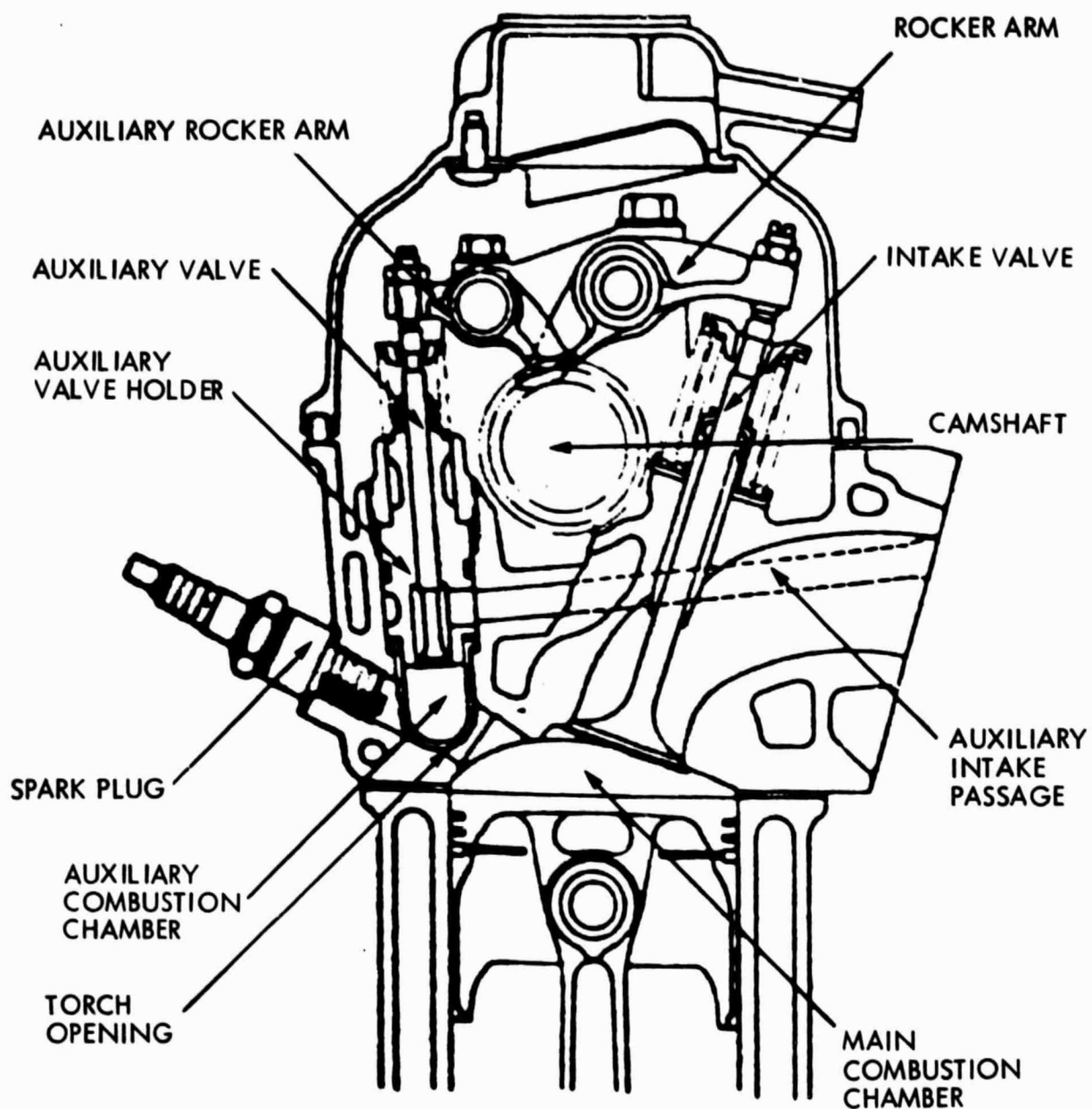


Figure 4-2. CVCC Engine Cylinder Head, Cutaway View
(Ref. 55)

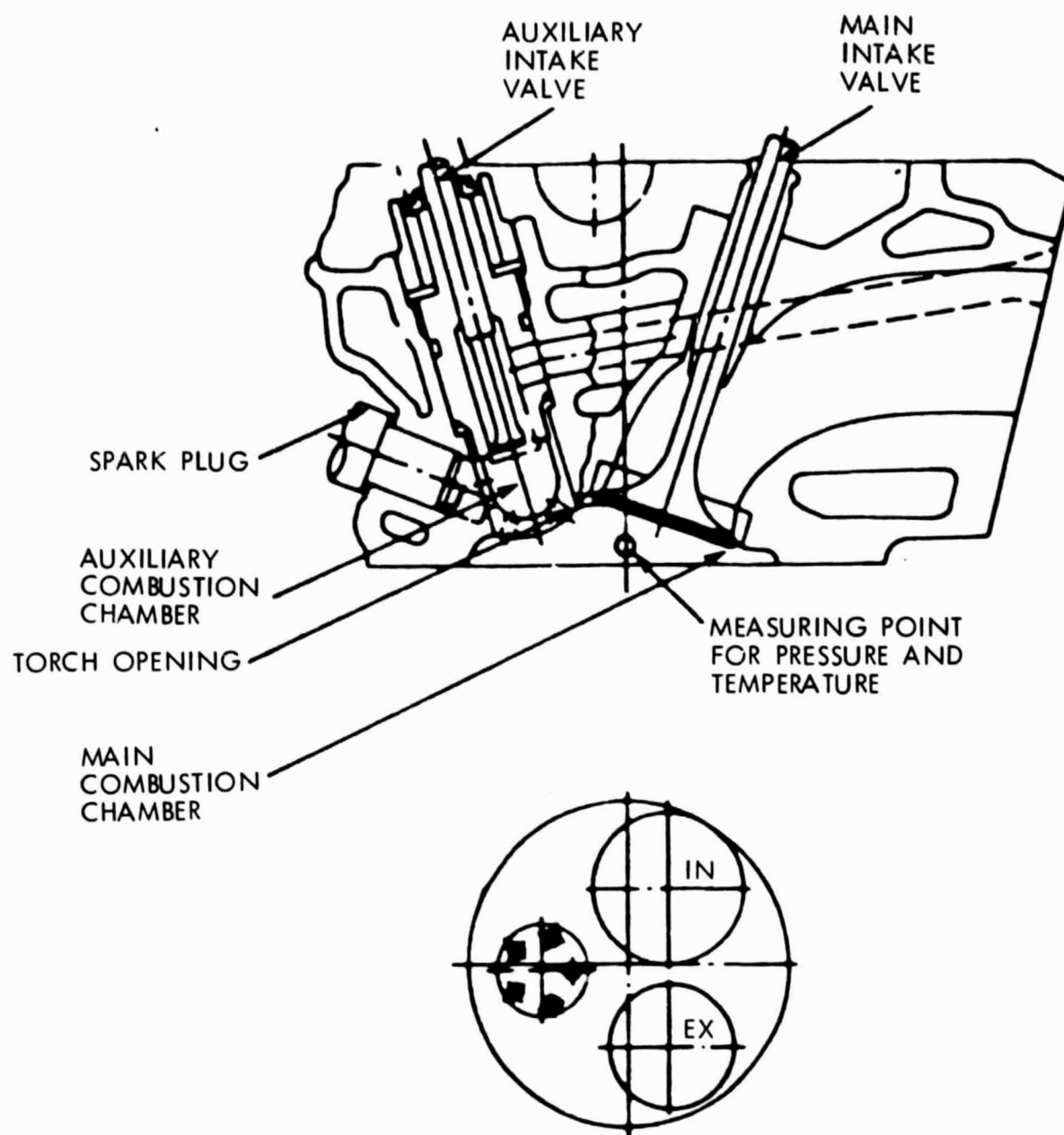


Figure 4-3. Cross Section of the New CVCC Engine Cylinder Head (Ref. 57)

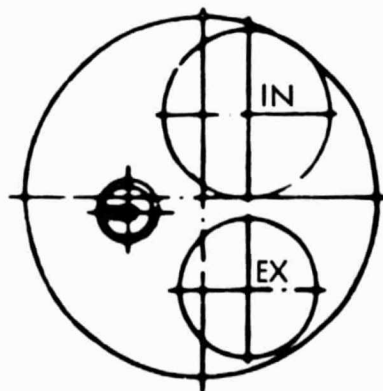
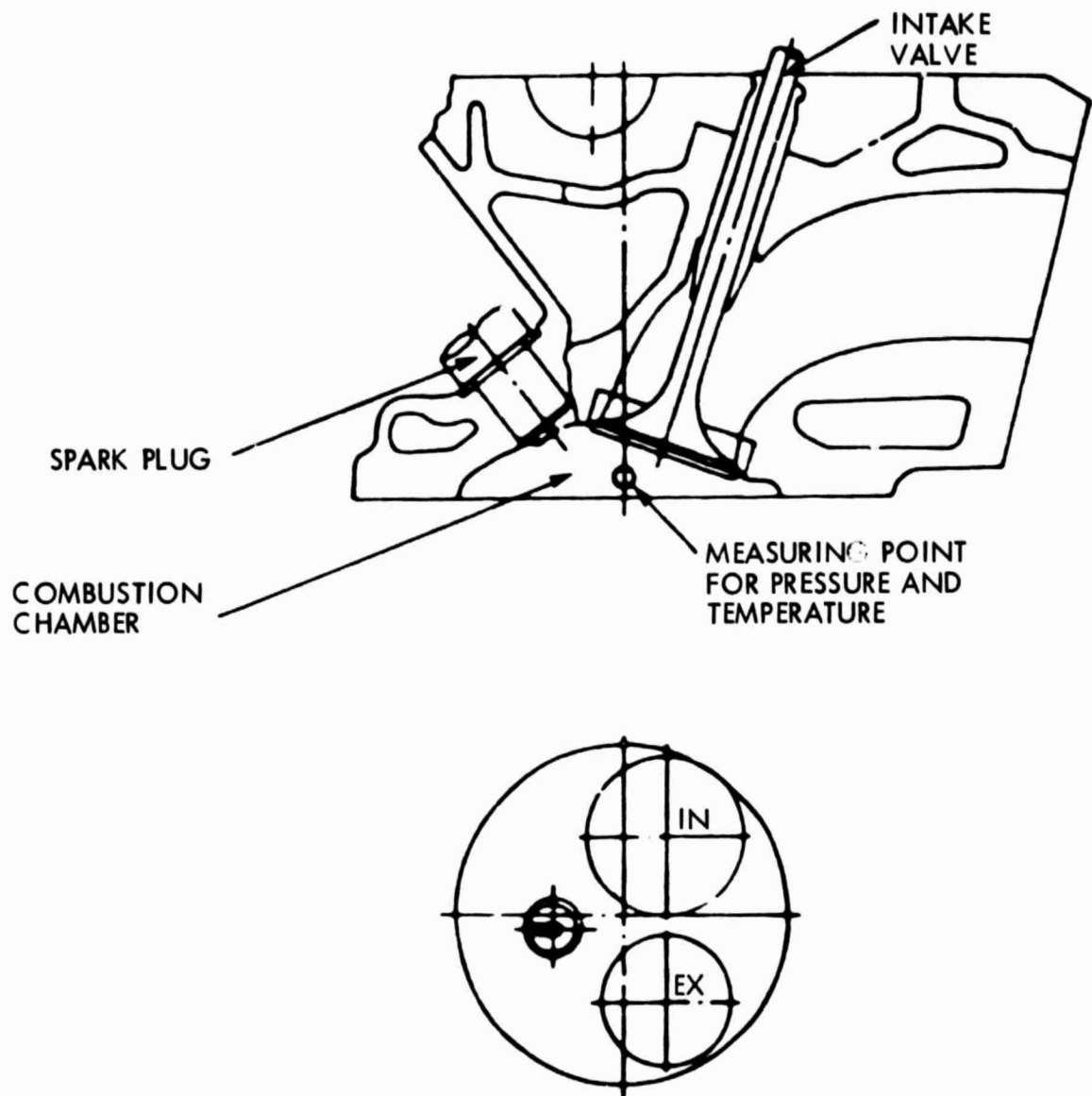


Figure 4-4. Cross-Section of the Conventional Engine Cylinder Head (Ref. 57)

and exhaust manifolds as the new CVCC engine. Tests were conducted at the following three load conditions:

	<u>Light Load</u> <u>(Load I)</u>	<u>Medium Load</u> <u>(Load II)</u>	<u>Heavy Load</u> <u>(Load III)</u>
Engine Speed, rpm	1500	3000	3000
Indicated Mean Effective Pressure, kg/cm ²	3.2	3.4	3.8

Comparisons of the fuel consumption and emissions characteristics of the CVCC engine and the conventional engine are given in Figures 4-5, 4-6, and 4-7. Circles identify the operating air-fuel ratios for the two engines. The CVCC engine is calibrated to operate under lean conditions (A/F of 18 to 19), while the conventional engine is set to operate at stoichiometric conditions (A/F of 14.7) assuming the use of a three-way catalyst for emissions control.

Fuel consumption characteristics of the two engines are shown in Figure 4-5. For all three load conditions, the CVCC engine has a flat fuel consumption characteristic in the lean region where it operates. The CVCC demonstrates significantly lower fuel consumption under lean conditions; however, the fuel consumption is about equal to that of the conventional engine at stoichiometric conditions.

The HC emissions characteristics are shown in Figure 4-6. Both have similar characteristics, with HC emissions reaching a minimum on the lean side of stoichiometric and then increasing for leaner mixtures. The minimum point in the CVCC engine is set to operate at air-fuel ratios leaner than the minimum HC emissions point for all three load conditions. This leaner calibration helps decrease fuel consumption (see Figure 4-5), and an exhaust catalyst is added to reduce the HC emissions to the desired level. The NO_x emissions characteristics are shown in Figure 4-7. Both engines have similar characteristics, with NO_x emissions reaching a peak at an air-fuel ratio of about 16. At any given air-fuel ratio, the NO_x emissions from the CVCC engine are 15-30% lower than the emissions from the conventional engine. Comparing the emissions from each engine at its respective operating air-fuel ratio for each load, the CVCC engine has a definite advantage.

To better understand the the differences in operating characteristics of the two engines, cylinder pressure-time measurements were made at the three load conditions. In Figure 4-8, typical average pressure diagrams for both engines are compared. The CVCC engine shows a slower pressure rise and lower peak pressure.

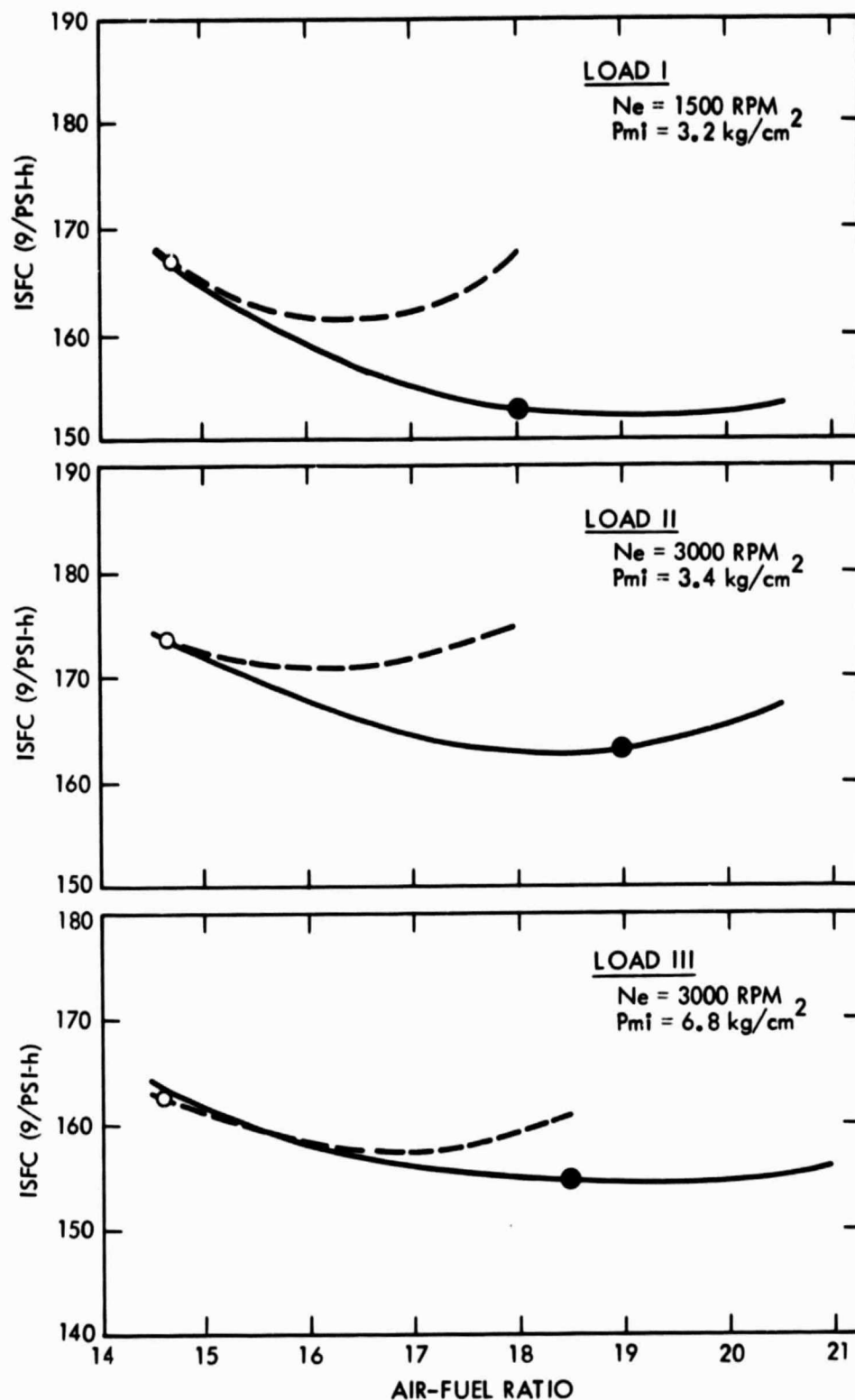


Figure 4-5. Comparison of ISFC Between the CVCC Engine and the Conventional Engine (Ref. 57)

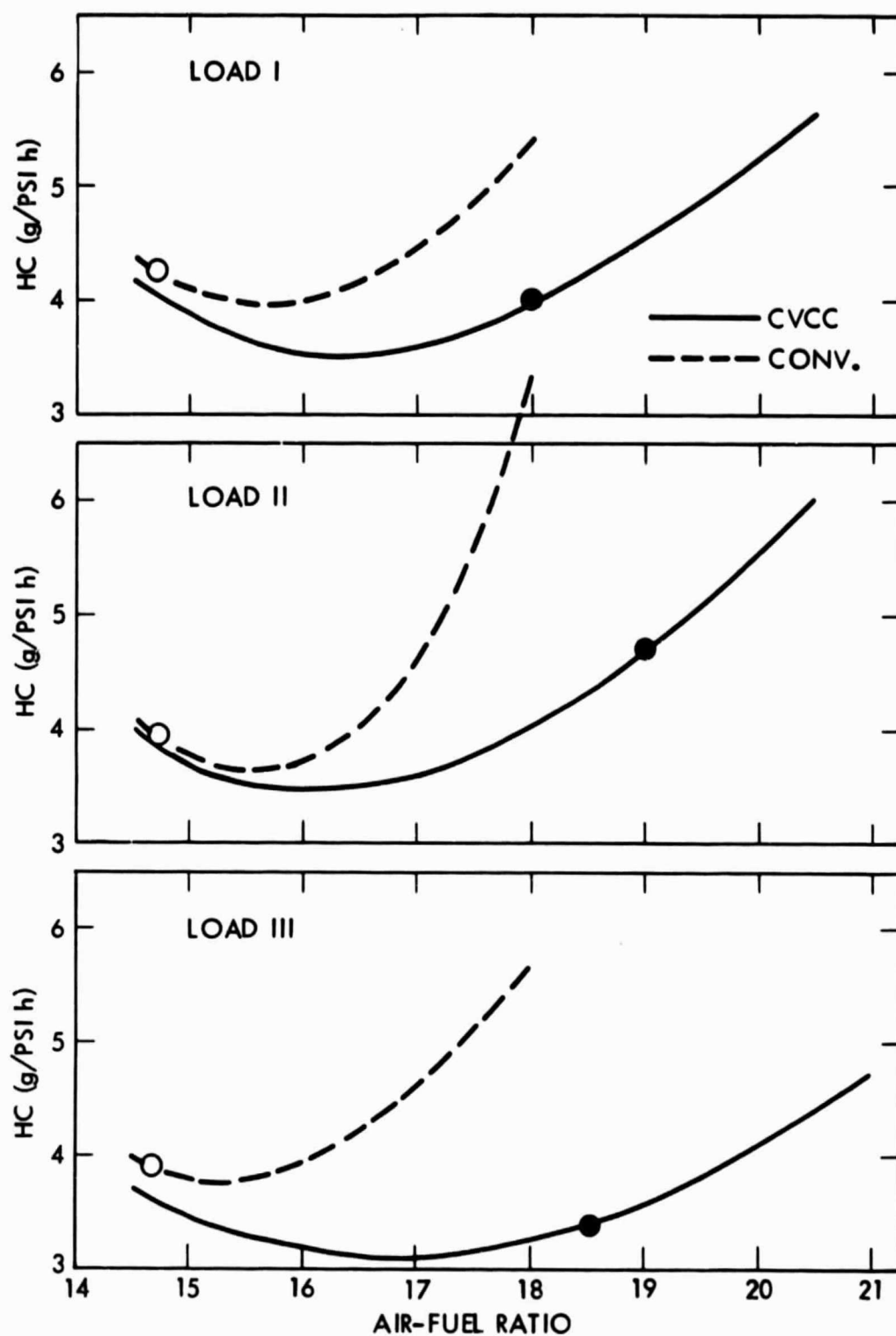


Figure 4-6. Comparison of HC Emission Between the CVCC Engine and the Conventional Engine (Ref. 57)

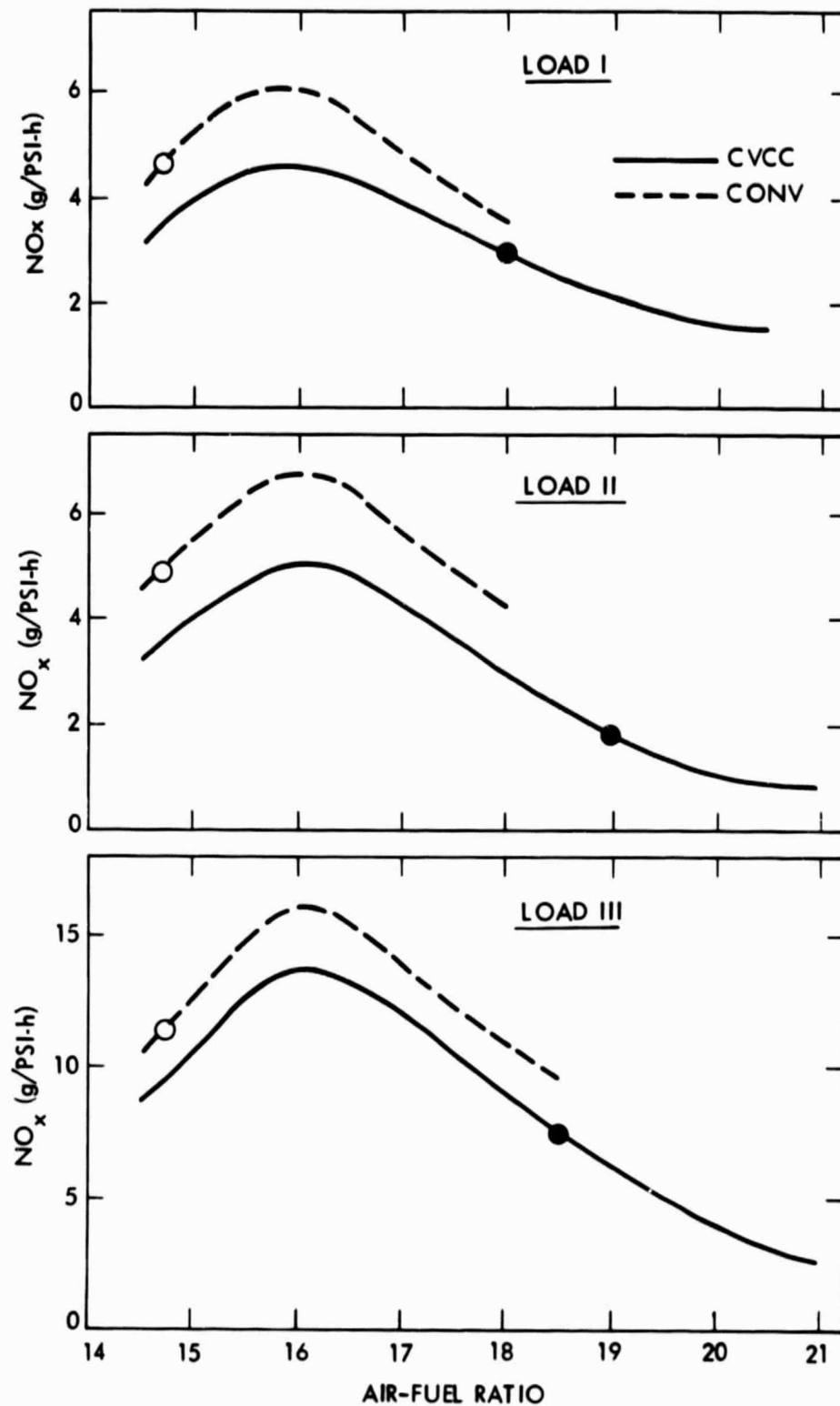


Figure 4-7. Comparison of NO_x Emission Between the CVCC Engine and the Conventional Engine (Ref. 57)

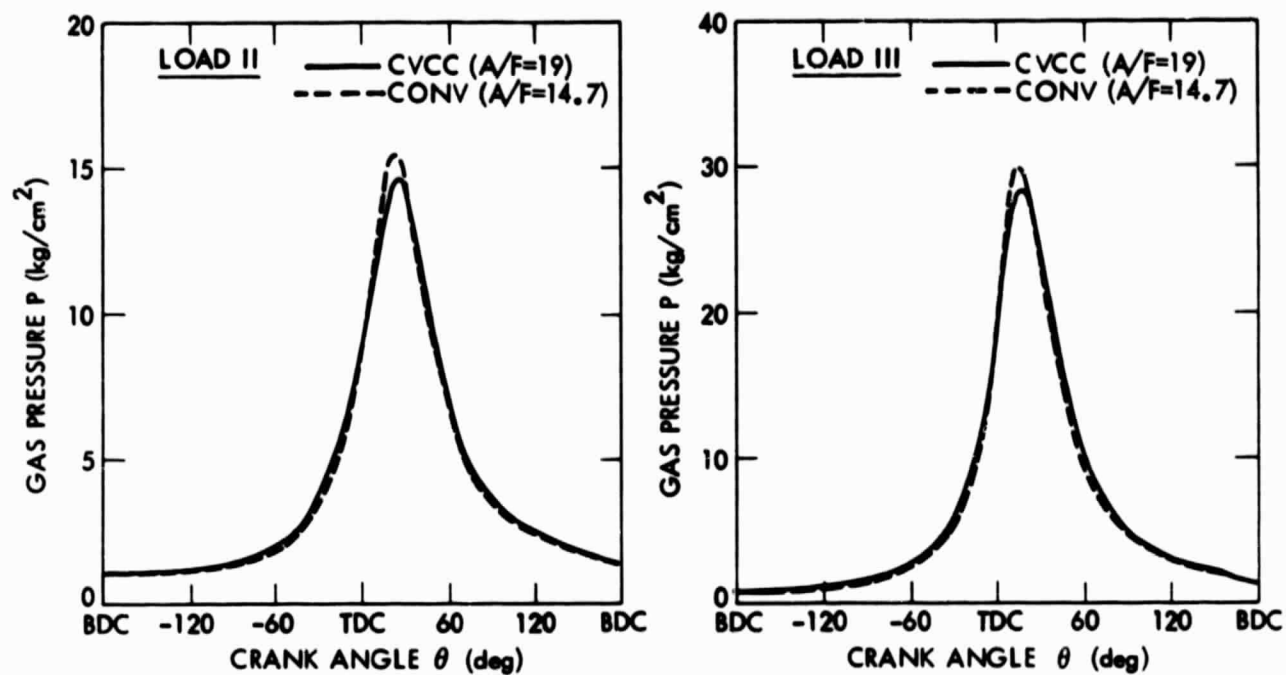


Figure 4-8. Comparison of Pressure Diagrams Between the CVCC Engine and the Conventional Engine (Ref. 57)

For the CVCC engine, the higher pressure during the compression stroke is a result of the leaner mixture. The lower peak pressure for the CVCC engine reflects a longer combustion interval (slower combustion) than that for the conventional engine. A comparison of the standard deviation of the cylinder pressure for the CVCC and conventional engines is shown in Figure 4-9. The standard deviation of pressure for an air-fuel ratio of 12 is larger than that for an air-fuel ratio of 14.7 on the CVCC engine. However, the standard deviation of pressure for an air-fuel ratio of 19 on the CVCC engine is still less than that of the conventional engine running at stoichiometric conditions. Thus, the CVCC engine is seen to show much less cyclic deviation than the conventional engine, even when operated in the lean regime. This is an indication of more stable combustion in the CVCC engine.

During development testing, the Texaco Controlled Combustion System (TCCS) (Refs. 58, 59 and 60) has demonstrated multifuel capability, low exhaust emissions, and good fuel economy. The TCCS concept, illustrated in Figure 4-10, involves a coordination of air swirl, direct-cylinder fuel injection and positive ignition in an open chamber configuration. The normally unthrottled air charge is forced to swirl, by suitably-shaped intake passages and the combustion chamber, at a rate about ten times the engine speed during the combustion event. The necessary swirl flow is produced by a cup-in-piston combustion chamber configuration, shown in Figure 4-11, which produces an increase in swirl rate near the end of the compression stroke. Fuel is injected into the swirling air in the same direction as the local swirl. The first fuel increment is ignited to establish a flame front immediately downstream from the nozzle. As injection continues, a combustible mixture is supplied to the stabilized flame and burned as rapidly as it is formed.

Load control in a TCCS engine is achieved by regulating the duration and quantity of fuel injection. For full load conditions, duration of the fuel injection corresponds to the time for one air swirl. Because there are mixing limitations, the engine cannot achieve the air utilization rates available with premixed fuel-air charges. Maximum power of the engine is determined by the exhaust smoke limit. For lower loads, the duration and quantity of fuel injection are decreased and the engine operates very lean. The direct cylinder injection produces good engine response, and the positive ignition results in good cold start and warmup characteristics.

One of the key advantages of the TCCS engine is its ability to use a variety of fuels. The positive immediate ignition of the first injected fuel increment eliminates the need for the high compression ratio and fuel cetane number required for diesel engine ignition. The injection of the first fuel increment just prior to the time of ignition eliminates the possibility of preignition of the fuel. Burning the fuel as rapidly as it is injected into the cylinder eliminates knock, regardless of the fuel octane rating, because the fuel-air mixture does not have sufficient residence time for preknock reactions to occur. This relative insensitivity to fuel properties will become more important as present fuel supplies dwindle and alternative fuels become more available.

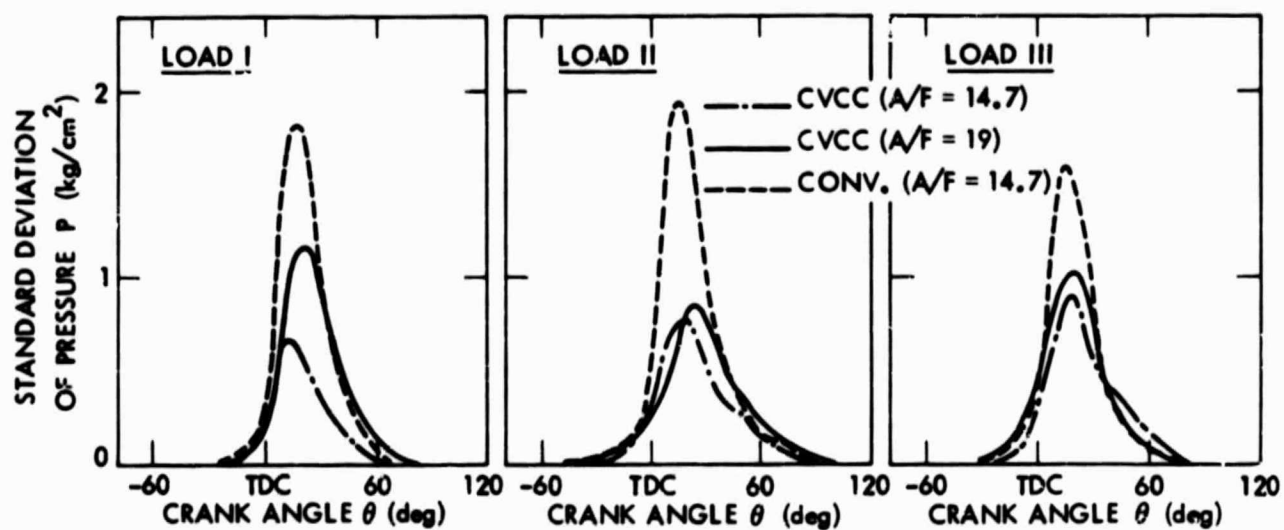


Figure 4-9. Comparison of Standard Deviation of Pressure Between the CVCC Engine and the Conventional Engine (Ref. 57)

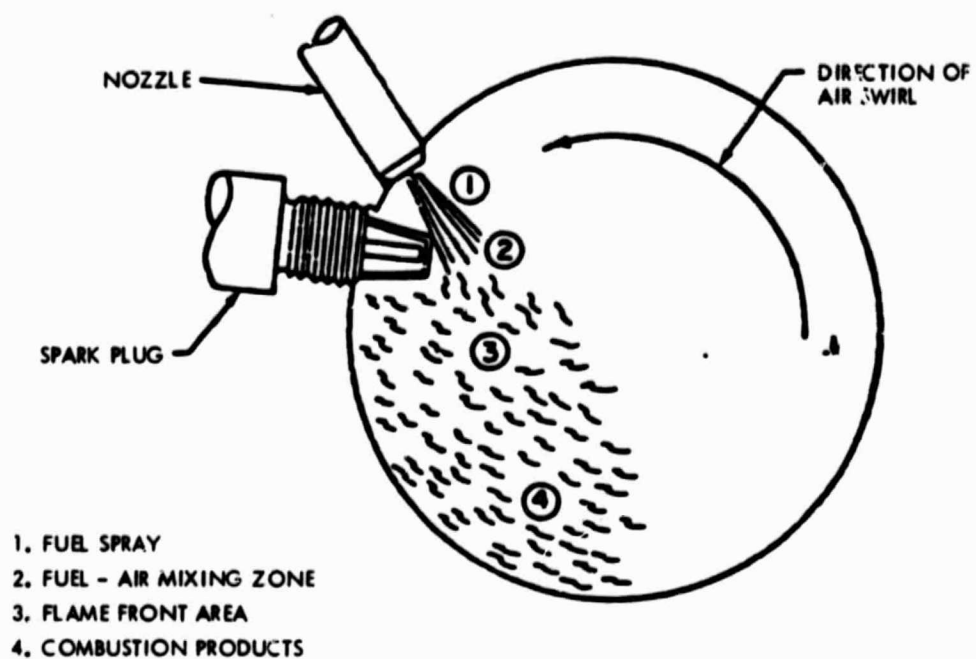


Figure 4-10. Texaco Controlled-Combustion System (Ref. 58)

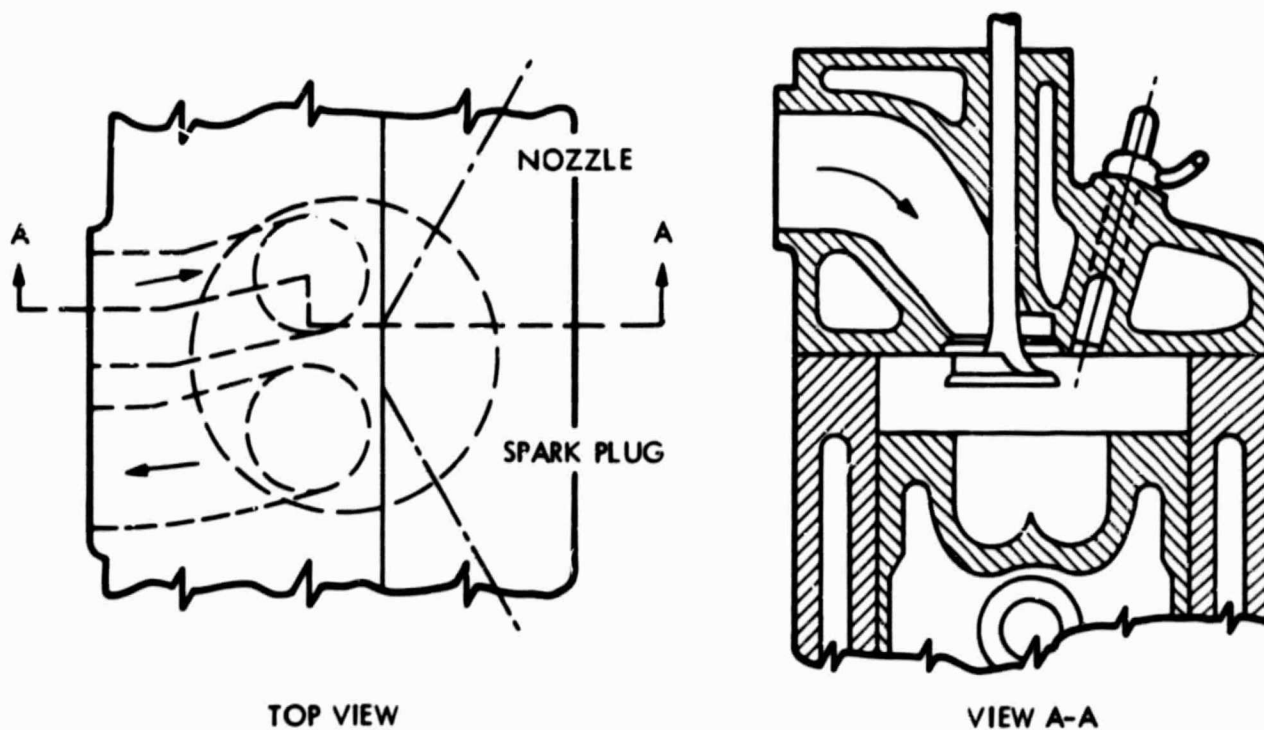


Figure 4-11. Cup Combustion Chamber (Ref. 58)

The TCCS concept offers the potential of high thermal efficiency because it can burn leaner overall fuel-air mixtures than can be used in uniform charge engines. Because the TCCS engine normally runs unthrottled, pumping losses are reduced. Because the engine is insensitive to fuel octane and cetane rating, there is freedom to choose compression ratio and turbocharging to achieve further increases in engine efficiency. Using an L-141 engine, whose specifications are given in Table 4-1, tests were made to compare performance of the TCCS engine with that of the standard premixed charge engine. Results from these tests are given in Figure 4-12, which shows data for the TCCS engine using a wide variety of fuels. The TCCS engine demonstrated a 30% lower specific fuel consumption than the standard engine. Essentially identical fuel consumption characteristics were measured for all the fuels tested. No changes in spark advance or injection advance were made when changing fuels. Performance with the various fuels was somewhat different under high load conditions, reflecting differing smoke-limited performance of the fuels. Using gasoline, the TCCS engine was shown to produce about the same full-load power as the standard engine.

Table 4-1. Engine Specifications, L-141 TCCS

Configuration	In-line
Operating cycle	4 stroke
Cooling	Liquid
Number of cylinders	4
Displacement	141.5 in. (2320 cc)
Bore	3.875 in. (98.4 mm)
Stroke	3.000 in. (76.2 mm)
Compr. ratio-nat.	
aspirated	10.1:1
turbocharged	9.3:1
Fuel	Avgas through No. 2 Diesel Fuel
Firing order	1-3-4-2
Weight (dry with accessories)	375 lb (170 kg)
Length	27.5 in. (69.8 cm)
Width,-nat. aspirated	24.5 in. (62.2 cm)
turbocharged	25.5 in. (64.8 cm)
Height	23.3 in. (59.2 cm)

The TCCS engine produces rather low engine-out emissions, mainly because the engine operates at all times with excess air. Even though the stratified combustion element may be considerably richer than stoichiometric, further post-flame oxidation of HC and CO occurs when the burned gases mix with this excess air. Also, because the fuel is consumed as it enters the combustion chamber, there is little contribution to HC emissions from wall-quenching effects. Fuel combustion under rich conditions limits formation of NO_x in

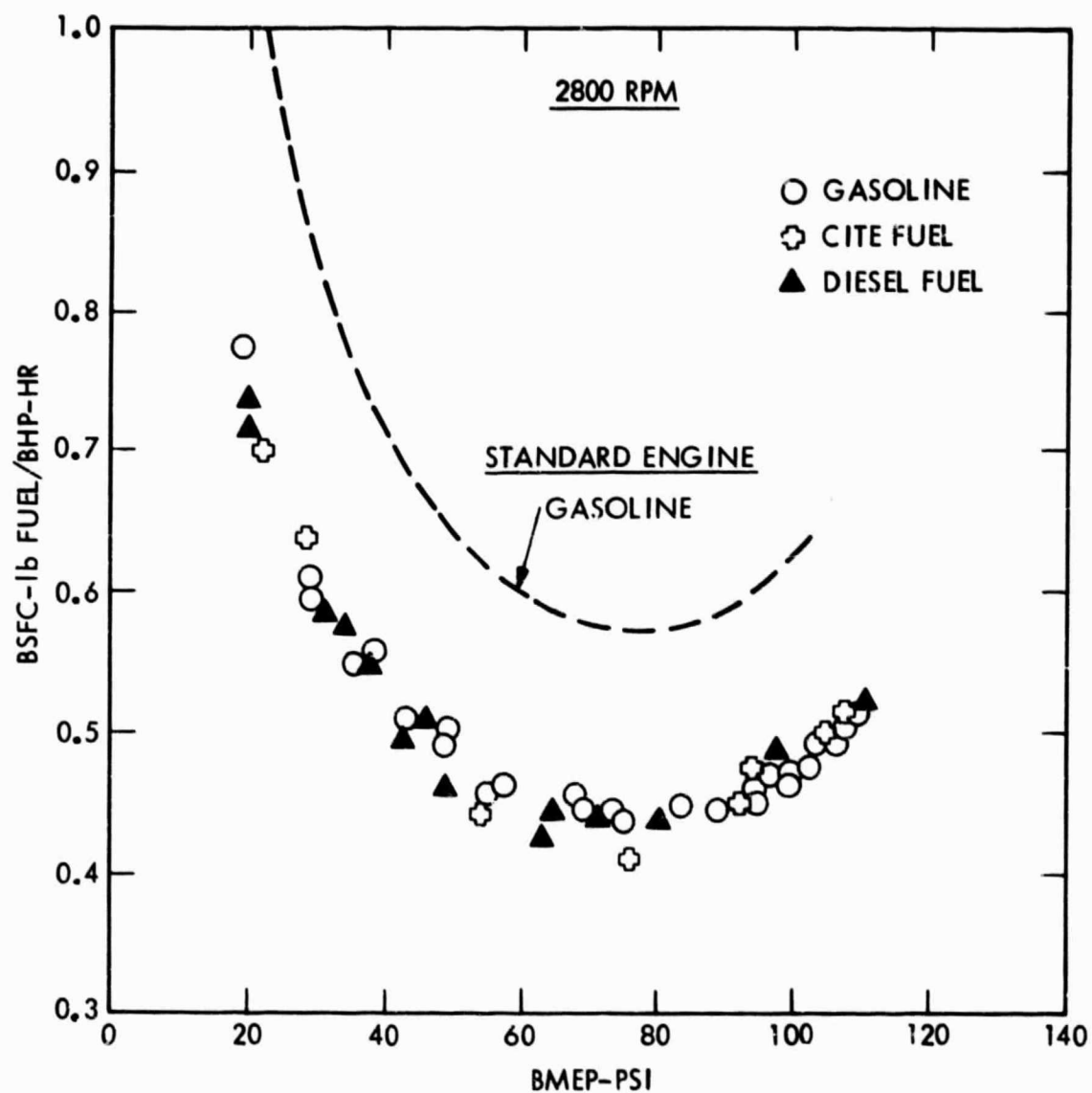


Figure 4-12. Naturally Aspirated L-141 TCCS Engine Multifuel Brake Performance (Ref. 58)

the flame zone. Quick quenching of the burned gases by the excess air pre-further NO_x formation in these post-flame gases. The direct fuel injection and positive ignition of the TCCS engine permit engine warmup without fuel enrichment, fuel cut-off during deceleration, and rapid fuel injection response, all of which contribute to low exhaust emissions under transient conditions.

Although engine-out emissions on the TCCS engine are low, additional emissions control measures are required to meet the most stringent emissions standards. Tests were made on a TCCS engine which has an emissions control system consisting of combustion event retard (ignition and injection retard), inlet air throttling under idle and deceleration conditions, dual-rate cooled EGR, and a catalytic converter unit. Results of these tests are shown in Table 4-2. Tests were conducted to evaluate the fuel economy penalty associated with meeting the low emissions levels. The effects of decreasing EGR rate on emissions and fuel economy are shown in Table 4-3. These results show that a very large fuel economy penalty is paid to achieve the low NO_x emissions level.

Another significant stratified-charge engine development activity is the Ford Programmed Combustion (PROCO) engine program (Ref. 61). In development tests, the PROCO concept has shown the potential for good fuel economy, low emissions, and limited multifuel capability. The PROCO concept, illustrated in Figure 4-13, includes air swirl, direct cylinder fuel injection, and positive ignition in an open chamber configuration. The intake port is designed to impart swirl to the inducted air, and substantial squish is applied during piston movement on the compression stroke. The piston contains a combustion bowl, and two spark plugs are used to increase EGR tolerance of the engine. Moderate air throttling at light and medium load conditions is used to help lower exhaust emissions.

A critical element of the PROCO engine is the fuel injection system and its control. The fuel injection system requirements could not be met by available diesel injector nozzles and injection pumps, and thus fuel injection system development was a key part of the PROCO program. The fuel injector nozzles operate with a differential pressure of 250-300 psi to provide adequate fuel atomization with low penetration. The fuel injection pump provides for specific injection timing requirements and good fuel distribution among cylinders while metering low viscosity gasoline. Optimum injection timing is a function of both engine speed and load. Under light loads, injection is completed just before the ignition spark. As the load is increased, fuel injection is advanced more to provide time for fuel vaporization and mixing prior to ignition in order to achieve high air utilization and high power output. Injection timing is adjusted for engine speed to compensate for injection lag.

It has been demonstrated in vehicle tests that the fuel octane requirement of the PROCO engine is lower than that for a homogeneous charge engine, permitting use of a compression ratio of 11 to 1 with 91 RON unleaded fuel. This lower octane requirement results from several factors. Direct injection of fuel into the combustion chamber and the subsequent fuel evaporation reduces gas temperature due to heat transfer from the

Table 4-2. Exhaust Emission Levels, Controlled

TCCS M-151 1975 Federal Test Procedure 2750-lb Inertia Lead-Free Gasoline			
Laboratory	Mass Emissions - gm/mi		
	HC	CO	NO _x
Texaco	0.25	1.17	0.33
Texaco	0.28	0.62	0.32
Texaco	0.30	0.79	0.29
EPA	0.40	0.26	0.30
EPA	0.33	0.15	0.31
EPA	0.37	0.30	0.31
1976 Standards	0.41	3.4	0.40

Table 4-3. Effect of Emissions Control on Fuel Economy, M-151 TCCS
1975 Federal Test Procedure 2750-lb Inertia Lead-Free Gasoline

Test Site and Engine Configuration	Mass Emissions - gm/mi			Fuel Economy mpg (L/100 km)
	HC	CO	NO _x	
Texaco-std. Configuration ^a	0.36	0.61	0.31	16.2 (14.5)
Texaco-reduced EGR ^b	0.48	0.57	0.45	17.6 (13.4)
EPA-std. Configuration ^a	0.37	0.24	0.31	15.8 (14.9)
EPA-reduced EGR ^b	0.50	0.14	0.70	21.9 (10.7)

^aAverage of three determinations.^bOne determination.

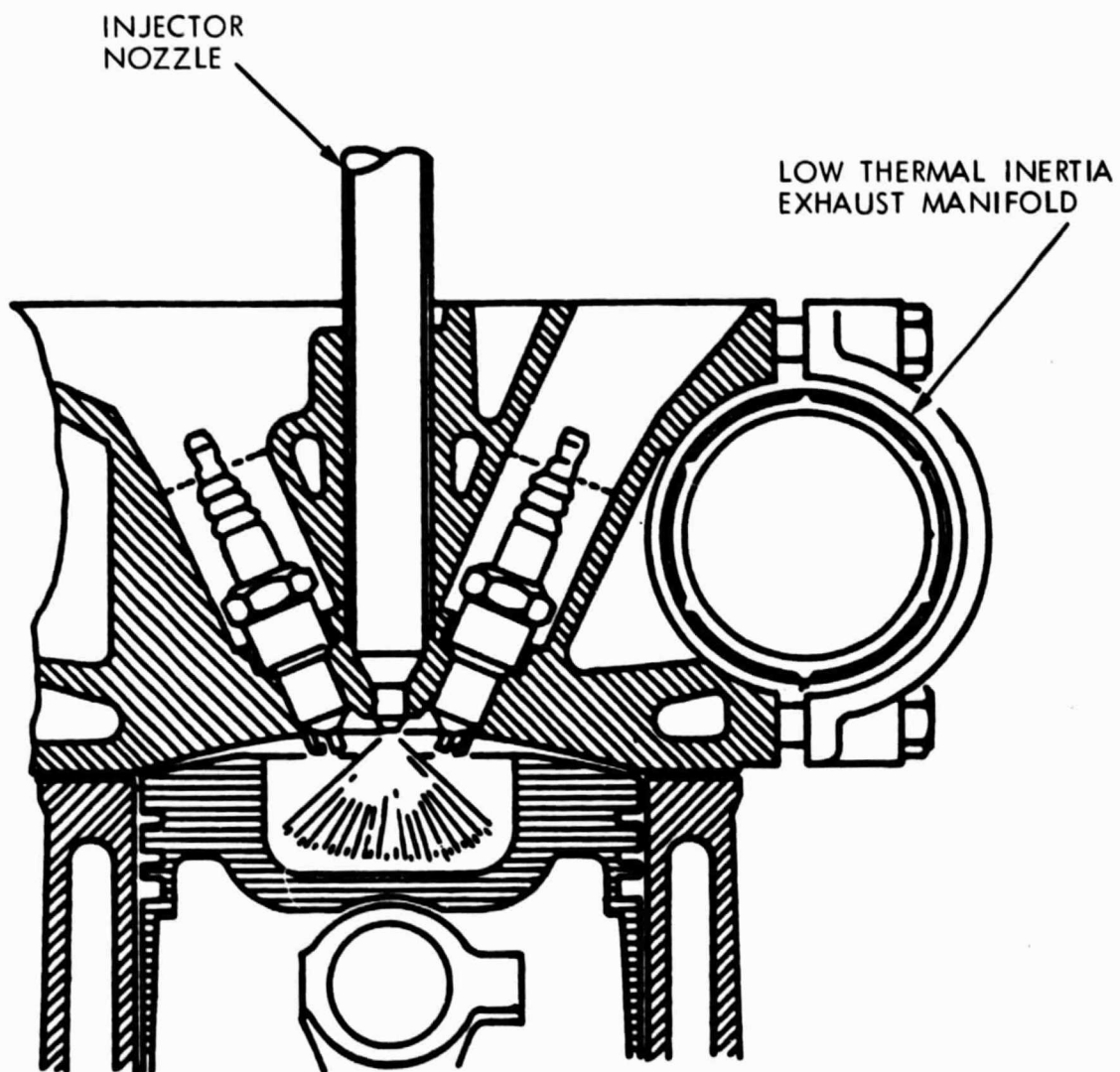


Figure 4-13. Cross-Section of a Typical PROCO Combustion Chamber (Ref. 61)

gas to the fuel. The direct fuel injection also provides less time for the fuel-air mixture to preignite or detonate. The fast burn rates (due to the use of two spark plugs) and charge stratification reduce the exposure time of the compressed end gas to high temperatures.

The potential fuel economy advantage of the PROCO concept is a result of its higher compression ratio, its highly diluted charge, and its reduced part-load throttling loss. As previously mentioned, the PROCO combustion process permits use of higher compression ratios; about three compression ratio units for the same octane fuel. With increasing compression ratio, there is a diminishing rate of improvement in indicated thermal efficiency, but a continual increase in friction (reduced mechanical efficiency). These factors result in an optimum compression ratio of about 11 to 1 for passenger cars, which use most of their fuel at relatively low specific power conditions. Another factor leading to the improved efficiency of the PROCO engine is related to the lean gas (air plus EGR) fuel mixture that can be used. Lean combustion leads to an increase in specific heat ratio, which improves efficiency by reducing the dissociation of gas molecules at the lower temperatures of lean combustion. At part-load conditions, the PROCO engine operates with 80-100% charge dilution, which is made up of about one-third air and two-thirds EGR. The excess air provides the oxygen required for complete combustion, while the EGR helps control NO_x emissions. At maximum power, charge dilution is eliminated to improve maximum performance. Another factor responsible for the PROCO fuel economy gain is the reduction in throttling loss made possible by the lean operation.

The PROCO engine concept is capable of achieving low exhaust emissions. Early work on the Ford stratified-charge engine demonstrated that the CO and NO_x emissions were inherently lower, while HC emissions were somewhat higher than those of a premixed charge engine. Also, the engine had an unpleasant odor that is characteristic of lean combustion. By introducing moderate air throttling at light and medium loads and using an oxidation catalyst, the HC emissions and exhaust odor were reduced without significantly reducing fuel economy. The CO emissions were further reduced by the oxidation catalyst. By using two simultaneously-fired spark plugs per cylinder, the EGR tolerance of the PROCO engine was increased significantly, permitting large reductions in NO_x emissions. After dynamometer tests to establish optimum control strategies for injection timing, air-fuel ratio, and EGR flow rate, three 6.6-liter PROCO engines, calibrated to meet the 0.41/3.4/1.0 g/mi (HC/CO/ NO_x) emissions levels, were installed in 1977 Cougar models or equivalent vehicles for fuel economy and emissions tests. Test results, obtained from a 15-test average of the three vehicles, are shown in Table 4-4. Compared to the fuel economy capability of a 1977 6.6-liter carbureted engine in a similar vehicle and calibrated to the 1.5/15/2.0 g/mi (HC/CO/ NO_x) emission standard, the PROCO engine, calibrated to the more stringent emissions level, provided a 20% improvement in fuel economy.

A typical modal breakdown of the results of individual bag data from CVS tests is given in Table 4-5. Operation during the cold 505-second transient portion of the test represents the most difficult period for control of HC and CO emissions. Further tests evaluated the capability of the PROCO engine with respect to acceleration performance, driveability, octane requirement, and startability. Results of these tests are given in Table 4-6.

Table 4-4. Emissions and Fuel Economy Test Results, 6.6L PROCO Vehicle at Low Mileage

3 Speed Automatic Transmission, 2.75:1 Rear Axle Ratio
5000-lb Inertia Weight Power, Absorption Unit Setting: 14.7 hp

	CVS-CH Emissions			Fuel Economy		
	HC gm/mi	CO gm/mi	NO _x gm/mi	Metro MPG	Highway MPG	M-H MPG
Objectives	0.24	2.5	0.82			
Car 1-5 Test Average	0.20	0.3	0.73	16.2	21.1	18.1
Car 2-5 Test Average	0.22	0.2	0.79	15.6	20.8	17.6
Car 3-5 Test Average	0.26	0.2	0.77	15.9	21.3	18.0
3 Car Average	0.23	0.2	0.76	15.9	21.1	17.9

Base Reference: Emission Standard:
(1.5 15 2.0)

Fuel Economy Capability
for the 6.6L
Carbureted Engine,
5000-lb IW, 2.75 axle ratio,
14.7-hp PAU

Table 4-5. Typical Modal CVS Bag Data, 6.6L PROCO Vehicle

3 Speed Automatic Transmission, 2.75:1 Rear Axle Ratio
5000-lb Inertia Weight, Power Absorption Unit Setting: 14.7 hp

(Average Data for 5 Tests)

Mode	HC	CO	NO _x	MPG
Cold 505 gm/bag	2.00	5.2	3.80	14.59
Stabilized gm/bag	0.40	0	2.44	15.39
Hot 505 gm/bag	0.37	0.04	2.55	17.34
CVS-H gm/mi	0.10	0	0.66	16.8
CVS-CH gm/mi	0.20	0.3	0.73	16.2
HWY				21.1
M-H				18.1

Table 4-6. Product Acceptance Tests,
6.6L V8 PROCO Vehicle

Automatic Transmission
2.75 Rear Axle Ratio

Test	PROCO Vehicle Test Results	Objective for Comparable Carbureted Engine Vehicle
<u>Performance</u>		
0-60 mph	12.0	12.4
25-60 mph	8.7	8.7
50-80 mph	13.3	13.1
<u>Octane Requirement</u>		
(WOT/Part Throttle)	88/<82	91/91
<u>Cold Start</u>		
0°F	Complied with Objective	5 seconds
-20°F	Complied with Objective	30 seconds

Results indicate a full-throttle octane requirement of 88 RON and a part-throttle octane requirement of 82 RON, both significantly less than the 91 RON requirement of the comparable carbureted engine.

Volkswagen has conducted research on the prechamber stratified-charge engine (PCI) concept, shown in Figure 4-14. A spherical prechamber, containing 25-30% of the compression volume, is connected to the main chamber by a relatively large flow passage. The fuel injection nozzle in the prechamber is positioned upstream from the spark plug with respect to the direction of air swirl. A carburetor or second fuel injection system provides a homogeneous air-fuel mixture to the main chamber. Load variations are primarily accomplished by varying the air-fuel ratio of the mixture introduced into the main chamber. A PCI engine was installed in a VW Beetle and a CVS test was conducted on a chassis dynamometer, using a 22500-lb inertia weight. Exhaust emissions with no exhaust gas after-treatment are shown in Table 4-7.

Table 4-7. Emissions from Third-Generation, 1.6-Liter PCI Volkswagen Engine

Emission	Amount
HC	2.1.-2.5 gm/mile
CO	4.4-8 gm/mile
NO _x	0.75-0.96 gm/mile
Fuel Economy	22-26 miles/gal (calculated from emissions)

Mitsubishi Heavy Industries, Ltd., has done development work on a stratified-charge combustion system called the Mitsubishi Combustion Process (MCP) concept (Ref. 59) shown in Figure 4-15. The MCP concept employs swirling air and direct-cylinder fuel injection. Fuel is injected toward the top of the cupped piston and is directed into the swirling air. The swirling air carries the evaporating fuel droplets to the spark plug, while the piston cavity prevents excessive fuel droplet diffusion.

4.3 VEHICLE FUEL ECONOMY AND EMISSIONS RESULTS

This section covers the fuel economy and emissions results for current production vehicles which use stratified-charge engine technology. Currently, only the Honda vehicles with stratified-charge engines fall in this category. The data is taken from EPA certification and fuel economy data for the 1980 model year in California. California data is used because it is felt that

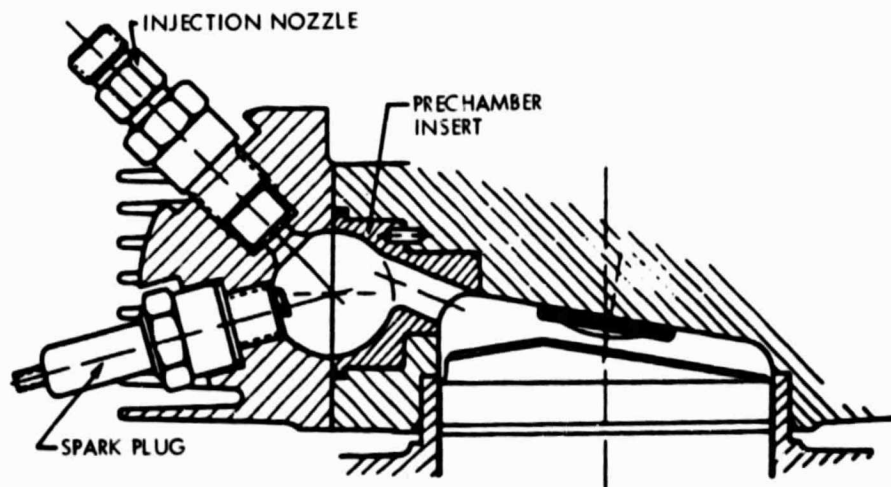


Figure 4-14. Second-Generation PCI Engine Combustion Chamber with Spherical Unscavenged Prechamber (Ref. 61)

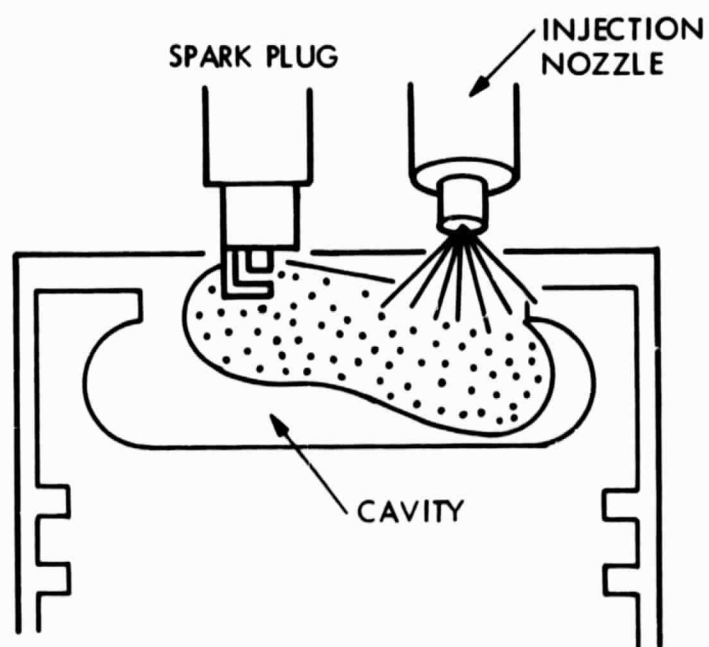
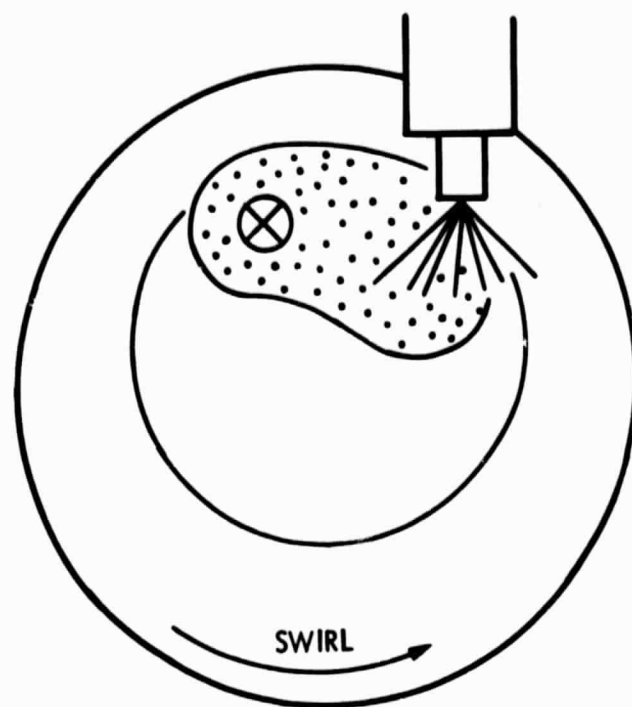


Figure 4-15. Illustration of MCP Engine (Ref. 63)

California emissions standards are more Representative of future emissions requirements for all states.

Figures 4-16 through 4-19 present fuel economy and emissions results for the 1980 California Honda vehicles using stratified charge engines and compared them with the results for all 1980 California vehicles using three-way catalyst emissions control. All of these vehicles are small, with inertia weights less than 2750 lb. As shown in Figure 4-17, the efficiencies of these vehicles, as indicated by the $1/W \times \text{MPG}$ parameter, are generally lower than the average for all California vehicles with three-way catalyst emissions control. HC and CO emissions are both low, and NO_x emissions fall between 0.7 g/mi and 0.9 g/mi. Comparisons of the fuel economy and emissions characteristics of the California and 49-state versions of these vehicles are given in Table 4-8 and Figure 4-20. Examination of this data indicates that a substantial fuel economy penalty is associated with meeting the lower California NO_x emissions level. The Honda stratified-charge engine system may have difficulty meeting the more stringent NO_x emissions requirement, especially without significant additional fuel economy penalties.

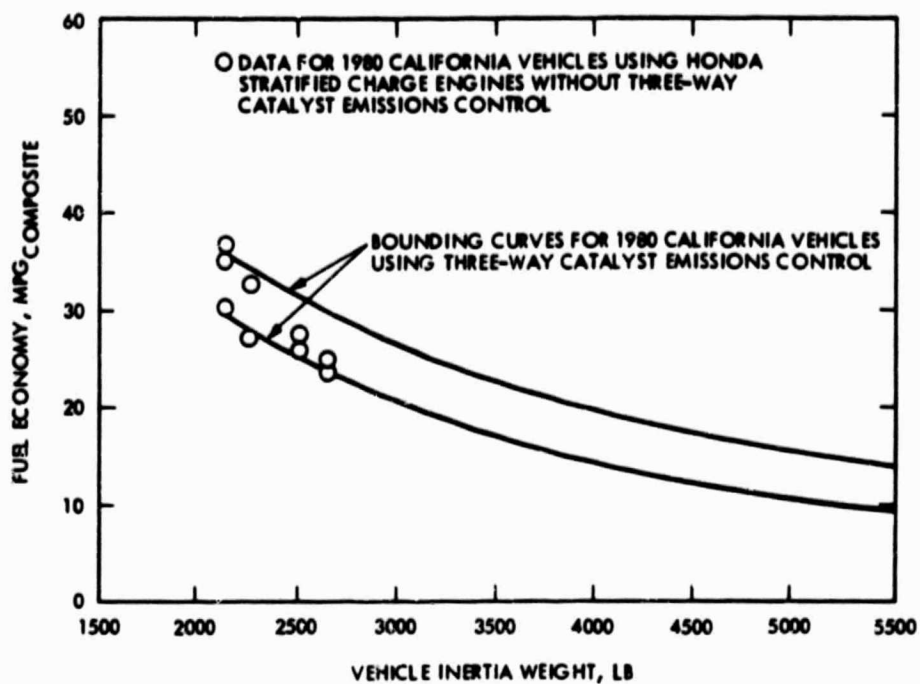


Figure 4-16. Composite Fuel Economy for California Vehicles Using the Honda Stratified-Charge Engine

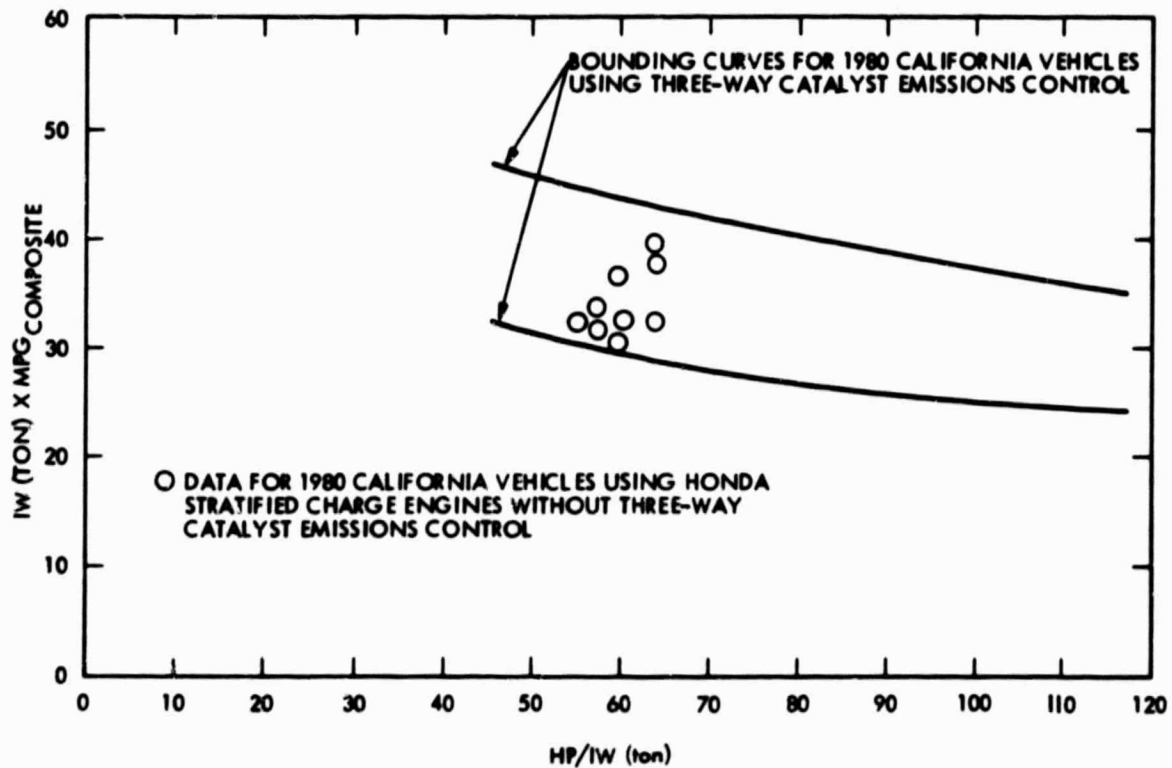


Figure 4-17. Fuel Economy Characteristics for California Vehicles Using the Honda Stratified-Charge Engine

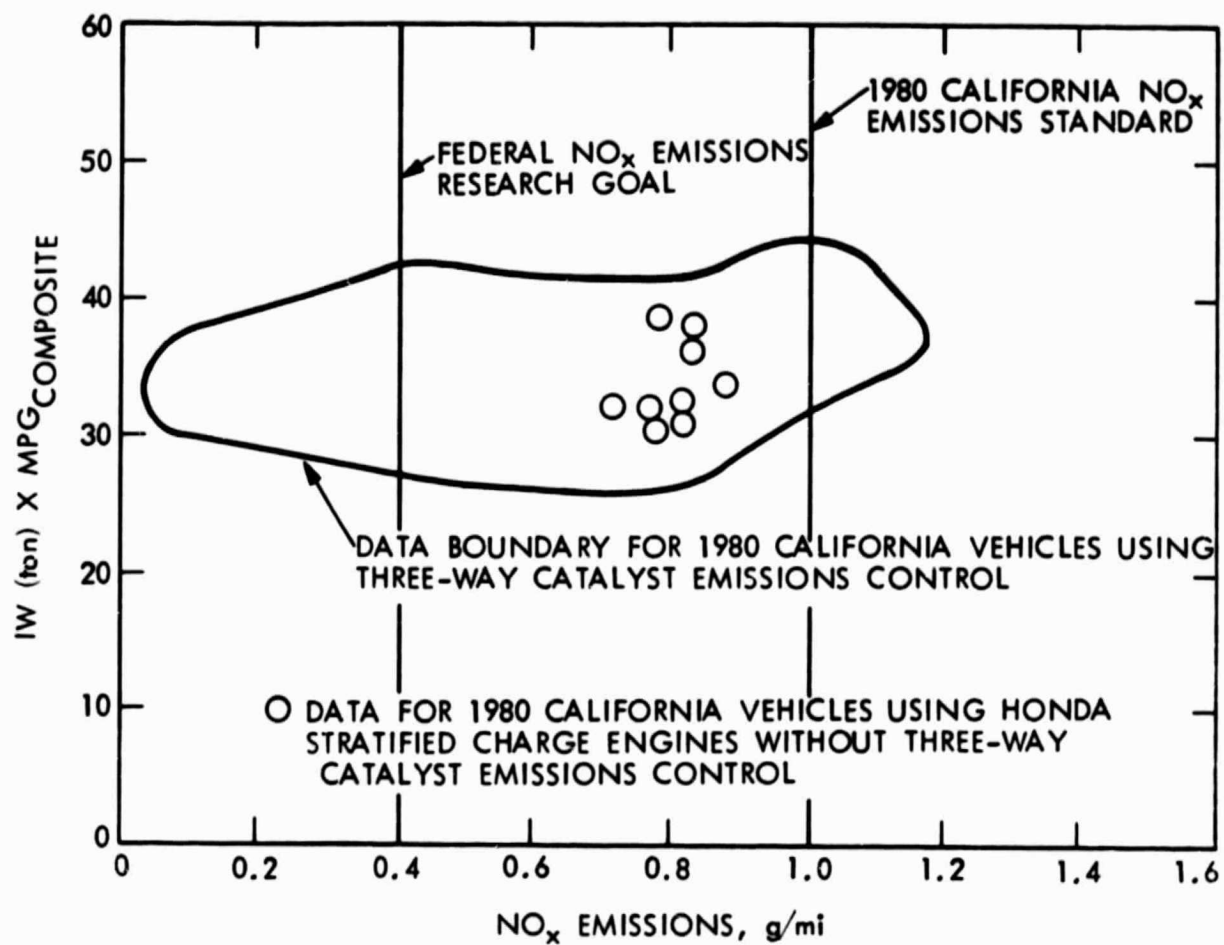


Figure 4-18. NO_x Emissions Characteristics for California Vehicles Using the Honda Stratified-Charge Engine

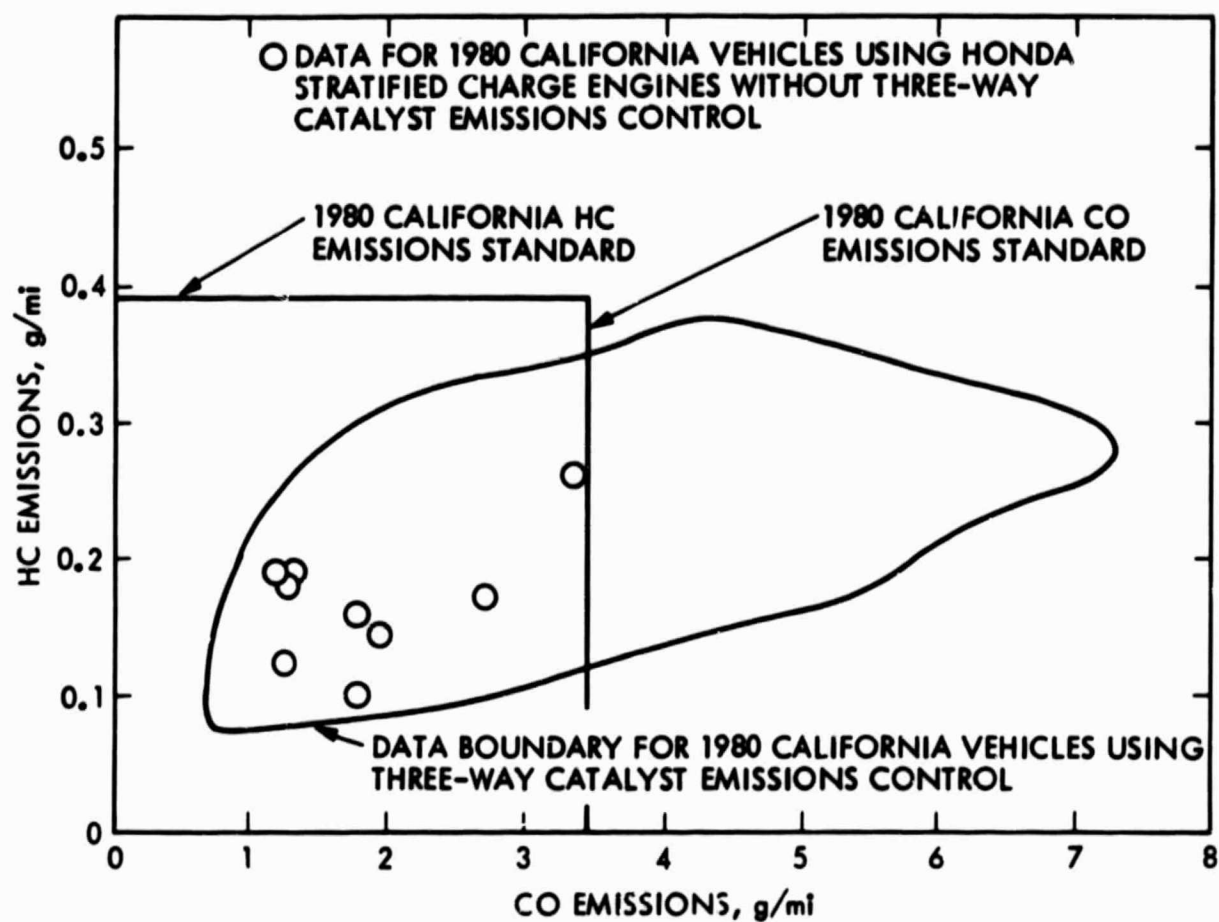
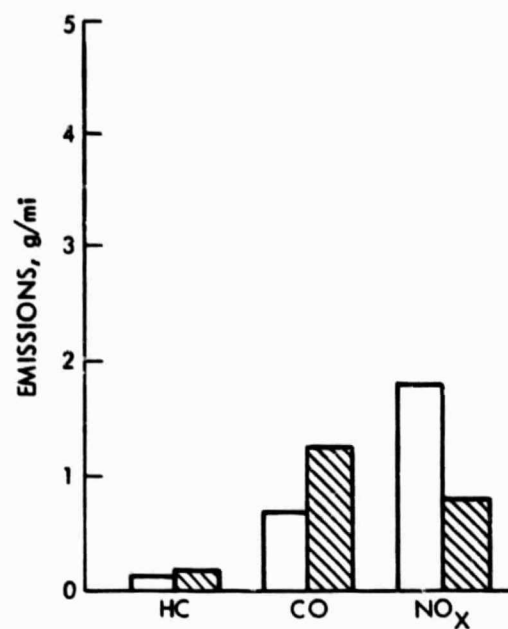
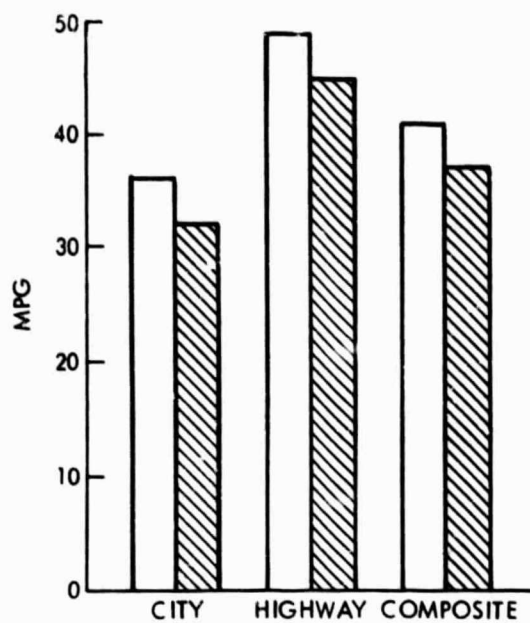


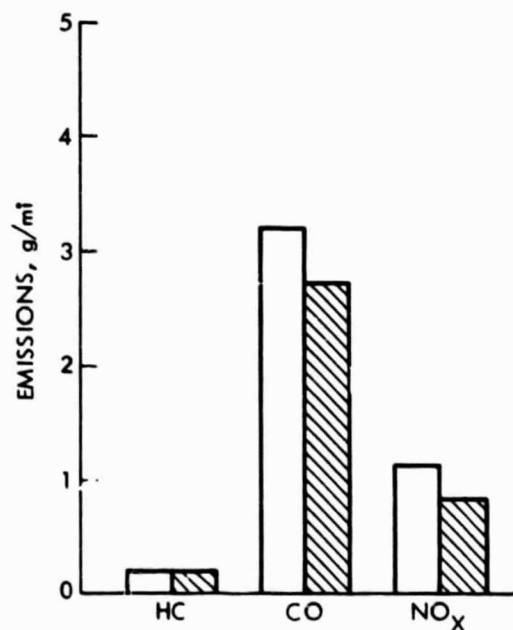
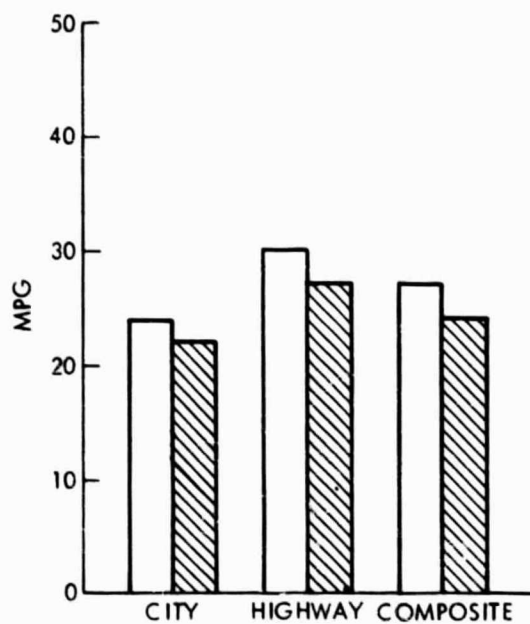
Figure 4-19. HC and CO Emissions Characteristics for California Vehicles Using the Honda Stratified-Charge Engine

Table 4-3. Characteristics of Honda Stratified-Charge Engines in 1980 California and 49-State Vehicles

Mfg	Car Line	CID	Carb FI	Comp Ratio	HP	Emission	Trans	Wt.	Axle	City	Hwy	Comb	HC	CO	NOx	Ton X mpg Comb	Ton HC/lw (Ton)
Honda	Civic	91	C-3	8.9	67	EGR/OXD	M4-2	2125	3.83	32	41	36	0.194	1.13	0.83	38.25	63.06
	Civic						M5-2	2125	3.88	32	45	37	0.185	1.25	0.79	39.31	63.06
	Civic Wg.						M5-2	2250	4.43	29	38	33	0.190	1.20	0.85	37.13	59.56
	Civic						M5-2	2125	4.12	27	35	30	0.122	1.23	0.77	31.88	63.06
	Civic Wg.						M5-2	2250	4.12	25	29	27	0.140	1.96	0.78	38.38	59.56
Prelude Accord		107	C-3	8.0	72	EM	M5-2	2500	4.38	24	33	27	0.264	3.37	0.87	33.75	57.60
							M5-2	2625	4.38	22	30	25	0.100	1.77	0.81	32.81	54.86
Accord Accord		107	C-3	8.8	75	EGR/OXD	A3-1	2500	3.59	24	28	26	0.163	1.78	0.71	32.50	60.00
							A3-1	2625	3.59	22	27	24	0.185	2.71	0.81	34.50	57.14
Honda (49- State)	Civic	91	C-3	9.0	67	OXD	M4-2	2125	3.88	35	45	39	0.106	0.42	1.81	41.44	63.06
	Civic						M5-2	2125	3.88	36	49	41	0.124	0.67	1.78	43.56	63.06
	Civic Wg.						M5-2	2250	4.43	31	42	35	0.109	0.60	1.45	39.58	59.56
	Civic						S2-2	2125	4.12	29	35	32	0.092	0.74	1.60	34.00	63.06
	Civic Wg.						S2-2	2250	4.12	28	32	29	0.143	1.73	1.70	32.63	59.56
Civic Civic		81	C-3	7.9	55	EM	M4-2	2000	4.93	28	36	31	0.256	3.58	1.15	31.00	55.00
							M5-2	2000	4.93	28	39	32	0.285	4.35	1.11	32.00	55.00
Accord Accord Accord Accord		107	C-3	8.0	68	EM	A3-1	2500	3.59	23	28	25	0.121	2.88	1.44	31.25	54.40
					68		A3-1	2625	3.59	24	30	27	0.178	3.19	1.40	35.44	51.81
					72		M5-2	2500	4.38	25	55	28	0.187	2.46	1.57	36.25	57.60
					72		M5-2	2625	4.38	26	36	30	0.278	3.76	1.34	39.38	54.86



FUEL ECONOMY AND EMISSIONS COMPARISONS FOR CALIFORNIA AND 49-STATE VEHICLES HONDA CIVIC (91 CID CVCC ENGINE)



FUEL ECONOMY AND EMISSIONS COMPARISONS FOR CALIFORNIA AND 49-STATE VEHICLES HONDA ACCORD (107 CID CVCC ENGINE)

 CALIFORNIA
 49-STATE

Figure 4-20. Fuel Economy and Emissions Comparisons for California and 49-State Vehicles Using the Honda Stratified-Charge Engine

SECTION 5

ROTARY ENGINE CONCEPTS

5.1 INTRODUCTION

The engine concepts discussed in earlier chapters of this report have all been of the reciprocating type, which consist of piston-in-cylinder configurations with power being removed through a rotating crankshaft. Rotary engine concepts (Ref. 64) have received varying amounts of attention during the last 20 years as an alternative to the more common reciprocating engine. Rotary engines have one or more 3-lobe rotors which are connected to an eccentric output shaft and which rotate within a rotor housing, whose geometry helps form the varying volume cavity where combustion occurs. Rotary designs are inherently compact, lightweight, and easy to package in automobile engine compartments. Also, rotary engines tend to have a much higher power density than their reciprocating counterparts.

Although many automobile manufacturers (e.g., General Motors, Toyo Kogyo, Audi NSU, Toyota and Curtiss-Wright) have done research and development on rotary engine concepts, only Toyo Kogyo has introduced a rotary engine in a production automobile, the Mazda. Unfortunately, the early production rotary engines had sufficient problems to establish a reputation for poor combustion chamber sealing, high HC emissions, excessive misfiring under idling conditions, and high fuel consumption. Most of these problems were significantly reduced in later rotary engine designs, but much of this early reputation remains. Under the pressure of emissions and fuel economy regulation, several automobile manufacturers have stopped work on rotary engine concepts and concentrated their efforts on new conventional gasoline and diesel engines of the reciprocating configuration. For example, General Motors and Audi NSU no longer have active rotary engine development programs.

From the beginning, sealing the rotating combustion chamber of the rotary engine has been a challenge. In attempting to combine durability with cost effectiveness, early production designs were not completely successful. However, through the use of improved materials and increasingly sophisticated seal geometries, rotary engine seal problems have all but been eliminated.

Rotary engine concepts characteristically produce higher HC emissions than their reciprocating counterparts; however, recent work indicates that rotor pocket design and selective cooling can help reduce engine-out HC emissions. The compact and continuous exhaust flow from a rotary engine matches well with the use of a thermal reactor for reducing engine-out HC emissions.

Rotary engines, by their inherent design, internally recirculate large amounts of exhaust gas relative to their reciprocating counterparts. This internal EGR sometimes results in excessive misfiring under idling conditions, producing poor driveability and lowering fuel economy. This problem can be minimized through the proper design of the combustion chamber and ignition source.

The fuel consumption characteristics of rotary engines are understood by considering the thermal and mechanical efficiencies of the engine. A typical rotary engine has a surface-to-volume ratio which is suboptimal from a thermal efficiency standpoint. On the other hand, the mechanical efficiency of a rotary engine is substantially higher than that for a comparable reciprocating engine due to the lower frictional losses. In spite of these factors, the fuel economy of early rotary engines was substantially below that of conventional engines. Some progress has been made in narrowing this fuel economy gap.

5.2 TECHNOLOGY DEVELOPMENTS AND VEHICLE SYSTEMS

Because only one rotary engine is presently being used on a production vehicle, much of the technology is contained in research studies and engine prototype developments. The results of some studies and engine developments will be reviewed to provide a basis for evaluating the potential of rotary engine concepts.

Toyo Kogyo (Ref. 65) began production of rotary engines in 1967 and introduced the first rotary engine available in this country for a production automobile in 1970. Two twin-rotor powerplants have been available in Mazda automobiles since that time. Both engines utilized carburetors, dual ignition, and a thermal reactor emission control system. One of the 1976 Mazda rotary engines is shown in Figure 5-1. When automotive fuel economy became more important in the mid-1970's, Toyo Kogyo made an increasing effort to improve the fuel economy of the rotary engine. Under pressure to improve vehicle fuel economy, Mazda finally dropped the rotary engine from all of their automobiles except the Mazda RX-7 sports car. Further developments in the production rotary engine have been concentrated on improving sealing techniques, a change to lean combustion, and developing a better thermal reactor which permits the use of more optimum ignition timing.

As shown in Figure 5-2, the sealing elements used on the rotor of a rotary engine includes a multi-piece apex seal mating with the trochoidal surface of the rotor housing, side seals running against the side housing, and an end (corner) seal to which the other seals converge. Initially, Toyo Kogyo used a one-piece carbon apex seal which was later replaced by a two-piece metallic seal. Further subtle refinement of the two-piece geometry have been made to reduce the geometrical leakage area at the seal interface with the side housings. When using an apex seal with a straight top in the axial direction, the trochoidal surface and the apex seal do not always maintain full contact, especially at low engine speeds. The resulting gas leakage caused a loss of engine power and increased fuel consumption. To overcome this problem, a slight crowning of the apex seal in the axial direction was added. Gas sealing performance of the corner seal is primarily influenced by the clearance between the corner seal and the seal bore. The corner seal has been modified by adding an off-center circular hole in the axial direction to increase the elasticity of the seal in the radial direction. This new design permits the use of reduced clearances which are compatible with achievable manufacturing tolerances. The design also reduces the seal contact area with the side housing, which decreases the sliding resistance.

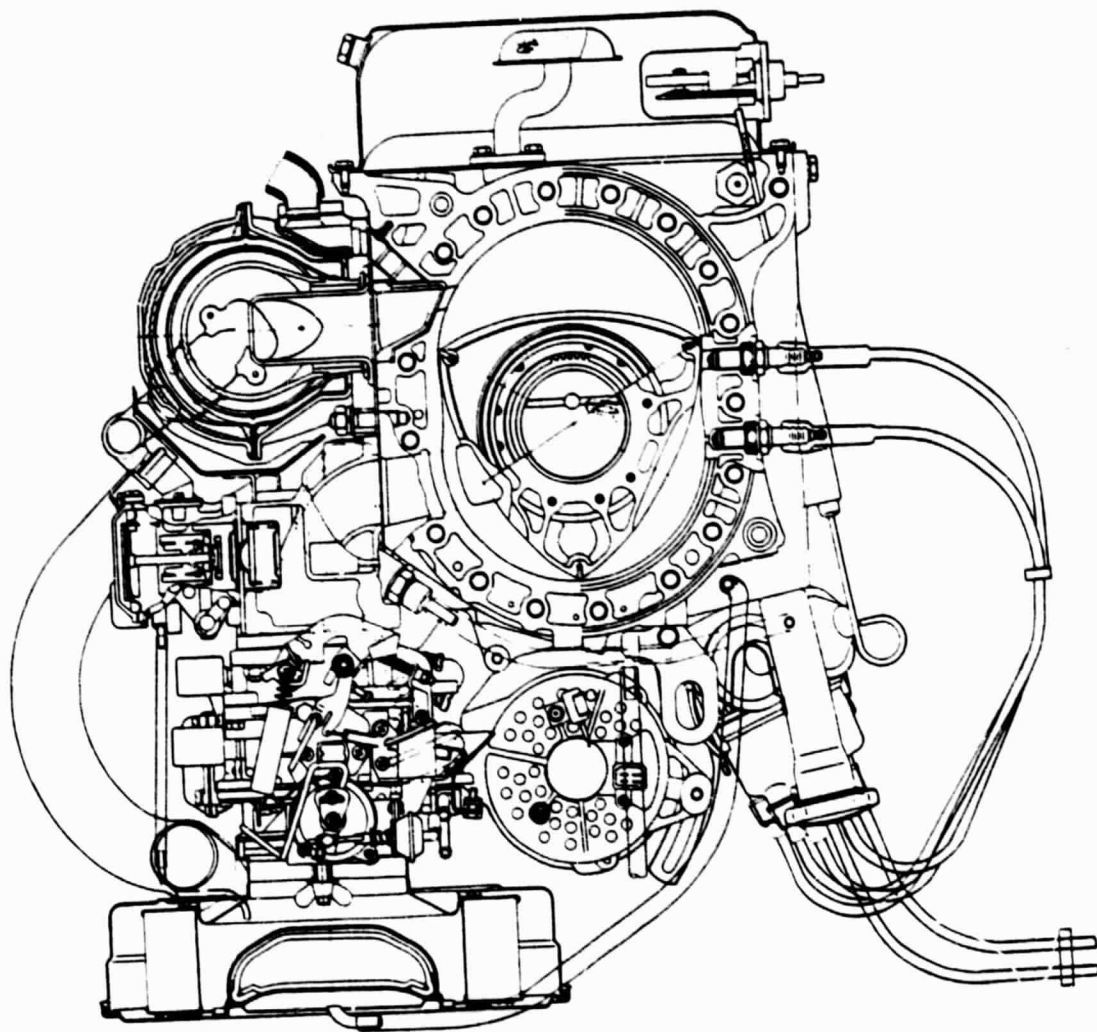


Figure 5-1. 1976 Mazda Rotary Engine (Ref. 65)

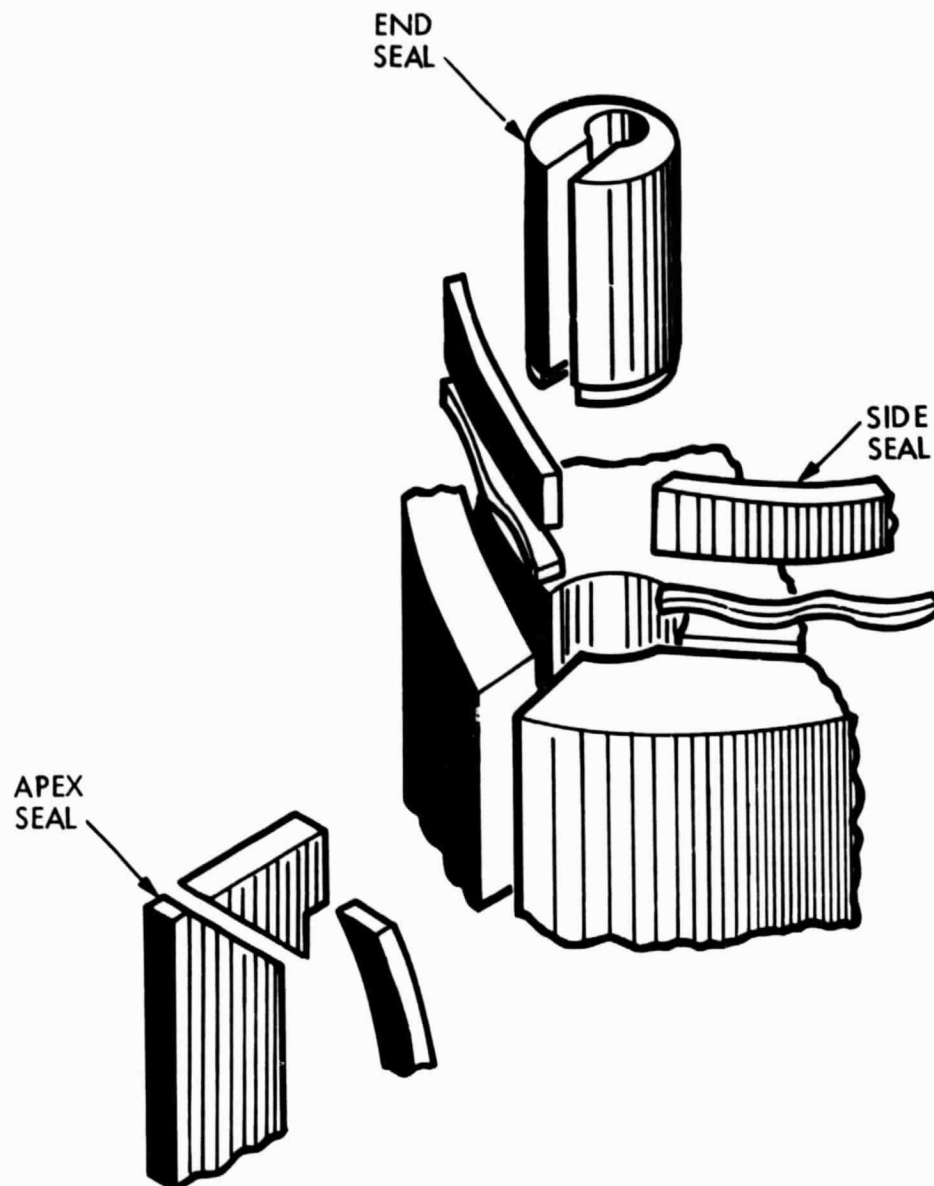


Figure 5-2. Rotor Sealing Elements Include Multi-Piece Apex Seal Mating with Trochoid Surface, Side Seals Running Against Side Housing, and End Seal to Which Others Converge (Ref. 64)

The shape of the combustion chamber recess in the rotor and the type and location of the spark plug have a significant influence on thermal efficiency and exhaust emissions. Early Mazda rotary engines used a medium deep recess-type (MDR) combustion chamber which is symmetrical with respect to the minor axis of the rotor, as shown in Figure 5-3. Later designs (after 1976) used a leading deep recess-type (LDR) combustion chamber which increases the squish in the rotating direction at TDC and increases the flame propagation speed. This improves fuel economy and reduces engine-out emissions, when coupled with part-load ignition by the leading plug alone. The LDR geometry was found to aggravate misfire tendencies at light load. To counteract this tendency, the spark plugs were changed from the conventional two-ground electrode type to a three-ground electrode type with an increased gap.

The rotary engine has a simpler structure around the exhaust port than does a conventional engine. This permits the use of a thermal reactor for the conversion of engine-out HC emissions. Later-production versions of the Mazda rotary engine have improved the reaction rate in the thermal reactor by using redesigned exhaust port liners and heated secondary air injection. The latest exhaust port liner uses an insulating ring to reduce the area of contact with the rotor housing, thereby reducing the heat transfer to the rotor housing. A heat-transfer ring is used between the exhaust port liner insert and the inlet pipe of the thermal reactor, to increase the temperature of the insert by providing a heat transfer path from the hot thermal reactor. Secondary air injection provides an oxygen-rich atmosphere for improved reaction rates in the thermal reactor. Unfortunately, when the secondary air is introduced at ambient temperature, it reduces the temperature of the exhaust gases entering the thermal reactor, resulting in reduced reaction rates. This negative effect on reactivity can be offset by preheating the secondary air, permitting the use of leaner engine air-fuel ratios, as shown in Figure 5-4. The leaner air-fuel ratios result in an increase in engine thermal efficiency. The Mazda vehicle implementation of the preheated secondary air concept is shown in Figure 5-5. Air from the air pump and control valve is routed through a heat exchanger which receives heat from the exhaust system. The heated air then travels to the thermal reactor in a sleeve surrounding the exhaust pipe. The preheated secondary air enters the reactor cavity through a nozzle incorporated into the port liner.

In addition to the improvements on the production engines, Toyo Kogyo has been pursuing other rotary engine developments to improve fuel economy. The spark plug arrangement and the shape and location of the combustion chamber recess are crucial for improving the thermal efficiency of rotary engines. It seems desirable to have multiple spark plugs located along the rotational direction because the combustion chamber moves in a rotational direction and is long and narrow. The production engines use two spark plugs located on the trailing side and the leading side of the minor axis. Before any modifications can be made to the spark plugs and combustion chamber to improve fuel economy emission control and driveability factors must also be considered. As shown in Figure 5-6, test results indicate that use of the leading spark plug alone at part load increases the exhaust gas temperature and permits leaner engine operation, which results in a better fuel economy than is obtainable by igniting two spark plugs, while maintaining the same level of emission control with the thermal reactor.

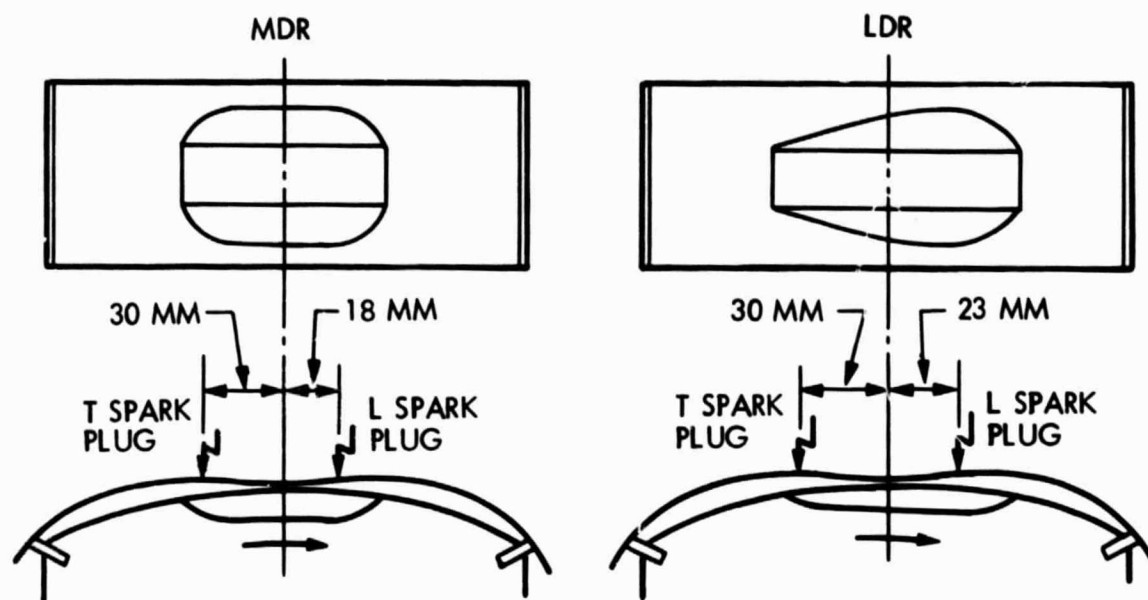


Figure 5-3. Alternate Designs for Combustion Chamber Recess (Ref. 65)

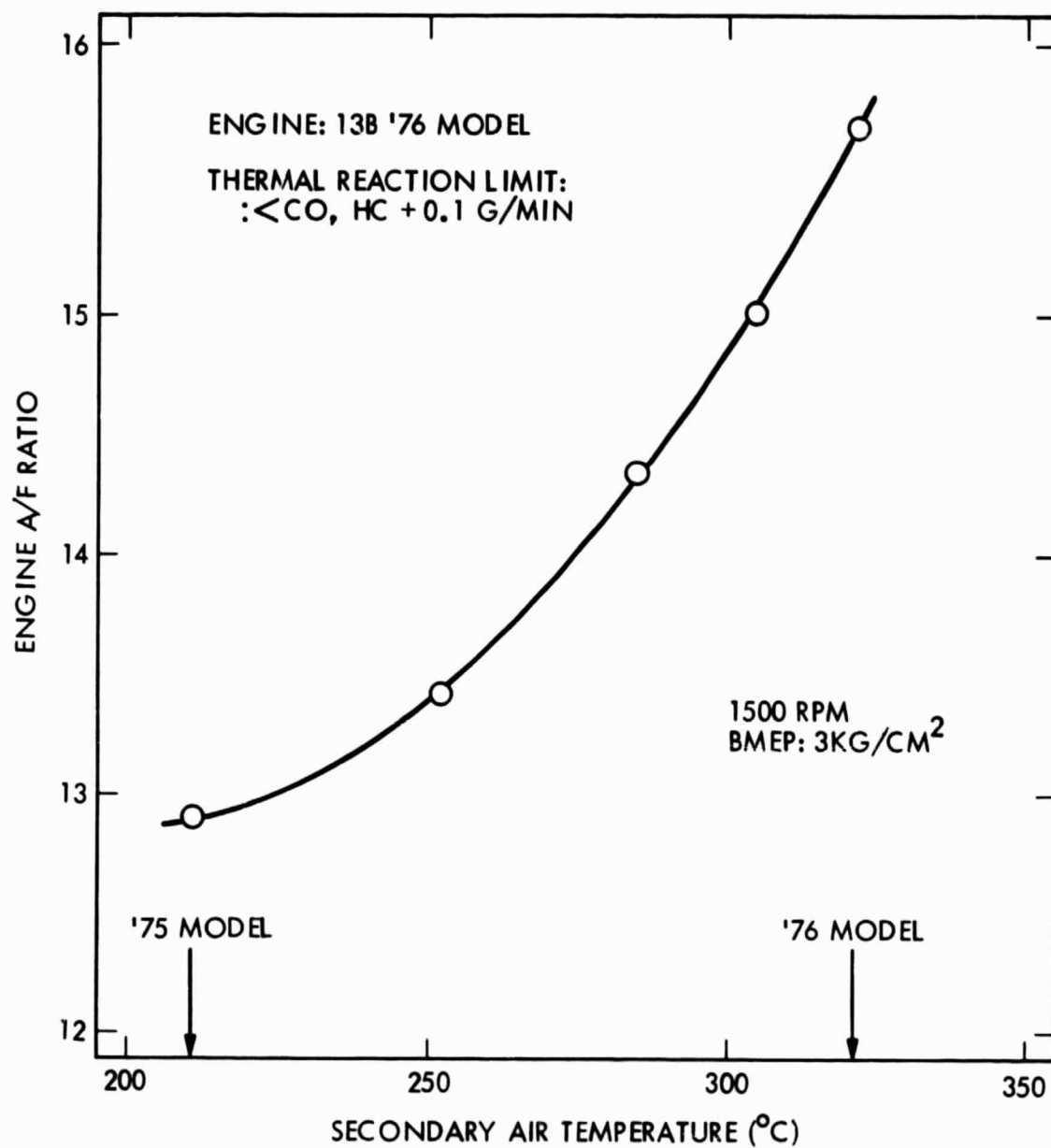


Figure 5-4. Effect of Secondary Air Temperature on Engine A/F Ratio for Thermal Reaction Limit (Ref. 65)

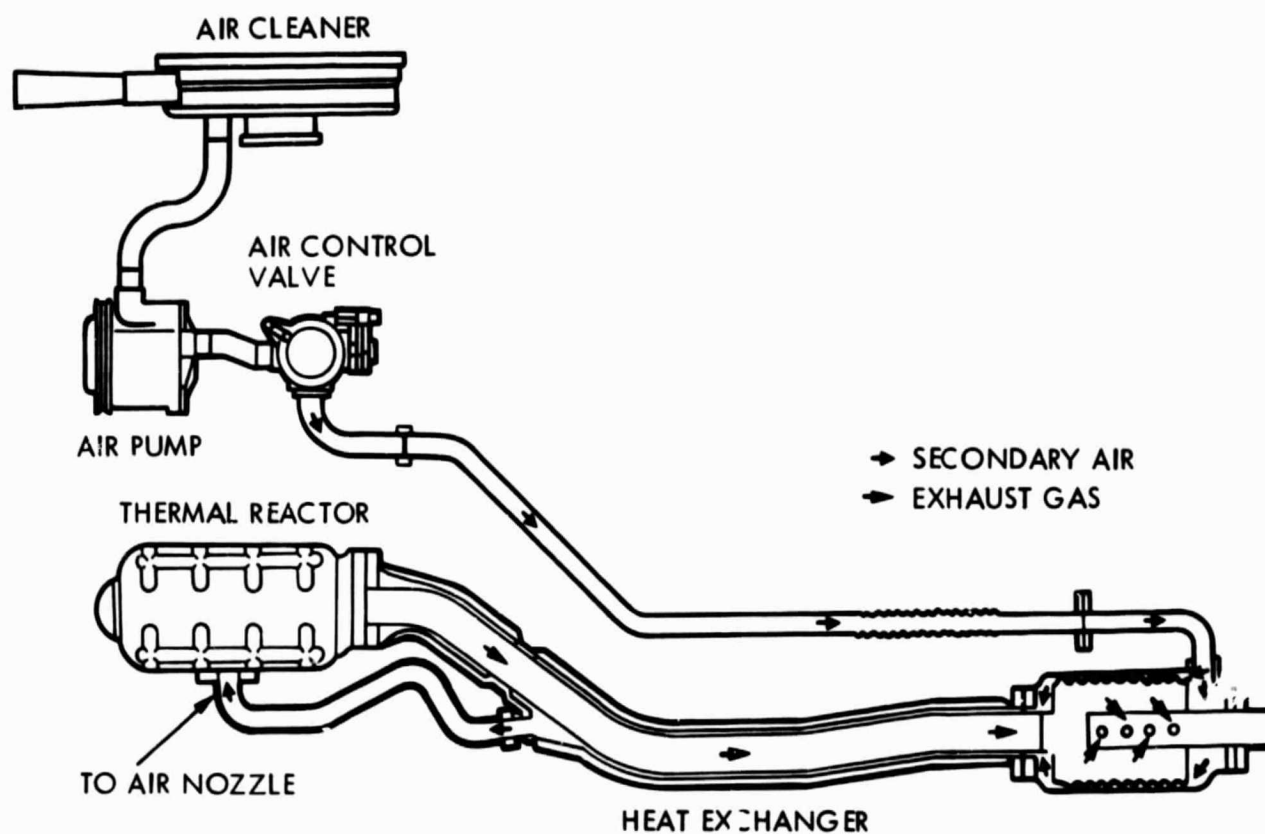


Figure 5-5. Secondary Air Pre-Heat System (Ref. 65)

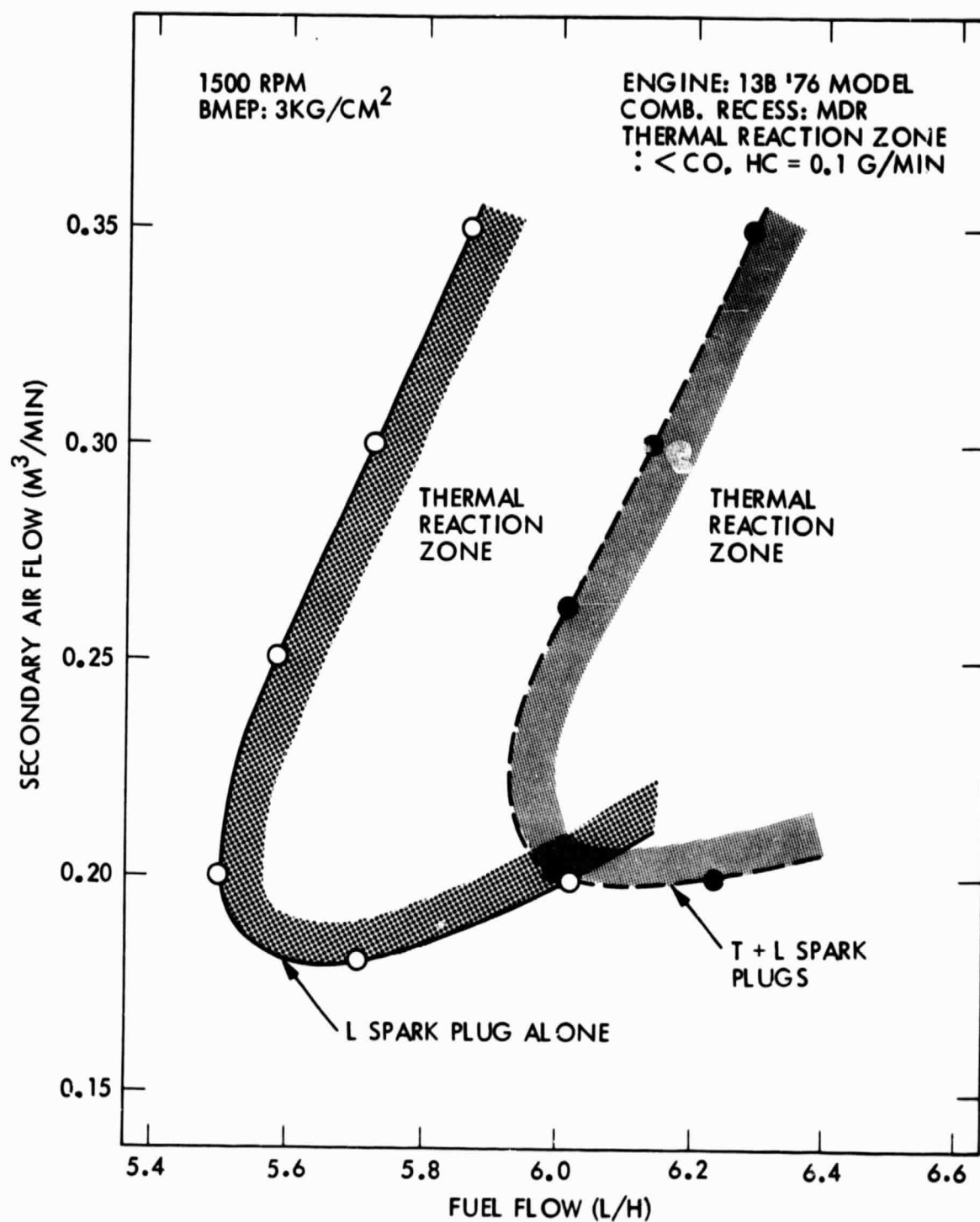


Figure 5-6. Effect of Spark Plug Location on Thermal Reaction (Ref. 65)

Toyo Kogyo made studies on the compression ratio as a means of increasing the thermal efficiency in rotary engines with the LDR type combustion chamber. Results of these tests indicated that by using the leading spark plug alone it would be possible to increase the compression ratio to a higher level than when two spark plugs were used, as shown in Figure 5-7. The octane number requirement (ONR) for a compression ratio of 10 when using the leading spark plug alone is equivalent to the ONR for a compression ratio of 9.2 when using two spark plugs, as on the current production engine. Raising the compression ratio generally improves performance and fuel economy, but HC and NO_x emissions tend to increase as well. At a given NO_x emission level achieved with EGR, the better fuel economy results were obtained with an engine having the LDR-type combustion chamber, a compression ratio of 10, and a disengaged trailing spark plug, as indicated in Figure 5-8.

The surface-volume ratio of the combustion chamber is larger on the rotary engine than on conventional piston engines. As a result, rotor and trochoid-housing temperatures have considerable influence on fuel economy (especially at light loads) and on engine-out HC emissions (especially when the engine is cold). Control of the cooling systems for the water-cooled housings and oil-cooled rotors can also produce significant benefits. Test results indicated that the LDR-type combustion chamber was particularly compatible with the use of EGR for NO_x emissions control. In addition to permitting the use of higher EGR rates, the LDR-type combustion chamber also demonstrated superior combustion stability (i.e., less peak-pressure fluctuation) over other designs.

Toyo Kogyo has evaluated two stratified-charge concepts as a means of achieving more efficient lean combustion in rotary engines. One of the concepts uses the Compound Induction Step Control (CISC) system shown in Figure 5-9. The CISC system combines a peripheral port and a side port. To reduce the amount of dilution gas introduced during intake and exhaust port overlap, the peripheral port has a slit shape with a reed valve. The peripheral port opens only at idling and low load conditions, and the side port supplies the additional mixture with increases in load. The small peripheral port area and vibrations of the reed valve aid fuel atomization at low load. The geometrical location of the peripheral port helps supply the mixture to the leading side of the combustion chamber. Compared to the conventional side-port rotary engine, the CISC engine gave substantially improved combustion stability with lean mixtures. It also showed a moderate reduction in fuel consumption, and some increase in HC and NO_x emissions. With regard to misfire characteristics, the CISC system was better than the side-port engine in the high speed range, but inferior in the low speed and low load ranges. The other advanced rotary engine under development by Toyo Kogyo uses direct fuel injection as a part of the Rotating Stratified Combustion (ROSCO) system shown in Figure 5-10. Fuel is injected directly into the chamber while air enters through both a conventional side port and a reed-valved peripheral port similar to the CISC system. The fuel spray is atomized through collision with the air flowing in at high speed from the peripheral port. This atomized mixture is then stratified into the leading portion of the combustion chamber recess. Compared to the carbureted engine, the ROSCO system demonstrated more stable combustion in the lean range and

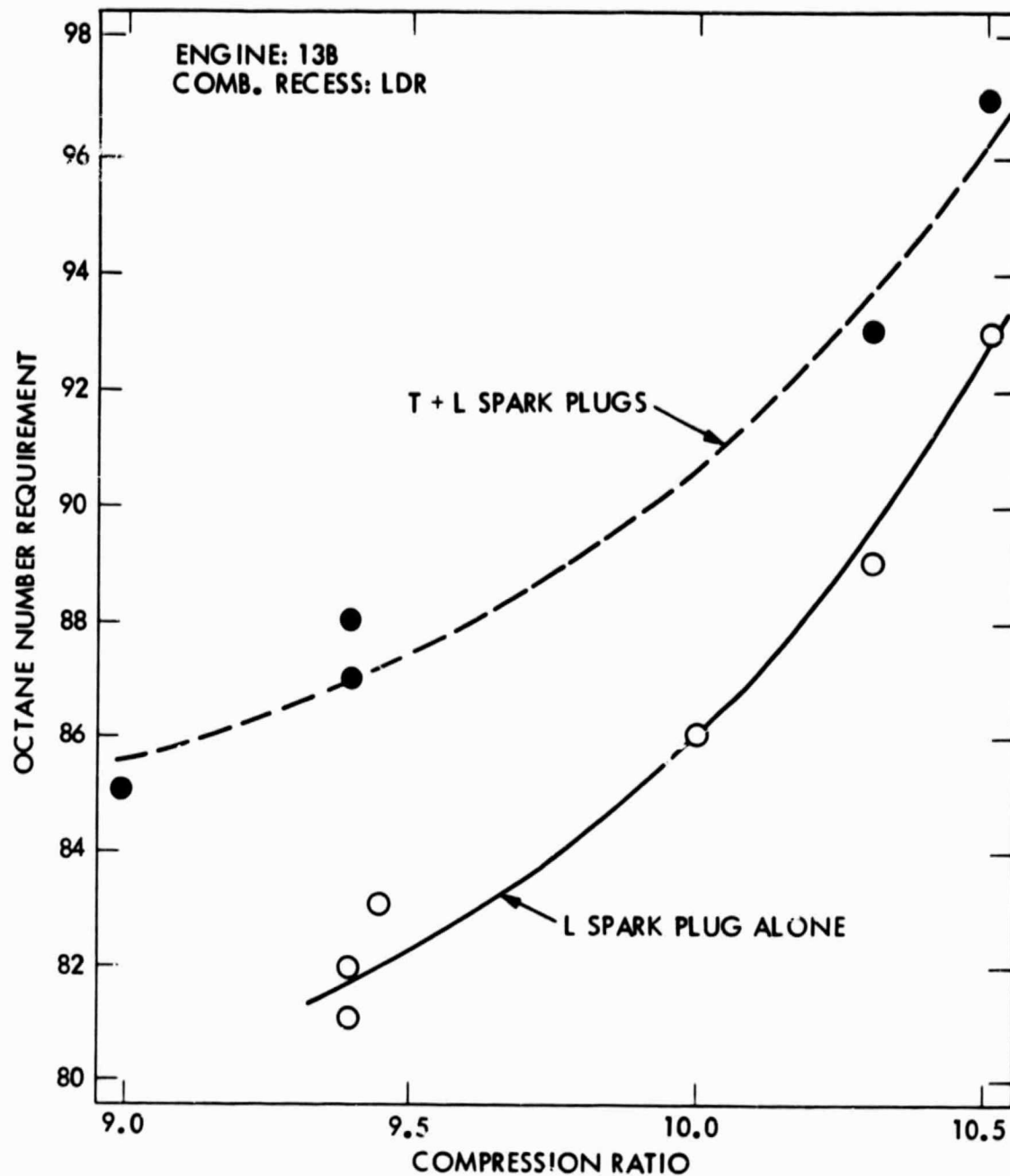


Figure 5-7. O.N.R. Related to Number of Spark Plugs

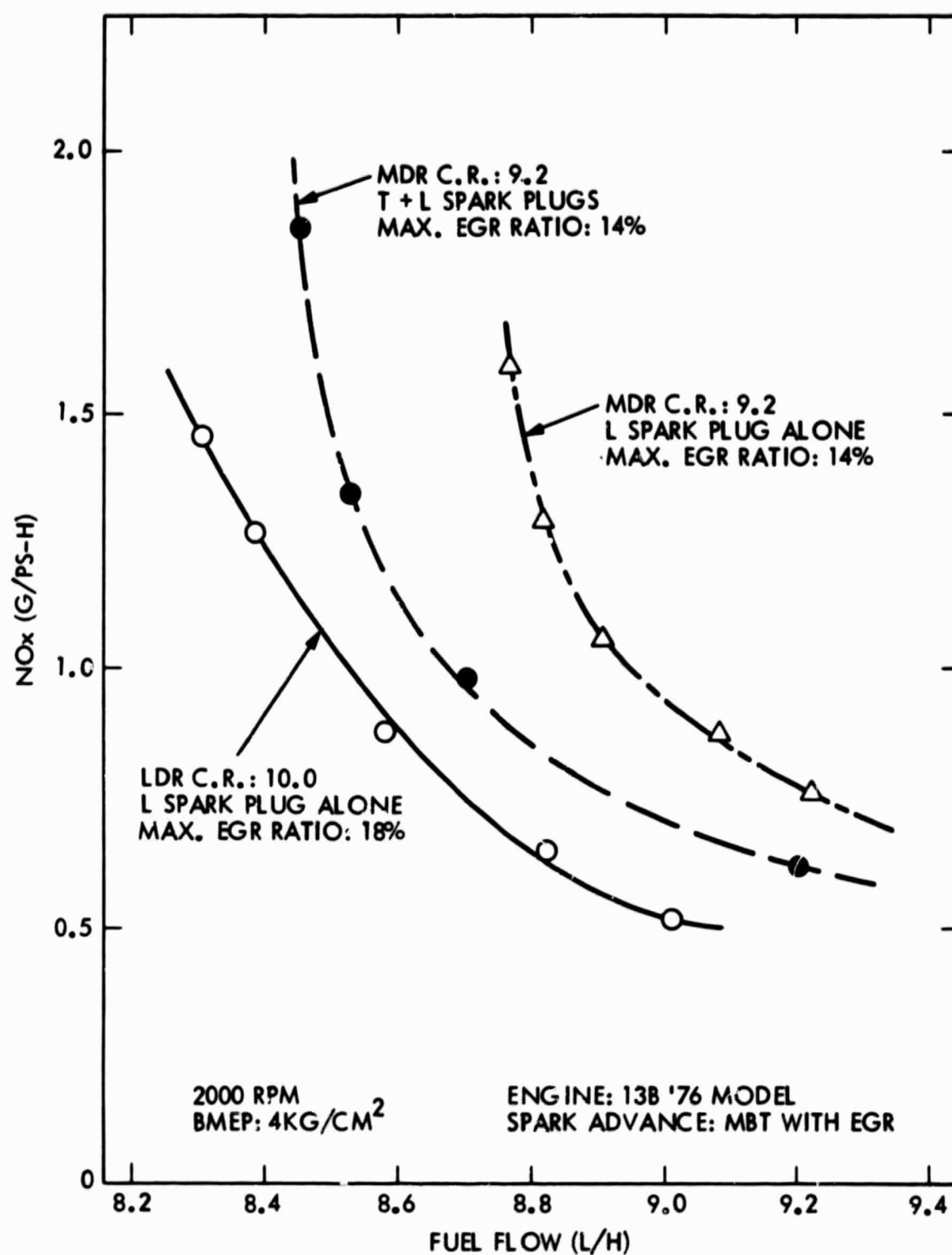


Figure 5-8. Effects of Combustion Recess and Spark Plug on NO_x Emission with EGR (Ref. 65)

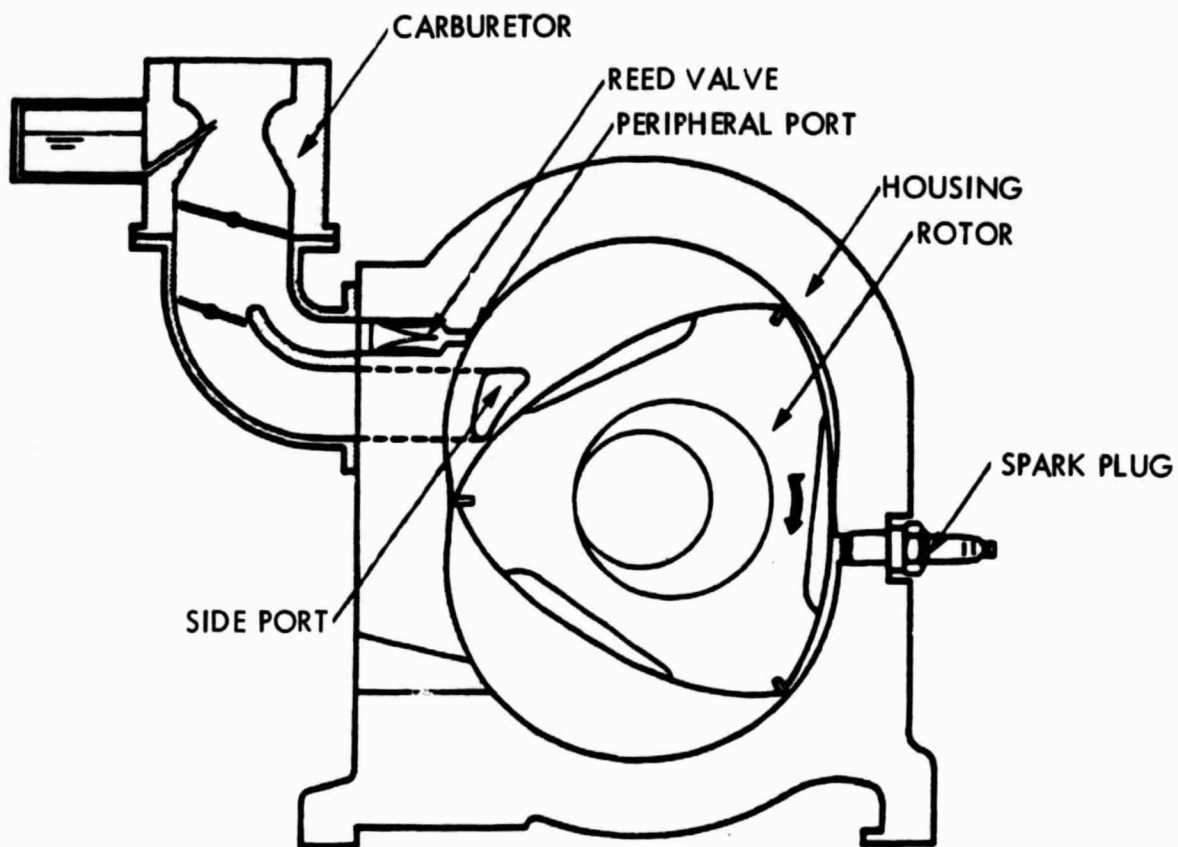


Figure 5-9. Compound Induction Step Control (CISC) System (Ref. 65)

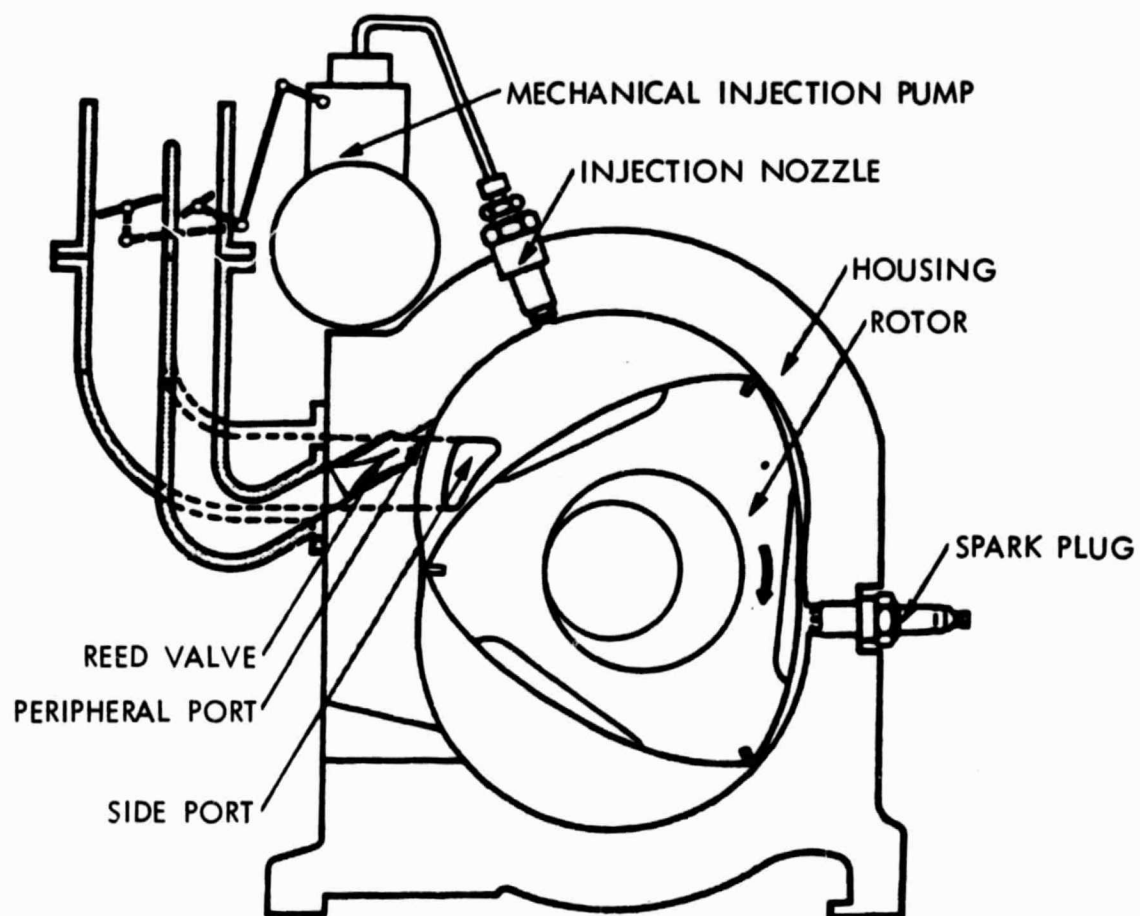


Figure 5-10. Rotating Stratified Combustion (ROSCO) System (Ref. 65)

somewhat better fuel economy. However, at rich air-fuel ratios, the ROSCO system exhibited more fluctuation in peak pressures than did the carbureted version. This less stable combustion was attributed to a poorer atomization of rich mixtures.

Rotary engine activities began at NSU (Ref. 66) in the mid-1950's and the single-rotor 1963 NSU Spider became the world's first production rotary-powered automobile. The twin-rotor RO-80 automobile followed in 1967. In 1969, NSU merged with Audi to form Audi NSU Auto Union AG, which began work on a new generation of rotary engines in 1971. Although this new rotary engine was intended as a powerplant for the Audi 5000 sedan, development work on the rotary was discontinued about a year ago. Some of the more significant developments resulting from the Audi NSU rotary program will be reviewed here.

One of the latest products of the Audi NSU rotary program is the two-rotor, fuel-injected, lean-combustion powerplant shown in Figure 5-11. This rotary engine design has dual side-port induction, two-point fuel injection, and thermostatically controlled oil-cooling of its twin rotors. A schematic of the fuel and air supply system for the engine is shown in Figure 5-12. Fuel is supplied by a mechanically-operated continuous-injection Bosch K-Jetronic unit. Each combustion chamber has two fuel-injection nozzles, and there is an auxiliary start-valve located upstream in a portion of the intake manifold common to both combustion chambers. One nozzle sprays directly into each rotor housing, supplying two-thirds of the incoming fuel. The remaining one-third of the fuel is supplied by a second nozzle, located in the intake manifold. Air is metered through a flow sensor in the mixture control unit. Engine speed and load determine the volume of air inducted, and the control unit meters an appropriate quantity of fuel to the injectors.

Downstream of the start-valve, the intake manifold splits into four sections for each of the four side ports. The two outer pipes are fitted with injection nozzles, while the inner pair carry air alone. Supplementary air enters the chamber under two control modes, one for idling and another for warmup. The idling valve functions whenever the throttle is closed, and the warmup valve supplies additional air to stabilize idle whenever the fuel start-valve is in operation.

As shown in the fuel-air schematic in Figure 5-13, part of the supplementary air enters at the rotor-housing injection location. Some of the air enters the chamber through a jacket surrounding the injection nozzle and promotes atomization of the fuel. The remaining air comes in through passages on either side of the housing and helps distribute lubricating oil to the side and trochoidal surfaces. The rotor, eccentric shaft and accompanying bearings and gears are lubricated by means of a thermostatically-controlled system, which optimizes temperatures as functions of engine speed and load. The emission control system needed to meet the U.S. emission standards is shown in Figure 5-14. The system includes both a main catalytic converter and a start-up device; however, no EGR is required. The main converter contains two metal-supported platinum catalysts with a small separation between them to generate turbulence and aid warmup. During cold starts, exhaust gas is directed through the start-up converter. When catalyst and

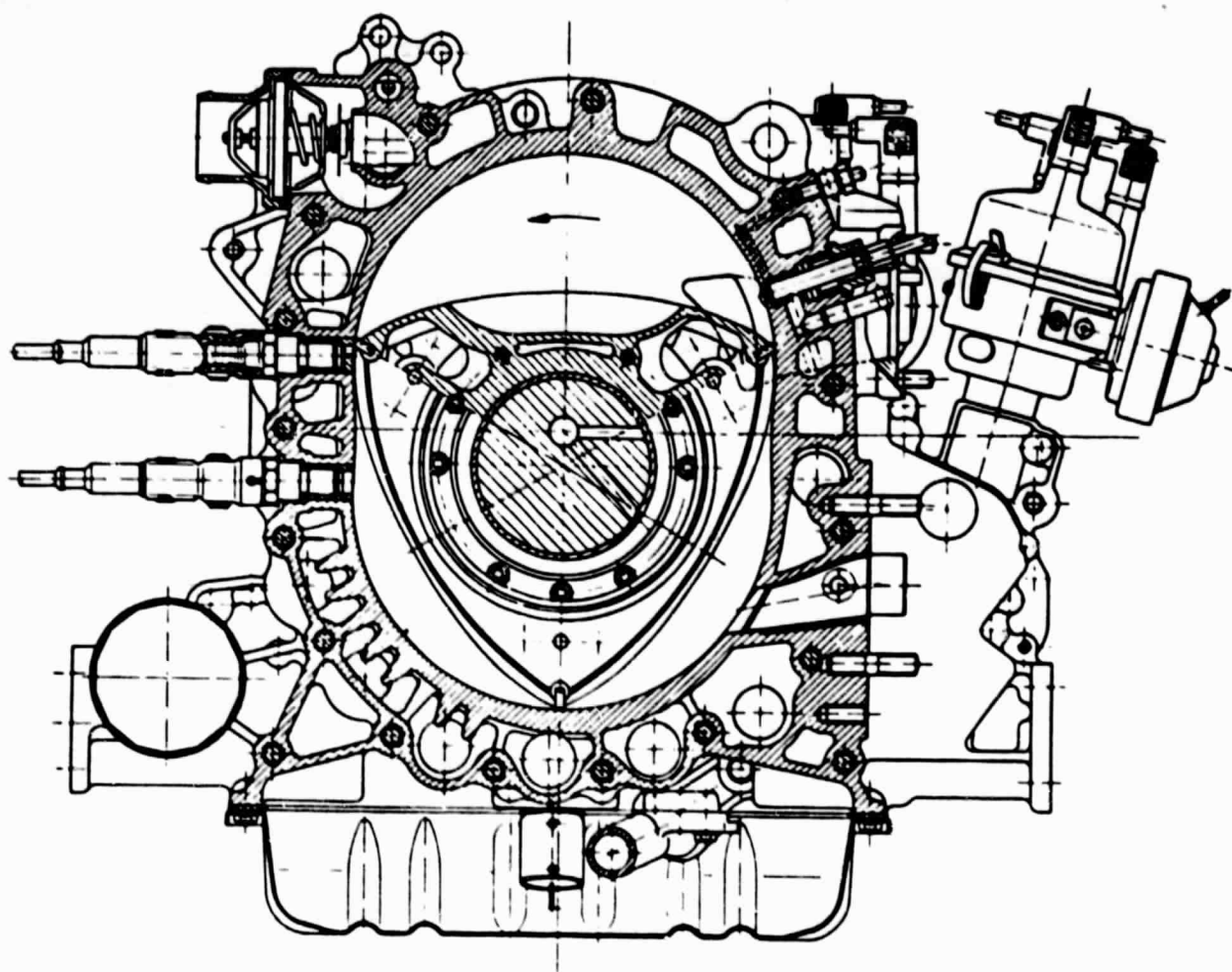
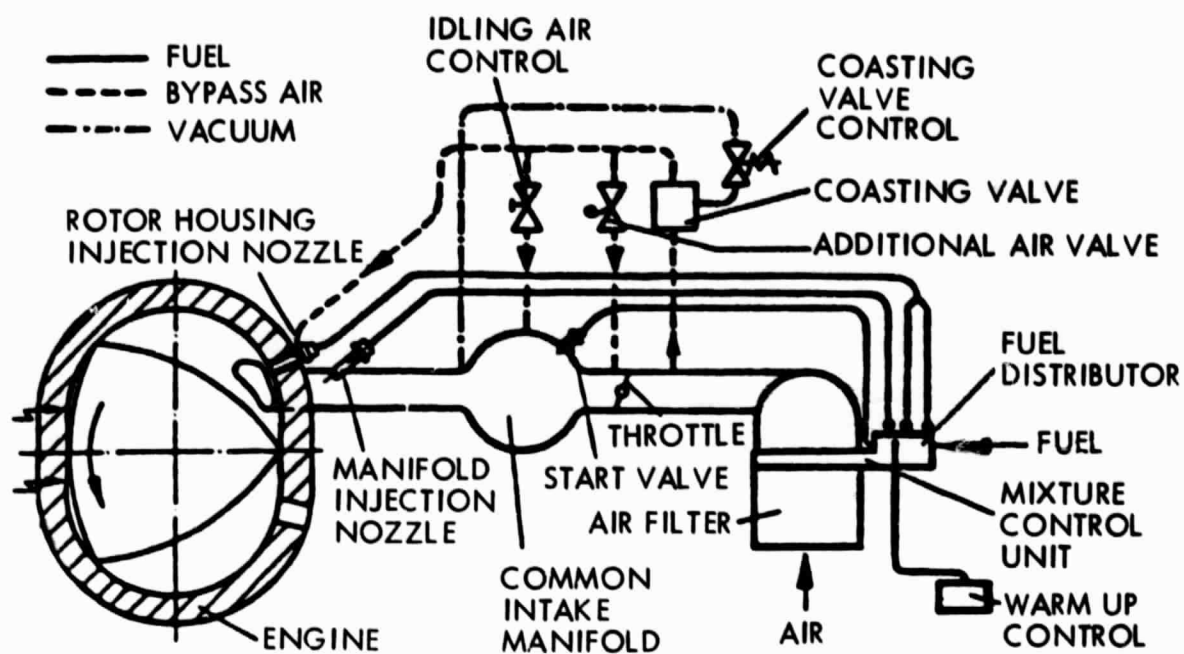
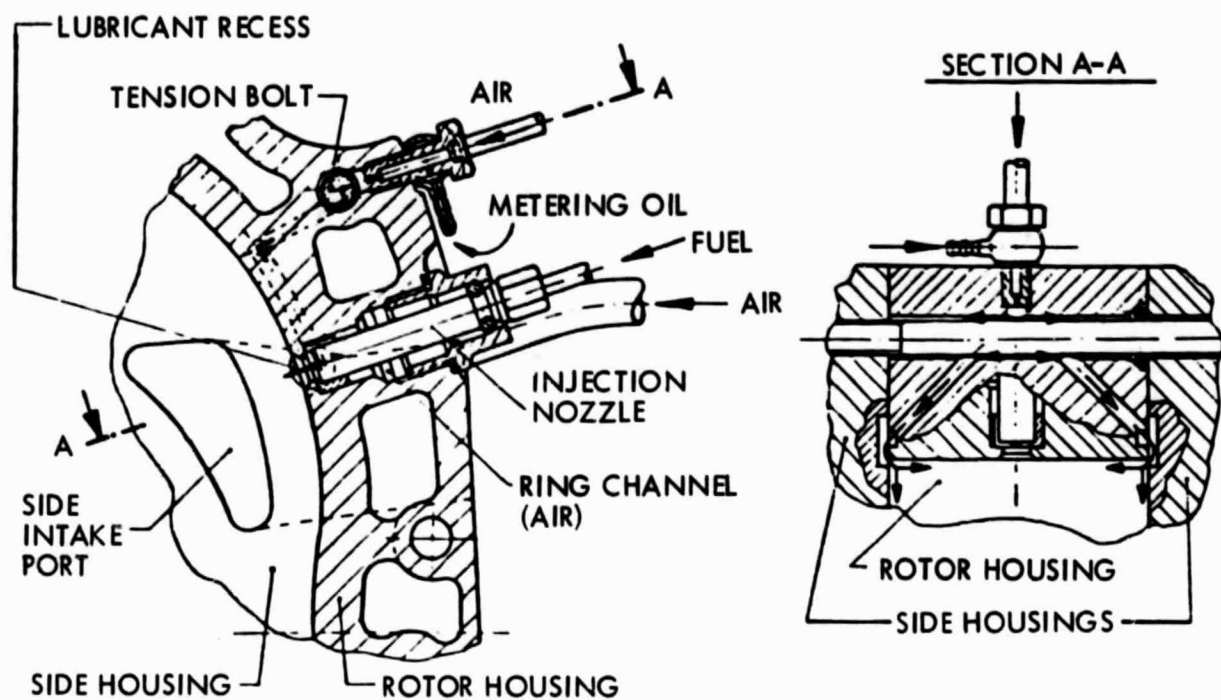


Figure 5-11. KKM 871 - Cross-Section (Ref. 66)



Note: Audi NSU's fuel and air enter at several sites: fuel is injected by rotor-housing nozzle, manifold nozzle, and upstream start-valve; air flows through manifold to side ports and through secondary passages. Secondary air control scheme is also shown.

Figure 5-12. Audi NSU Fuel and Air Intake Configuration (Ref. 66)



Note: Nozzle has annular channel for secondary air. Additional air enters with metered oil through passages above, shown in section at right.

Figure 5-13. Rotor-Housing Nozzle (Ref. 66)

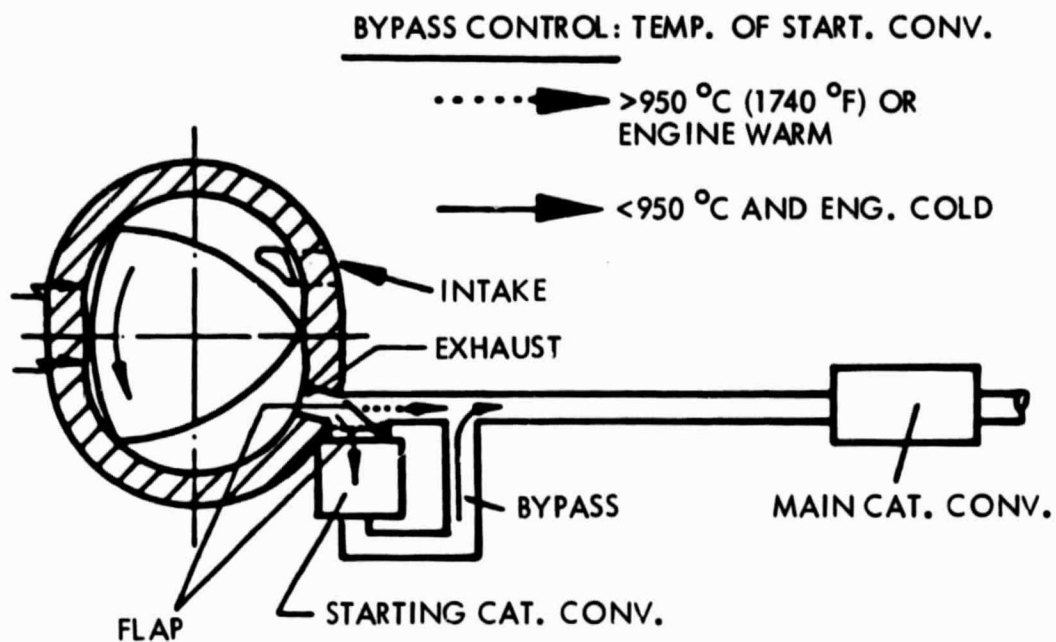


Figure 5-14. Exhaust Emission Control System for U.S. Standards (Ref. 66)

engine oil reach specified temperatures, the start-up unit is bypassed and the exhaust goes directly to the main converter. To offset the rich air-fuel ratios during cold start, secondary air is injected into the exhaust port region until coolant temperature reaches a preset temperature. The engine-driven pump supplying this secondary air then vents to the atmosphere.

Audi NSU has also done some development on two stratified-charge rotary engine concepts, one with partial direct injection of the fuel and the other with full direct injection.

Curtiss-Wright (Ref. 67) has developed a family of rotary powerplants featuring dual direct-injection stratified charge. These designs use a pilot fuel nozzle to initiate combustion near the spark plug, and a main fuel nozzle to supply additional fuel under increased load conditions. Various engine configurations developed at Curtiss-Wright have demonstrated engine-out HC emissions comparable to reciprocating engines, plus diesel-like fuel economy.

The HC emissions reductions achieved are principally attributed to rotor inserts that restrict heat transfer to the rotor body. Each "hot rotor" insert occupies most of the rotor face and has undergone steady geometric refinement. Pocket geometry, nozzle spray patterns, and injection system dynamics are all important elements in reducing engine-out HC emissions. Fuel-injected stratified-charge also plays a major role in reducing HC emissions. The stratified-charge approach concentrates combustion in a compact region surrounded by layers of successively leaner mixtures. Thus, quench and crevice volumes, and any apex leakage, are essentially air rather than air-fuel mixtures that can increase HC emissions.

The fuel economy of the Curtiss-Wright rotary engine was improved by replacing the engine's aluminum rotor housing by one of cast iron. The change of material provides higher surface temperature by virtue of reduced thermal conductivity, and also allows a significant increase in engine coolant temperature. The cast iron housing appeared to have little effect on engine-out HC emissions, compared to an identical configuration in aluminum. Thus, there appears to be no significant tradeoff with respect to hot-rotor and cast iron housing configurations.

5.3 VEHICLE FUEL ECONOMY AND EMISSIONS RESULTS

This section covers the fuel economy and emissions results for current production vehicles which use rotary engines. Currently, only the Mazda RX-7 with the Toyo Kogyo rotary engine falls in this category. The data is taken from EPA certification and fuel economy data for the 1980 and 1981 model years in California. Both 1980 and 1981 data are used because a significant change in emissions control technology was introduced on 1981 vehicles with rotary engines. California data is used because it is felt that California emissions standards are more representative of future emissions requirements for all states.

Fuel economy and emissions results for the 1980 and 1981 California Mazda vehicles using rotary engines are compared with the results for all 1980 California vehicles using three-way catalyst emissions control in Figures 5-15 through 5-18. These data represent essentially one vehicle type, the Mazda RX-7 sports model. In 1980 models, emissions were controlled using an exhaust thermal reactor and exhaust gas recirculation. In 1981 models, emissions control is accomplished using both a three-way catalyst and an oxidation catalyst with air injection. The 1980 vehicle inertia weight of 2750 lb was reduced to 2625 lb on the 1981 models. The vehicles are performance models with (HP/IW) values around 75. As shown in Figure 5-16, the efficiencies of these vehicles, as indicated by the (IW X MPG) parameter, are lower than the average for all California vehicles with three-way catalyst emissions control. However, the efficiency of the 1981 models has improved substantially over that of the 1980 models as a result of the introduction of improved emissions control systems. Emissions levels are reduced for 1981 models compared with 1980 models. For the 1981 models, both HC and CO emissions are low, and NO_x emissions fall between 0.4 g/mi and 0.6 g/mi. Comparisons of the fuel economy and emissions characteristics of the California and 49-state versions of these vehicles are given in Table 5-1 and in Figures 5-19 and 5-20. Examination of this data indicates that engine calibrations are about the same for California and 49-state versions of the 1981 vehicles, because both emissions and fuel economy are almost identical.

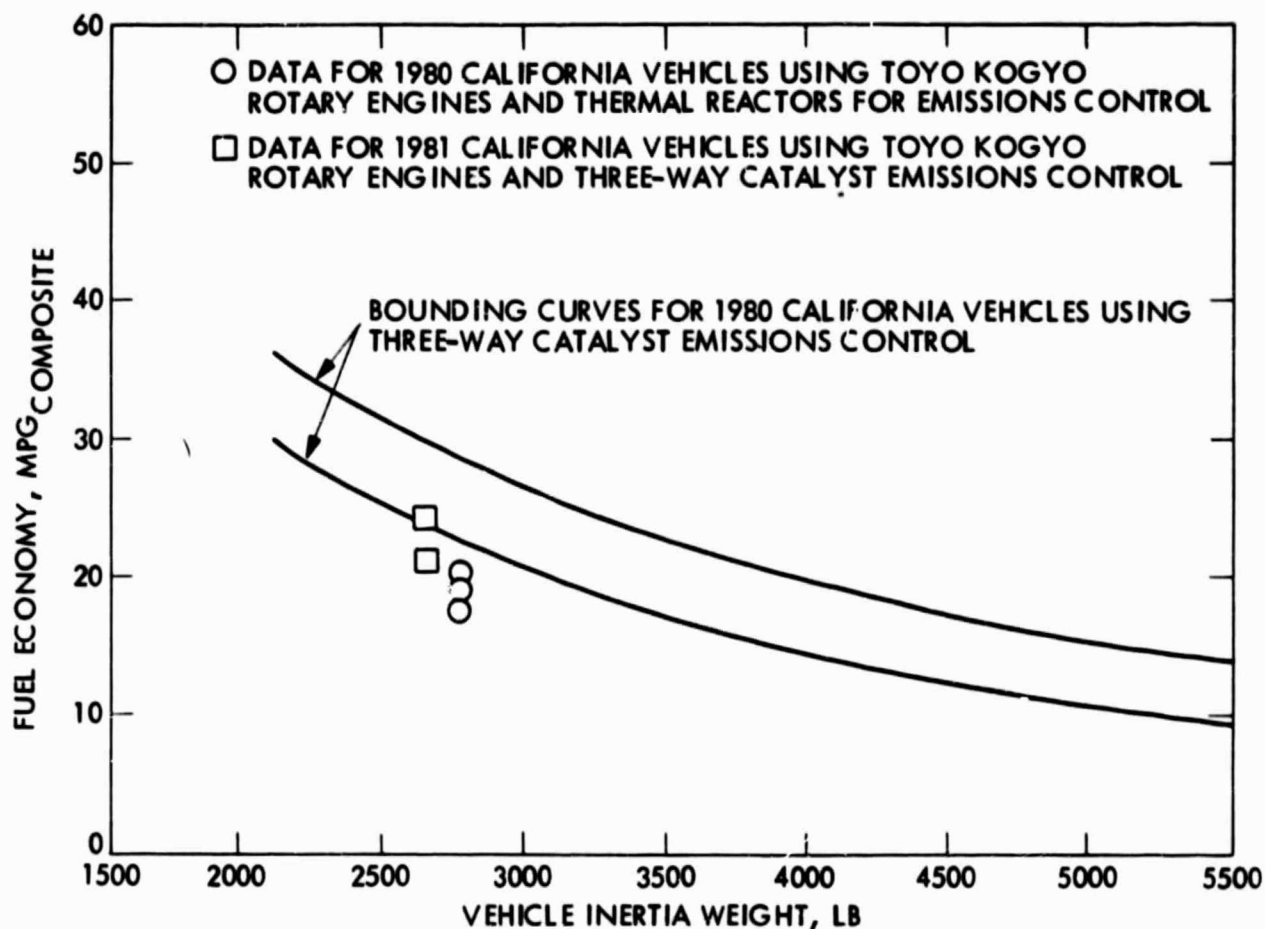


Figure 5-15. Composite Fuel Economy for California Vehicles Using the Toyo Kogyo Rotary Engine

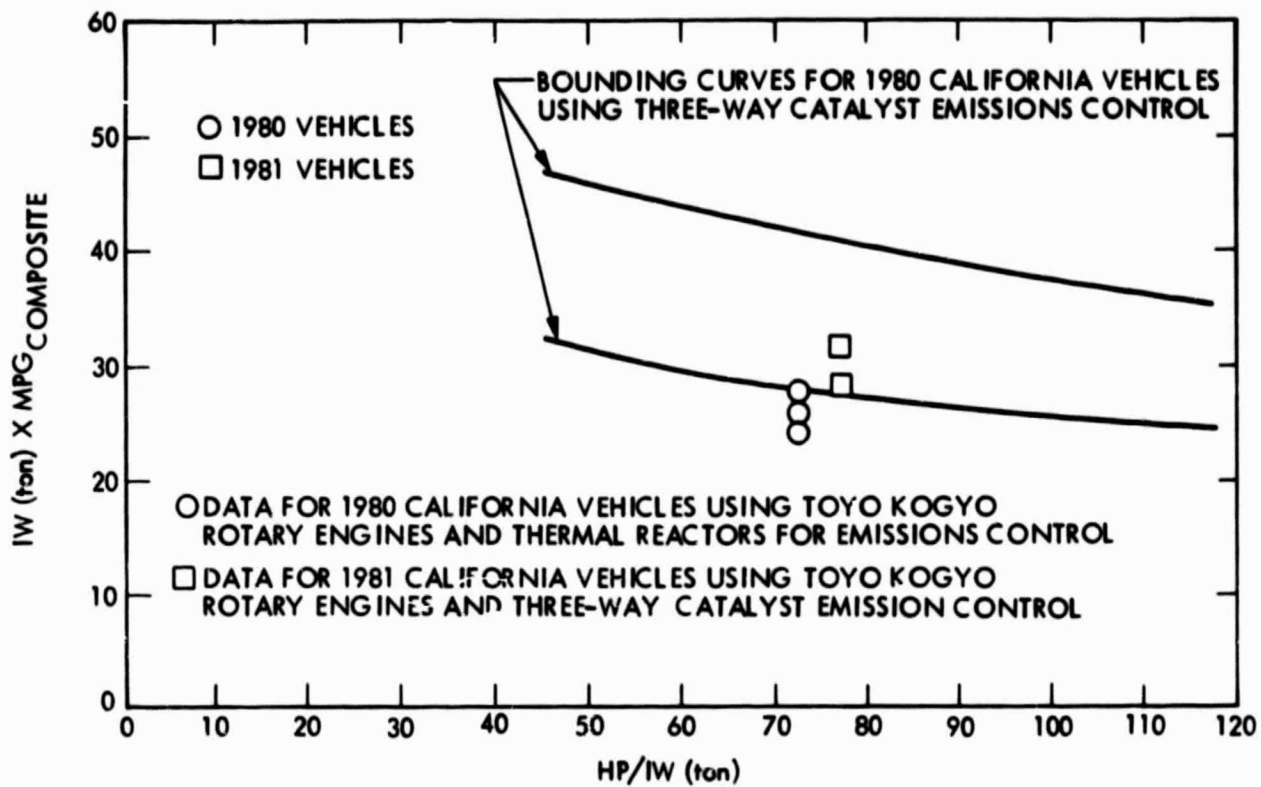
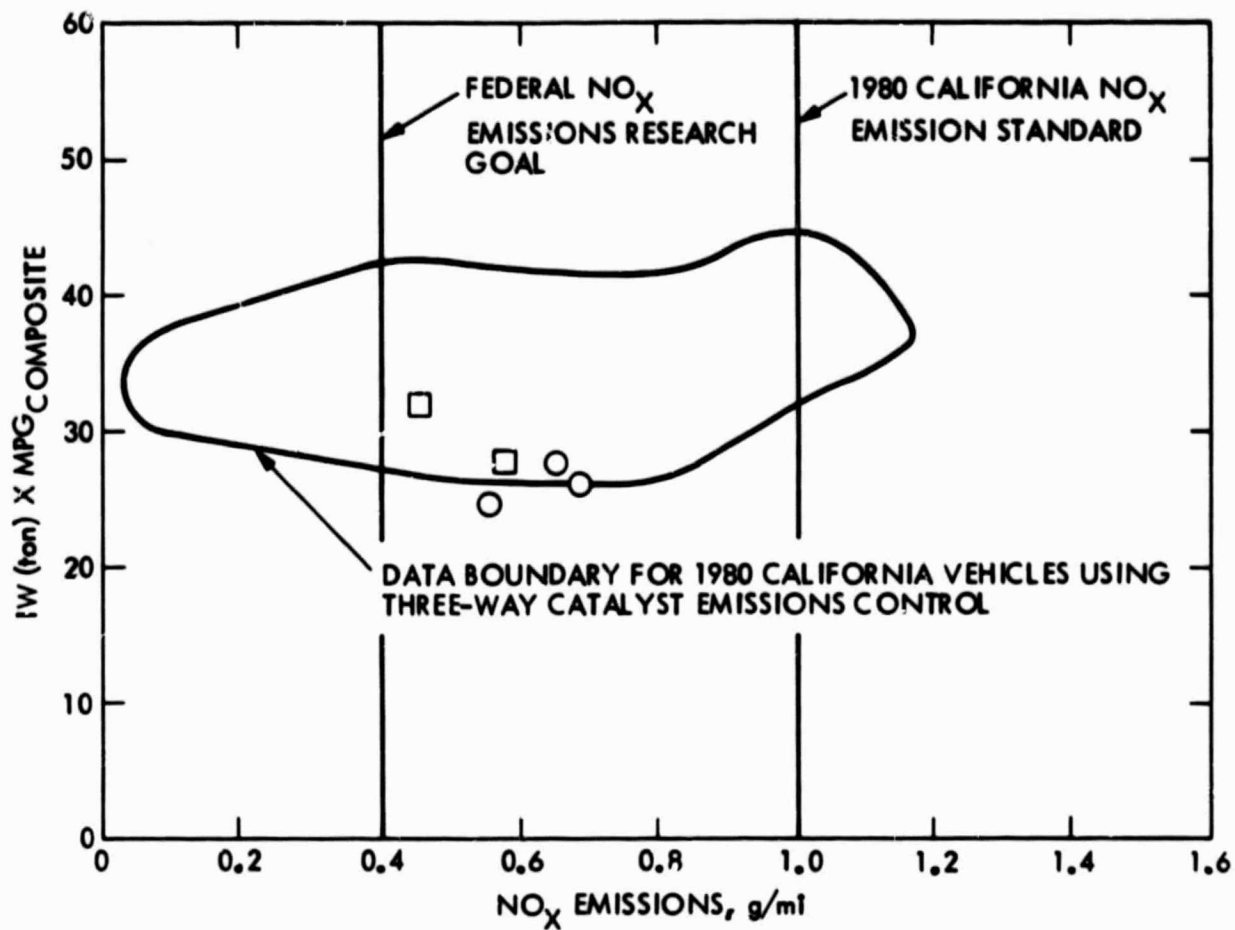


Figure 5-16. Fuel Economy Characteristics for California Vehicles Using the Toyo Kogyo Rotary Engine



- DATA FOR 1980 CALIFORNIA VEHICLES USING TOYO KOGYO ROTARY ENGINES AND THERMAL REACTORS FOR EMISSIONS CONTROL
- DATA FOR 1981 CALIFORNIA VEHICLES USING TOYO KOGYO ROTARY ENGINES AND THREE-WAY CATALYST EMISSIONS CONTROL

Figure 5-17. NO_x Emissions Characteristics for California Vehicles Using the Toyo Kogyo Rotary Engine

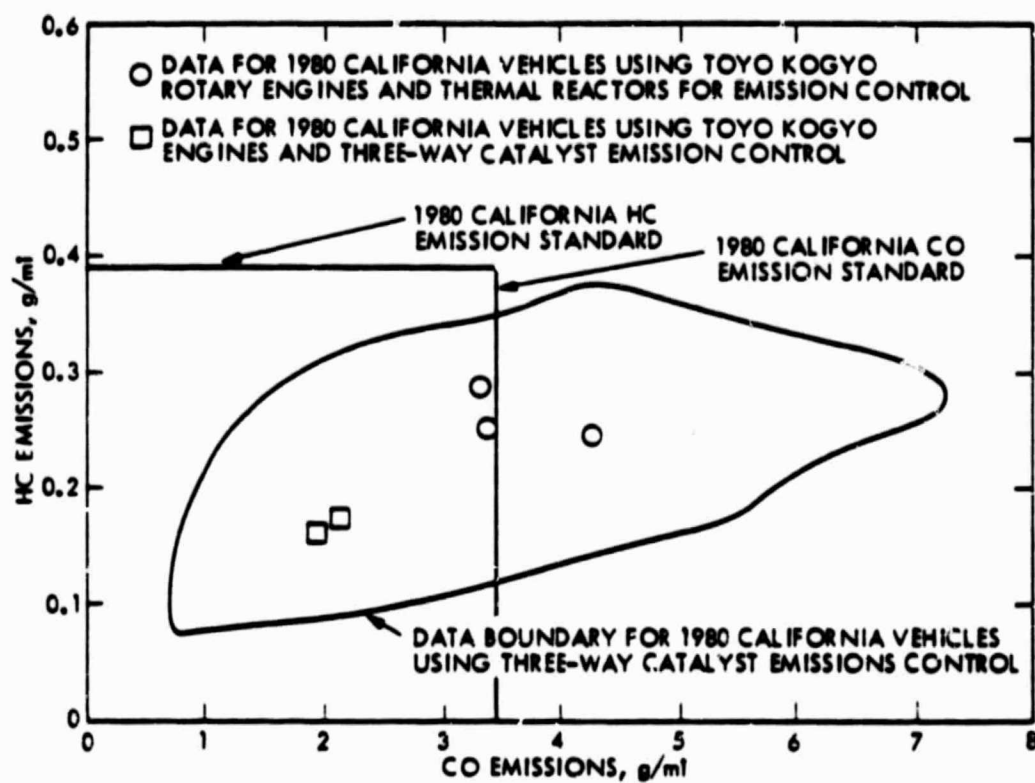
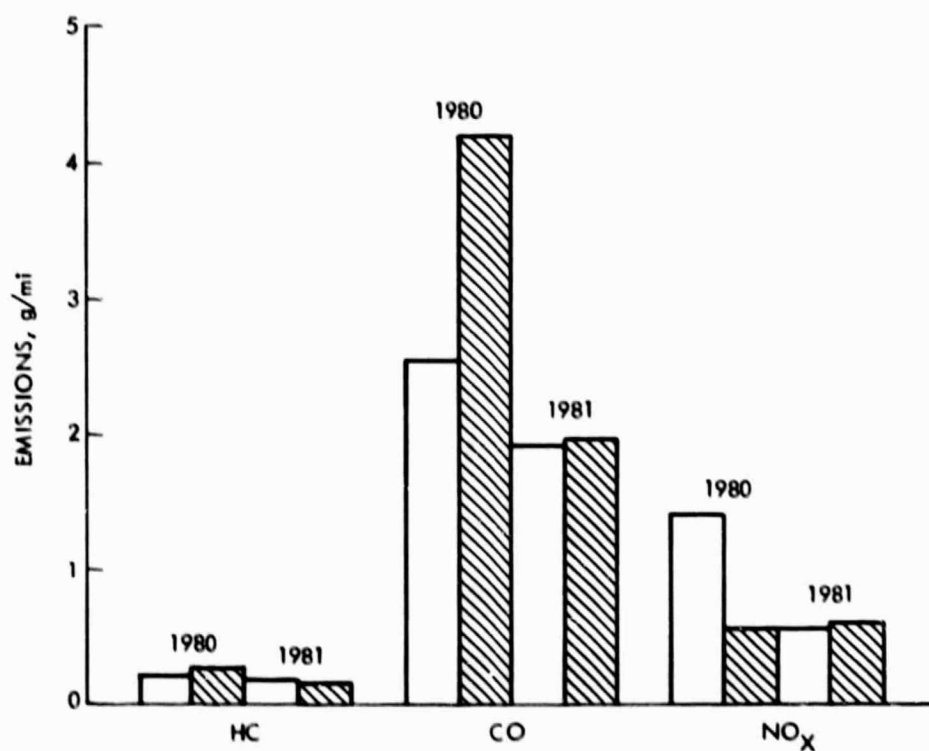
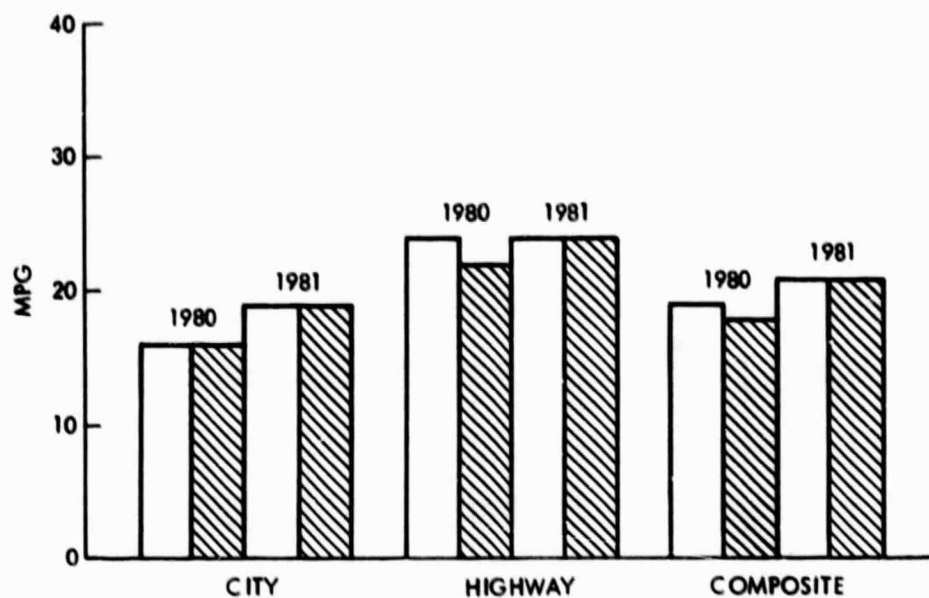


Figure 5-18. HC and CO Emissions Characteristics for California Vehicles Using the Toyo Kogyo Rotary Engine

Table 5-1. Characteristics of Toyo Kogyo Rotary Engines in 1980-81 California and 49-State Vehicles

Mfg	Car Line	CID	Carb FI	Comp Ratio	HP	Emission	Trans	Wt	Axle	City	Hiway	Comb	HC	CO	NOx	X mpg Comb	HP/lW (Ton)
TKM (1981)	RX-7 (Cal)	70	C-4	9.4	100	PMP/OXY/3WY	A3-1	2625	A3-1	19	24	21	0.164	1.96	0.58	27.56	26.19
	RX-7 (Cal)	70	C-4	9.4	100	PMP/OXY/3WY	M5-2	2625	M5-2	20	30	24	0.169	2.07	0.45	31.50	26.19
	RX-7 (49-St)	70	C-4	9.4	100	PMP/OXY/3WY	A3-1	2625	A3-1	19	24	21	0.194	1.92	0.54	27.56	26.19
	RX-7	70	C-4	9.4	100	PMP/OXY/3WY	M5-2	2625	M5-3	20	30	24	0.162	1.54	0.46	31.50	26.19
TKM	RX-7 (Cal)	70	C-4	9.4	100	THM/EGR/PMP	A3-1	2750	A3-1	16	22	18	0.242	4.19	0.56	24.75	72.73
	RX-7 (Cal)	70	C-4	9.4	100	THM/EGR/PMP	M4-1	2750	M4-1	16	24	19	0.253	3.39	0.69	26.13	72.73
	RX-7 (Cal)	70	C-4	9.4	100	THM/EGR/PMP	M5-1	2750	M5-2	16	27	20	0.288	3.32	0.64	27.50	72.73
	RX-7 (49-St)	70	C-4	9.4	100	THM/PMP	A3-1	2750	A3-1	16	24	19	0.208	2.53	1.39	26.13	72.73
TKM	RX-7 (49-St)	70	C-4	9.4	100	THM/PMP	M4-1	2750	M4-1	16	25	19	0.170	3.70	1.05	26.13	72.73
	RX-7 (49-St)	70	C-4	9.4	100	THM/PMP	M5-1	2750	M5-2	17	28	20	0.202	4.26	1.17	27.50	72.73



FUEL ECONOMY AND EMISSIONS COMPARISONS FOR CALIFORNIA AND 49-STATE VEHICLES - MAZDA RX-7 (70 CID ROTARY ENGINE, A3-1 TRANSMISSION)


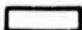
 CALIFORNIA
 49-STATE

Figure 5-19. Fuel Economy and Emissions Comparisons for California and 49-State Vehicles Using Toyo Kogyo Rotary Engine (Automatic Transmission)

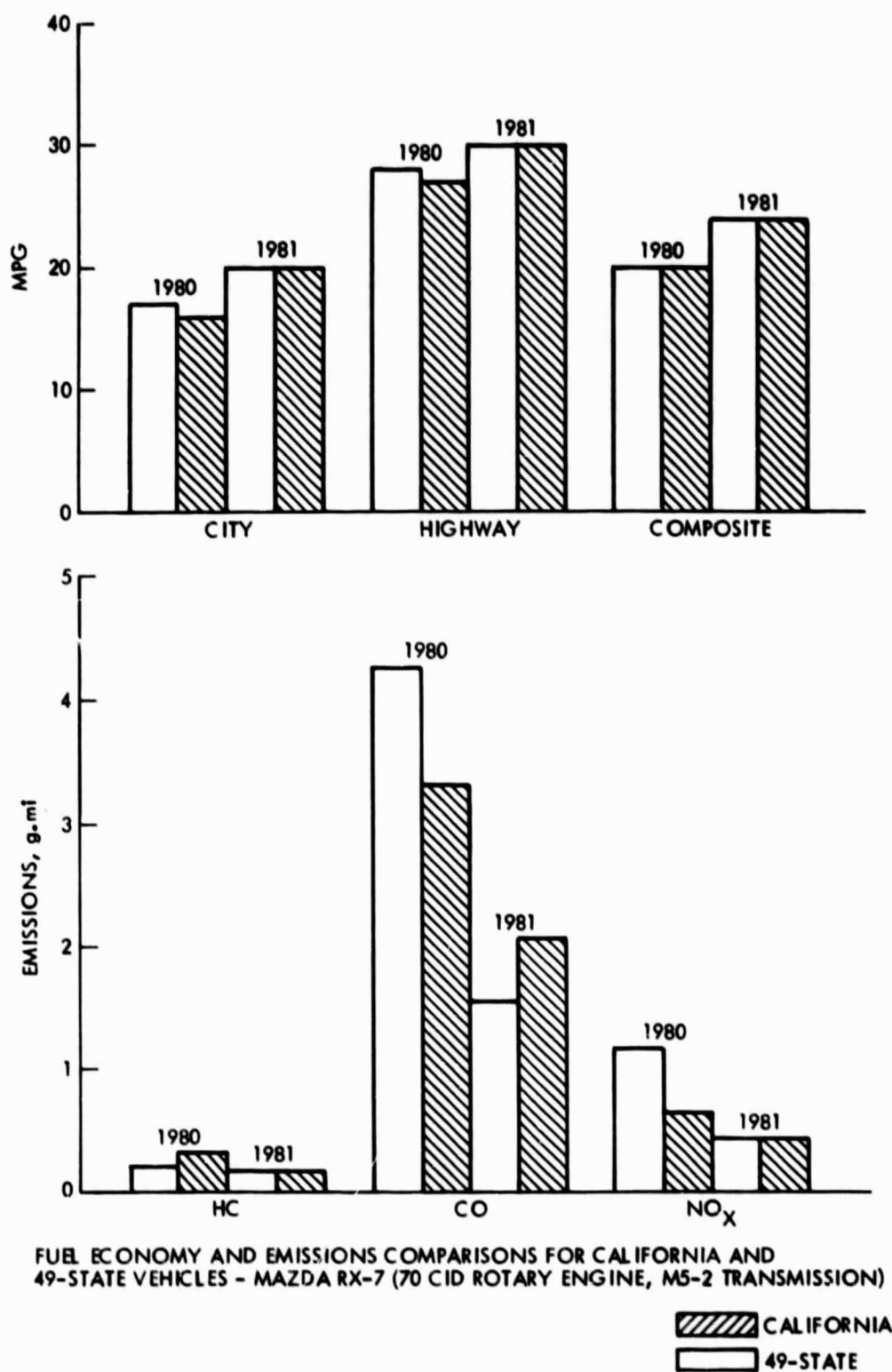


Figure 5-20. Fuel Economy and Emissions Comparison for California and 49-State Vehicles using Toyo Kogyo Rotary Engine (Manual Transmission)

SECTION 6

REFERENCES

1. Cross, R.H., "Emissions from Catalyst Equipped California Cars in Customer Service," SAE Paper 800395, February 1980.
2. Volvo News and Information, Volvo of America Corporation, 14 July 1976.
3. "Lambda-Sond: Complete Emission Control?" Automotive Engineering, February, 1977.
4. "MCA-Jet Swirls Mixture for Improved Combustion," Automotive Engineering, April 1978.
5. Engh, G.T. and Wallman, S., "Development of the Volvo Lambda-Sond System," SAE Paper No. 770295, February 1977.
6. Hughmark, G.A., and Sobel, B.A., "A Statistical Analysis of the Effect of MMT Concentration on Hydrocarbon Emissions," SAE Paper No. 800393, February, 1980.
7. Gruber, H.V. and Weidenmann, H.M., "Three Years Field Experience with the Lambda-Sensor in Automotive Control Systems," SAE Paper No. 800017, February 1980.
8. Young, C.T. and Bode, J.D., "Characteristics of ZrO_2 -Type Oxygen Sensors for Automotive Applications," SAE Paper No. 790143, February 1979.
9. "Oxygen Sensors Revisited," Automotive Engineering, April 1980.
10. Hamann, E., Manger, H. and Steinke, L., "Lambda-Sensor with Y_2O_3 -Stabilized ZrO_2 -Ceramic for Application in Automotive Emission Control Systems," SAE Paper No. 770401, February 1977.
11. Reddy, J.N., "Sensors for Automotive-Engine Control," SAE Paper No. 770399, February 1977.
12. Glockler, O., Knapp, H. and Manger, H.Y., "Present Status and Future Development of Gasoline Fuel Injection Systems for Passenger Cars," SAE Paper No. 800467, February 1980.
13. Rivard, J.G., "Closed-Loop Electronic Fuel Injection Control of the Internal Combustion Engine," SAE Paper No. 730005, January 1973.
14. Bosch Technische Berichte, Vol. 4 (1973) 5, pp 200-214.
15. Spilski, R.A. and Creps, W.D., "Closed-Loop Carburetor Emission Control System," SAE Paper No. 750371, February 1975.

16. Bantzert, T.R., Hicks, D.L. and Jeffries, M.A., "A Feedback Controlled Carburetion System Using Air Bleeds," SAE Paper No. 770352, February 1977.
17. "A Carburetor for Three-Way Conversion," Automotive Engineering, June 1977.
18. Ford Motor Company Advanced Emission Control Program Status Report, submitted to EPA in December 1976.
19. Berriman, L.P., "Special Report to the Environmental Protection Agency," Dresser Industries, Inc., November 1975.
20. Bowler, L.L., "Throttle Body Fuel Injection (TBI)-An Integrated Engine Control System," SAE Paper No. 800164, February 1980.
21. Engh, G.T. and Wallman, S., "Development of the Volvo Lambda-Sond System," SAE Paper No. 770295, February 1977.
22. Grimm, R.A., Bremer, R.J. and Stonestreet, S.P., "GM Micro-Computer Engine Control System," SAE Paper No. 800053, February 1980.
23. Ikeura, K., Hosaka, A. and Yano, T., "Microprocessor Control Brings about Better Fuel Economy with Good Driveability," SAE Paper No. 800056, February 1980.
24. "Lambda-Sond: Complete Emission Control?" Automotive Engineering, February 1977.
25. "GM Expands C-4 System Use," Automotive Engineering, August 1980.
26. "Microprocessor Control Improves Economy, Reduces Emissions," Automotive Engineering, February 1980.
27. Gorille, I., Rittmannsberger, H. and Werner, P., "Bosch Electronic Fuel Injection with Closed Loop Control," SAE Paper No. 750368, 1975.
28. Toyoda, T., Yamakawa, Y., Inoue, T., Oishi, K. and Hattori, K., "Development of Closed Loop Secondary Air Control Three-Way Catalyst System," SAE Paper No. 800399, February 1980.
29. "Exhaust Gas Composition Tailored Downstream," Automotive Engineering, April 1980.
30. "Engineering Highlights of the 1981 Automobiles," Automotive Engineering, October 1980.
31. "Engineering Highlights of the 1980 Automobiles," Automotive Engineering, October 1979.
32. "LEC-1 + 3-way = EEC-11," Automotive Engineering, August 1978.

33. Dowdy, M.W., Hoehn, F.W. and Vanderbrug, T.G., "Lean Mixture Engines Testing and Evaluation Program," Volumes I, II and III, Report No. DOT-TSC-OST75-26.1, prepared for U.S. Department of Transportation, November 1975.
34. Schweitzer, P.H., "Control of Exhaust Pollution Through a Mixture-Optimizer," SAE Paper 720254, January 1972.
35. Hansel, J.G., "Lean Automobile Engine Operation-Hydrocarbon Exhaust Emissions and Combustion Characteristics," SAE Paper 710164, January 1971.
36. Lindsay, R. and Wilson, J., "Heat Pipe Vaporization of Gasoline-Vapour," presented at First Symposium on Low Pollution Power and Alternative Automotive Power Systems Coordination Meeting, October 14-19 1973.
37. Hurter, D.A., "A Study of Technological Improvement in Automobile Fuel Consumption" DOT-TSC-OST-74-40, Department of Transportation/Environmental Protection Agency, December 1974.
38. Quader, A.A., "Effects of Spark Location and Combustion Duration on Nitric Oxide and Hydrocarbon Emissions," SAE Paper No. 730153, January 1973.
39. Peters, B.D. and Quader, A.A., "'Wetting' the Appetite of Spark Ignition Engines for Lean Combustion" SAE Paper 780234, February 1978.
40. Gabele, P.A., "The Effect of Intake Valve Modification on Cycle-by-Cycle Variations in an SI Engine," MS.S. Thesis, Pennsylvania State University, March 1971.
41. Tanuma, T., Sasaki, K., Kaneko, T. and Kawasaki, H., "Ignition, Combustion and Exhaust Emissions of Lean Mixtures in Automotive Spark Engines," Nissan Motor Co. Ltd., SAE Paper 710159, SAE Transactions, Vol. 80, 1971.
42. Kuroda, H., Nakajima, Y., Sugihara, K., Takagi, Y. and Muranaka, S., "The Fast Burn with Heavy EGR, New Approach for Low NO_x and Improved Fuel Economy," SAE Paper 780006, February 1978.
43. Brandstetter, W., "The Volkswagen Lean Burn PC-Engine Concept," SAE Paper 800456, February 1980.
44. Nakamura, H., Ohinouye, T., Hori, K., Kiyota, Y., Nakagami, T., Akishino, K. and Tsukamoto, Y., "Development of a New Combustion System (MCA-Jet) in Gasoline Engine," SAE Paper 780007, February 1978.
45. Mattavi, J.N., "The Attributes of Fast Burning Rates in Engines," SAE Paper 800920, February 1980.
46. Quader, A.A., "What Limits Lean Operation in Spark Ignition Engines-Flame Initiation or Propagation?" SAE Paper 760760, October 1976.

47. "What Limits Lean Combustion-Spark or Propagation?" Automotive Engineering, January 1977.
48. "Homogeneous Mixtures May Not Be Optimal for Lean Combustion," Automotive Engineering, November 1980.
49. "Fast-Burn Chamber Design Improves Efficiency, Lowers Emission," Automotive Engineering, November 1980.
50. "Fast Burn-Heavy EGR Improves Economy, Reduces NO_x," Automotive Engineering, August 1978.
51. May, M.G., "Lower Specific Fuel Consumption with High Compression Lean Burn Spark-Ignited 4-Stroke Engines," SAE Paper 790386, February 1979.
52. Stephenson, R.R., et al, "Should We Have a New Engine?" Jet Propulsion Laboratory, Report SP 43-17, August 1975.
53. Bracco, F.V., "Toward an Optimal Automobile Powerplant," Combustion Science and Technology, Volume 12, pp. 1-10, 1976.
54. Date, T., Yagi, S., Ishizuya, A. and Fujii, I., "Research and Development of the Honda CVCC Engine," SAE Paper 740605, February 1974.
55. Inoue, Kazuo, Ukawa, Haruo and Fujii, Isao, "Fuel Economy and Exhaust Emissions of the Honda CVCC Engine," Combustion Science and Technology, Volume 12, pp. 11-27, 1976.
56. Yagi, Shizuo, Fujii, Isao, Nishikawa, Masayasu, and Shirai, Hiroshi, "A New Combustion System in the Three-Valve Stratified-Charge Engine," SAE Paper 790439, February 1979.
57. Yagi, Shizuo, Fujii, Isao, Nishikawa, Masayasu, and Shirai, Hiroshi, "A Newly Developed 1.5 L CVCC Engine for Some 1980 Models," SAE Paper 800321, February 1980.
58. Mitchell, E. and Alperstein, M., "Texaco Controlled-Combustion System-Multifuel, Efficient, Clean and Practical," Combustion Science and Technology, Vol. 8, pp. 39-49, 1973.
59. Alperstein, M. Schafer, G.H. and Villforth, F.J., "Texaco's Stratified-Charge Engine-Multifuel, Efficient, Clean and Practical," SAE Paper 780699, August 1978.
60. "Stratified-Charge Mixing Strategies Compared," Automotive Engineering, August 1978.
61. Scussel, A.J., Simko, A.O. and Wade, W.R., "The Ford PROCO Engine Update," SAE Paper 780699, August 1978.
62. Brandstetter, W.R., Decker, G., Schafer, H.J. and Steinke, D., "The Volkswagen PCI Stratified-Charge Concept-Results from 1.6 Liter Air Cooled Engine," SAE Paper 741173, 1974.

63. Miyake, M., Okada, S., Kawahara, Y. and Asai, K., "A New Stratified-Charge Combustion System (MCP) for Reducing Exhaust Emission," *Combustion Science and Technology*, Vol. 12, pp. 29-46, 1976.
64. "A Worldwide Rotary Update," Automotive Engineering, Volume 86, Number 2, February 1978.
65. Yamamoto, K. and Muroki, T., "Development of Exhaust Emission and Fuel Economy of the Rotary Engine at Toyo Kogyo," SAE Paper 780417, February 1978.
66. van Basshuysen, R. and Wilmers, G., "An Update of the Development on the New Audi NSU Rotary Engine Generation," SAE Paper 780418, February, 1978.
67. Jones, C., Lamping, H.D., Myers, D.M. and Loyd, R.W., "An Update of the Direct Injected Stratified-Charge Rotary Combustion Engine Developments at Curtiss-Wright," SAE Paper 770044, February 1977.

SECTION 7

BIBLIOGRAPHY

Bradow, R.L. and Stump, F.D., "Unregulated Emissions from Three-Way Catalyst Cars," SAE Paper No. 770369, February 1977.

Cooper, B.J., Harrison, B., Shutt, E. and Lichtenstein, I., "The Role of Rhodium in Rhodium/Platinum Catalysts for CO/HC/SO₄ Emission Control: The Influence of Oxygen on Catalytic Performance," SAE Paper 770367, February 1977.

Ernest, M.V. and Kim, G., "Development of More Active and Durable Automotive Exhaust Catalysts," SAE Paper 800083, February 1980.

Falk, C.D. and Mooney, J.J., "Three-Way Conversion Catalysts,: Effect of Closed-Loop Feed-Back Control and Other Parameters on Catalyst Efficiency," SAE Paper 800462, February 1980.

Ghandi, H.S., Piken, A.P., Stepien, H.K., Shelaf, M., Delosh, R.G. and Heyde, M.E., "Evaluation of Three-Way Catalysts-Part II," SAE Publication SP-414, February 1977.

Holl, W.J., "Air-Fuel Control to Reduce Emissions: Vol. I: Engine Emissions Relationships," SAE Paper 800051, February 1980.

Howitt, J.W., "Thin Wall Ceramics as Monolithic Catalyst Supports," SAE Paper 800082, February 1980.

Kaberstein, E., "Characterization and Application of Multifunctional Catalysts for Automotive Exhaust Purification," SAE Paper 770366, February 1977.

Kaneko, Y., Kobayashi, J., Komagome, R., Nakagami, T. and Fukui, T., "Catalyst Systems Development," SAE Publication SP-414, February 1977.

Kim, G. and Maselli, J.M., "Effect of Support on Noble Metal Catalysts for Three-Way Conversions," SAE Paper 770368, February 1977.

Mooney, J.J., Thompson, C. and Dettling, J., "Three-Way Conversion Catalysts-Part of the New Emission Control System," SAE Paper 770365, February 1977.

Oser, P., "Catalyst Systems with an Emphasis on Three-Way Conversion and Novel Concepts," SAE Paper 790306, February 1979.

Prigent, M., Raynal, B. and Courty, P., "A Three-Way Catalytic Muffler Using Progressive Air Injection for Automotive Exhaust Gas Purification," SAE Paper No. 770298, February 1977.

Urban, C.M. and Garbe, R.J., "Exhaust Emissions from Malfunctioning Three-Way Catalyst-Equipped Automobiles," SAE Paper 800511, February 1980.

Wang, Wei-Ming, "Air-Fuel Control to Reduce Emissions, Vol. II: Catalyst Characterization Under Cyclic Conditions," SAE Paper 800052, February 1980.